

Aus dem
Deutschen Krebsforschungszentrum (DKFZ) Heidelberg
(Wissenschaftlicher Vorstand: Prof. Dr. med. Michael Baumann)

in Zusammenarbeit mit dem
Nationalen Centrum für Tumorerkrankungen Dresden (NCT/UCC)
(Geschäftsführende Direktoren:
Prof. Dr. med. Martin Bornhäuser, Prof. Dr. med. Hanno Glimm,
Prof. Dr. med. Mechthild Krause, Prof. Dr. med. Jürgen Weitz)
Abteilung Translationale Medizinische Onkologie
Abteilungsleiter: Prof. Dr. med. Hanno Glimm

Characterization of G Protein Subunit Beta 1 as Regulator of Tumour Initiating Cell Activity in Human Pancreatic Cancer

Inauguraldissertation
zur Erlangung des Doctor scientiarum humanarum (Dr. sc. hum.)
an der
Medizinischen Fakultät Heidelberg
der
Ruprecht-Karls-Universität

vorgelegt von
Na Kang

aus
Harbin, China

2021

Dekan: Herr Prof. Dr. med. Hans-Georg Kräusslich

Doktorvater: Herr Prof. Dr. med. Hanno Glimm

Index of Contents

Index of Contents	3
List of Figures	6
List of Tables.....	8
List of Abbreviations.....	9
1 Introduction	13
1.1 Pancreatic cancer.....	13
1.1.1 The human pancreas.....	13
1.1.2 Epidemiology of pancreatic cancer	13
1.1.3 Development of pancreatic cancer	14
1.2 Treatment of pancreatic cancer	15
1.3 Tumour initiating cells in cancer.....	16
1.4 Functional heterogeneity in human pancreatic cancer	17
1.4.1 Identification of potential TIC activators	18
1.5 Aims of the study	21
2 Material and Methods.....	22
2.1 Materials.....	22
2.1.1 Equipment	22
2.1.2 Plastic and Disposables	23
2.1.3 Cell Culture Related Reagents	25
2.1.4 Cell Culture Media and Buffers	26
2.1.5 Antibodies	26
2.1.6 Commercial Kits	28
2.1.7 Western Blot Buffers.....	29
2.1.8 Plasmids and Primers	29
2.1.9 GNB1 Codon-optimized sequence with flanking restriction enzyme sequences (5' – 3') (Gao 2017, pg. 27-28).....	30
2.1.10 Oligonucleotides for specific gene knockdowns.....	31
2.1.11 Cell lines.....	31
2.1.12 Commercial Bacteria Strains.....	31
2.1.13 Mouse Strains.....	31
2.1.14 Other Reagents and Chemicals for Molecular and Cloning Technologies	32
2.1.15 Primary patient-derived PDAC cultures	33
2.1.16 Software	33
2.2 Methods	35
2.2.1 Cell culture techniques	35
2.2.2 Single-cell RNA Sequencing (sc-RNA-Seq)	37
2.2.3 Flow cytometry and cell sorting.....	39
2.2.4 Production of concentrated lentiviral particles.....	40
2.2.5 Measurement and calculation of the infectivity of produced lentiviral stocks.....	40

2.2.6 Generation of stably transduced cultures for gene overexpression or knockdown studies.....	41
2.2.7 Molecular Techniques	42
2.2.8 Cell cycle analysis	49
2.2.9 Cloning of GNB1-FLAG constructs into pCCL pptPGK_IRES_GFP_PRE Vector ..	50
2.2.10 Colony formation assay.....	53
2.2.11 Culture contamination test	53
2.2.12 Cloning of SLC35F5 shRNAs into pRSIT17-U6Tet-sh-HTS6-CMV-TetRep-2A-TagGFP2-2A-Puro vector	54
2.2.13 <i>In vivo</i> mouse xenotransplantation experiments	55
2.2.14 Statistical Analysis	56
3 Results	58
3.1 Patient-derived PDAC cell cultures	58
3.2 Validation experiments of the identified TIC regulators GNB1 and SLC35F5 in established primary PDAC cultures	60
3.2.1 Validation of GNB1 as regulator of TIC activity in human PDAC	60
3.2.2 Validation experiments of SLC35F5 as TIC regulator in PDAC.....	76
3.2.3 Summary 3.2	84
3.3 Deciphering the transcriptional heterogeneity in pancreatic cancer patient tumours by single-cell RNA sequencing.....	85
3.4 GNB1 induced pathway alterations in pancreatic cancer cells	89
3.4.1 Generation of a model system to assess GNB1 induced pathway alterations in pancreatic tumorigenesis	89
3.4.2 Ectopic overexpression of GNB1 expression in H6C7 cells on mRNA and protein levels.....	92
3.4.3 Investigation of Akt and ERK1/2 activation in H6C7 transduced cells.....	93
3.4.4 Comprehensive evaluation of PI3K and MAPK signalling pathway deregulation by DigiWest multiplex protein profiling	94
3.4.5 Validation of PDPK1 expression in GNB1 dysregulated cells	97
3.4.6 Validation of mTOR expression and mTOR phosphorylation level in GNB1 dysregulated cells	101
3.4.7 Investigation of the PI3K pathway activity in GNB1 overexpressed normal pancreatic epithelial cells.....	103
3.4.8 Summary 3.4	104
3.5 Identification of GNB1 binding partners in primary PDACs.....	106
3.5.1 Cloning of FLAG-tagged GNB1 expression constructs	106
3.5.2 GNB1-FLAG-Tag lentiviral particle production and titration	107
3.5.3 Establishment of constitutive GNB1-FLAG-Tag expression in primary PDACs	108
3.5.4 Validation of GNB1-FLAG-Tag protein expression by Immunofluorescence staining	109
3.5.5 Identification and validation of GNB1 binding partners by mass-spectrometry after co-immunoprecipitation	112
3.5.6 Summary 3.5	114
4 Discussion	115

4.1 GNB1 possesses PDAC TIC regulator activity.....	115
4.1.1 TICs are transiently activated in PDAC.....	115
4.1.2 Overexpression of GNB1 promotes PDAC progression.....	115
4.1.3 GNB1 is heterogeneously expressed in PDAC.....	117
4.2 Gβ1 expression seems to be strictly controlled in cancer cells.....	118
4.3 GNB1 may regulate PDAC TIC activation via PI3K-Akt-mTOR signalling.....	119
4.4 GNG12, GNAI1 and KCTD5 are characterized as the binding partners of GNB1 in primary PDACs.....	121
4.5 Role of SLC35F5 in PDAC TIC activation.....	122
4.6 Conclusion.....	122
4.7 Outlook.....	123
5 Summary.....	125
6 Zusammenfassung.....	127
7 References.....	129
8 Personal Contribution to Data Acquisition, Assessment and Publications.....	148
Curriculum Vitae.....	149
Acknowledgement.....	150
EIDESSTATTLICHE VERSICHERUNG.....	152

List of Figures

Figure 1: Illustration of two clonal TIC dynamic models (Ball et al. 2017).....	18
Figure 2: Stable marker gene expression by flow cytometry after lentiviral transduction of PDAC cultures for deregulated target gene expression (n=3).....	62
Figure 3: GNB1 overexpression is detectable on RNA level in patient-derived cultures (n=3) after lentiviral transduction.	63
Figure 4: LV. GNB1 OE vector showed mild influence on endogenous GNB1 expression on RNA level in patient-derived cultures (n=3) after lentiviral transduction.	64
Figure 5: GNB1 expression on protein level in three patient-derived GNB1 overexpression and knockdown cultures (n=3).....	65
Figure 6: Marker gene expression after flow cytometric enrichment of freshly transduced cells (n=2).	66
Figure 7: GNB1 overexpression was detectable on protein level in newly transduced PC1 and PC3 cultures (n=2).	67
Figure 8: Summary of values of total identified proteins which detected by Mass-spectrometry based whole protein analysis (n=3).....	69
Figure 9: GNB1 expression on protein level was detected by mass-spectrometry (n=3).....	70
Figure 10: GNB1 overexpression and knockdown on protein level is detected by Mass-spectrometry based whole protein analysis (n=3).	70
Figure 11: Heat-map of G protein alpha subunits LFQ intensity detected by mass-spectrometry in genetically engineered PCs (n=3).	71
Figure 12: GNB1 overexpression detected by immunofluorescence staining on PC1 (n=1). .	72
Figure 13: Influence of GNB1 expression on cell cycle in three PCs (n=3).....	74
Figure 14: SLC35F5 expression in five primary PDAC cultures compared to HeLa cells on RNA level (n=6).....	76
Figure 15: FACS analysis showed efficient marker gene expression in PC1 three days post transduction (n=1).	77
Figure 16: Measurement of lentiviral SLC35F5 overexpression vector transduction efficiency in PC1 (n=1).	78
Figure 17: Investigation of SLC35F5 expression on RNA and protein level in PC1 transduced cells (n=1).....	79
Figure 18: Pre-experiment of PC1 colony formation assay (n=1).	80
Figure 19: Colony formation of PC1 after lentiviral mediated SLC35F5 knockdown (n=3)..	81
Figure 20: Colony formation of PC1 after lentiviral mediated SLC35F5 overexpression (CDS and TR) (n=3).....	82
Figure 21: The influence of SLC35F5 knockdown on TIC activation in serial transplantation (n=18).....	84

Figure 22: Identification of cell clusters and cell sub-types in PC1 using sc-RNA seq data (n=1).	86
Figure 23: Heterogeneous expression of GNB1 in PC1 on single-cell RNA level.	87
Figure 24: High GNB1 expression correlates with β -arrestin signalling pathway signatures (n=1).	88
Figure 25: Illustration of established H6C7 cultures with lentiviral mediated GNB1 overexpression and transduction efficiency measurements.	90
Figure 26: Enrichment of GFP positive cells in H6C7 GFP control by cell sorting.	91
Figure 27: Validation of GNB1 overexpression in pancreatic epithelial cells with and without <i>KRAS</i> mutation (n=1).	92
Figure 28: Investigation of PI3K and MAPK signalling after GNB1 overexpression in <i>KRAS</i> wildtype or mutated pancreatic epithelial cells (n=1).	93
Figure 29: Illustration of the timeline and protein samples generation for DigiWest multiplex protein profiling analysis and consecutive validation experiments.	94
Figure 30: Summary of DigiWest multiplex protein profiling array data analysis (n=2).	96
Figure 31: PDPK1 validation by western blot in R2 set and independent transduced (R4) set samples (n=2).	97
Figure 32: Validation of PDPK1 expression by western blot in the original screening sample set (n=2).	98
Figure 33: PDPK1 validation by western blot in the newly generated (replicates 5, R5) H6C7 cells (n=1).	99
Figure 34: Investigation of PDPK1 expression in three primary PDACs after GNB1 gene dysregulation (n=3).	100
Figure 35: Validation of mTOR and p-mTOR expression in R2 Set (n=1).	101
Figure 36: Validation of mTOR and p-mTOR expression in R1 and R3 Sets (n=2).	102
Figure 37: Dose-response curves of inhibitors targeting Akt, PIK3CA, PI3K alpha, PI3K, PDPK1 and GNB1.	104
Figure 38: PCR amplification of GNB1-FLAG-Tag sequences.	106
Figure 39: GNB1-FLAG-Tag virus titration using FACS (n=1).	107
Figure 40: Efficient enrichment of lentivirally transduced cells using a vector for GNB1-FLAG-Tag expression after sorting (n=3).	108
Figure 41: Validation of GNB1 and FLAG-Tag protein expression (n=1).	110
Figure 42: FLAG-Tagged GNB1 expression was detectable in transduced PC2 and PC3 samples (n=2).	111
Figure 43: Validation of identified GNB1 binding partners by co-immunoprecipitation (n=3).	113

Figure 44: Validation of GNG12 as the binding partner of GNB1 by co-immunoprecipitation (n=3).....	114
--	-----

List of Tables

Table 1: Clinical information of established primary pancreatic cancer cultures used in this study (n=7).	59
Table 2: Transduction efficiency of three PDAC patient-derived cultures after transduction with lentiviral based GNB1 overexpression or knockdown vectors as well as the corresponding controls analysed by flow cytometry (n=3).....	61
Table 3: Unique peptide numbers of identified G protein gamma subunits detected by mass-spectrometry (n=3).	71
Table 4: Summary of the influence of GNB1 on cell cycle (n=3).	75
Table 5: Transduction efficiency of transduced and transplanted PDAC patient-derived culture PC1.	83
Table 6: Transduction efficiency of transduced H6C7 cells with lentiviral based GNB1 overexpression and mock vector.	91
Table 7: Unique peptide numbers of GNG12 detected by mass-spectrometry based whole cell protein analysis in PC1, PC2 and PC3 (n=3).	112

List of Abbreviations

Abbreviations	Full name
°C	Celsius scale
4E-BP1	Eukaryotic translation initiation factor 4E-binding protein 1
5-FU	5-fluorouracil
A	Area
AC	Adenylyl cyclase
ADP	Adenosine diphosphate
Akt	Protein kinase B
APC	Allophycocyanin
Asp	Aspartic acid
ATP	Adenosine triphosphate
BCA	Bicinchoninic acid
bp	Base pairs
BRCA	BRCA DNA repair associated
BSA	Bovine serum albumin
Ca ²⁺	Calcium
CAF	Cancer-associated fibroblast
cAMP	Cyclic adenosine monophosphate
CD	Cluster of differentiation
<i>CDKN2A</i>	Cyclin Dependent Kinase Inhibitor 2A
cDNA	Complementary DNA
CDS	Full coding sequence
CFMP	Core Facility for Mass-spectrometry & Proteomics
CIP	Calf alkaline phosphatase
cm	Centimeter
CO ₂	Carbon dioxide
Codon.	Codon-optimized
con.	Control
CRC	Colorectal cancer
DC-TIC	Delayed contributing tumour initiating cell
DKFZ	German Cancer Research Center
DMSO	Dimethylsulfoxide
DNA	Deoxyribonucleic acid
dNTP	Deoxynucleotide phosphate
Dox	Doxycycline
ECL	Enhanced chemiluminescence
EDTA	Ethylenediaminetetraacetic acid
EGF	Epidermal growth factor
EGFR	Epidermal growth factor receptor
Endo.	Endogenously expressed
EpCAM	Epithelial cell adhesion molecule
ERK1/2	Extracellular signal-regulated kinase 1/2
EV	KRAS wildtype
FACS	Fluorescence-activated cell sorting
FASTA	Fast-All
FBS	Fetal Bovine Serum
FCS	Forward scatter

FG	Hydroxystilbamidine (Fluoro-Gold)
FGF	Fibroblast growth factors
FITC	Fluorescein isothiocyanate
g	Gram
G protein	Guanine nucleotide-binding protein
GBA protein	Guanine nucleotide-binding protein subunit alpha - binding and activating motif-containing protein
GDP	Guanosine diphosphate
GEF	Guanine nucleotide exchange factor
GEM	Gel beads in emulsion
GIV	Guanine nucleotide-binding protein subunit alpha-interacting vesicle-associated protein
GNA15	Guanine nucleotide-binding protein subunit alpha 15
GNAI1	Guanine nucleotide-binding protein subunit alpha I1
GNB1	Guanine nucleotide-binding protein subunit beta 1
GNB2	Guanine nucleotide-binding protein subunit beta 2
GNG12	Guanine nucleotide-binding protein subunit gamma 12
GNG5	Guanine nucleotide-binding protein subunit gamma 5
GPCRs	Guanine nucleotide-binding protein-coupled receptors
GPRs	Guanine nucleotide-binding protein regulators
Grb2	Growth factor receptor bound protein
GRKs	Guanine nucleotide-binding protein-receptor kinases
GTP	Guanosine triphosphate
G α	Guanine nucleotide-binding protein subunit alpha
G β 1	Guanine nucleotide-binding protein subunit beta 1
G γ	Guanine nucleotide-binding protein subunit gamma
H	Height
HEK Cell	Human embryonic kidney cell
HF	Hank's Balanced Salt Solution with 2% FBS
HIV	Human immunodeficiency viruses
IC ₅₀	Half maximal inhibitory concentration
IgG	Immunoglobulin G
IMDM	Iscove's Modified Dulbecco's Medium
IP	Immunoprecipitation
IS	Integration site
JAK/STAT	Janus tyrosine kinase/signal transducers and activators of transcription
K ⁺	Potassium
kb	Kilobases
KCTD5	Potassium channel tetramerization domain containing 5
KD	Knockdown
kDa	Kilodalton
<i>KRAS</i> (gene)	Kirsten rat sarcoma viral oncogene homolog
KRAS (in sample name)	KRAS mutated
LAM-PCR	Linear amplification-mediated polymerase chain reaction
LB	Luria-Bertani
LFQ	Label-free quantification
LGR5	Leucine-rich repeat-containing G protein-coupled receptor 5

LPA	Lysophosphatidic acid
LT-TIC	Long-term TIC
LV	Lentiviral vector
M	Molar
MAPK	Mitogen-activated protein kinase
mg	Milligram
min	Minute (s)
miRNA	MicroRNA
ml	Milliliter
mM	Millimolar
MOI	Multiplicity of infection
mRNA	Messenger RNA
mTOR	Mechanistic target of rapamycin kinase
Mut.	Mutation
NF- κ B	Nuclear factor 'kappa-light-chain-enhancer' of activated B-cells
nM	Nanomolar
NRG1	Neuregulin 1
NSG	NOD.Cg-Prkdc ^{scid} Il2rg ^{tm1Wjl} /SzJ
OE	Overexpression
P70 S6 Kinase	Ribosomal protein S6 kinase beta-1
PAGE	Polyacrylamide gel electrophoresis
PanIN	Pancreatic intraepithelial neoplasia
PARs	Protease-activated receptors
PBS	Phosphate Buffered Saline
PBST	Phosphate-Buffered Saline with Tween 20
PC	Patient-derived pancreatic cancer cultures
PCR	Polymerase chain reaction
PDACs	Pancreatic ductal adenocarcinomas
PDCL	Phosducin-like protein
PDPK1/PDK1	3-phosphoinositide-dependent protein kinase-1
PEI	Polyethylenimine
PH	Pleckstrin homology domain
PI	Propidium iodide
PI3K	Phosphatidylinositol 3-kinase
PIK3CA	Phosphatidylinositol-4,5-bisphosphate 3-kinase catalytic subunit alpha
PIP2	Phosphatidylinositol (4,5)-bisphosphate
PKA	Protein kinase A
PKA	protein kinase A
PKC	Protein kinase C
PLC β	Phospholipase C β
PP2A	Serine/threonine-protein phosphatase 2A
PTEN	Phosphatase and tensin homolog
qRT-PCR	Semi-quantitative reverse transcriptase PCR
R1-R5	Replicates 1-5
RGS protein	Regulators of G protein signalling protein
RNA	Ribonucleic acid
rpm	Rounds per minute

SA	Splice acceptor
Scr.	Scramble
sc-RNA-Seq	Single-cell RNA Sequencing
SD	Splice donor
SD (in statistic)	Standard deviation
SDS	Sodium dodecyl sulfate
Ser	Serine
SGK1	Serum/glucocorticoid regulated kinase 1
Shc	SHC adaptor protein
shRNA	Short hairpin TNA
SLC	Solute carrier family
SLC35F5	Solute Carrier Family 35 Member F5
SMAD4	SMAD family member 4
SOS2	Ras/Rho guanine nucleotide exchange factor 2 Also known: Son of sevenless Homolog 2
SSC	Side scatter
STAR	Spliced transcripts alignment to a reference
TBE	Tris-Borat-EDTA
TBST	Tris-Buffered Saline with Tween 20
TGF- β	Transforming growth factor- β
TIC	Tumour initiating cell
TP53	Tumour Protein p53
TR	Truncated
Trp	Tryptophan
TSC2	TSC complex subunit 2
t-SNE	t-Distributed Stochastic Neighbor Embedding
T-TAC	Transient amplifying cell
Tyr	Tyrosine
U	Unit
UDP	Uridine 5'-diphosphate
UDP-GlcNAc	UDP-N-acetylgluc osamine
UMI	Unique molecular identifiers
V	Volt
WNT	Wingless and INT-1
WT	Wildtype
Xyl	Xylose
YM155	Sepantronium bromide
μ g	Microgram
μ l	Microliter
μ m	Micrometer
μ M	Micromolar

1 Introduction

1.1 Pancreatic cancer

1.1.1 The human pancreas

The human pancreas is a glandular organ, with a weight of approximately 100 g and an average length of 14-20 cm (Franjic 2019). It locates in the upper left abdomen behind the stomach, surrounded by the liver, spleen, and small intestine. The pancreas can be divided into head, neck, body, and tail (Franjic 2019; Longnecker 2021). The main function of the pancreas is the regulation of energy consumption and metabolism by secreting different enzymes and hormones (Zhou and Melton 2018). 95% of the pancreas consists of exocrine tissue (Zhou and Melton 2018). The exocrine part of the pancreas is mainly formed by acinar and ductal cells, which produce and secrete digestion enzymes (Zhou and Melton 2018). These enzymes are exported together with bile into the intestine to digest fatty acids, proteins, and carbohydrates together with small intestinal fluids to transform them into the molecules that can be absorbed by the human body. The remaining 5% of the pancreas mass consists of the endocrine islets (Zhou and Melton 2018). Five major types of endocrine cells that secrete hormones have been described, α -cell: glucagon; β -cell: insulin; δ -cell: somatostatin; ϵ -cell: ghrelin and PP cell: pancreatic polypeptide (Zhou and Melton 2018). Among these hormones, insulin and glucagon are directly released into the blood and essential to regulate the blood glucose level (Zhou and Melton 2018).

1.1.2 Epidemiology of pancreatic cancer

Pancreatic cancer is a highly malignant tumour disease and ranks as the 7th highest mortality cancer entity in the world (McGuigan et al. 2018). In US Cancer Facts & Figures, 2020, the estimated number of newly diagnosed pancreatic cancer cases in 2020 is 57,600 (both gender, Female: 27,200, Male: 30,400) and the pancreatic cancer related death cases are predicted as 47,050 (both gender, Female: 22,410, Male: 24,600) in 2020 (American Cancer Society 2020a).

The common cancer risk factors are separated into two groups: modifiable and non-modifiable factors. Modifiable risk factors include lifestyle associated behaviors like smoking, alcohol consumption, obesity, and occupational exposures (Rawla et al. 2019). Non-modifiable risk factors include gender, age, ethnicity, diabetes mellitus, family history, genetic factors, and infection (Rawla et al. 2019). Moreover, among them, the modifiable risk factor tobacco smoking and the non-modifiable factor family history are reported as the most significant pancreatic cancer risk factors (Vincent et al. 2011). The risk of pancreatic cancer development for smokers is two times higher compared to non-smokers. A study showed that 20% of pancreatic cancers are caused by or related to smoking (Blackford et al. 2009; Rawla et al. 2019). 10% of pancreatic cancers are found to have a genetic origin, and evaluation of the family history revealed an increase of individual's risk by the discovery of first-degree relatives with pancreatic cancer (Hruban et al. 2010; Kamisawa et al. 2016; Klein et al. 2004). However, not only inherited genetic factors can be considered as the main cause, shared environmental exposure, similar lifestyle, or the combination of different risk factors might lead to this finding (Klein et al. 2004). Several germline mutated genes have been identified to be related to inherited pancreatic cancer. As an example, in 5-17% of families with familial pancreatic cancer germline *BRCA2* deoxyribonucleic acid (DNA) repair associated (*BRCA2*) gene mutations have been identified (Couch et al. 2007; Hahn et al. 2003; Murphy et al. 2002; Rawla et al. 2019).

1.1.3 Development of pancreatic cancer

Pancreatic cancer evolves through pancreatic intraepithelial neoplasias (PanINs), intraductal papillary mucinous neoplasms and mucinous cystic neoplasms (Vincent et al. 2011). Pancreatic ductal adenocarcinomas (PDACs) develop from the exocrine pancreas and represent the most common type of pancreatic cancer (Zhou and Melton 2018). The most prevalent genetic alterations in pancreatic cancer are mutations in the kirsten rat sarcoma viral oncogene homolog (*KRAS*) proto-oncogene which can be found in more than 90% of all patients (Buscail et al. 2020). This mutation happens in the early stage of PanIN-1, and with tumour progression, inactivation of tumour-suppressors like Cyclin Dependent Kinase Inhibitor 2A (*CDKN2A*), Tumour Protein p53 (*TP53*), SMAD family member 4 (*SMAD4*) and *BRCA2* also take place (Vincent et al. 2011).

KRAS is a small GTPase protein serving as a simple binary molecular on-off switch in signalling pathways. *KRAS* is predominantly bound to guanosine diphosphate (GDP) at the inactive status, and *KRAS* is activated when guanosine triphosphate (GTP) is exchanged to GDP (Waters and Der 2018). Two studies showed that *KRAS* G12D alone could induce ductal lesions and resulted in PanIN (Aguirre et al. 2003; Hingorani et al. 2003). The initiation role of oncogenic mutated *KRAS* in PDAC was further supported by studies utilizing genetically engineered mouse models (Gopinathan et al. 2015; Lee et al. 2016). *KRAS* is mutated in over 90% of all PDAC patients (van Geel et al. 2020). The mutation is commonly found at codon 12 (exon 2) with a frequency between 70-95% of G12V, G12D, G12R and G12A as the four subtypes, and other less frequent mutations have been reported at codon 11, codon 13, codon 61 and codon 146 (Buscail et al. 2020). *KRAS* proteins engage with various downstream effectors, but signal mainly through three major pathways namely mitogen-activated protein kinase (MAPK) signalling pathway, phosphatidylinositol 3-kinase (PI3K) -3-phosphoinositide-dependent protein kinase-1 (PDPK1/PDK1) - Protein kinase B (Akt), and the Ral guanine nucleotide exchange factor pathway (Collisson et al. 2012; Eser et al. 2013; Eser et al. 2014; Feldmann et al. 2010; Lim et al. 2005). The activation of these three pathways mainly controls cell survival, differentiation, proliferation and metabolism (Mendoza et al. 2011). *CDKN2A* is a tumour suppressor gene and regulates cell cycle progression (Cicenas et al. 2017). *CDKN2A* inactivation can be detected in early PanIN stage, but *TP53* and *SMAD4* mutations are commonly detected in the advanced stage of PanIN (Vincent et al. 2011). *TP53* mutation is one of the most common genetic lesions in cancer, at the frequency of 20%-76%, and a study showed that a PDAC pro-metastasis phenotype requires mutant *TP53* (Cicenas et al. 2017; Weissmueller et al. 2014). Tumour suppressor *SMAD4* is normally inactivated in PDACs, and mutated *SMAD4* has been associated with transforming growth factor- β (TGF- β) induced tumour proliferation and migration in advanced PDAC (Bardeesy et al. 2006). These genetic alterations can lead to deregulated signaling pathways which contribute to the transformation of normal pancreatic cells to tumor lesions.

Another layer of controlling signalling pathway can be achieved by micro ribonucleic acids (miRNAs). Dysregulation of miRNAs was demonstrated by multiple studies to be related to tumour progression in different types of human cancer (Macha et al. 2014; Rawat et al. 2019). Numerous studies identified multiple dysregulated miRNAs that target genes involved in activated signalling pathways which influenced PDAC progression (Yonemori et al. 2017). Yonemori et al. found 36 upregulated and 22 downregulated miRNAs in at least three studies. Within the identified downregulated miRNAs, miR-217, miR-141, miR-148a, and miR-375 were quite common (Yonemori et al. 2017). miR-217 directly targets *KRAS* messenger RNAs

(mRNAs) and is predicted as a tumour suppressor in PDACs (Zhao et al. 2010). Phosphatase and tensin homolog (PTEN), one of the critical regulators of the PI3K-Akt signalling pathway, which involves cell proliferation and apoptosis, is targeted by miR-21 (Meng et al. 2007). A clinical study showed that with high miR-21 expression in primary tumours, PDAC was more aggressive and gemcitabine resistant (Giovannetti et al. 2010). The Janus tyrosine kinase/signal transducers and activators of transcription (JAK/STAT), Wingless and INT-1 (WNT)/ β -catenin, TGF- β signalling pathways and cell cycle, apoptosis could also be influenced by these dysregulated miRNAs (Yonemori et al. 2017), thereby providing an additional layer of gene regulation on the post-transcriptional level.

The interaction between tumour cells with the tumour microenvironment formed by non-malignant immune cells, stromal cells, endothelial cells, and blood vessels contribute to PDAC tumour progression (Balkwill et al. 2012; Ligorio et al. 2019). As the critical component in the tumour microenvironment, cancer-associated fibroblasts (CAFs) show multiple functions in promoting growth, suppressing the immune system, or remodelling the extracellular matrix (Liu et al. 2019; Sahai et al. 2020). A recent study analyzed 195 PDAC tumours by using single-cell technologies (Ligorio et al. 2019). This study showed that stromal cells in the microenvironment could shape the intra-tumoral architecture of human PDAC by altering inherent patterns of tumour glands (Ligorio et al. 2019). PDAC has been described to have low immunogenicity and to provide an immunosuppressive microenvironment which leads to rapid tumour progression, and till now, the administration of cancer immunotherapy, which shows promising responses in many cancer types, has quite limited effects on PDAC patients (Karamitopoulou 2019; Murakami et al. 2019). In a recent study, whole transcriptome data from 24 pancreatic cancers which determined the sequence of 23,219 transcripts revealed that an average of 63 genetic alterations in pancreatic cancers define a core set of 12 core signalling pathways (Jones et al. 2008). Three distinct tumour subtypes, classical, quasi-mesenchymal and exocrine-like identified in resected PDACs (Collisson et al. 2011). Moreover, Moffitt et al. identified two 'basal-like' tumour-specific subtypes which led to a worse outcome and further defined 'normal' and 'activated' stromal subtypes by accessing a collection of PDAC gene expression microarray data (Moffitt et al. 2015). 456 PDACs were analyzed by integrated genomic analysis and 32 recurrently mutated genes were identified being involved in ten pathways (Bailey et al. 2016). Four subtypes namely, squamous, pancreatic progenitor, immunogenic, and aberrantly differentiated endocrine exocrine were further classified by the expression analysis (Bailey et al. 2016). These findings may further refine the distinct subtypes of PDAC and may help to improve personalized treatments of PDAC patients.

1.2 Treatment of pancreatic cancer

The treatment options for pancreatic cancer are yet a challenge for both patients and doctors. The high mortality rate of pancreatic cancer patients and the low 5-year survival rate are partly due to the difficulties of early detection. Up to now, the most effective treatment is surgery. However, surgery is not suitable for all patients, and surgery alone is not sufficient for more than 90% of patients due to the high relapse rate and early metastasis (Kleeff et al. 2016). Therefore, adjuvant treatment is commonly used in combination with surgery. Besides surgery, other treatment options are assessed, including chemotherapy, radiation therapy, immunotherapy, or targeted therapy.

Chemotherapy is a drug treatment which can be given before surgery to shrink the tumour size and after surgery to eradicate remaining cancer cells or to target micro-metastasis, which cannot

be removed by the primary operations, thereby preventing relapse. However, the outcome of chemotherapy treatment of pancreatic cancer patients is very disappointing. Although a lot of agents and different combination regimens were tested in clinical trials, the 5-year relative overall survival rate for localized PDAC is only 39% and 3% for patients with distant metastatic tumours (American Cancer Society 2020b). With increasing in-depth molecular studies of PDAC, revolutionizing targeted therapies directly focusing on specific genes, proteins or microenvironment to block cancer growth, progression, and metastasis evolved (Lee et al. 2018). However, most of the tested agents failed to improve the mean of patients' survival time (Neoptolemos et al. 2018).

The failure of targeted therapies might be explained by the existence of the high amount of tumour stroma, hypoxia, and the mediation of high molecular heterogeneity in PDACs (Barati Bagherabad et al. 2019; Neoptolemos et al. 2018). To further develop more reliable and effective therapeutic agents, a better understanding of PDACs, including alterations of signalling pathways, intra- and inter-tumoural heterogeneity, and the PDAC microenvironment are required. On the one hand, over 90% of PDACs harbour activating mutations in KRAS genes (Kent 2018). The downstream effectors of oncogenic KRAS are commonly selected as specific targets in PDAC targeted therapy. Mueller et al. well demonstrated that the aggressive phenotypes of PDAC are positively related to the dosage gain of oncogenic KRAS (Kent 2018; Mueller et al. 2018). On the other hand, one study showed KRAS wild-type PDAC may harbour targetable oncogenic fusions, and in this study, they reported that neuregulin 1 (NRG1) fusion might be a novel therapeutic target (Heining et al. 2018).

1.3 Tumour initiating cells in cancer

Normal adult stem cells are tissue-specific cells which have self-renewal ability and capability to differentiate into all cell types (Tan et al. 2006). In most tissues, the self-renewal ability of adult stem cells maintains long-term tissue regeneration (O'Brien et al. 2011). Some progenitor cells also have self-renewal ability, but this ability is only short-term compared to the long-term self-renewal of stem cells (O'Brien et al. 2011).

Recent data supports the existence of a small subpopulation of tumour cells, called tumour initiating cells (TICs) which share many characteristics with normal adult stem cells existing in several types of cancer, for example, human breast cancer, brain tumours, colon cancer, liver cancer and pancreatic cancer (Al-Hajj et al. 2003; Li et al. 2007; O'Brien et al. 2007; Singh et al. 2004; Yang et al. 2008). TICs are responsible for tumour initiation, progression, maintenance, and metastasis (Hermann et al. 2007; O'Flaherty et al. 2012; Rahman et al. 2011). Furthermore, TICs are involved in drug resistance and relapse of cancer which can affect tumour therapy (Vinogradov and Wei 2012).

In adult tissues, normal stem cells can be identified by cell surface markers. With the marker-enrichment and lineage-tracing strategies, a heterogeneous cell population could be found containing a mixture of stem cells and mature progenitors (Tang 2012). In many human tumours, cell surface markers have been used to enrich for a population of cells with TIC activity. Interestingly, TICs are both phenotypically and functionally heterogeneous in some types of tumours (Tang 2012). Phenotypically diverse TICs were observed in human breast cancer as well as in glioma (Bradshaw et al. 2016; Tang 2012). Li et al. found that cluster of differentiation 44 (CD44), CD24 and epithelial cell adhesion molecule (EpCAM) expressing tumour cells are highly tumorigenic and possess self-renewal ability in human pancreatic

cancers (Li et al. 2007). Hermann et al. showed that cells expressing CD133⁺ had enhanced proliferative capacity in both pancreatic cancer primary tumours and cell lines (Hermann et al. 2007). However, recent evidence from gastrointestinal patient-derived cultures shows that also the cell populations negative for CD133 and CD44 can form tumours with similar frequency upon xenotransplantation in immune-deficient mice, suggesting that the tumour-forming capacity is not linked to the expression of these cell surface markers (Ball et al. 2017).

1.4 Functional heterogeneity in human pancreatic cancer

In 2011, a previous study from Prof. Dr. med. Hanno Glimm's lab (ref: Dieter et al. 2011), self-renewing long-term TIC (LT-TIC) were identified which maintained tumour formation, and were composed of delayed contributing TICs (DC-TICs) and transient amplifying cells (T-TACs) in human colon cancer by using genetic clonal marking in serial xenografts (Dieter et al. 2011; Kreso et al. 2013). LT-TICs are characterized by a high self-renewal activity in vivo, compared to T-TACs with minimal self-renewal ability and this study suggested that LT-TICs might be a potential therapeutic target for colon cancer (Dieter et al. 2011).

The same strategy was used in PDAC to investigate whether a similar clonal organization could be identified that drove PDAC tumour growth in serial xenotransplantation (Ball et al. 2017). In this study, the PDAC cell model is derived from primary PDAC patient tumours. Three diverse PDAC cultures were transduced with lentiviral vectors to achieve molecular marking, and these cells were serially transplanted into NOD.Cg-Prkdc^{scid}Il2rg^{tm1Wjl}/SzJ (NSG) mice (Ball et al. 2017). Highly sensitive linear amplification-mediated polymerase chain reaction (LAM-PCR) was used to identify the unique fusion sequence of the vector and host genomic DNA at the integration site (IS) which is inherited by all daughter cells and serves as a unique clonal marker (Ball et al. 2017). The finding of this study shows a distinct set of clones which contribute to tumour formation in each generation. These individual clones can hardly be detected in other xenograft generations (Ball et al. 2017). These results demonstrated that unlike the classical model of a rather fixed TIC compartment like in colorectal cancer (CRC), pancreatic cancer progression is driven by a succession of transient active TIC clones (Ball et al. 2017) (Figure 1).

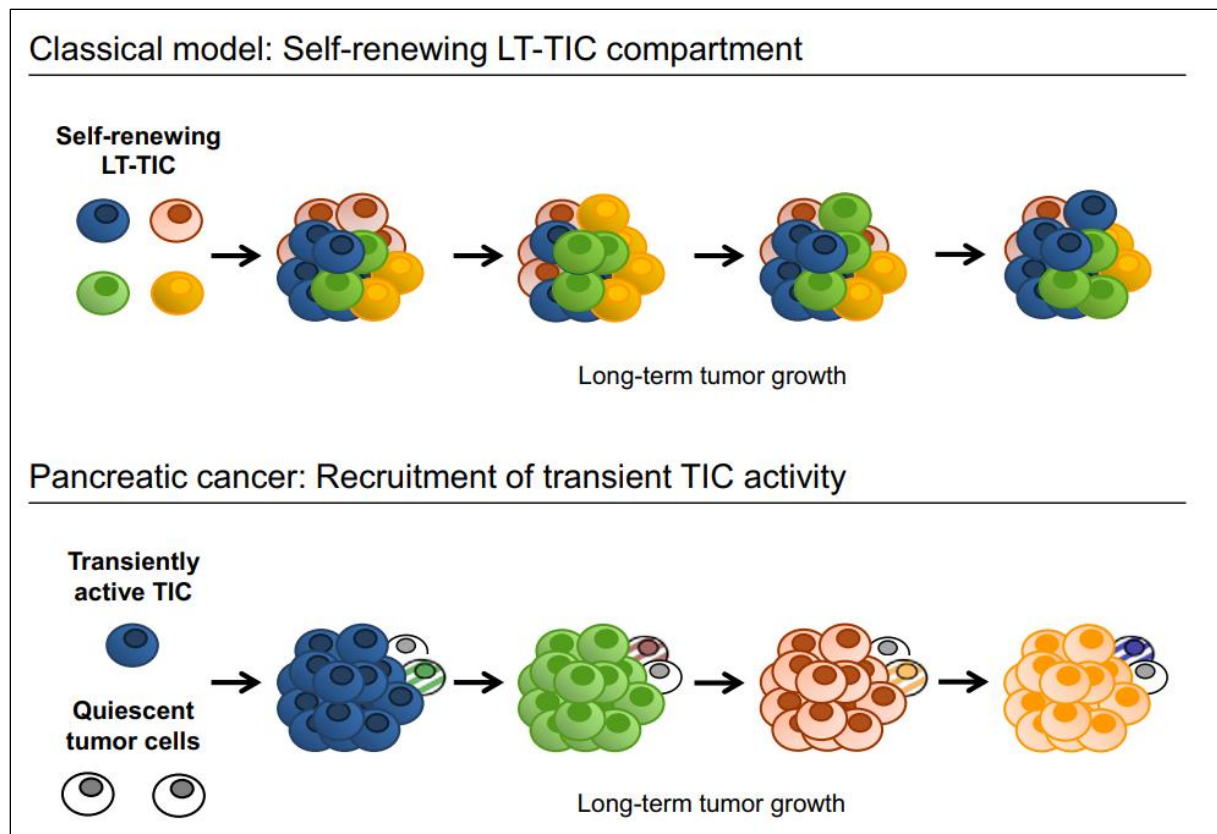


Figure 1: Illustration of two clonal TIC dynamic models (Ball et al. 2017).

The upper panel depicts represents the self-renewing long-term tumour initiating cell (LT-TIC) in long-term tumour growth. The lower panel represents the recruitment of transient active TICs in pancreatic cancer. In PDACs, LT-TICs are not identified. In each serial generation, one set of TICs contribute to tumour formation, and in the next generation a new set of TICs are recruited and form the tumour. The overlap of activated TICs is hardly detected in different generations. (Ball et al. 2017) LT: long-term; TIC: tumour initiating cell.

1.4.1 Identification of potential TIC activators

To further investigate how transient TIC activity is regulated in PDAC progression, an overexpression screen was performed in Prof. Dr. med. Hanno Glimm's lab to identify potential TIC activators (Gao 2017). Therefore, semi-adherent PDAC cultures derived from patient tumours were transduced with a lentiviral trapping vector. The enhancer-promoter region of this vector contains a strong splice donor (SD) and a weak splice acceptor (SA) to achieve insertional mutagenesis (Montini et al. 2009; Ranzani et al. 2013). The trapping vector enables the trans-splicing from the SD to the SA of nearby exons of the host genome leading to overexpression of the genes located downstream of integration sites. Transduced PDAC patient-derived cultures) were serially transplanted into NOD.Cg-Prkdc^{scid}Il2rg^{tm1Wjl}/SzJ (NSG) mice and the unique fusion of vector and host DNA sequences was utilized to trace the fate and the dynamics of clones in each xenograft by high throughput insertion site analysis. In this system, the integration sites of trapping vectors were used as inherited markers for clonal dynamics. Genes overexpressed by trapping vectors insertions constantly induced TIC activation. These genes were identified by genome-wide high throughput sequencing. Within this study, guanine nucleotide-binding protein (G protein) subunit beta 1 (*GNB1*), Ras/Rho guanine nucleotide exchange factor 2 (also known as son of sevenless homolog 2, *SOS2*) and solute carrier family 35 member F5 (*SLC35F5*) were identified as potential TIC activators (Gao 2017, pg. 60-64). In line with this, initial technical validation experiments of the trapping vector

screens showed that GNB1 knockdown (KD) led to a loss of transduced PDAC cells (PDAC cultures, n=2) during serial transplantation into NSG mice and significantly reduced the average tumour size upon GNB1 KD, while GNB1 overexpression cells were found to continuously contribute to tumour formation in all generations (Gao 2017, pg. 60-64). These data showed that the trapping vector screen is suitable to identify potential regulators of TIC activity in human PDAC.

1.4.1.1 G Protein-Coupled Receptor Signalling

G protein-coupled receptors (GPCRs) are the largest family of cell surface receptor proteins and are encoded by over 800 individual genes in humans (Wootten et al. 2018). Ligands, including biogenic amines, amino acids and ions, lipids, peptides and proteins, and others bind to GPCRs and induce the transmembrane signalling exchange (Dorsam and Gutkind 2007). The same underlying architecture, including a seven-transmembrane α -helical region, an extracellular amino-terminal segment and an intracellular carboxy-terminal tail are shared by most of the members of the GPCR family (Tuteja 2009). Three intracellular polypeptide and three extracellular loops connect the seven-transmembrane α -helices, and the extracellular loops of GPCRs can be glycosylated (Tuteja 2009). The intracellular carboxy-terminal tail of GPCRs contains serine (Ser) and tyrosine (Tyr) residues providing the sites for phosphorylation and receptor desensitization which is mediated by G protein-receptor kinases (GRKs) (Komolov and Benovic 2018; Tuteja 2009). GPCR desensitization mediated by GRKs is a well-characterized mechanism (Ribas et al. 2007). Structural studies of GRKs elucidated that GRK2 subfamily members interact with G protein subunits α_q 11 ($G\alpha_q11$) to block its interaction with their downstream effectors (Carman et al. 1999; Salcedo et al. 2006). Moreover, studies showed that the pleckstrin homology domain (PH) on the C-terminal region of GRK2 and GRK3 could interact with phosphatidylinositol (4,5)-biphosphate (PIP₂) and free $G\beta\gamma$ subunits (Homan and Tesmer 2015; Murga et al. 2019; Nogués et al. 2017). GPCR phosphorylation also triggers the binding of arrestin proteins, which blocks the activation of downstream G proteins (Ribas et al. 2007). G proteins are formed by three subunits namely, G protein subunit α ($G\alpha$), G protein subunit β ($G\beta$) and G protein subunit γ ($G\gamma$). $G\alpha\beta\gamma$ subunits are the intracellular components of GPCRs (Hilger et al. 2018). They bind to the cell membrane and interact with the intracellular face of GPCRs (Hilger et al. 2018). Commonly, $G\alpha$ -GDP binds tightly to $G\beta\gamma$ subunits, when ligand-bound GPCRs trigger the release of GDP on $G\alpha$ and lead to the 'GDP to GTP' exchange on $G\alpha$, then $G\alpha$ -GTP disassociates with $G\beta$ (McCudden et al. 2005). Separated $G\alpha$ subunits and $G\beta\gamma$ subunits further bind to downstream effectors to trigger cellular signalling pathway alterations. A variety of downstream effectors are regulated by four subtypes of $G\alpha$ subunits, including $G\alpha_s$, $G\alpha_i$, $G\alpha_q$ and $G\alpha_{12}$ (McCudden et al. 2005). PI3K γ , phospholipase C β (PLC β) and ion channels are found as the downstream effectors of $G\beta\gamma$ subunits (Dorsam and Gutkind 2007). Many cell functions are regulated by GPCRs, for example, cell proliferation, survival, inflammation and angiogenesis (Dorsam and Gutkind 2007). Moreover, the central role of GPCRs in tumour cell-growth, metastasis, and tumour-induced angiogenesis have been revealed (Dorsam and Gutkind 2007). As an example, protease-activated receptors (PARs) belong to the GPCR family, and PAR1 is reported to play a critical role in thrombosis, tumour growth and metastasis in many types of tumours (Arakaki et al. 2018; Boire et al. 2005; Lappano and Maggiolini 2011). GPCRs are the largest class of drug targets (Campbell and Smrcka 2018). Nowadays, inhibitors designed to target G protein subunits have been tested in multiple preclinical studies including cancer, thrombosis, asthma,

melanoma, chronic inflammatory disease, heart failure, and fibrosis (Campbell and Smrcka 2018).

1.4.1.2 G protein subunit beta 1 (GNB1)

GNB1 encodes G protein subunit beta 1 (G β 1), and so far, five human G β s are identified (McCudden et al. 2005). Each G β subunit consists of an α -helix on the N-terminal, and a seven Trp-Asp (tryptophan-aspartic acid) repeat, so called 7-WD repeat, forming a torus-like structure on the C-terminal part (Neer et al. 1994). G γ bind on the α -helix to G β 1 and form heterodimers, whereas G α binds to the C-terminal end of G $\beta\gamma$ subunits (Clapham and Neer 1997).

Free G $\beta\gamma$ subunits have various effectors. In 1987, the first effector of G $\beta\gamma$, G protein-regulated inward rectifier potassium (K⁺) channels (GIRK), was identified by Logothetis et al. (Logothetis et al. 1987; McCudden et al. 2005). In 1996, Luttrell et al. showed that Shc-c-Src complex formation is mediated by G $\beta\gamma$ subunits (Luttrell et al. 1996). The direct interaction between G $\beta\gamma$ and calcium (Ca²⁺) channel was identified, and this interaction is responsible for maintaining a G protein-dependent modulation of Ca²⁺ channel activity (Waard et al. 1997). The extracellular signal-regulated kinase 1/2 (ERK1/2) activation can be mediated by G $\beta\gamma$ through the PI3K canonical pathway, exchange protein directly activated by cyclic adenosine monophosphate (cAMP), protein kinase A (PKA) and protein kinase C (PKC), or through noncanonical pathways via β -arrestins (Crespo et al. 1994; Koch et al. 1994; Kolch et al. 1993; Lev et al. 1995; Lopez-Illasaca et al. 1997; Paradis et al. 2015). A GNB1 and G protein subunit beta 2 (GNB2) mutation study indicated that oncogenic alterations in G β subunits might be responsible for transformed and resistance phenotypes of multi-types of human cancer which further suggests that G β subunits may be a potential therapeutic target (Yoda et al. 2015).

1.4.1.3 Solute carrier family 35

Solute carrier family (SLC) is one of the superfamilies of transporters, and more than three hundred transporters have been identified. These transporters are organized into 52 families (Lin et al. 2015; Liu 2019). SLC transporters are widely expressed in the epithelia of major organs and involved in the uptake of small molecules (Lin et al. 2015). It has been demonstrated that alanine cross-talk between pancreatic stellate cells and PDACs rely on specific transporters (Parker et al. 2020). Alanine concentrations are exchanged by SLC1A4 and other transporters, and to fulfil the supplement of alanine demand, SLC38A2 is found to be upregulated in PDAC cells (Parker et al. 2020). SLC35 is described as a nucleoside-sugar transporter family which transports nucleotide sugars into the Golgi apparatus or endoplasmic reticulum and can be further divided into six subfamilies (from SLC35 A to SLC35 F) with 23 members in total (Hadley et al. 2019; He et al. 2009). In the SLC35 family, SLC35A1 is reported as the CMP-sialic acid transporter; SLC35A2 and SLC35A3 are identified as the uridine 5'-diphosphate (UDP)-galactose transporter and acetylglucosamine transporter; SLC35A4 and SLC35A5 are described as the probable UDP-sugar transporter; SLC35B1 is the adenosine diphosphate (ADP)/adenosine triphosphate (ATP) exchanger; SLC35B4 is revealed as the UDP-xylose (Xyl)/UDP-N-acetylglucosamine (UDP-GlcNAc) transporter (Hadley et al. 2019). One study suggested that SLC35D3, another member of SLC35, regulate platelet-dense granules (Chintala et al. 2007). SLC35F2 was reported to enable YM155 (sepantronium bromide)-mediated DNA damage toxicity in leukaemia (Winter et al. 2014). In 2017, SLC35F2 was further reported to play a key role in papillary thyroid carcinoma progression (He et al. 2018). SLC35F5 mRNAs are found to be higher expressed in 5-fluorouracil (5-FU) responding tumours compared to non-responders in colorectal cancers (Matsuyama et al. 2006).

1.5 Aims of the study

PDAC is a highly malignant type of cancer with poor overall survival. Targeted therapies on PDACs as a single treatment or assisting conventional surgical treatment have not efficiently prevented tumour relapse and metastasis formation so far. Therefore, it is urgently required to study the mechanisms of PDAC progression. Previous results have shown that PDAC tumour progression is driven by a succession of transiently activated TIC clones in serial transplantation. Recent data suggest that these TIC clones are not a fixed cell population but represent a functional state. It is pivotal to understand the mechanism of how this transient TIC activation is regulated to further develop targeted treatment strategies against this functional population. To gain more insights of the mechanisms regulating this functional state, a lentiviral vector-based insertional mutagenesis (trapping vector) *in vivo* screening was performed which identified GNB1 and SLC35F5 as potential regulators of PDAC TIC activity.

To validate the identified potential target genes and to further investigate the mechanism of TIC activation, this project aimed:

1. To evaluate and validate GNB1 and SLC35F5 as regulators of TIC activity.
 - a) Here, the experimental portfolio of preliminary experiments will be expanded to address proliferation, cell cycle analysis, apoptosis to study molecular processes potentially involved in GNB1-mediated TIC activation.
 - b) For SLC35F5, colony formation and an *in vivo* tumour formation assay will be performed to validate this target as TIC activation regulator.
2. To further strengthen the hypothesis, single-cell RNA sequencing of primary PDAC cultures will be performed to assess the expression of the identified TIC regulator candidates of Aim 1.
3. To further characterize the pathway alterations induced by GNB1 regulating clonal TIC activity in PDAC. A cell model system will be generated and utilized which allows to access the impact of GNB1 expression in KRAS mutated and wild type background. Pathway alterations will be revealed in the same genetic background by using a systematically antibody-based screening.
4. To identify the specific $G\alpha$, $G\gamma$ subunits and the regulators which bind to $G\beta 1$ in the established patient-derived PDAC cultures. Therefore, co-immunoprecipitation and mass-spectrometry protein analysis will be performed to identify the binding partners of $G\beta 1$.

This study will help to gain a better understanding of the underlying mechanisms of $G\beta 1$ in regulating the clonal TIC activity in PDACs. The identification of GNB1 as PDAC TIC regulator may help to develop novel therapeutic strategies to efficiently target pancreatic cancer.

2 Material and Methods

2.1 Materials

2.1.1 Equipment

Equipment	Producer
Agarose gel documentation	NIPPON Genetics, Dueren, Germany
Agarose gel electrophoresis system (Chamber and power supply)	Biometra, Dublin, Ireland
Analytical balance TE124S	Sartorius, Goettingen, Germany
Avanti J-30I ultracentrifuge	Beckman Coulter, Krefeld, Germany
Beckman L8-70M Ultracentrifuge	Beckman Coulter, Krefeld, Germany
Cell counting chamber	Immune Systems, Paignton, UK
Centrifuge 5430/5424	Eppendorf, Hamburg, Germany
Centrifuge Fresco1	ThermoFisher Scientific, Waltham, Massachusetts, USA
Centrifuge Multifuge® 3SR	Heraeus, Hanau, Germany
CFX96™ Real-Time System	Bio-rad, Hercules, California, USA
ChemiDoc™ MP Imaging System	Bio-rad, Hercules, California, USA
Cryo-freezing container (Nalgene®)	ThermoFisher Scientific, Waltham, Massachusetts, USA
Dynabeads™ MPC™ -S (Magnetic Particle Concentrator)	ThermoFisher Scientific, Waltham, Massachusetts, USA
Flow Cytometer BD™ FACS Aria™ cell sorter	BD Biosciences, San Jose, California, USA
Flow Cytometer BD™ LSRII	BD Biosciences, San Jose, California, USA
Fluorescence microscope AxioCAM MRC/&MRm	Zeiss, Jena, Germany
Fluorescence microscope Axiovert 200	Zeiss, Jena, Germany
Freezer (-20°C)	Liebherr, Bulle, Switzerland
Freezer (-80°C)	Sanyo, Osaka, Japan
HERAEUS FRESCO 17 Centrifuge	ThermoFisher Scientific, Waltham, Massachusetts, USA
Incubator HeraCell 150i	ThermoFisher Scientific, Waltham, Massachusetts, USA
Leica TCS SP5 II (Confocal Microscope)	Leica, Wetzlar, Germany
Light microscope (cell culture application)	Zeiss, Jena, Germany

Microplate Reader Infinite M200	Tecan, Maennedorf, Switzerland
Microwave oven	Bartscher, Salzkotten, Germany
Mini-centrifuge Galaxy mini	VWR, Radnor, Pennsylvania, USA
Mini-plate SpinnerSpinner	Labnet, Edison, New Jersey, USA
NanoDrop® Spectrophotometer ND-1000	ThermoFisher Scientific, Waltham, Massachusetts, USA
PCR-Thermocycler	Biometra, Goettingen, Germany
Pipetboy	INTEGRA, Zizers, Switzerland
Pipette	Eppendorf, Hamburg, Germany
PowerPac™ HC Power Supply	Bio-rad, Hercules, California, USA
Refrigerator (4°C)	Liebherr, Bulle, Switzerland
Rotating Incubator	Heidolph, Schwabach, Germany
Safety cabinet Herasafe® KS	ThermoFisher Scientific, Waltham, Massachusetts, USA
Thermomixer comfort	Eppendorf, Hamburg, Germany
VIAFLO multichannel pipette	INTEGRA, Zizers, Switzerland
Western blot Mini-PROTEAN® Tetra Cell Systems	Bio-rad, Hercules, California, USA
Western blot Trans-Blot® Turbo™	Bio-rad, Hercules, California, USA

2.1.2 Plastic and Disposables

Disposable Materials	Producer
4-15% Mini-PROTEAN® TGX Stain-Free™ Precast Gels (10 wells, 30 µl, 50 µl)	Bio-rad, Hercules, California, USA
Absorbable Thread PGA Resorba 4-0	Resorba, Nuernberg, Germany
Adhesive Clear qPCR Seals, Sheets	Biozym Biotech, Wien, Austria
Alcohol Pads	B. Braun, Melsungen, Germany
Baytril® (enrofloxacin)	Bayer, Leverkusen, Germany
BD™ Falcon™ FACS tube	BD Biosciences, San Jose, California, USA
BD™ Falcon™ FACS tube with filtering strainer	BD Biosciences, San Jose, California, USA
BD™ Falcon™ Polypropylene Conical Tube (15 ml, 50 ml)	BD Biosciences, San Jose, California, USA
BlackSeal-96/384 Black, Black Adhesive Bottom Seal for 96-well and 384-well Microplate	PERKInElmer, Waltham, Massachusetts, USA

Cell culture flask (T25; T75; T225)	Nunc (ThermoFisher Scientific), Roskilde, Denmark
Cell culture plate (150 mm x 25 mm)	BD Biosciences, San Jose, California, USA
Cell culture plate (Multi-well plate)	Greiner Bio One, Frickenhausen, Germany
Cell filtering strainer (0,4 – 1 µm pore size)	BD Biosciences, San Jose, California, USA
Cell scraper	BD Biosciences, San Jose, California, USA
Collagenase IV	Invitrogen, Life® Technologies, Carlsbad, California, USA
Cryogenic tubes Nalgene system 100™	Corning, New York, USA
Eppendorf Protein LoBind Tube (1.5 ml)	Eppendorf, Hamburg, Germany
Eppendorf Safe-lock Tubes (1.5 ml, 2 ml)	Eppendorf, Hamburg, Germany
Eye protection lotion	Bayer, Leverkusen, Germany
Hard-Shell PCR Plates 96-well, thin wall	Bio-rad, Hercules, California, USA
Heating Pad	Thermolux, Meix-devant-Virton, Belgium
Injection needle 100 sterican	B. Braun, Melsungen, Germany
Injection needle blunt	B. Braun, Melsungen, Germany
Injection syringe	B. Braun, Melsungen, Germany
Isoflurane	Abbott, Chicago, Illinois, USA
Lab Gloves, MICROFLEX® XCEED® Powder-Free Nitrile Examination Gloves	Ansell, Iselin, New Jersey, USA
PCR reaction strip	Biozym, Hessisch Oldendorf, Germany
PCR reaction tube (200 µl)	Corning, New York, USA
Pipette tips (10 µl, 20 µl, 200 µl, 1 ml)	Greiner Bio One, Frickenhausen, Germany
Pipette tips (125 µl)	INTEGRA, Zizers, Switzerland
Pipettes (2 ml, 5 ml, 10 ml, 25 ml, 50 ml)	Corning, New York, USA
PluriStrainer 20 µm	PluriSelect, Leipzig, Germany
Precision Wipes	Kimberly-Clark Professional™, Milsons Point NSW, Australia
PVDF membrane	Bio-rad, Hercules, California, USA
Reagent Reservoirs	INTEGRA, Zizers, Switzerland
Sterile cell filter (0.22 µm, 0.45 µm pore size)	Merck Millipore, Burlington, Massachusetts, USA
Sterile cotton swab	Paul Böttger, Bodenmais, Germany
Surgical tools	Fine Science Tools, Heidelberg, Germany
TERUMO® SYRINGE (20 cc/ml)	TERUMO, Eschborn, Germany

TERUMO® syringe (5 ml, 20 ml, 50 ml)	TERUMO, Eschborn, Germany
Tissue Culture Treated Plate (384-well, Black/Clear)	BD Biosciences, San Jose, California, USA
Tissue-mincing scalpel	Dr. JUNGHANS Medical GmbH, Bad Lausick, Germany
Ultracentrifuge tube	Beranek Laborgeräte, Weinheim, Germany
Virus production parafilm	Pechiney, Paris, France
Wound Clip kit	Fine Science Tools, Heidelberg, Germany

2.1.3 Cell Culture Related Reagents

Reagents	Company
Advanced DMEM/F12 (1x) Reduced Serum Medium (1:1)	Gibco by Life Technologies, New York, USA
Accutase® solution	Sigma-Aldrich, St. Louis, Missouri, USA
Ampicillin Sodium Salt	Sigma-Aldrich, St. Louis, Missouri, USA
B-27™ Supplement	Gibco by Life Technologies, New York, USA
D-Glucose Dextrose	Gibco by Life Technologies, New York, USA
Dimethylsulfoxide (DMSO)	Sigma-Aldrich, St. Louis, Missouri, USA
Fetal Bovine Serum (FBS)	PAN Biotechnology, Aidenbach, Germany
FGF10	R&D Systems, Minneapolis, Minnesota, USA
FGF2	R&D Systems, Minneapolis, Minnesota, USA
Heparin sodium salt	Sigma-Aldrich, St. Louis, Missouri, USA
HEPES solution	Sigma-Aldrich, St. Louis, Missouri, USA
Iscove's Modified Dulbecco's Medium (IMDM, 1x)	Gibco by Life Technologies, New York, USA
Keratinocyte-SFM (1x)	Gibco by Life Technologies, New York, USA
L-glutamine (200 mM)	Invitrogen, Carlsbad, California, USA
Luria Broth (LB) base	Invitrogen, Carlsbad, California, USA
Medium 199 (1x)	Gibco by Life Technologies, New York, USA
Nodal	R&D Systems, Minneapolis, Minnesota, USA
Phosphate Buffered Saline (PBS)	Gibco by Life Technologies, New York, USA
RPMI Medium 1640 (1x)	Gibco by Life Technologies, New York, USA
SOC-Medium Invitrogen	Invitrogen, Carlsbad, California, USA
Supplements for Keratinocyte-SFM	Gibco by Life Technologies, New York, USA

Trypan Blue Stain (0.4%)	Gibco by Life Technologies, New York, USA
Trypsin-EDTA 0.05%	Invitrogen, Carlsbad, California, USA

2.1.4 Cell Culture Media and Buffers

Medium	Composition
CSCN (Primary PDAC culture)	Advanced DMEM-F12 added with: D-Glucose (0.6%), 6.0 mg Heparin sodium salt, 5 mM HEPES buffer, 2 mM L-glutamine, 10 ml B27-supplement (1x); Cytokines mix: FGF2 10 ng/ μ l, Nodal and FGF10 20 ng/ μ l
293T and HeLa culture media	IMDM added with 10% FBS, 2 mM L-glutamine
H6C7 culture media	Keratinocyte-SFM (1x) added with commercial supplements
LB Medium	25 g LB powder, 1 L H ₂ O, sterile
Cell freezing solution (Primary PDAC cells)	Per sample: 385 μ l RPMI medium (10% FBS), 210 μ l FBS, 105 μ l DMSO
Cell freezing solution (293T/HeLa cells)	Per sample: 385 μ l IMDM medium (10% FBS), 210 μ l FBS, 105 μ l DMSO
Cell freezing solution (H6C7 cells)	Full medium with 10% DMSO
Cell thawing solution	50% Culture medium with 50% FBS

2.1.5 Antibodies

2.1.5.1 Antibodies for Western Blot

Antibody	Concentration	Product Number	Supplier
Akt (pan) (11E7)	1:1000	4685	Cell Signaling Technology, Danvers, Massachusetts, USA
FLAG-Tag	1:1000	NBP1-06712	Novus Biologicals, Littleton, Colorado, USA
G gamma 12	1:1000	ab21791	Abcam, Cambridge, UK
GNAI1	1:1000	12617-1-AP	Proteintech Group, Rosemont, Illinois, USA
GNB1	1:5000	ab137635	Abcam, Cambridge, UK
GNB1	1:1000	SAB2701168	Sigma-Aldrich, St. Louis, Missouri, USA
GNB1	1:1000	PA1-725	Invitrogen, Carlsbad, California, USA
KCTD2/5/17	1:500	15553-1-AP	Proteintech Group, Rosemont, Illinois, USA

mTOR (7C10)	1:1000	2983	Cell Signaling Technology, Danvers, Massachusetts, USA
P44/42 MAP Kinase (L34F12)	1:1000	4696	Cell Signaling Technology, Danvers, Massachusetts, USA
PDK1	1:1000	3062	Cell Signaling Technology, Danvers, Massachusetts, USA
Phospho-Akt (Ser473) (D9E) XP®	1:1000	4060	Cell Signaling Technology, Danvers, Massachusetts, USA
Phospho-mTOR (Ser2448) (D9C2) XP®	1:1000	5536	Cell Signaling Technology, Danvers, Massachusetts, USA
Phospho-p44/42 MAPK (Thr202/Tyr204) (20G11)	1:1000	4376	Cell Signaling Technology, Danvers, Massachusetts, USA
A-Tubulin (DM1A) (HRP Conjugate)	1:1000	12351	Cell Signaling Technology, Danvers, Massachusetts, USA
SLC35F5	1:1000	PA5-42494	Invitrogen, Carlsbad, California, USA

2.1.5.2 Antibodies for Flow Cytometry

Antigen	Clone	Dilution	Isotype	Conjugated	Product Number	Supplier
Ki-67	B56	1:1000	Mouse IgG1, κ	Alexa Fluor® 647	561126	BD Biosciences Pharmingen, San Diego, California, USA
EpCAM	EBA-1	1:20	Mouse IgG1	APC	347200	BD Biosciences Pharmingen, San Diego, California, USA
H2KD	SF1-1.1	1:100	Mouse IgG2a	PE	553566	BD Biosciences Pharmingen, San Diego, California, USA
CD45	-	1:100	Mouse IgG1	PE	555483	BD Biosciences Pharmingen, San Diego, California, USA

2.1.5.3 Antibodies for Immunofluorescence

Antigen	Dilution	Product Number	Supplier
FLAG-Tag	1:100	NBP1-06712	Novus Biologicals, Littleton, Colorado, USA
GFP	1:2000	Ab5450	Abcam, Cambridge, UK

GNB1	1:200	Ab137635	Abcam, Cambridge, UK
GNB1	1:100	SAB2701168	Sigma-Aldrich, St. Louis, Missouri, USA
Goat anti-rabbit Alexa Fluor Plus 488	1:100	A32731	Life technologies, Carlsbad, California, USA
Goat anti-rabbit Alexa Fluor Plus 647	1:100	A32733	Life technologies, Carlsbad, California, USA
Goat anti rat Cy3	1:100	Ab6953-100	Abcam, Cambridge, UK

2.1.6 Commercial Kits

Product Name	Supplier
ATPlite 1step	PERKInElmer, Waltham, Massachusetts, USA
Chromium Single Cell 3' Library & Gel Bead Kit v2, 16 rxns	10x Genomics, Pleasanton, California, USA
Chromium Single Cell A Chip Kit, 16 rxns	10x Genomics, Pleasanton, California, USA
Clarity Max™ Western ECL Substrate	Bio-rad, Hercules, California, USA
FLAG® Immunoprecipitation Kit	Sigma-Aldrich, St. Louis, Missouri, USA
HiSpeed Plasmid Maxi Kit	QIAGEN, Hilden, Germany
Phusion High-Fidelity PCR Kit	New England BioLabs, Frankfurt, Germany
Pierce™ BCA Protein Assay Kit	ThermoFisher Scientific, Waltham, Massachusetts, USA
Plasmid Miniprep	Roboklon, Berlin, Germany
QIAquick Gel Extraction Kit	QIAGEN, Hilden, Germany
RevertAid First Strand cDNA Synthesis Kit	ThermoFisher Scientific, Waltham, Massachusetts, USA
RNeasy® Mini Kit	QIAGEN, Hilden, Germany
TOPO TA Cloning® Kit	Invitrogen, Carlsbad, California, USA
Trans-Blot Turbo RTA Transfer Kit, LF PVDF	Bio-rad, Hercules, California, USA
Western Lightning® Plus-ECL	PERKInElmer, Waltham, Massachusetts, USA

2.1.7 Western Blot Buffers

Buffer	Composition
Running Buffer	1:10 diluted from 10x Tris/Glycine/SDS Buffer (Bio-rad)
Blotting Buffer	Trans-Blot Turbo RTA Transfer Kit
Washing Buffer	1x TBST: 100 mM Tris/HCL, pH 7.5, 1.5 M NaCl, 0.5% Tween 20
Blocking Buffer	5% Slim milk powder dissolved in 1x TBST, 5% BSA powder dissolved in 1x TBST
Antibody Buffer	5% BSA powder dissolved in 1x TBST
Stripping Buffer	Restore™ PLUS Western Blot Stripping Buffer (ThermoFisher)
Sample Buffer	4x Laemmli Sample Buffer (Bio-rad)

2.1.8 Plasmids and Primers

2.1.8.1 Plasmids

Application	Plasmid	Explanation	Supplier
Lentiviral vector packaging system	pMDLg/pRRE	CMV-driven HIV1 gag pol and RRE	Naldini Lab, Milan, Italy
	pRSV-REV	RSV driven HIV1 Rev	Naldini Lab, Milan, Italy
	pMD2.VSV.G	CMV-driven VSV.G	Naldini Lab, Milan, Italy
Genetic labelling and gene of interest overexpression	GFP control	PGK driven lentiviral eGFP expression vector (pCCL pptPGK_IRES_GFP_PRE)	Naldini Lab, Milan, Italy
shRNA mediated knockdown	Lentiviral shRNA vector with GFP as a marker gene	pRSIT17-U6Tet-sh-HTS6-CMV-TetRep-2A-TagGFP2-2A-Puro	Collecta, Mountain View, California, USA
	Lentiviral shRNA vector with RFP as a marker gene	pRSI12-U6-(sh)-UbiC-TagRFP-2A-Puro	Collecta, Mountain View, California, USA

2.1.8.2 Real-time PCR Primers

Primers	Direction	Sequence 5'-3'
GNB1_en_1	F	GGCCACGAGTCTGACATCAA
	R	CATCCACATGCTACTGGCGT

GNB1_en_2	F	CTTGCTGGGTACGACGACTT
	R	TCCACATGCTACTGGCGTTA
GNB1_en_3	F	GCTGGGTACGACGACTTCAA
	R	TCCACATGCTACTGGCGTTAG
GNB1_co_1	F	GGACGACAACCAGATCGTGA
	R	GCTCATCACGTCGCCTGTAT
GNB1_co_2	F	GGACATACAGGCGACGTGAT
	R	GCAGATGATGTTGTCGTGGC
GNB1_co_3	F	ATACAGGCGACGTGATGAGC
	R	GAACAGTCTACAGGTGGCGT
SLC35F5	F	GGGGCTGCTTTCTTACCTCA
	R	CTCTCACACTGTTGCTGTCT
β-Actin	F	CACCATTGGCAATGAGCGGTTC
	R	AGGTCTTTGCGGATGTCCACGT

2.1.8.3 Sequencing Primers

Primers	Sequence 5'-3'
GNB1_1	TACGCTCCTAGCGGCAATTATG
GNB1_2	ACCGGCTCTGATGACGCCAC

2.1.8.4 PCR Primers

Primers	Direction	Sequence 5'-3'
GNB1-FLAG-Tag-N	Forward	GGATCCATGGATTACAAGGATGACGACGATAAGAGTGAGCTTGACCA GCTGAG
	Reverse	GCGATCGCTTAGTTCCAGATCTTGAGGAAG

2.1.9 GNB1 Codon-optimized sequence with flanking restriction enzyme sequences (5' – 3') (Gao 2017, pg. 27-28)

GGATCCATGAGTGAGCTTGACCAGCTGAGACAAGAGGCCGAGCAGCTGAAGAACCAGATCAGAGATGCCAGAAAGGCCTGCGCCGATGCCACACTGAGCCAGATACCAACAACATCGACCCCGTGGGCA GAATCCAGATGCGGACCAGAAGAACAAGACTGAGAGGCCACCTGGCCAAGATCTATGCCATGCACTGG GGCACCGATAGCAGACTGCTGGTGTGAGCCAGCCAGGACGGAAAGCTGATCATCTGGGACAGCTA CACCACCAACAAGGTGCACGCCATTTCCTCTGAGAAGCAGCTGGGTCATGACATGCGCCTACGCTCC TAGCGGCAATTATGTGGCTTGTGGCGGCCTGGACAACATCTGCAGCATCTACAACCTGAAAACCCG CGAGGGCAACGTGCGGGTTTCAAGAGAAGTGGCCGACACACAGGCTACCTGAGCTGCTGTAGAT TCCTGGACGACAACCAGATCGTGACCAGCAGCGGCATACAACATGCGCCCTGTGGGATATCGAG ACAGGCCAGCAGACCACCACCTTTACAGGACATACAGGCCGACGTGATGAGCCTGTCTCTGGCCCT

GATACCAGACTGTTTGTGTCTGGCGCCTGTGATGCCAGCGCCAAGCTTTGGGACGTCCGCGAGGGA
 ATGTGCAGACAGACATTCACAGGCCACGAGAGCGACATCAACGCCATCTGCTTTTTCCCAACGGC
 AATGCCTTTGCCACCGGCTCTGATGACGCCACCTGTAGACTGTTTCGACCTGAGAGCCGACCAAGAG
 CTGATGACCTACAGCCACGACAACATCATCTGCGGCATCACCAGCGTGTCTTCAGCAAGAGTGGT
 AGACTGCTGCTGGCCGGCTACGACGACTTCAACTGTAATGTGTGGGACGCCCTGAAGGCCGATAGA
 GCTGGTGTCTGGCTGGCCACGATAACAGAGTGTCTTGCCTGGGCGTGACCGATGATGGAATGGCC
 GTTGCCACAGGCAGCTGGGATAGCTTCTCAAGATCTGGAACCTAAGCGATCGC

2.1.10 Oligonucleotides for specific gene knockdowns

Knockdown Oligo	Sequence 5' – 3'
GNB1	GCTGAAACCAAGAGCACAATT
SLC35F5 shRNA 1 FW	ACCGGCGCATGTCATATCCTGTGAAAGTTAATATTCATAGCTTTCACAGGATATGACATGCGTTTT
SLC35F5 shRNA 1 RV	CGAAAAAACGCATGTCATATCCTGTGAAAGCTATGAATATTAACCTTTCACAGGATATGACATGCGC
SLC35F5 shRNA 5 FW	ACCGGGCTTTCTTACCTCATCATTGAGTTAATATTCATAGCTCAATGATGAGGTAAGAAAGCTTTT
SLC35F5 shRNA 5 RV	CGAAAAAAGCTTTCTTACCTCATCATTGAGCTATGAATATTAACCTCAATGATGAGGTAAGAAAGCC

2.1.11 Cell lines

Cell line	Suppliers
HEK 293T	ATCC, Manassas, Virginia, USA
HeLa	ATCC, Manassas, Virginia, USA
H6C7	Provided by Prof. Dr. Med. Claudia Scholl's group, DKFZ, Heidelberg, Germany

2.1.12 Commercial Bacteria Strains

Competent cells	Company
One Shot® TOP10 chemically competent Escherichia coli (E. coli)	Invitrogen, Carlsbad, California, USA

2.1.13 Mouse Strains

Mouse Strain	Company
NOD.Cg- <i>Prkdc</i> ^{scid} Il2rg ^{tm1Wjl} /SzJ (NSG)	The Jackson Laboratory, Bar Harbor, Maine, USA

All animal experiments were approved by the Regierungspräsidium Karlsruhe. Application number: G-233/15 and G-76/12

2.1.14 Other Reagents and Chemicals for Molecular and Cloning Technologies

Reagents and Chemicals	Suppliers
4% Paraformaldehyde Solution	HiMedia Laboratories, Einhausen, Germany
Agarose SERVA Wide Range	SERVA Electrophoresis, Heidelberg, Germany
Anisomycin	Sigma-Aldrich, St. Louis, Missouri, USA
Anti-FLAG [®] M2 Magnetic Beads	Sigma-Aldrich, St. Louis, Missouri, USA
Benzonase [®] Nuclease	Merck Millipore, Burlington, Massachusetts, USA
Bovine Serum Albumin	Sigma-Aldrich, St. Louis, Missouri, USA
BYL-719 (Alpelisib)	Hölzel Diagnostika Handels, Koeln, Germany
Copanlisib	Hölzel Diagnostika Handels, Koeln, Germany
Crystal Violet	Sigma-Aldrich, St. Louis, Missouri, USA
Doxycycline hyclate	GENAXXON Bioscience, Ulm, Germany
Ethanol absolute	VWR, Radnor, Pennsylvania, USA
Fluorescence Mounting Medium	Dako (Agilent Technologies), Santa Clara, California, USA
Gallein	Tocris Bioscience, Bristol, UK
GDC-0032	Hölzel Diagnostika Handels, Koeln, Germany
Gel Loading Dye, Purple (6x)	New England BioLabs, Frankfurt, Germany
GSK2334470	Selleck Chemicals, Houston, Texas, USA
Halt [™] protease and phosphatase inhibitor cocktails	ThermoFisher Scientific, Waltham, Massachusetts, USA
Hanks' Balanced Salt Solution	Sigma-Aldrich, St. Louis, Missouri, USA
Hoechst 33342	Life technologies, Carlsbad, California, USA
Hydroxystilbamide	Invitrogen, Carlsbad, California, USA
Incidin [™] Foam	Ecolab, Saint Paul, Minnesota, USA
Isopropanol	Honeywell Specialty Chemicals, Seelze, Germany
Lysis Buffer 6	R&D Systems, Minneapolis, Minnesota, USA
MK-2206 2HCL	Hölzel Diagnostika Handels, Köln, Germany
Mouse IgG - Agarose	Sigma-Aldrich, St. Louis, Missouri, USA
Nonidet [®] p40 (Substitute) – Solution 10% peroxide-free	PanReac AppliChem, Darmstadt, Germany
OSU-03012	Selleck Chemicals, Houston, Texas, USA
Pen Strep Penicillin Streptomycin	Gibco by Life Technologies, New York, USA
Polybrene	Merck Millipore, Burlington, Massachusetts, USA
Polyethyleneimine (PEI)	Sigma-Aldrich, St. Louis, Missouri, USA

PowerSYBR® Green PCR Master Mix	Applied biosystems, Foster City, California, USA
Precision Plus Protein™ All Blue Prestained Protein Standards	Bio-rad, Hercules, California, USA
Propidium iodide	Invitrogen, Carlsbad, California, USA
Protector RNase Inhibitor	Sigma-Aldrich, St. Louis, Missouri, USA
Rapamycin	Cayman Chemical Company, Ann Arbor, Michigan, USA
Restriction enzymes	New England BioLabs, Frankfurt, Germany
Restriction reaction buffer	New England BioLabs, Frankfurt, Germany
RNase A Solution	QIAGEN, Hilden, Germany
SKIM MIL POWER	GERBU Biotechnik, Heidelberg, Germany
Sodium chloride	Fisher Scientific, Hampton, New Hampshire, USA
TOTO™-3 iodide (642/660) (Toto-3)	Invitrogen, Carlsbad, California, USA
Tris-borate-EDTA (TBE) buffer	GENAXXON Bioscience, Ulm, Germany
Tween® 20	Sigma-Aldrich, St. Louis, Missouri, USA
UltraPure™ 1 M Tris-HCL pH 7.5	Invitrogen, Carlsbad, California, USA

2.1.15 Primary patient-derived PDAC cultures

All human tumour tissues were collected from the Surgery Department of Heidelberg University Hospital, Germany, and all experiments with human materials were performed according to the guidelines of the Declaration of Helsinki. The ethics committee of the Medical Faculty at the University Heidelberg approved all experiments (Ethic vote number 323/2204, Amendment 03). (Ehrenberg et al. 2019)

2.1.16 Software

Program	Company/Url
Bio-rad CFX Maestro 1.1 v4.1.2433	Bio-rad, Hercules, California, USA
Endnote X9	The licence provided by Heidelberg University, Germany
FACS Diva Software v6.1.3	Becton, Dickinson and Company, Franklin Lakes, New Jersey, USA
featureCounts (included in Subread package) v2.0.0	GNU GPL v3 Licence http://subread.sourceforge.net/
Garnett v0.1.13	MIT Licence https://cole-trapnell-lab.github.io/garnett/docs/
Grammarly for Microsoft® Office Suite	https://www.grammarly.com/office-addin
GraphPad Prism 8.4.2.679	https://www.graphpad.com/

ImageLab 6.1	Bio-rad, Hercules, California, USA
LAS AF v2.6.0	Leica, Wetzlar, Germany
Microsoft Office 365 Professional	The licence provided by Heidelberg University, Germany
NanoDrop® ND-1000 v3.2.1	ThermoFisher Scientific, Waltham, Massachusetts, USA
NEBioCalculator® v1.12.0	https://nebiocalculator.neb.com/#!/ligation
R v3	https://www.R-project.org
Scaffold™ v4.10.0	http://www.proteomesoftware.com/products/scaffold/download/
SEURAT v3.0.0	GNU GPL-3 Licence https://satijalab.org/seurat/
STAR 2.7.0	MIT Licence https://github.com/alexdobin/STAR
UMI-tools 1.0.0	MIT Licence https://umi-tools.readthedocs.io/en/latest/index.html

2.2 Methods

2.2.1 Cell culture techniques

2.2.1.1 Culturing of patient-derived primary PDAC

Tumour tissues of patients were obtained from the surgery department in PBS on ice, Heidelberg University Hospital, Germany. To expand the tumour, two pieces were subcutaneously transplanted into NSG mice, and the rest of tumours (weight >1 g) were purified to obtain single tumour cells in addition to xenotransplants (All animal experiments were approved by the Regierungspräsidium Karlsruhe. Application number: G-233/15 and G-76/12). In brief, the tumour tissues were washed three times with PBS plus antimycotics to prevent fungus contamination and then disinfected by incubating with 5 ml Braunol solution for 5 min under the cell culture hood at room temperature. 2 ml PBS was added to dilute the Braunol solution and incubated for additional 2 min. Tumour tissues were washed twice with cold PBS plus antimycotics and centrifuged at 300 rpm for 5 min in Centrifuge Multifuge® 3SR to remove Braunol solution. Tumour pieces were transferred into a 10 cm culture dish, and then cut into small pieces (which could pass through the 25 ml pipette tips) by using the scalpel. Tumour pieces were collected in a conical 50 ml Falcon tube, centrifuged at 900 rpm for 5 min in Centrifuge Multifuge® 3SR, and then washed with PBS plus Pen strep twice. To isolate individual tumour cells, tumour pieces were rotated with 20 ml digestion solution (40 mg/ml Collagenase IV, 1.5 μ M CaCl₂, filled up to 20 ml with Medium 199) at 37 degrees for 2.5 hours. After the digestion, the mixture was pipetted through a 100 μ m filter and the filter was washed with 10 ml cold PBS. The cells were centrifuged at 1000 rpm for 5 min in Centrifuge Multifuge® 3SR. The cell suspension was pipetted through 40 μ m filter twice (after each filtering, cold PBS was used to wash the filter once). Cells were collected by centrifugation at 1000 rpm. In case of a reddish cell pellet, the cell pellet was treated with 5 ml cold erythrocyte lysis buffer for 5 min at room temperature to remove the red blood cells. Cells were washed with 10 ml cold PBS once and the cell pellet was re-suspended in 5-10 ml cold PBS (dependent on the size of the cell pellet) followed by cell number counting. Cells were seeded in a T25 or T75 cell culture flask (T25: total cell number less than 1x10⁶; T75: total cell number more than 1x10⁶) with 6 ml (T25 cell culture flask) or 13 ml (T75 cell culture flask) CSCN medium plus cytokines. On the second day, seeded cells were checked under the microscope.

The established PDAC cultures were maintained in T25 or T75 attachment flasks and cultured at 37 degrees, under 5% CO₂ in an incubator. 6 ml CSCN medium (cell culture medium for patient-derived PDAC cultures, see materials) containing cytokines mix (FGF2 10 ng/ μ l, Nodal and FGF10 20 ng/ μ l) were used in T25 flasks, and 13 ml in T75 flasks. Fresh cytokines were added every 3-4 days. The cell confluency and status were checked twice per week. The medium was changed when the confluency reached 50%, and cells were split at the time point of 90% confluency.

To split cells, cells were detached from the cell culture flasks by treating with 5 ml (T75 culture flask) or 1 ml (T25 culture flask) Accutase for 15-30 min at 37 degrees. Detached cells were transferred to a 50 ml falcon and centrifuged at 1,200 rpm for 5 min at room temperature. The supernatant was discarded, and the cell pellet was re-suspended in 1 ml fresh CSCN medium. Cells were re-seeded (1:5-1:20 dilutions) in the new cell culture flask and fresh CSCN medium with cytokines was added to the final volume of 6 ml (T25 cell culture flask) or 13 ml (T75 cell

culture flask). Passage number was recorded on the cell culture flask and in electronic lab book. Cells were discarded when the passage number reached to 20.

2.2.1.2 Culturing of cell lines

Commercial cell lines used in this project were normal pancreas epithelial cells H6C7, HeLa and 293T cells.

To culture H6C7 cells, H6C7 cells were seeded in T25 or T75 attachment flasks. Keratinocyte-SFM medium (1x) added with Supplements (Gibco by Life Technologies) were used as the growth medium. Health status and confluency of cells were checked, and the growth medium was changed twice per week. Cells were detached when the confluency reached up to 80%. 5 ml cold PBS was used to wash the cells after the culture medium was discarded. 1 ml Accutase (Sigma) was used for detaching the cells by incubating the cells for 5 min at 37 degrees, using the 5% CO₂ incubator. The detached cells were transferred into a 1.5 ml Eppendorf tube by using 1 ml pipette tips and centrifuged at 1,200 rpm for 5 min at room temperature. Cells were 1:10 split in the new cell culture flask and added Keratinocyte-SFM (with supplements) growth medium to the final volume of 6 ml in a T25 flask, and 13 ml for the T75 flask.

HeLa and 293T cells were cultured in T25, T75 or T225 attachment flasks. IMDM (Gibco by Life Technologies) with 10% FBS and 2 mM L-glutamine were used for culturing these cells. Cells were checked twice per week. Medium was changed when the colour turned to yellow. Cells were detached when the confluency reached to 80%. Cells were pre-washed with 1x cold PBS and Trypsin-EDTA 0.05% (Invitrogen) was used for detaching the cells (1 ml for T25 flask, 5 ml for T75 flask, and 10 ml for T225 flask). Cells were incubated with Trypsin-EDTA 0.05% under the cell culture hood for 5 min, room temperature, and then cells were gently shaken then centrifuged down in 50 ml falcon tubes at 1,200 rpm, 5 min, room temperature. 1:10 dilution was applied for splitting cells into the new cell culture flasks.

2.2.1.3 Thawing and freezing of primary PDAC cultures and cell lines

To thaw the cells, vital freezing cell stocks were transferred from liquid nitrogen to the cell culture room on dry ice thawed by the hand warming, and then they were transferred under the cell culture hood. Cells, along with freezing solutions, were transferred into a 50 ml falcon tube. The cryotube was washed with 1 ml thawing solution (50% cell growth medium plus 50% FBS), and the solution was transferred into the same falcon tube drop by drop in 20 seconds. 2 ml, 4 ml, 8 ml thawing solution were added into the falcon in 20 seconds every time. The cells were centrifuged at 1,200 rpm, room temperature followed with 1x washing step and resuspended in 1 ml culture medium. Then the total cell suspension was transferred into a new cell culture flask with cell growth medium and supplements. On the second day, cell culture medium was changed.

For freezing cultures, cells were first detached from cell culture flasks by using 1 ml Accutase (Sigma) for primary PDAC cultures and H6C7 cell line or 1 ml Trypsin-EDTA 0.05% (Invitrogen) for HeLa and 293T cells per flask, and then cells were transferred into 50 ml falcon tubes and centrifuged at 1,200 rpm, room temperature. Cell pellets were resuspended in 1,400 µl of freezing solution (per sample: 210 µl FBS, 105 µl DMSO and 1085 µl cell growth medium, pre-warmed in room temperature). Then cryotubes were labelled and stored in the freezing box.

The freezing box was immediately transported and kept at -80 degrees for 24 hours, followed by a transfer to liquid nitrogen tank for longer storage.

2.2.2 Single-cell RNA Sequencing (sc-RNA-Seq)

10x Genomics Chromium Single Cell Gene Expression Assay is a droplet-based sc-RNA-seq (Freytag et al. 2018). The single-cell 3' protocol has the power to provide 3' digital gene expression profiling for up to 10,000 individual cells per sample with low doublet rates, but in the meantime offers up to 65% cell capture rate (10x Genomics 2019).

For the sample preparation, primary patient-derived cells were seeded into T25 cell culture flasks in culture medium with cytokines at 37 degrees, in a 5% CO₂ incubator. Cells were harvested when the cell confluency reached 50-60%. Cell suspensions were transferred into 50 ml falcon tubes and spun down at 1,200 rpm for 5 min at 4 degrees. To remove the cell debris, dead cells, and remaining culture medium, cell pellets were washed twice with cold 500 µl PBS (plus 1 U/µl RNases inhibitors (Sigma)). To prepare the single cell suspension, cells were filtered through 35 µm and 20 µm filters. To ensure the single cell status, filtered cells were checked under the microscope. Then the cell number was counted and adjusted to a concentration of 600 cells/µl and total volume of 40 µl per sample. All steps were performed at 4 degrees as fast as possible. Cells were transported on ice to the ScOpenLab, DKFZ, Heidelberg, Germany offering the 10x Genomics' single-cell RNA sequencing platform. The following procedures were done by following Chromium Single Cell 3' Reagent Kits v2 User Guide (10x Genomics 2019).

The major workflow of 10x Genomics (10x Genomics 2019; Zheng et al. 2017) can be described as:

1. 10,000 singularized cells (29.0 µl prepared single cell suspension + 4.8 µl cold PBS) per sample were loaded on a microfluidics chip, mixed with barcoded primer gel beads from another channel, and then further mixed with oil formed gel beads in emulsion (GEM). During this step, all cells were labelled with barcodes.
2. GEMs were carefully transferred into polymerase chain reaction (PCR) tubes. PolyA tails were added to RNAs. Then, these RNAs-polyA were reverse transcribed to complementary DNAs (cDNAs) by using the thermal cycler. The lid temperature of thermal cycler was set at 53 degrees, and the reaction mix was incubated at 53 degrees for 45 min and then heated to 85 degrees for 5 min and then hold at 4 degrees. Beads were pulled and further cleaned up.
3. Oil was first removed and then cDNAs were amplified by using the PCR method in the thermal cycler followed with reaction clean-up. The cycle number depends on the input cell number. In this study, 14 cycles were used.

Details of PCR settings (Table modified based on Chromium Single Cell 3' Reagent Kits v2 User Guide (10x Genomics 2019, pg. 24)):

Step	Temperature	Time
1	98°C	3 min
2	98°C	15 seconds
3	67°C	20 seconds
4	72°C	1 min
5	Go to Step 2, 14 cycles	
6	72°C	1 min
7	4°C	Hold

4. cDNAs were quantified by using the 4200 TapeStation System (Agilent Technologies) and analysed using TapeStation Analysis Software A.02.02 (SR1).
5. 35 µl purified cDNAs were further used for fragmentation, end repair & A-tailing following with size selection.
6. 50 µl sample from step 5 were used for adaptor ligation followed by a post ligation clean-up step.
7. Sample index PCR was performed. The cycle number used in this step was dependent on the amount of DNA input for the library construction. In this project, eight cycles were used. Details PCR settings (Table modified based on Chromium Single Cell 3' Reagent Kits v2 User Guide (10x Genomics 2019, pg. 36)):

Step	Temperature	Time
1	98°C	45 seconds
2	98°C	20 seconds
3	54°C	30 seconds
4	72°C	20 seconds
5	Go to Step 2, 8 cycles	
6	72°C	1 min
7	4°C	Hold

8. Size selection was performed post sample index PCR following with clean-up step.
9. Prepared libraries from step 8 were quantified by using a 4200 TapeStation System (Agilent Technologies) and analysed by using TapeStation Analysis Software A.02.02 (SR1).
10. To further sequence the libraries, prepared libraries were diluted in nuclease-free water to a final concentration of 10 nM in 30 µl total volume. The libraries were sequenced at the Genomics & Proteomics Core Facility of DKFZ, Heidelberg, Germany. HiSeq 4000 Paired-End 100 base pairs (26+74 bp) sequencing was performed.

Analysis:

Single cell RNA sequencing data was retrieved from the Genomics & Proteomics Core Facility, DKFZ, Heidelberg, Germany and stored in the DKFZ NGS hard disk. The retrieved sequence data was further processed and analysed by bioinformatician Dr. Mario Huerta, Nationalen Centrum für Tumorerkrankungen, Heidelberg, Germany.

Dr. Mario Huerta provided the following information:

To obtain the counts from retrieved Fast-All (FASTA) files of sc-RNA-seq, unique molecular identifiers (UMI)-tools using a whitelist (Smith et al. 2017), spliced transcripts alignment to a reference (STAR) (Dobin et al. 2013) and featureCounts (Liao et al. 2014) tools were used (version and licences in section 2.1.16). The default parameters which suitable for the type of sequencing data were used. Cells with a drop in the number of counts were discarded in the knee analysis. Then the counts were analysed by using SEURAT (version and licences in section 2.1.16) (Stuart et al. 2019). Cells susceptible of being artifacts due to an abnormal number of counts or features and death cells due to an excessive percentage of mitochondrial expressed genes were discarded. The feature expression measurements for each cell were normalized to the total expression, then multiplied by a scale factor (10,000 default), and the results were log-transformed. Counts were clustered by K-nearest neighbour. 2,000 genes with highest variability and the most significant dimensions which obtained from a Principal Components dimension reduction were used for clustering. Cell classification by cell type was performed by using the gene signatures provided in the publication of Peng et al. Cell type was classified by the maximum gene-expression mean among the different gene signatures for each cell or by using the cell-classification method of Garnett package. A cell-type hierarchy was set between cell types and subtypes based on the publication of Peng et al 2019. Cells were classified by the expression levels of GNB1, and further distinguished as no-expression, low-expression, medium-expression, and high-expression. Cut-offs were set to limit each class by quartiles or by cell-density fluctuations. Differentially expressed genes between clusters and classes were obtained by using Wilcoxon rank sum test of SEURAT package.

2.2.3 Flow cytometry and cell sorting

To prepare cells for flow cytometry analysis, up to 1×10^6 cells were detached from cell culture flasks, and spin down at 1,200 rpm, 5 min at room temperature. Then cells were washed 1x in 300 μ l cold HF (Hank's Balanced Salt Solution with 2% FBS) and then cells were stained with 300 μ l prepared Hydroxystilbamidine (Fluoro-Gold) (1:1000 dilution) or Toto-3 (1:5000 dilution) viability dye in fluorescence-activated cell sorting (FACS) tubes. Then cells were centrifuged and washed with 300 μ l cold HF to remove the remaining nucleus staining solution. To prepare the single cell suspension for analysis, the cells was filtered through the 35 μ m filter before samples loaded on LSRII or AriaII. Samples were stored on ice until loaded on the flow cytometry. In the working sheet of FACS Diva software (BD Company, v6.1.3), side scatter versus forward scatter (SSC-A vs. FCS-A, A stands for Area) dot plot was created to select of desired cell size and granularity. Parameter settings were adjusted to show all the events. Then, debris in the left bottom were excluded by gating around the events. The single parameter dot plot was created to further gate around living cells. In cell sorting settings, to select for single cells, SSC-H (H stands for Height) versus SSC-A and FSC-H versus FSC-A dot plots were created. Single parameter histogram was created to distinguish the single marker expression. In this project, green fluorescent protein (GFP) and red fluorescent protein (RFP)

were commonly used. If two markers were used in the experiments, two parameter histograms were used. The populations were gated by using the quadrant gate for further compensation adjustments and readouts. Within flow cytometry and cell sorting experiments, a negative control without any staining, a viability dye staining sample, experiment samples (viability dye and markers staining) were measured. Compared to the negative control sample cells, marker positive cells were identified. For compensation, the statistic table was created, and the compensation was adjusted until the medians of two populations match. In cell sorting experiments, only strong marker expressed cells were sorted.

2.2.4 Production of concentrated lentiviral particles

Day 1 To prepare the producer cells, 1×10^7 /plate 293T cells were seeded in ten 15 cm cell culture plates with 13 ml IMDM culture medium with 10% FBS and 2 mM L-glutamine. Cells were cultured overnight at 37 degrees, 5% CO₂.

Day 2 To transfect the packaging plasmids with the gene of interest transfer vectors, DNA-PEI mixtures (1:3 ratio) were prepared. DNA mixtures contained 12.5 µg p101, 12.5 µg p102, 9.0 µg p103 and 32 µg DNA constructs for each plate. Polyethylenimine (PEI) solution (Sigma) contained 179.25 µg per plate and diluted in IMDM medium (without FBS inside) to the final volume 500 µl per sample. DNA mixtures were 1:1 mixed with PEI solution to the final volume of 1 ml and further incubated for 30 min at room temperature. Within 30 min incubation time, fresh cell growth medium was added to each cell culture plate. Then, the DNA-PEI solution was evenly distributed on the cell culture plates. Cell culture plates with DNA-PEI solution were gently shaken horizontally and they were transported into 37 degrees 5% CO₂ incubator culturing for 16 hours.

Day 3 After 16 hours incubation, cell culture medium with DNA-PEI solution was discarded to end the transfection. Fresh cell growth medium was added to cell culture plate. Cells were further incubated for additional 56 hours to produce viral particles.

Day 4 GFP or RFP fluorescence signals in transfected cells were checked under the fluorescence microscopy to check whether the transfection working or not.

Day 5 Viral particles were harvested and concentrated 72 hours post-transfection. Viral supernatant was filtered through a 0.22 µm filter and centrifuged at 20,000 g for 2 hours at 20 degrees by using ultracentrifuge L8-70M with Rotor SW27 (Beckman Coulter). The supernatant was discarded, and the tubes were left upside down on the wipe tissues for 10 min at room temperature to remove the remaining medium in tubes. 50 µl PBS was added in each tube, and the tubes were covered using parafilm and further incubated at room temperature for 30 min. The liquid was pipetted 25 times (by avoiding the generation of air bubbles and touching the virus pellets). Then the virus suspensions were collected and transferred into the 1.5 ml Eppendorf tubes and rotated for 20 min at room temperature. Virus suspensions were equally aliquoted 10 µl per 0.5 ml Eppendorf tube and immediately transported to -80 degrees for longer storage. 3 µl virus suspensions were used for the titer assay.

2.2.5 Measurement and calculation of the infectivity of produced lentiviral stocks

Day 1 To measure the titer of produced lentiviral particles, 5×10^4 HeLa cells were plated in each well of a 6-well-plate, with 2 ml IMDM culture medium (with additional 10% FBS), and

let the cells attached to cell culture plate and doubled the cell number overnight in the 37 degrees, 5% CO₂ incubator.

Day 2 104 µl Polybrene (1 mg/ml) (MERCK) was added into 6.5 ml IMDM (with additional 10% FBS) for 2 virus production. Cell growth culture medium was discarded, and 500 µl prepared Polybrene-IMDM mix was added into each well. The virus was diluted from 1:10e3 to 1:10e7 in IMDM medium and adjust the final volume to 500 µl for each concentration. 500 µl virus solution in IMDM was added in 6-well-plate. One well was left as the negative control by adding 500 µl IMDM cell growth medium. Then cells were incubated for 72 hours, at 37 degrees, under 5% CO₂ in a cell culture incubator.

Day 5 To prepare the cells for flow cytometry measurement, cell growth medium with the remaining viral particles was discarded and the cells were prepared following the sample preparation protocol for flow cytometry (see 2.2.3 Flow cytometry and cell sorting) and measured the percentage of fluorochrome positive cells. Percentage of fluorochrome-positive cells are between 3%-25% was used for virus titer calculation.

The following formula was used to determine the titer of the lentiviral vector stocks:

$$[(1 \times 10^5) \times (\% \text{ of fluorochrome-positive living cells})] / (100 \times \text{dilution factor}) = \text{Transduction units/ml (TU/ml)}$$

Multiplicity of infection (MOI): number of transducing lentiviral particles per cell.

Desired MOI = total transduction units needed / total number of cells waiting for transduction

2.2.6 Generation of stably transduced cultures for gene overexpression or knockdown studies

To stably overexpressed or knockdown genes in primary PDAC and cell lines, concentrated lentiviral particles were first produced and then lentivirus transduction was performed.

Day 1 Preparation of cells for transduction. Cells were freshly detached from the cell culture flasks. 1×10^5 cells were seeded into a 6-well-plate, and in each well, 2 ml cell growth medium was added plus supplements. Cells were cultured overnight in 5% CO₂, 37 degrees.

Day 2 Lentivirus transduction. The cell confluency was first checked under the light microscope. Old culture medium was discarded and 2 ml fresh cell growth medium (plus supplements) with 8 µg/ml polybrene was added into each well. Then, to achieve high transduction efficiency at the initial point, 5 µl concentrated lentivirus were added into each well, and spread evenly by gently shaken the plate. MOI was calculated afterwards. If the transduction efficiency needed to control under 50% to achieve single integration site per cell, four different MOIs (MOI1, MOI2, MOI5, MOI10) were used.

Day 3 Cell growth medium was discarded to end the transduction and cells were further washed with cold PBS twice to remove the lentivirus completely. Fresh cell growth medium plus supplements were added into each well, and the transduced cells were further cultured for two days.

Day 5 Transduction efficiency determination. Transduction efficiency was measured on day 3 post virus transduction by using flow cytometry (flow cytometry detailed protocol see 2.2.3 Flow cytometry and cell sorting).

When the experiments required a high purity of transduced cells, the transduced cells were further expanded and sorted to increase the purity of transduced cells in the total cell population over 95%.

2.2.7 Molecular Techniques

2.2.7.1 RNA isolation and quantification

In this project, all experiments which need RNA as the primary material followed the same RNA isolation and quantification protocol. As the source of RNA, primary patient-derived PDAC cultures and tumour cell lines were freshly detached from the cell culture flask, and washed twice with cold PBS to remove the remaining reagents. Up to 5×10^5 cells were counted and used for RNA isolation. RNAs were isolated by using QIAGEN RNeasy Mini Kit according to the provided protocol in the kit. Isolated RNAs were quantified by Nanodrop. Absorbance ratio of 260/280 was used to analyse the purity of RNA. RNAs were either stored at -80 degrees for further usages or directly used for cDNA synthesis.

2.2.7.2 cDNA synthesis and semi-quantitative reverse transcriptase PCR

RNA was reversely transcribed for further semi-quantitative reverse transcriptase PCR (qRT-PCR) analysis. RevertAid First Strand cDNA Synthesis Kit (ThermoFisher Scientific) was used for cDNA synthesis. 1 μ l of oligo-dT primer was mixed with 1 μ g RNA to the final volume by adding ddH₂O of 12 μ l in the PCR reaction tube and incubated for 5 min at 65 degrees. Then the mixture was chilled on ice. The 4 μ l of reaction buffers (5x), 2 μ l of dNTP mix (10 mM), 1 μ l of RiboLock RNase inhibitor and 1 μ l of RevertAid M-MuLV RT enzyme were added into the reaction system according to manufacturer's instruction. Then the RNA was reversely transcribed at 42 degrees for 60 min and 5 min at 70 degrees. At the end of the reaction, the temperature held at 4 degrees. The final product was 1:10 diluted by adding ddH₂O and could be further used for qRT-PCR. The rest of the product was stored at -20 degrees.

qRT-PCR master mix per well:

Reagent	Volume
Power SYBR Green PCR Master mix	10 μ l
Primer Mix (Forward+Reverse, 10 μ M working solution)	2 μ l
ddH ₂ O	5 μ l
cDNA	3 μ l
Final Volume	20 μ l

To prepare the sample reaction plate for qRT-PCR, 96-well PCR-reaction plate was placed on ice. And then the master mix was prepared on ice as well. 20 μ l prepared master mix was distributed into each well, and then the plate was sealed by sealing membrane. The plate was shaken shortly and then centrifuged by using Mini-plate Spinner (VWR). In the next step, the plate was loaded on CFX96™ Real-Time System (Bio-Rad) and the program started.

PCR program steps were:

Step	Temperature	Time
1	95 °C	10 min
2	95 °C	15 seconds
3	58 °C	30 seconds
4	72 °C	30 seconds
5	Plate read	
6	Go to step 2, 39 cycles	
7	95 °C	5 seconds
8	65 °C	31 seconds
9	65 °C	5 seconds (+0.5 °C/cycle)
10	Plate read	
11	Go to step 9, 64 cycles	
12	40 °C	30 seconds

Beta-actin was used for the housekeeping gene for the relative quantification. Relative mRNA levels were calculated by using the formula of $2^{-(\Delta\Delta Ct)}$:

Δ stands for delta.

$\Delta Ct = \text{mean Ct (gene of interest)} - \text{mean Ct (housekeeping gene)}$

$\Delta\Delta Ct = \Delta Ct (\text{treated sample}) - \Delta Ct (\text{control sample})$

Fold of gene of interest expression = $2^{-(\Delta\Delta Ct)}$

Standard deviation (SD) of the mean of each sample was further calculated.

2.2.7.3 Protein extraction

To prepare the sample cells, primary PDACs and cell lines were detached from cell culture flask following the cell detaching protocol (see 2.2.1.1). Up to 1×10^7 cells per plate were seeded in 15 cm cell culture plates and incubated overnight in 37 degrees, 5% CO₂ incubator. On the second day, culture medium was discarded, and cells were washed twice with cold PBS. Washing PBS was discarded completely, and in each plate 1 ml fresh cold PBS was re-added. Then cells were collected by scrappers, and then transferred into 1.5 ml Eppendorf tubes. Cell pellets were collected after centrifuged at 2,000 rpm, at 4 degrees. The supernatant was discarded, and cell pellets were kept on ice for further usages.

Protein extraction procedures were performed as follows: 100 μ l cell lysis buffer (plus 1x proteases inhibitors and 1x phosphatase inhibitors) were used for resuspending the cell pellets and the reaction system incubated on ice for 30 min, and then centrifuged at 13,000 rpm for 15 min at 4 degrees. The supernatant was transferred into new Eppendorf tubes and either

stored on ice for later protein concentration quantification or transferred into -80 degrees for further usages.

2.2.7.4 Quantification of protein concentration and western blot

To measure the protein concentration, 6 μl extracted proteins solution were first 1:10 diluted to the final volume 60 μl . 25 μl diluted proteins were mixed with reagents provided in Pierce BCA Protein Assay Kit (ThermoFisher Scientific) including a replicate. Bovine serum albumin (BSA) standers which provided by the kit were prepared according to the user guide. The sample plate was incubated at 37 degrees for 30 min (avoid light). The chemiluminescence was measured by Tecan plate reader. A scatter plot was created in the excel for the reading of BSA standers. The mean of readings of protein samples were calculated. By using the formula determined by BSA standers, unknown protein concentration was extrapolated.

In pre-experiments, 30 μg proteins were used, and according to the results, protein loading amount was adjusted, and the proteins amount ranged from 2 μg to 30 μg in all western blot experiments in this project. To prepare the loading protein samples, proteins were mixed with 4x Laemmli sample buffer and ddH₂O to the final volume of 20-40 μl per sample. And then protein samples were boiled for 5 min to protein denaturation and then chilled on ice. To separate proteins according to the their size, the following procedures performed: isolation tape and comb were removed from 4-15% mini-PROTEAN TGX Stain-Free protein gels (Bio-rad) and then the gel was fitted into the electrophoresis chamber; 1x running buffer was filled in the chamber until completely cover gels; loading wells were flushed with 1x running buffer to remove the air bubbles inside; prepared protein samples and 3 μl Precision Plus Protein™ All Blue Prestained Protein Standards (Bio-rad) were loaded into wells and electrophoresis were performed for approximately 1 hour at 110 volts. The separation of total loading proteins in gels was checked under ChemiDoc MP Imager (Bio-rad) by using Stain-Free Gel function (Auto). To detect specific protein, proteins were transferred to 0.45 μm PVDF membranes (Bio-rad) by using the Trans-Blot Turbo instrument (High-MW programme) (Bio-rad). After the trans-membrane step, total loading proteins were detected on PVDF membranes under the ChemiDoc MP Imager with Stain-Free Blot function (Auto) to evaluate the trans-membrane efficiency and the detected chemiluminescence of each lane which was further quantified in ImageLab software (Bio-rad) and used as the loading control. 5% slim milk with 1x TBST blocking buffer was used as blocking buffer. Blocking buffer was changes to 1x TBST with 5% BSA when detecting phosphorylated proteins. PVDF membranes were incubated with blocking buffer for 2 hours on the rock shaker at room temperature. During the blocking time, primary antibodies were diluted at the desired dilution (section 2.1.5.1) in 1x TBST with 5% BSA or 1x TBST with 5% slim milk according to the date sheets which provided by the manufacturers. After blocking step, membranes were transferred into 50 ml falcon tubes and incubated with prepared primary antibodies overnight at 4 degrees. On the second day, membranes were washed three times, 10 min of each, with 1x TBST. 2nd antibodies were 1:10,000 prediluted in 1x TBST and incubated with membranes for 40 min, following with 3x washing steps, 10 min of each in 1x TBST. ECL solutions were 1:1 pre-mixed shortly before the exposure step and stored avoid light at 4 degrees for short-term (less than 30 min). Membranes were treated with pre-mixed ECL solutions for 1 min, and then the chemiluminescence of protein bands were detected by ChemiDoc MP Imager (Bio-rad). The following quantification steps were done by using ImageLab software (Bio-rad).

The second target protein could be detected on the same membranes if the primary antibody was generated by a different species and the protein molecular weight was not the same as the previous proteins. If the primary antibody for the second target protein was generated from the same species, then the membranes could be stripped by using 5-10 ml stripping buffer and incubated on the rotator for 10-15 min. The stripped membranes were washed with 1x TBST twice, and then the chemiluminescence was detected by using ChemiDoc MP Imager after incubating with prepared ECL solutions mixture to check the efficiency of stripping step. Then the membrane was re-blocked with blocking buffer followed with normal procedures. The PVDF membranes can be shortly stored in 1x TBST and air dried for long-term storage.

Analysis:

To quantify the fold of protein expression, two loading controls (reference) were used in this project. One was total loading protein, and the other one was alpha-tubulin protein. The chemiluminescence of total loading proteins of each sample was determined by using ImageLab software. The frame tool was used to detect each lane in the multichannel PVDF membrane images. Then, to select all the loaded proteins in each lane, the frame was adjusted to the width and the height in each lane to cover all protein bands, and both width and height were the same between each lane. The background chemiluminescence was adjusted by using Adjust Background Tool. The readout of each lane was used as the loading control for further analysis. Target protein bands were identified by using Rectangle Tool. The first rectangle was created to mark the target protein band in the first lane, and then this rectangle was copied and pasted to mark all the target protein bands in the other lanes. Background readout of each protein bands were also eliminated by using the Adjust Background Tool. The reference alpha-tubulin protein bands were quantified by using the same strategy. Both lanes and bands readout were exported into an excel worksheet. The fold protein expression was calculated according to the formula:

Fold protein expression = (readout value of protein band S / readout value of reference S) x (readout value of reference C / readout value of protein band C)

S stands for target protein in target protein overexpressed or knockdown sample. C stands for target protein in control samples.

2.2.7.5 Sample preparation and analysis of mass-spectrometry based whole cell protein analysis

To prepare the protein samples, 1×10^7 primary PDAC cells were freshly detached from cell culture flasks and then seeded into 15 cm cell culture dishes with 13 ml cell growth medium (plus cytokines) per plate. On the second day, cell growth medium was discarded, and the cells were washed with cold PBS twice. Then cells were harvested by using scrappers. Collected cells were centrifuged at 2000 rpm for 5 min at 4 degrees. 100 μ l cell lysis buffer (150 mM NaCl, 50 mM Tris pH 7.5, 1% Nonidet P-40, 0.5% Na-Desoxycholat, 10% SDS, 1x proteases inhibitors and 1x phosphatase inhibitors) were used to extract proteins from cells. Then the reaction system was incubated on ice for 30 min followed with 15 min at 13,000 rpm centrifugation. The protein concentration was measured by using the bicinchoninic acid (BCA) assay (see 2.2.7.4). The cell lysates were further treated with Benzonase endonuclease (1% of total volume of cell lysis buffer) to remove the DNA. Protein samples were stored in -80 degrees until transferred to the Genomics and Proteomics department of the core facility in DKFZ, Heidelberg, Germany for further mass-spectrometry analysis.

Analysis:

Mass-spectrometry based whole cell protein data analysis was based on the Filtered Protein Groups readout. It included unique peptides numbers of identified proteins and label-free quantification (LFQ) intensity values (LFQ intensity is normalized protein intensities to correct errors between samples). LFQ intensity is commonly used for comparison of one protein expression in different samples. I further analysed the retrieved mass-spectrometry data. The protein expression was evaluated by considering unique peptides number (greater than two). LFQ intensity value was used for fold protein expression calculation.

2.2.7.6 Co-immunoprecipitation and sample preparation for mass-spectrometry after protein pull-down

To prepare the cells for protein extraction, 1×10^7 cells per plate were plated in the 15 cm cell culture plates and incubated overnight at 37 degrees, under 5% CO₂ in a cell incubator. On the second day, cell culture medium was discarded, and then cells were washed with cold PBS twice. PBS should be discarded completely before adding 1 ml cell lysis buffer per plate (plus 1x protease inhibitors and 1x phosphatase inhibitors) which offered in FLAG Immunoprecipitation Kit (Sigma). Cells were incubated with cell lysis buffer for 30 min at 4 degrees on the shaker. Cells and cell lysates were collected by using scrapers and transferred into the 1.5 ml low protein binding Eppendorf tubes. Tubes were stored on ice shortly until all the samples were collected, and then all tubes were centrifuged at the 13,000 rpm, 15 min at 4 degrees. Cell lysates were transferred into new 1.5 ml low protein binding Eppendorf tubes and stored on ice for short-term usage (not exceed 30 min) or stored at -80 degrees for long-term storage (not exceed one week).

To prepare the samples for pull-down mass-spectrometry protein analysis, 100 μ l packed Anti-FLAG M2 Magnetic Beads (Sigma) were used with the binding capacity of up to 60 μ g proteins. The same amount IgG1 κ Magnetic Beads and IgG Agarose Beads from the same company were used for the IgG controls. The following beads washing steps were done according to the manufacturer's instructions provided in the FLAG Immunoprecipitation Kit (Sigma) and Anti-FLAG M2 Magnetic Beads (Sigma). The used buffers were provided by FLAG Immunoprecipitation Kit (Sigma). The loading amount of protein samples were adjusted to the 900 μ g (in this study). Pre-washed beads were added into protein samples and rotated overnight at 4 degrees. On the second day, beads were pulled by using the DynabeadsTM MPCTM-S (Magnetic Particle Concentrator) (ThermoFisher Scientific) and washed with washing buffer according to the manufacturer's instructions. To elute the proteins from the beads, 40 μ l 2x sample buffer which provided in the kit were mixed with beads and boiled for 5 min, at 95 degrees. Beads were eluted twice by using the same method. The first set of eluted protein samples were stored in -80 degrees and further analysed in the Core Facility for Mass-spectrometry & Proteomics (CFMP) at Zentrum für Molekulare Biologie der Universität Heidelberg (ZMBH) after FLAG-Tag and GNB1 proteins were confirmed by evaluation experiments. The second eluted protein sample set was further used for the protein evaluation by western blot method.

To evaluate pull-down proteins on the SDS-PAGE gel (PAGE: polyacrylamide gel electrophoresis), 20 μ l eluted protein samples were loaded into the 4-15% mini-PROTEAN TGX Stain-Free protein gel (Bio-rad) and proceed the western blot procedures. In western blot evaluation, FLAG-Tag antibody (1:1000, NBP1-06712, Novus Biologicals) and GNB1 antibody (1:5000, ab137635, Abcam) were used to evaluate the pull-down efficiency.

Analysis:

The results of identified peptides identified after protein pull-down mass-spectrometry were exported to an excel spread-sheet. The quality of pull-down mass-spectrometry was evaluated according to the spectrum of identified unique peptides of the bait protein GNB1 using the Scaffold v4.10.0 software. To identify the binding partners of GNB1, proteins detected in the IgG controls and GFP-controls were excluded by using the filter function in the Microsoft Office Excel. This step eliminated the unspecific proteins, heavy and light chains of antibody that bound to the beads. Next, only proteins were left in the list only if the identified unique peptides number was greater than two. The same strategy was performed in the three submitted primary PDAC cultures to identify the binding partners of GNB1.

2.2.7.7 Immunofluorescence

To prepare the imaging sample slides, 1×10^5 PC1 cells were plated on the coverslip into 48-well-plate and incubated for 40 hours allowing the attachment at 37 degrees in a 5% CO₂ cell incubator. Cells were gently washed once with 300 μ l cold PBS per well (avoiding direct pipette PBS onto cells) and the PBS was removed completely. Cells were fixed in 4% freshly prepared paraformaldehyde buffer for 20 min at room temperature under the fume hood. 4% paraformaldehyde was discarded in the special container and then cells were washed three times for 10 min each with PBST on the shaker, in total 30 min. And then cells were permeabilized by incubating with 100 μ l permeabilization buffer (1x PBS plus 0.1% Triton X-100) per well for 5 min. Cells were washed three times for 10 min with 300 μ l 1x PBST per well each. Then fixed cells were blocked for 60 min in 100 μ l blocking solution (10% normal goat serum or 10% normal donkey serum diluted in 1x PBST, depended on the species of the primary antibodies) and then incubated with primary antibodies (GNB1, 1:100, Abcam; Flag-Tag, 1:100, Novus Biologicals; GFP, 1:2000, Abcam) which diluted in blocking buffer overnight at 4 degrees on the shaker. Primary antibodies were washed away with 300 μ l 1x PBST per well, 3x washing, in total 30 min. 2nd antibodies were 1:100 pre-diluted in 1x PBST. The following steps needed to avoid light. Then cells incubated with 100 μ l pre-diluted 2nd antibodies for one hour at room temperature followed with 3x washing 1x PBST, 300 μ l per well, for 30 min in total. Cells were stained with 1:300 diluted Hoechst nucleus staining in washing buffer for 15 min at room temperature. Coverslips were washed in ddH₂O shortly, and then gently dried on tissue paper (quick, avoid complete dry of coverslips). Coverslips were gently put on the mounting medium (cells side faced to the mounting medium). Air bubbles were removed by gently pressing the coverslips with forceps. Let the mounting medium became solid, and then coverslips were cleaned by using 70% ethanol. Prepared coverslips were stored at 4 degrees and avoid the light until imaging. Immunofluorescence images were taken in the Light Microscopy Facility, DKFZ, Heidelberg, Germany by using the Leica TCS SP5 confocal microscope. All images with in one experiment were scanned under the same microscope settings.

2.2.7.8 Sample preparation for western blot based DigiWest multiplex protein profiling array

To extracted proteins which could match the lowest required protein amount of DigiWest multiplex protein profiling array, the number of seeded cells in each plate was pre-tested. 3×10^6 H6C7 cells were the proper cells number that on the second day the cell confluency can reach to 80% and the amount of total protein could reach to at least 30 μ g. Therefore, 3×10^6

H6C7 cells per plate were seeded in 15 cm cell culture plates with 13 ml cell growth medium and cultured overnight in 37 degrees, 5% CO₂ incubator. On the second day, culture medium was discarded, and then cells were washed three times with 5 ml PBS each to remove dead cells and the remaining culture medium. Then the PBS was discarded completely and then 1 ml fresh cold PBS was added in the plate. Cells were collected with scrappers together with PBS transferred into 1.5 ml Eppendorf tubes, centrifuged at 2,000 rpm, 5 min at 4 degrees. The supernatant was discarded, and cell pellets were directly transported to -80 degrees for long-term storage. The cell pellets were shipped on dry ice to NMI TT Technologietransfer GmbH, Reutlingen, Germany (NMI Technologietransfer GmbH 2020) for further analysis.

Analysis:

Two sets of samples were sent for analysis. Quality analysis was performed by NMI TT Technologietransfer GmbH, Reutlingen, Germany. The readout values of identified proteins were retrieved and calculated the mean in the lab. Then, the fold protein expression (GNB1 overexpression versus GFP control) was calculated. The bar graph was created to show the fold. Threshold was set at 1.5. Identified proteins which fold protein expression above 1.5 was selected as the candidate targets followed by evaluation western blot experiments.

2.2.7.9 IC₅₀ determination of inhibitors measured by ATP-Lite assay

Day 1 – Sample plate preparation

To prepare the sample plate for inhibitors treatments, 500 H6C7 transduced cells were seeded at the volume of 40 µl in 3 x 14 wells per culture on the tissue treated clear F-bottom black 384-well-plate (BD Biosciences), and cultured overnight in 37 degrees, 5% CO₂ incubator. Cells were evenly spread by gently shaking the plate. The rest of wells were filled with 40 µl PBS.

Day 2 – Compounds preparation and treatments

The concentration of all compounds used in this study were pre-adjusted to 10 mM. 1 ml 5x working solution (Initial concentration in the figure) of inhibitors in culture medium was prepared and added into a separate 384-well-plate (90 µl each well). 12 dilutions were used in this study, for the rest 11 wells, filled the wells with 45 µl culture medium, then performed the serial 1:2 dilutions, 5x pipette up and downs in each dilution. DMSO controls were prepared in the same way to guarantee the concentration of DMSO control match with the lowest concentration of DMSO in the inhibitors working solution. 10 µl working solution inhibitors were added into each well in the sample plate. 50 µM anisomycin was used as a positive control. Then the plate was gently shaken and put back to 37 degrees, 5% CO₂ incubator.

Name	Initial concentration	Lowest concentration	Times of dilutions	Number of dilutions
Gallein	25 μ M	12.2 nM	1:2	12
GSK2334470	25 μ M	12.2 nM	1:2	12
OSU-03012	2 μ M	0.9 nM	1:2	12
Copanlisib	10 μ M	4.8 nM	1:2	12
Alpelisib	25 μ M	12.2 nM	1:2	12
GDC-0032	25 μ M	12.2 nM	1:2	12
MK-2206	25 μ M	12.2 nM	1:2	12

Day 5 - ATP-Lite Assay

After 72 hours treatment, sample plates were taken out and covered the bottom with black stickers to avoid the light reflection. The following steps were performed according to the instructions of ATPlite 1step kit (PERKInElmer). 10 ml ATPlite 1 step buffer were used to dissolve the lyophilized substrate, and the mixture was left in the room temperature for 5 min (avoid light). 25 μ l mixed reagent were added into each well and shaken for 2 min in the dark. The luminescence was measured by Tecan plate reader.

2.2.8 Cell cycle analysis

In this project, to evaluate the influence of GNB1 alteration in PDAC cultures, GNB1 overexpressed and GNB1 knockdown cultures were used. These cultures were lentiviral transduced to generate GNB1 overexpression (GFP positive) and GNB1 knockdown (RFP positive) which expressed GFP and RFP fluorochrome. Therefore, to faithfully reflected the cell cycle of the bulk population, before evaluating the cell cycle, the purity of transduced cells was first measured by flow cytometry. The purity of GFP and RFP positive cells should over 90% of total measured population.

Cells were detached from culture flasks. All the following procedures were handling on ice. 5×10^5 cells were transferred into FACS tubes and centrifuged at 1,200 rpm for 5 min, at 4 degrees. The supernatant was discarded and then cells were washed 1x with 300 μ l cold 1x PBS per tube. Then cells were first resuspended in 250 μ l cold PBS and then 750 μ l 100% ice cold Ethanol (final concentration 75%) was added drop by drop while vortex. Cells were fixed in 75% ice-cold ethanol overnight. On the second day, 2 ml cold PBS was filled into FACS tubes, and then cells were centrifuged at 1,200 rpm, 10 min at 4 degrees. Cells were washed with 300 μ l 1x cold PBS once and then resuspended in 100 μ l ice cold 1x PBS. 5 μ l Ki67 antibody (APC colour, BD Biosciences, 561126) per sample and 20 μ l isotype control (BD Biosciences, 557783) per sample were incubated with cells on ice (avoid light) for 30 min. Then cells were washed twice with 300 μ l ice cold 1x PBS each time. PI (Sigma) was prediluted to 50 μ g/ml and mixed with 100 μ g/ml RNase A in 1x PBS. 300 μ l pre-prepared PI with RNase solution was incubated with fix cells for 20 min (avoid light) on ice following 1x washing step.

Prepared samples can be stored shortly at 4 degrees (avoid light). Cells were filtered through 35 μm filters before FACS measurement and measured within 24 hours.

Analysis:

In the FACS settings, dot plot SSC-A versus FSC-A was set for determine the cell population. To gate the singlets, dot plots FSC-H versus FSC-A and SSC-W versus SSC-A were set. A PI single parameter histogram was set to distinguish cell cycle G0+G1, S, and G2+M phase. On the X-axis, the peak of G0+G1 was adjusted to the value of 50. An APC versus PI dot plot was used for separating G0 phase to G1 phase. The population of APC negative (Ki67 non-expressing) cells was the cells still in G0 phase.

2.2.9 Cloning of GNB1-FLAG constructs into pCCL pptPGK_IRES_GFP_PRE Vector

2.2.9.1 Preparation for cloning

Amplification primers were designed to amplify the N-terminal part of the GNB1 codon-optimized sequence, with 1x FLAG-Tag protein-coding sequence in the forward primer (Forward: 5'- GGATCCATGGATTACAAGGATGACGACGATAAGAGTGAGCTTGACC AGCTGAG - 3'; Reverse: 5'- GCGATCGCTTAGTTCCAGATCTTGAGGAAG - 3'). A stop codon, restriction enzyme sequences and six base-pair protection nucleotides were included in forward and reverse primers. Two more sequence primers were designed to target on GNB1 codon-optimized sequence (GNB1_1: 5' – TACGCTCCTAGCGGCAATTATG - 3'; GNB1_2: 5' – ACCGGCTCTGATGACGCCAC - 3'). All primers were dissolved to 100 μM in nuclease-free water, and then 1:10 dilute to 10 μM working concentration. Prepared primers were stored at -20 degrees.

2.2.9.2 Amplifying PCR

GNB1 codon-optimized expression pCCL pptPGK_IRES_GFP_PRE vector (GFP control) was used as template. The reaction system of amplifying PCR was prepared on ice and the details of master mix as follow:

Component	Reaction	Final Concentration
Nuclease-free water	to 50 μl	
5X Phusion GC Buffer	10 μl	1x
10 mM dNTPs	1 μl	200 μM
10 μM Forward Primer	2.5 μl	0.5 μM
10 μM Reverse Primer	2.5 μl	0.5 μM
Template DNA	Variable	50 ng
DMSO (optional)	1.5 μl	3%
PhusionDNA Polymerase	0.5 μl	1 Unit

Gradient PCR was performed, annealing temperature range from 55 degrees to 65 degrees, 12 gradients. The length of GNB1-FLAG is 1050 bp. Therefore, elongation time at 72 degrees was set for 2 min.

The thermocycling conditions:

Step	Temperature	Time
1	98°C	30 seconds
2	98°C	10 seconds
3	55°C-65°C	30 seconds
4	72°C	2 min
5	Go to step 2, 34 cycles	
6	72°C	5 min
7	4°C	Hold

2.2.9.3 Gel electrophoresis and gel purification

Gel electrophoresis was used to separate DNA bands according to the length. To prepare the 0.5% agarose gel, 3 g agarose powder were dissolved in 60 ml 1x TBE buffer by microwaving for 5 min. 0.5% agarose gel matrix was chilled to approximately 55 degrees and one drop of ethidium bromide was added into gel matrix. The agarose gel matrix was mixed well with ethidium bromide and poured into the casting tray with comb. The agarose gel was ready to use after solidifies.

Agarose gel was transferred into a chamber filled with 1x TBE buffer. The buffer in the chamber should cover the gel completely. 20 µl PCR products were mixed with 4 µl 6x gel loading dye (BioLabs) and then shortly spined down. 20 µl prepared samples and 6 µl DNA ladder (1 kb, Invitrogen by Life Technologies) were loaded into prepared 0.5% agarose gel separately in wells and then the gel was run for one hour in 1x TBE buffer at 140 volts. The DNA bands at the size of 1050 bp were cut out and DNA extracted from agarose gel by using QIAquick Gel Extracting Kit according to the instructions which provided by the manufacturer.

2.2.9.4 TOPO® TA Cloning

2 µl extracted insert DNAs were ligated to the TOPO TA vector by using TOPO® TA cloning Kit (Invitrogen). The reaction master mix was listed below:

Reagent	Volume
Fresh PCR product	2 µl
Salt Solution	1 µl
Water	2 µl
TOPO® vector	1 µl
Final Volume	6 µl

The reaction master mix was left incubation for 20 min at room temperature.

2 μ l ligated products were transfected into 50 μ l Invitrogen™ One Shot™ TOP10 competent cells following the manufacturer's instructions. The reaction was firstly incubated on ice for 30 min, and then heat-shocked at 42 degrees for 30 seconds. And then transfected competent cells were immediately transferred on ice and left on ice for 5 min. 300 μ l room temperature S.O.C. medium (Fisher BioReagents) was added into each tube and shake 300 rpm at 37 degrees for one hour.

LB-agar plates were pre-warmed at 37 degrees until ready for use. And then 50 μ l transfected TOP 10 competent cells were spread on the LB-agar plate (containing 100 μ g/ml ampicillin) for each transformation and cultured overnight at 37 degrees. On the second day, 10-20 colonies were picked up and further expand them in LB-medium (containing 100 μ g/ml ampicillin), 160 rpm shaken overnight at 37 degrees. Plasmids were extracted from TOP10 competent cells by using Plasmid Miniprep DNA Purification Kit according to the provided protocol in the kit. Plasmids were sent to Eurofins Genomics Europe Sequencing GmbH (sample picked up in Heidelberg, Germany) for sequencing to confirm the sequence of inserts was successfully cloned into the TOPO TA vectors.

2.2.9.5 Double digestion by restriction enzymes

1 μ g GFP control vector was linearized by using AsiSI (1 μ l, 10,000 units/ml) and BamHI (1 μ l, 10,000 units/ml) restriction enzymes. And TOPO TA vectors which carry correct insert were also double digested by 1 μ l AsiSI (10,000 units/ml) and 1 μ l BamHI (10,000 units/ml) per reaction. The details of reaction system were listed as follow:

Component	Reaction
CutSmart Buffer	2 μ l
DNA	1 μ g
BamHI-HF	1 μ l
AsiSI	1 μ l
Nuclease-Free Water	To 20 μ l

The reaction system was prepared on ice and further incubated at 37 degrees for one hour, 1 μ l calf alkaline phosphatase (CIP) was added into tubes of GFP control vector and further incubated at 37 degrees for additional 20 min, then heat to 80 degrees to deactivate enzymes.

Products were loaded into prepared 0.5% agarose gel and repeat the steps of gel electrophoresis followed with gel purification to purify the linearized GFP control and inserts.

2.2.9.6 Ligation

50 ng backbone GFP control vector was used for ligation. The required insert DNA mass was calculated by using NEBioCalculator[®] and the final reaction system used here was:

Component	Reaction
10x T4 DNA Ligase Buffer	2 μ l
Vector DNA	50 μ g
Insert DNA	18.31 μ g
T4 DNA Ligase	1 μ l
Nuclease-Free Water	To 20 μ l

This reaction system was incubated at 16 degrees for 16 hours.

2.2.9.7 Selection of clones and plasmid purification

2 μ l of the ligation products from the last step was transferred into 50 μ l TOP 10 competent cells following the protocol which provided by Invitrogen company, and then bacteria were cultured on LB-agar plate (contains selection antibiotics, 100 μ g/ml ampicillin) at 37 degrees, overnight. On the second day, 10-20 colonies were picked up and performed mini- or maxi-prep for plasmids purification by using Qiagen plasmids purification kits according to the protocol provided in kits. Plasmids were sent to Eurofins Genomics Europe Sequencing GmbH (sample picked up in Heidelberg, Germany) for sequencing to confirm the inserts' sequence.

2.2.10 Colony formation assay

PDAC cells were first detached from cells culture flask by using Accutase (5 ml for T75 flask and 1 ml for T25 flask) and filter through 35 μ m filters to remove cell clumpy. Then cells numbers were counted and seeded 400 cells/well in a 6-well-plate with 2 ml/well CSCN culture medium, with cytokines mix (FGF2 10 ng/ μ l, Nodal and FGF10 20 ng/ μ l). Cells were cultured for 14 days, and the culture medium was changed twice per week. On Day 14, the cell culture medium was discarded, and cells were washed with 1 ml cold PBS per well twice. Then cells were fixed and stained with 2% crystal violet with 2% methanol for 30 min. And then cells were washed by using running tap water and then dried overnight. Images were taken by ChemiDoc MP (Bio-rad).

2.2.11 Culture contamination test

All cultures used in this study were tested mycoplasma contamination every three months. Contamination tests were done in Multiplexion GmbH, Heidelberg, Germany.

Samples for Multiplex Cell Contamination Test were prepared as follow (Multiplexion 2020):

To extract genomic DNA for contamination analysis from cells, 1x10⁶ cells were pelleted in a 1.5 ml Eppendorf tube by centrifugation at 600 rpm for 5 min at room temperature. Then the cell pellet was resuspended in 100 μ l PBS and heated to 95 degrees for 15 min. Cellular debris

was removed by centrifuged at 10,000 g for 5 min at 4 degrees. The supernatant was transferred into a new 1.5 ml Eppendorf tube and kept at 4 degrees (short-term). Samples were prepared within one hours before delivery to Multiplexion GmbH, Heidelberg, Germany.

2.2.12 Cloning of SLC35F5 shRNAs into pRSIT17-U6Tet-sh-HTS6-CMV-TetRep-2A-TagGFP2-2A-Puro vector

To validate SLC35F5 as the candidate regulator of tumour initiating cells, SLC35F5 was first knocked down by shRNAs. shRNAs oligoes (sequence see section 2.1.10) were designed according to the user manual by Collecta company (Logue Ave. USA). shRNA oligonucleotides were diluted in ddH₂O to the final concentration of 20 µM. To clone the shRNAs into pRSIT17-U6Tet-sh-HTS6-CMV-TetRep-2A-TagGFP2-2A-Puro vector, the shRNA oligonucleotides annealing reaction mix was prepared on ice as follow:

Competent	Volume
Sense shRNA oligo (20 µM)	1 µl
Antisense shRNA oligo (20 µM)	1 µl
10x T4 Polynucleotide Kinase Buffer	2 µl
ATP (5 mM)	2 µl
ddH ₂ O	13 µl
T4 Polynucleotide Kinase (10 U/µl)	1 µl
Final volume	20 µl

The reaction mix was incubated at 37 degrees for 30 min in a thermal cycler, and heated to 95 degrees for 2 min. Then, the reaction mix was removed from the thermal cycler and cooled down to room temperature.

A 2 µl aliquot from the reaction was diluted 1:5 by adding 1x T4 kinase buffer and mixed. Then, 0.5 µl diluted product was further used to ligate with the linearized pRSIT17-U6Tet-sh-HTS6-CMV-TetRep-2A-TagGFP2-2A-Puro vector. The ligation reaction mix were prepared on ice as follow:

Competent	Volume
Linearized expression vector (10 ng/µl)	1 µl
shRNA template (0.2 µM)	0.5 µl
10x T4 DNA Ligase Buffer	1 µl
ddH ₂ O	6.5 µl
T4 DNA Ligase (40 U/µl)	1 µl
Final volume	10 µl

The reaction mix was incubated at 16 degrees for 2 h on the thermal cycler.

The following selection of clones and plasmid purification steps were claimed in section 2.2.9.7.

2.2.13 *In vivo* mouse xenotransplantation experiments

2.2.13.1 Transplantation of patient-derived PDAC cells orthotopically in NSG mice

PDAC cells were freshly detached from cell cultures flasks and washed with 500 µl cold PBS per sample once. 1 million cells for one mouse transplantation were counted, and centrifuged (1,200 rpm, room temperature, 5 min) in the 1.5 ml Eppendorf tube. Cell pellet was resuspended in 20 µl cold PBS and 1:1 mixed with 20 µl matrigel. The cells in Matrigel were transferred into an insulin syringe with a blunt needle and the syringe was stored on ice until transplantation.

In compliance with the animal application (application no.: G-233/15 and G-76/12), NSG mice were anaesthetized under 1.75% isoflurane and then kept on the heating pad until mice woke up after the transplantation. Bepanthen was used to cover the eyes of the mice to prevent drying. 100 µl per 10 g bodyweight metamizole was injected subcutaneously. The left abdomen was shaved with a scalpel and disinfected with alcohol pads. A 1 cm incision was made to expose pancreas connected to the spleen. Prepared cells were carefully injected into the subserosa of mouse pancreas and waited for 30 seconds to ensure that matrigel was completely solidified. If during the injection, the matrigel leaked out of pancreas, it was cleaned gently by cotton swabs which moisturised by sterile PBS. Then, pancreas was slowly placed back in the abdomen. During the time of organs exposure to air, sterile PBS was applied by cotton swabs to prevent drying. Then the peritoneum was closed with resorbing thread, and the skin was clipped. Iodide solution was applied to the clipped skin to prevent further infection. The transplanted mouse was earmarked and put back to the cage after the mouse woke up. 50 µg Baytril per ml was added into the drinking water. The status of transplanted mice was checked on the second day morning, with the following bodyweight and tumour growth observation twice a week. Clips were removed on Day 10 after transplantation. 2 g/L Doxycycline Hyclat (GENAXXON) was added into the drinking water to treat mice.

Mice status was checked at least three times per week. The expected endpoint for transplanted mice was the tumour size reached to 1 cm³. However, if the transplanted cells were not formed tumour, these mice were kept for one year (since the date of birth). Before the expected endpoint, according to the human endpoint defined in the animal application, in brief, the transplanted mouse was sacrificed once over 20% body weight loss per week, suffering from pain or abnormal behaviours were observed after discussing with the animal doctors and care takers. All sacrificed mice were opened and carefully checked whether the visible tumour formed in the lung, pancreas, stomach, liver, spleen, kidneys, and colon.

2.2.13.2 Resection of tumours from mice

Once the size of tumours reached to 1 cm³, the mouse was sacrificed by cervical dislocation. Tumours were taken out and stored in sterile PBS with 1x Pen strep (Gibco by Life Technologies), and metastases tumours were carefully checked through all organs. The tumours and organs with metastatic tumours were further purified in the laboratory.

2.2.13.3 Purification of primary pancreatic tumour tissues

Tumours were transferred into a 10 cm dish and weighed. Then a small piece from the middle part of the tumour tissue was cut and embedded in the labelled pathology cassette and fixed in 4% formalin. The rest of the tumour tissues were cut into small pieces to pass through a 25 ml pipette. Tumour pieces were transferred into a 50 ml falcon and washed with 10 ml PBS with 1x Pen strep, and then centrifuged down at 1,200 rpm, 5 min at room temperature. Discard the supernatant and resuspend the tumour pieces in 20 ml Medium 199 with 1 ml 40 mg/ml Collagenase IV and 120 μ l CaCl₂ (25 mM). Incubate the tumour pieces with enzyme mix on the rotator for 2.5 h, 37 degrees. Filter digested tumour pieces through 100 μ m (1x), 40 μ m filters (2x) and then centrifuged at 1,200 rpm, 5 min at room temperature. Cell pellets were resuspended in 5 ml PBS with 1x Pen strep and then counted the cell number. 100 μ l cell suspension was transferred into a FACS tube, in total 6 FACS tubes and kept on ice for later usage. The rest of the cells were separated into three Eppendorf tubes and stored in -80 degrees.

Purified tumour cells in FACS tubes were further stained with EpCAM (APC, 1:20), CD45 (PE, 1:100) and H2KD (PE, 1:100) primary antibodies, and then Toto-3 was used to distinguish living and dead cells. Cells were stained with primary antibodies for 30 min on ice, avoiding the light and then analysed by flow cytometry.

Quality control: The transplanted target gene altered human tumour cells were traced in this project to show the tumour formation ability. EpCAM is the human tumour cell marker. Therefore, the EpCAM expression was used to trace the transplanted human tumour cells. In the flow cytometry analysis, the percentage of EpCAM positive cells were first identified. In this project, the target gene altered cells expressed GFP fluorochromes (GFP positive cells). To determine the transplanted target gene altered human tumour cells in the xenografts, single parameter fluorescein isothiocyanate (FITC) was set to trace the percentage of GFP positive cells. Then, percentage of GFP out of isolated human tumour cells from the xenograft was calculated as percentage of GFP / percentage of EpCAM positive cells. The dot plot was created to show the percentage of GFP positive cells out of isolated human tumour cells from xenografts. Every single dot represented the data of one mouse. The median number in each generation of the serial transplantation was calculated and showed in the dot plot as well.

2.2.14 Statistical Analysis

Data was analysed by Graphpad Prism (8.4.2.679) and Microsoft Office 365 Professional Excel. Data are presented as relative values (experimental groups versus their respective controls). If other controls were used for calculation, this is indicated in the main text and figure legends. Error bars which presented in graphs indicated the standard deviation of the mean values of samples. The number of samples and the type of replicates (technical or biological) were noted in the main text, figure or table titles and legends. Furthermore, t-test was performed to calculate the statistical significance of the observed difference between each sample vs control group in cell cycle analysis, colony formation assay, and DigiWest multiplex protein profiling by using Graphpad Prism (8.4.2.679). $P < 0.05$ is statistically significant.

Cell cycle analysis was performed three times (n=3, technical replicates) with three patient-derived PDAC cultures (n=3, biological replicates). The mean value and the standard deviation of each cell cycle phase were calculated by using Microsoft Office 365 Professional Excel.

In colony formation assay, triplicates were set for each culture (n=3, technical replicates). In each well, the colony number was counted by using ImageJ software. A dot plot was created to show the number of colonies in each well, the median value by using GraphPad Prism (8.4.2.679). P-value was further calculated by using the GraphPad Prism (8.4.2.679).

Protein samples in duplicates were analysed by DigiWest multiplex protein profiling. In NMI Technologietransfer GmbH, Reutlingen, Germany, detected protein peak single values normalized to the control was calculated and the normalized data was log₂ transformed. NMI Technologietransfer GmbH calculated the mean values of duplicates as well as the standard deviation. I re-calculated the mean values of duplicates and the sample versus control fold-change, and further p-value was calculated to determine the significance by using Graphpad Prism (8.4.2.679).

For each inhibitor concentration, triplicates were used. Experiments were performed twice, in total six technical replicates for each concentration (n=6). To calculate the IC₅₀ of inhibitors, log concentration was first calculated in Microsoft Office 365 Professional Excel. Mean values from wells of each concentration were calculated. Next, cell viability was calculated as [(mean readout of inhibitors treated sample wells – mean readout of blank control wells) / (mean readout of DMSO wells – mean readout of blank control wells)], and then standard deviation was calculated. Log concentration value, calculated cell viability and standard deviation were transferred into created GraphPad Prism 8.4.2.679 worksheet, then IC₅₀ was calculated by this software, and the cell responding curve was created at the same time.

3 Results

This project was based on results gained within a previous PhD thesis project in Prof. Dr. med. Hanno Glimm's group performed by Dr. med. Jianpeng Gao (Gao 2017). Dr. Gao had identified GNB1 as a potential TIC regulator in a screening approach and performed initial validation experiments in patient derived cultures. Within my thesis, I completed the dataset for experimental validation of the identified candidate. After successful validation, I further investigated the underlying mechanisms and aimed to identify relevant binding partners of GNB1 in human pancreatic cancer.

Since the experiments done by Dr. med. Jianpeng Gao are relevant for the rationale of my project, I will recapitulate the findings that were in part already presented in his (Gao 2017) in the results section. In brief, Dr. Gao generated the lentiviral vectors used in my thesis and performed initial functional analysis on two patient derived cultures. I further extended this initial dataset within my thesis to complete the analysis. All experiments and analyses described in this thesis have been performed by me unless explicitly mentioned in the respective section.

3.1 Patient-derived PDAC cell cultures

Primary pancreatic cancer patient-derived cultures can reflect some of the complexity and heterogeneity of PDAC, and can capture the biological properties and have stable phenotypes after multiple passages (Ehrenberg et al. 2019; Krempley and Yu 2017). Seven patient-derived semi-adherent pancreatic cancer cell cultures (PC1-7) established previously in Prof. Dr. med. Hanno Glimm's lab (Ehrenberg et al. 2019) were used in this study. These established patient-derived PDAC cell cultures were further analysed the *KRAS* mutation, and I provided the cell pellets of PC1 and PC3 for analysis. All seven cultures harboured *KRAS* mutations (PC1: *KRAS*^{G12D}; PC2: *KRAS*^{G12V}; PC3: *KRAS*^{G12D}, PC4, PC5, PC6 and PC7 also harbour *KRAS* mutations, but the specific type of the mutation is unknown). PC1 and PC7 were pathologically classified as adenosquamous carcinoma. PC2, PC3, PC4, PC5 and PC6 were classified as ductal adenocarcinoma (Table 1). The primary tumour tissues from these patients were further expanded in NOD.Cg-Prkdc^{scid}Il2rg^{tm1Wjl}/SzJ (NSG) mice (Ehrenberg et al. 2019). The purity of human tumour cells was characterized by flow cytometry which revealed that no contamination from murine stromal cells (H2KD⁺) or human blood cells (CD45⁺) were detectable (Ehrenberg et al. 2019). All xenograft cells expressed the human epithelial cell marker EpCAM indicating human tumour cells without murine cell contamination (Ehrenberg et al. 2019). The absence of bacterial, fungal, and viral cell culture contamination and the unique sequence of each PC to assure sample identity were previously assessed in Multiplexion GmbH, Heidelberg, Germany. In this thesis, I re-submitted the samples of PC1, PC2 and PC3 for contamination analysis (Multiplexion 2020) to confirm no contamination in the cell cultures which used in the following experiments.

Table 1: Clinical information of established primary pancreatic cancer cultures used in this study (n=7).

Thesis ID	Histological Tumour Type	KRAS Mutation Status	Age	Gender	UICC-Stage	Weight of patient sample
PC1	Adenosquamous carcinoma	G12D	74	Male	IIB	N/A
PC2	Ductal adenocarcinoma	G12V	69	Female	IIA	0.30 g
PC3	Ductal adenocarcinoma	G12D	67	Female	IIB	0.26 g
PC4	Ductal adenocarcinoma	Mut.	69	Male	III	0.25 g
PC5	Ductal adenocarcinoma	Mut.	62	Male	IV	0.68 g
PC6	Ductal adenocarcinoma	Mut.	62	Male	IIB	0.10 g
PC7	Adenosquamous carcinoma	Mut.	86	Male	IIB	0.25 g

Thesis ID is the unique culture ID that was used in this thesis. Patients' tumour tissues were pseudonymised which is showed as PC-Number. All three PCs contained *KRAS* mutations, both PC1 and PC3 contained *KRAS*^{G12D} mutation, and the *KRAS* mutation status of PC2 is *KRAS*^{G12V}. From PC4 to PC7, *KRAS* mutation (Mut.) was confirmed, but the information of mutation type was unavailable.

3.2 Validation experiments of the identified TIC regulators GNB1 and SLC35F5 in established primary PDAC cultures

3.2.1 Validation of GNB1 as regulator of TIC activity in human PDAC

3.2.1.1 Generation of primary PDAC cultures with stable GNB1 knockdown or overexpression

The contribution in section 3.2.1.1: Dr. med. Jianpeng Gao generated LV. GNB1.OE and LV. GNB1-shRNA KD and LV. sh-scramble vectors and concentrated lentiviral vector stocks. I transduced PC1, PC2 and PC3 by using LV. GNB1. OE, LV. GFP con. to generate PC1 GNB1 OE, PC1 GFP con., PC2 GNB1 OE, PC2 GFP con., PC3 GNB1 OE and PC3 GFP con. I also transduced PC3 by using LV. GNB1-shRNA KD and LV. sh-scramble to generate PC3 GNB1 KD and PC3 Scr. I measured the transduction efficiency by using flow cytometry which showed in this section.

To further decipher the role of GNB1 in TIC activation, Dr. med. Jianpeng Gao ectopically knocked down and overexpressed GNB1 to validate its role in the established PDAC patient-derived cell models (Gao 2017). Dr. Gao cloned one shRNA into a lentiviral-based knockdown vector encoding for RFP as a marker gene. After lentiviral vector production, 1x10⁵ PC1 and PC2 cells were transduced with either the GNB1 knockdown lentiviral vector (LV. GNB1-shRNA KD) or scrambled control (LV. sh-scramble) vector and sorted for RFP expression on day five after transduction (Gao 2017). The RFP enriched cultures were expanded and vitally frozen (Gao 2017).

I followed the same transduction protocol to generate PC3 GNB1 knockdown (KD) and scramble control cultures by using the LV. GNB1-shRNA KD and LV.sh-scramble concentrated lentiviral vector stock. The transduction efficiency of PC3 with LV. GNB1 KD and LV.sh-scramble was 42% and 47%, respectively (Table 2). These cells were further expanded in T75 culture flasks and sorted for RFP positivity on day 5 post expansion. This lentiviral transduction protocol, transduction efficiency measurement and cell sorting were used for all the patient-derived PDACs.

The GNB1 coding sequence used for lentiviral mediated overexpression was codon-optimized and therefore was not targeted by the designed GNB1 shRNAs. This allowed for a stable GNB1 expression rescue in GNB1 KD cultures, by preventing shRNA mediated degradation of the ectopic GNB1 RNA (Gao 2017). By following the lentiviral transduction procedures, I transduced PC1, PC2 and PC3 by using LV. GNB1 OE and LV. GFP con. On Day 3 after transduction, I measured the transduction efficiency by flow cytometry. The transduction efficiency of PC1 with LV. GNB1 OE was 58%, and the same percentage of 58% was detected with the GFP control vector; 15% and 21% of PC2 GNB1 OE and PC2 GFP control; 72% and 83% of PC3 GNB1 OE and PC3 GFP control. I further sorted these cells for GFP expression and kept in culture for further experimental usages (Table 2).

Table 2: Transduction efficiency of three PDAC patient-derived cultures after transduction with lentiviral based GNB1 overexpression or knockdown vectors as well as the corresponding controls analysed by flow cytometry (n=3).

Culture	GNB1 OE (% of living cells)	GFP con. (% of living cells)
PC1	58%	58%
PC2	15%	21%
PC3	72%	83%

Culture	GNB1 KD (% of living cells)	Scr. (% of living cells)
PC3	42%	47%

N=3, biological replicates. The experiment was performed once and showed in the table. Abbreviation in the table: OE: overexpression; KD: knockdown; con.: control; scr.: scramble; PC: patient-derived PDAC culture.

I detected stable GFP marker gene expression after transduction (Day 3) by flow cytometry in three lentiviral transduced primary PDACs which was shown in Figure 2. I prepared samples for flow cytometry analysis on the same day with the same procedure and measured under the same flow cytometry settings. As the GFP positive population showed in the dot plots of PC1 GNB1 OE and PC1 GFP control groups, the cell populations were different, therefore the same value from both groups were not due to any mistake (Figure 2).

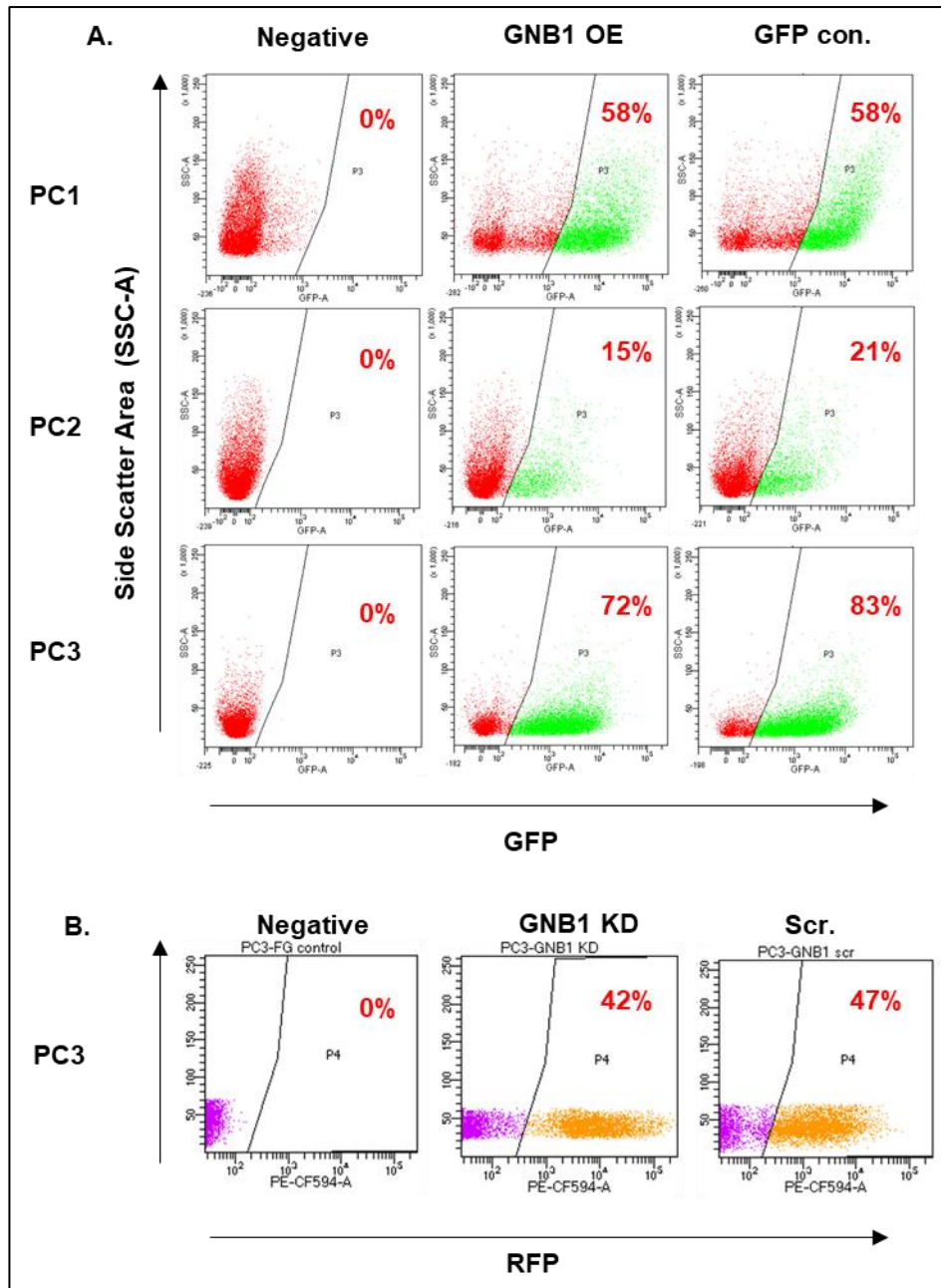


Figure 2: Stable marker gene expression by flow cytometry after lentiviral transduction of PDAC cultures for deregulated target gene expression (n=3).

The transduction efficiency was measured on Day 3 post transduction. PC1 with LV. GNB1 OE was 58%, 58% with the GFP control vector; 15% and 21% of PC2 GNB1 OE and PC2 GFP control; 72% and 83% of PC3 GNB1 OE and PC3 GFP control. N=3, biological replicates. Single values collected from each sample. SSC-A: side scatter Area. PE-CF594-A: flow cytometry parameter used for detecting RFP positive cells. PC: patient-derived PDAC culture; OE: overexpression; KD: knockdown; con.: control; scr.: scramble. GFP: green fluorescent protein; RFP: red fluorescent protein.

3.2.1.2 GNB1 overexpression is detectable on RNA level in the lentiviral mediated overexpression cultures

To validate the expression of GNB1 in the generated PDAC cultures stably overexpressing or knocked-down GNB1 on RNA level, I performed the cell sorting to enrich GNB1 OE, GFP con., GNB1-shRNA KD and sh-scramble vectors transduced cells (GNB1 OE, GFP control, GNB1 KD and scramble control) for the expression of the marker genes GFP and RFP. Next, I examined the GNB1 mRNAs expression in sorted cultures. I designed primer pairs that specifically amplify the codon-optimized (Codon.) and endogenously expressed (Endo.) GNB1 coding sequence. I performed semi-quantitative real-time PCR (qRT-PCR) to determine the GNB1 mRNA level in cells. From the qRT-PCR results, in GNB1 OE of three primary PCs (n=3, biological replicates), mRNAs that transcribed from GNB1 codon-optimized sequence could be detected. In PC1 GNB1 OE, codon-optimized GNB1 mRNA expression levels were 19.3-fold increase compared to endogenous GNB1 mRNAs expression levels, 2.72-fold increase in PC2 GNB1 OE and 13.86-fold increase in PC3 GNB1 OE. As codon-optimized GNB1 coding sequence was not present in GFP control cells, no signal was detectable (Figure 3).

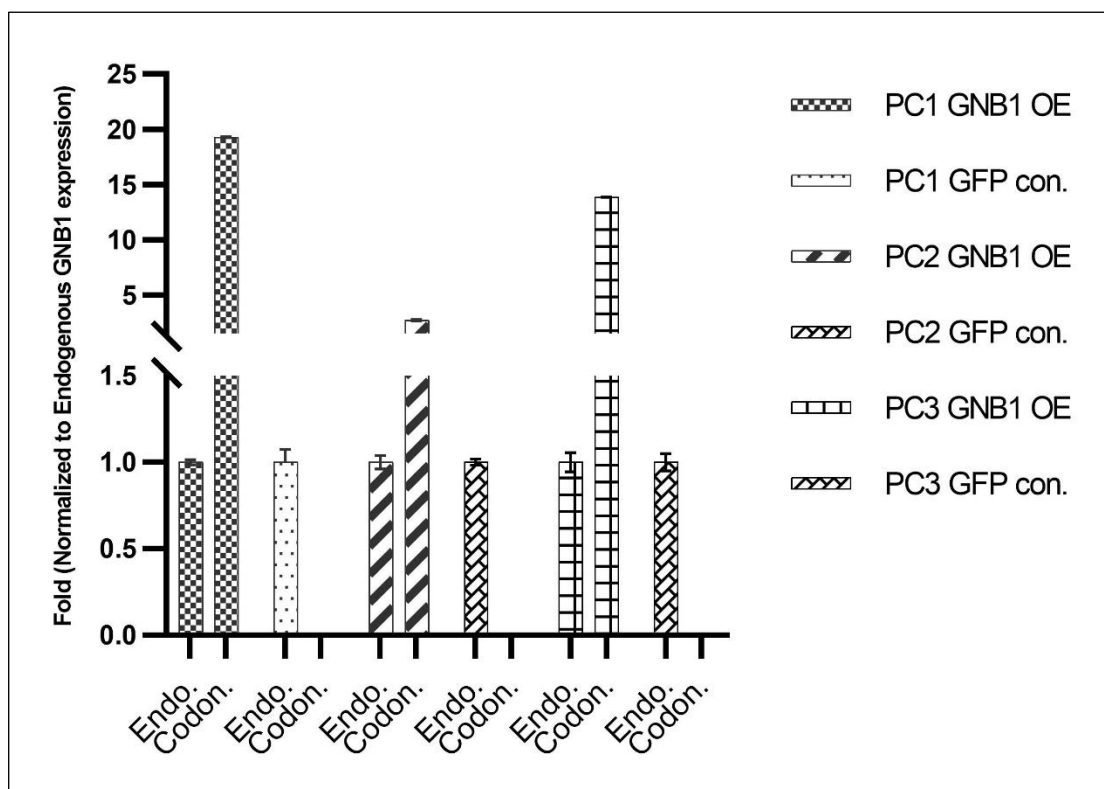


Figure 3: GNB1 overexpression is detectable on RNA level in patient-derived cultures (n=3) after lentiviral transduction.

GNB1 expression on RNA level was detected by qRT-PCR method. In PC1 GNB1 OE, a 19.3-fold increase was observed compared to endogenous GNB1 mRNAs expression level, and 2.72-fold, 13.86-fold increase in PC2 and PC3 GNB1 OE. N=3, technical and biological replicates. Y axis: calculated fold change. β -Actin was used as the reference gene. GNB1 codon-optimized mRNAs expressions were normalized to endogenous GNB1 mRNAs levels. In all GFP con. groups, due to no GNB1 codon-optimized sequence was expressed, therefore no data showed in here. Endo.: endogenous GNB1, and Codon.: codon-optimized GNB1 group. Error bar: standard deviation (SD). OE: overexpression; GFP con.: green fluorescent protein control; PC: patient-derived PDAC culture.

The endogenous GNB1 expression between GNB1 OE and GFP con. of PC1 and PC3 showed less than 10% difference. In PC2, LV. GNB1 OE led to a 41% decreased of endogenous GNB1 compared to PC2 GFP con. (Figure 4). Comparing the endogenous GNB1 expression on the RNA level, PC2 showed the highest GNB1 expression among the three PCs, and the lowest was detected in PC3 (Figure 4).

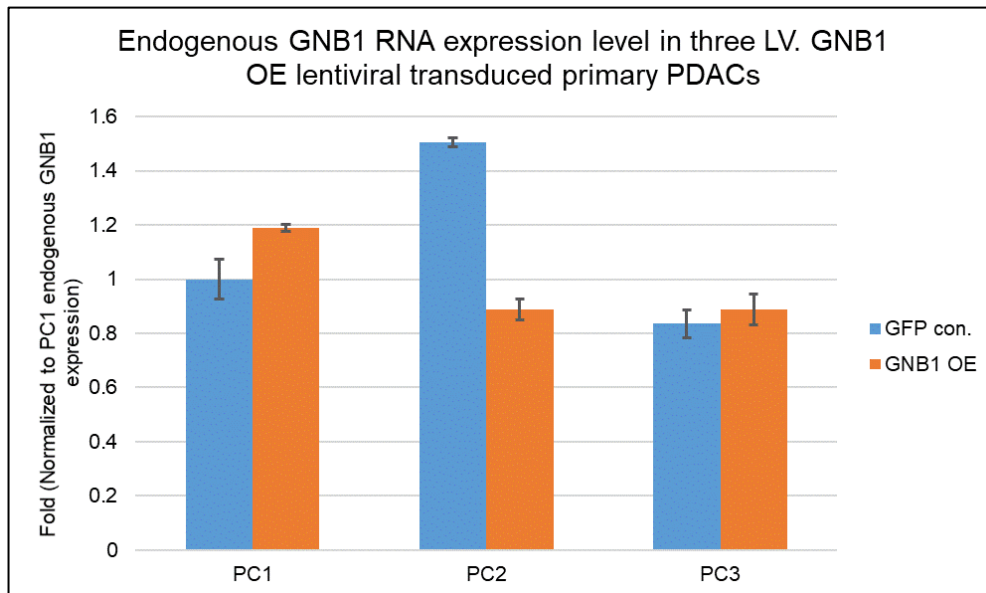


Figure 4: LV. GNB1 OE vector showed mild influence on endogenous GNB1 expression on RNA level in patient-derived cultures (n=3) after lentiviral transduction.

Endogenous GNB1 expression on RNA level was detected by qRT-PCR method. In PC1 and PC3, LV. GNB1 OE vector did not have an influence on the endogenous GNB1 expression. However, in PC2, endogenous GNB1 decreased 41%. Endogenous GNB1 showed highest expression in PC2. Endogenous GNB1 showed less than 10% difference between PC1 and PC2. Endogenous GNB1 expression on RNA level was normalized to PC1 GFP con. culture (n=3, technical and biological replicates). β -Actin was used as the reference gene. Y axis: calculated fold change. Error bar: standard deviation (SD). OE: overexpression; GFP con.: green fluorescent protein control; PC: patient-derived PDAC culture.

These data demonstrated that cells transduced with LV. GNB1 OE vectors stably expressing GNB1 mRNAs and GNB1 mRNAs that transcribed from GNB1 codon-optimized vectors were highly expressed in three PCs GNB1 OE cultures.

3.2.1.3 Validation of deregulated GNB1 expression on protein level in primary PDAC

The contribution in section 3.2.1.3: Previously, Dr. med. Jianpeng Gao generated PC1 GNB1 KD, PC1 Scr., PC2 GNB1 KD and PC2 Scr. cultures. I thawed the vital frozen stocks of these four cultures which stored by Dr. med. Jianpeng Gao and used these cells in the following experiments. I used PC1 GNB1 OE, PC1 GFP con., PC2 GNB1 OE, PC2 GFP con., PC3 GNB1 OE, PC3 GFP con., PC3 GNB1 KD and PC3 Scr. cultures which generated by myself in the following western blot experiments. Further, I performed all western blot experiments.

In the next step, I performed western blot to investigate the expression of GNB1 on protein level. Proteins were extracted from GNB1 OE, GFP control cultures, GNB1 KD and scrambled control transduced cell of all three patient-derived PDAC cultures. After SDS-PAGE and blotting on three membranes, GNB1 and a tubulin antibody were used to examine the GNB1 protein levels. The western blot results indicated that GNB1 was successfully knocked down in PC1, PC2 and PC3 (90%, 70% and 30% knockdown respectively, compared to scramble controls). In GNB1 OE cultures, a 1.2-fold increase (in PC1 and PC2) of GNB1 and up to 1.5-fold in PC3 compared to GFP control transduced cells could be detected (n=3, biological replicates) (Figure 5).

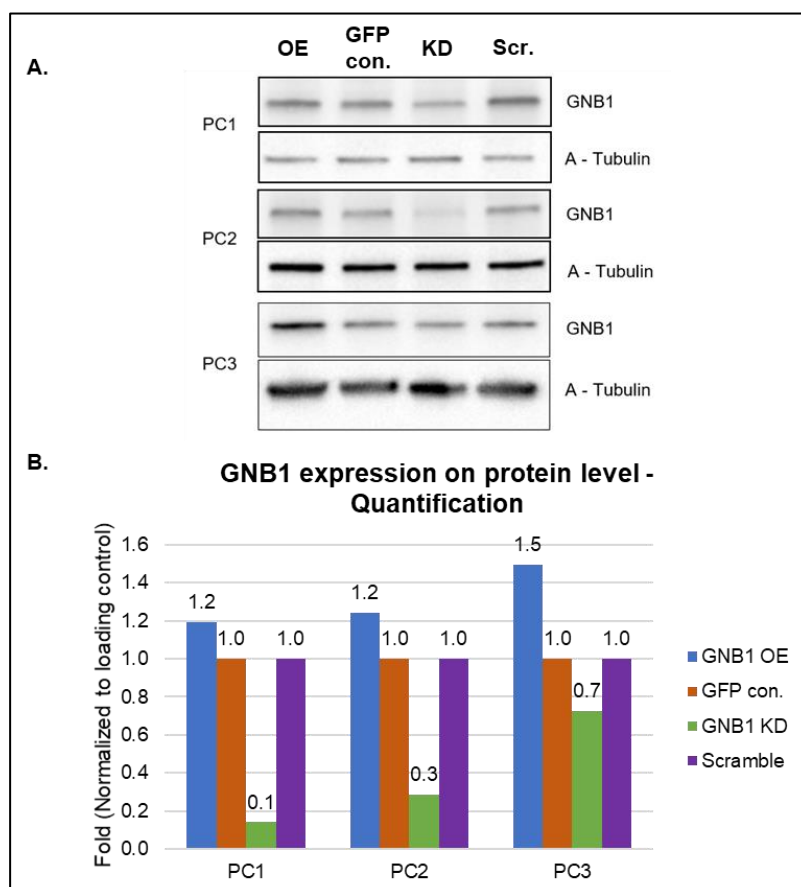


Figure 5: GNB1 expression on protein level in three patient-derived GNB1 overexpression and knockdown cultures (n=3).

A. GNB1 expression on protein level detected by western blot method in PC1, PC2 and PC3 with LV. GNB1 OE, LV. GFP con., LV. GNB1 shRNA KD and LV.sh-scramble. B. Quantification figure depicts the fold change (showed on Y axis) between GNB1 OE vs GFP control, GNB1 KD vs scramble control. Alpha-tubulin was used as loading control. 30 μ g total proteins were loaded in each lane. The results showed GNB1 overexpression could be detected on protein level. In PC1 and PC2, the GNB1 protein knockdown efficiency reached to 90% and 70%. And in PC2, the efficiency was 30%. N=3, biological replicates. OE: overexpression; KD: knockdown; GFP con.: green fluorescent protein control; scr.: scramble; A-Tubulin: alpha-tubulin; PC: patient-derived PDAC culture.

Of note, although on RNA level the detected GNB1 overexpression transcribed from the lentiviral vector exceeded endogenous GNB1 levels 2.7 - 19.3-fold, only moderate overall GNB1 protein overexpression (less than 2-fold) was detectable. One explanation could be that overexpressed GNB1 proteins were degraded, or cells could not tolerate high GNB1 overexpression during culture period. To rule out the technical challenges, I repeated lentiviral transduction of PC1 and PC3 using the LV. GNB1 OE vector by using the same transduction conditions, lentiviral particles from the same batch and similar sorting steps. In the flow cytometry settings, the gate was first set according to the un-transduced control (no GFP or RFP expression) to identify the un-transduced cell population. To increase the purity of GFP positive cells, the sorting gate was applied at 50% of the GFP positive population to sort out highly GFP expressing cells (Figure 6). After sorting, 200 sorted cells were re-measured (Figure 6).

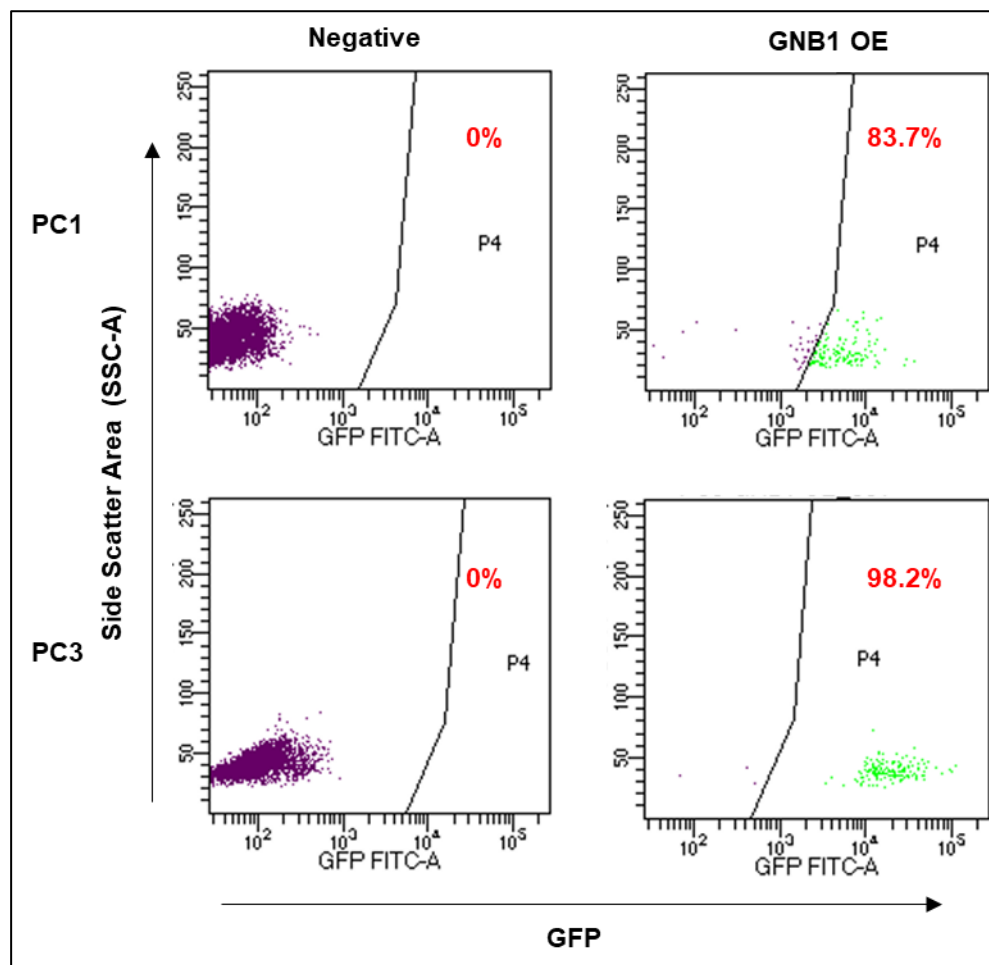


Figure 6: Marker gene expression after flow cytometric enrichment of freshly transduced cells (n=2).

In both PC1 flow cytometry results, sorting gate was set as shown in the images. In negative control of PC3, this gating represented sorting gate. But in GNB1 OE PC3, the gating showed the percentage of GFP positive cells. Sorting efficiency was measured directly after sorting, therefore total 200 cells were measured. GFP positive cells were transduced PC cells. In PC1 and PC3, after the sorting, the GFP positive cells were enriched to 83.7% and 98.2% of total measured living cells. N=2, biological replicates. The experiment was performed once. SSC-A: side scatter area; FITC: the flow cytometry parameter used to detect GFP signal. OE: overexpression; GFP: green fluorescent protein; PC: patient-derived PDAC culture.

In PC1 and PC3, 83.7% and 98.2% are GFP positive respectively after sorting (n=2, biological replicates). Both PC1 and PC2 sorted cells were further expanded for further experimental usages. I performed the western blot to analyse the GNB1 expression in newly generated PC1

and PC3 GNB1 OE cultures. On the protein level, the GNB1 overexpression level in LV. GNB1 OE transduced PC1 was again 2-fold increase compared to GFP control transduced cells and 1.2-fold increase in GNB1 OE transduced PC3 (Figure 7).

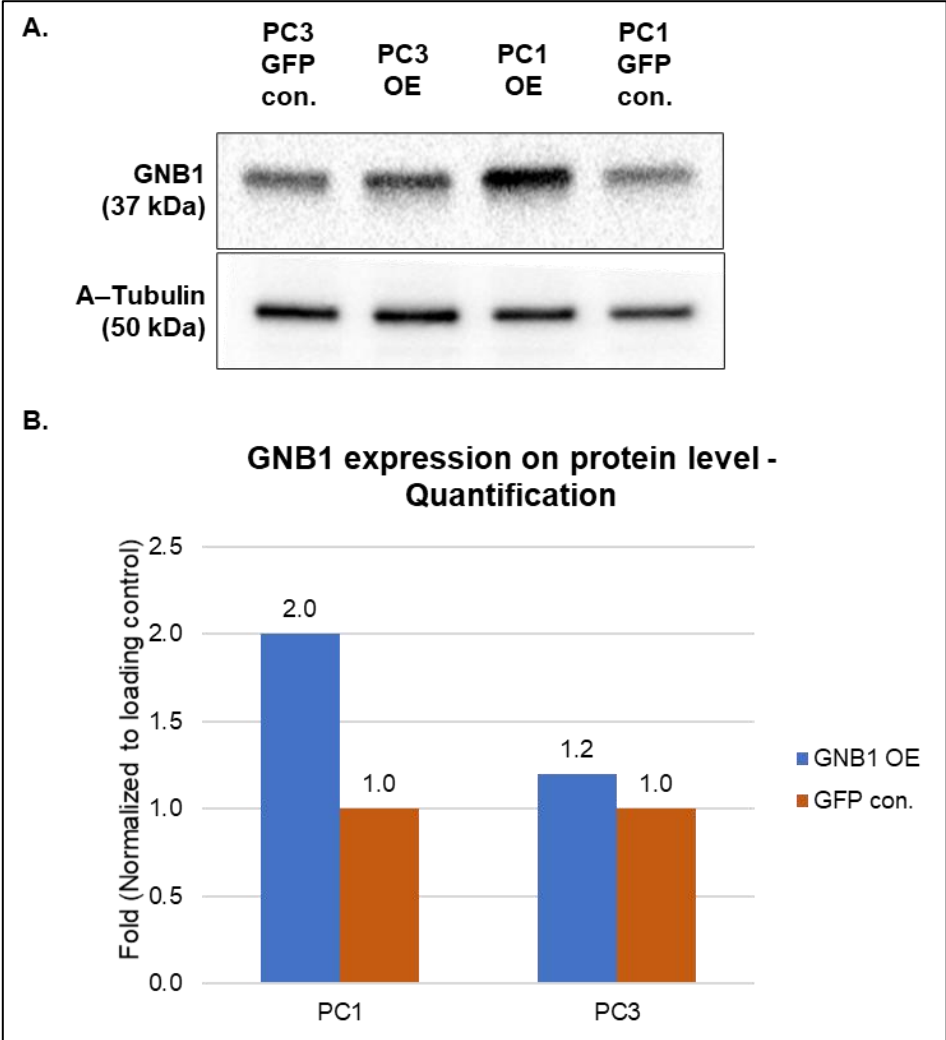


Figure 7: GNB1 overexpression was detectable on protein level in newly transduced PC1 and PC3 cultures (n=2).

A. Western blot results show GNB1 expression level in another independent transduced PC1 and PC3. B. GNB1 protein expression was quantified according to western blot images. GNB1 expression was normalized to A-Tubulin and the fold change GNB1 OE versus GFP con. were calculated. In PC1, 2-fold increase of GNB1 protein detected in PC1 GNB1 OE compared to GFP control, and 1.2-fold increase in PC3. Y axis: calculated fold change. GNB1: 37 kDa; A-Tubulin: 50 kDa. N=2, biological replicates. OE: overexpression; GFP con.: green fluorescent protein control; A-Tubulin: alpha-tubulin; PC: patient-derived PDAC culture.

3.2.1.4 Detection of GNB1 expression by mass-spectrometry based whole protein analysis

The contribution in section 3.2.1.4: I prepared all protein samples for mass-spectrometry based whole protein analysis and submitted samples to the Genomics and Proteomics Core Facility of DKFZ, Heidelberg, Germany for analysis. Mass-spectrometry raw data was first analysed in the core facility. Then data was retrieved from the core facility including the values of proteins pass the quality control. I further analysed the retrived data and generated the figures showed in this section.

While in the GNB1 OE transduced PCs mRNAs that were transcribed from GNB1 codon-optimize lentiviral delivered constructs were highly expressed, only moderate (1.2 - 2-fold increase) GNB1 protein levels could be detected by western blot. To exclude methodological problems of the available three antibodies, western blot procedures, GNB1 protein was detected by mass-spectrometry based whole-protein analysis as an independent methodology. Further this approach could provide additional insights into downstream regulations which are induced by GNB1 overexpression in primary PDAC cultures. I prepared one set of protein samples with three biological replicates (n=3) and sent for analysing by mass-spectrometry.

I submitted PC1, PC2, and PC3 GNB1 overexpression (GNB1 OE), GFP control, GNB1 knockdown (GNB1 KD) and scramble control for the analysis. The submitted proteins were digested and measured the unique peptides and intensity of proteins in the Genomics and Proteomics Core Facility of DKFZ, Heidelberg, Germany. The raw data of the mass-spectrometry was first analysed in the core facility. Then the data was retrieved which included values of proteins that passed the quality control. According to the retrieved data of mass-spectrometry, the identified number of peptides in three PCs which passed the quality control were above 60,000. The average number of identified proteins was 5597, and 4813 of quantified proteins (Figure 8).

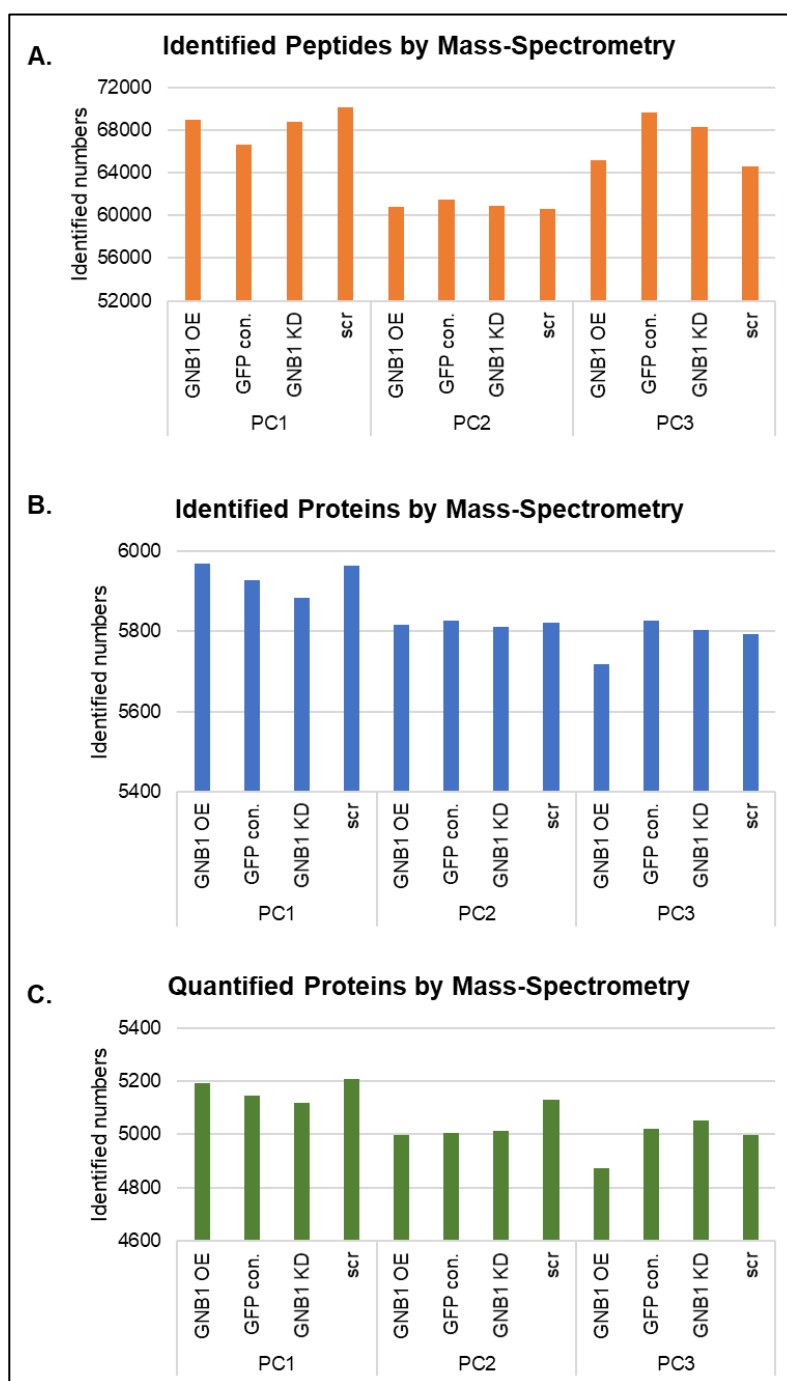


Figure 8: Summary of values of total identified proteins which detected by Mass-spectrometry based whole protein analysis (n=3).

A. Total identified peptides of each sample, B. Total identified proteins of each sample and C. Quantified proteins of each sample. N=3, biological replicates. Y axis: identified numbers. OE: overexpression; KD: knockdown; con.: control; scr.: scramble; GFP con.: green fluorescent protein control; PC: patient-derived PDAC culture.

The GNB1 identified peptide numbers were above 10 in all samples (commonly, peptide numbers more than two mean the detection is reliable) (Figure 9). Then GNB1 expression in GNB1 OE and GFP control, GNB1 KD and scramble were compared in three PCs by using Label-Free Quantification (LFQ) intensity values.

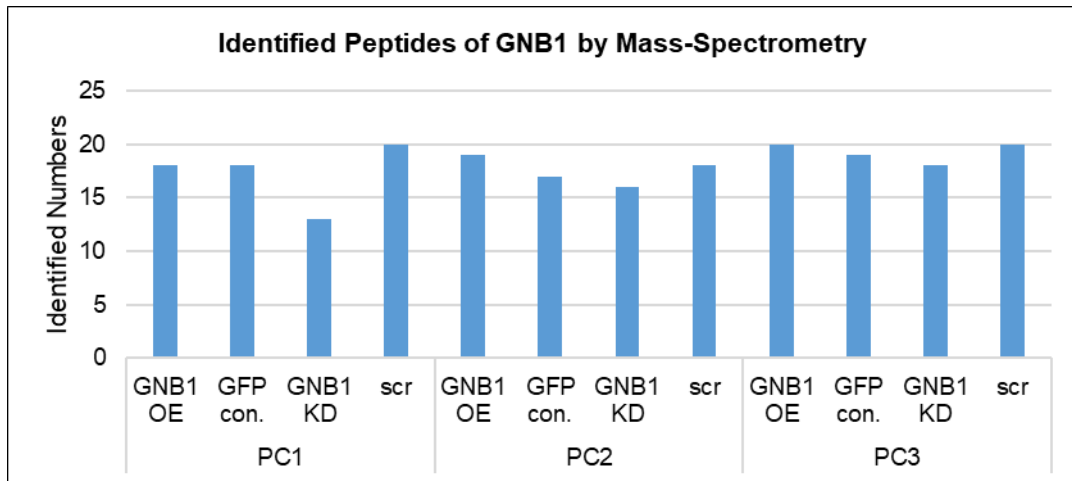


Figure 9: GNB1 expression on protein level was detected by mass-spectrometry (n=3).

The figure shows that the identified peptides of GNB1 by mass-spectrometry in all three PCs transduced cells are above 10. N=3, biological replicates. Y axis: identified numbers. OE: overexpression; KD: knockdown; GFP con.: GFP green fluorescent protein control; scr.: scramble; PC: patient-derived PDAC culture.

In GNB1 overexpression cultures, it was detected a 1.5-fold increase in PC1 GNB1 OE, and 2-fold in PC3 GNB1 OE, and no change in PC2 GNB1 OE compared to each GFP controls (Figure 10). In GNB1 KD PCs, in PC3, 20% less GNB1 protein was detected compared to scramble controls, respectively (Figure 10). In PC1 and PC2, the GNB1 knockdown efficiencies were 70% and 60% (Figure 10). Therefore, the antibody-mediated detection of GNB1 protein by western blot was in line with peptide detection using mass spectrometry.

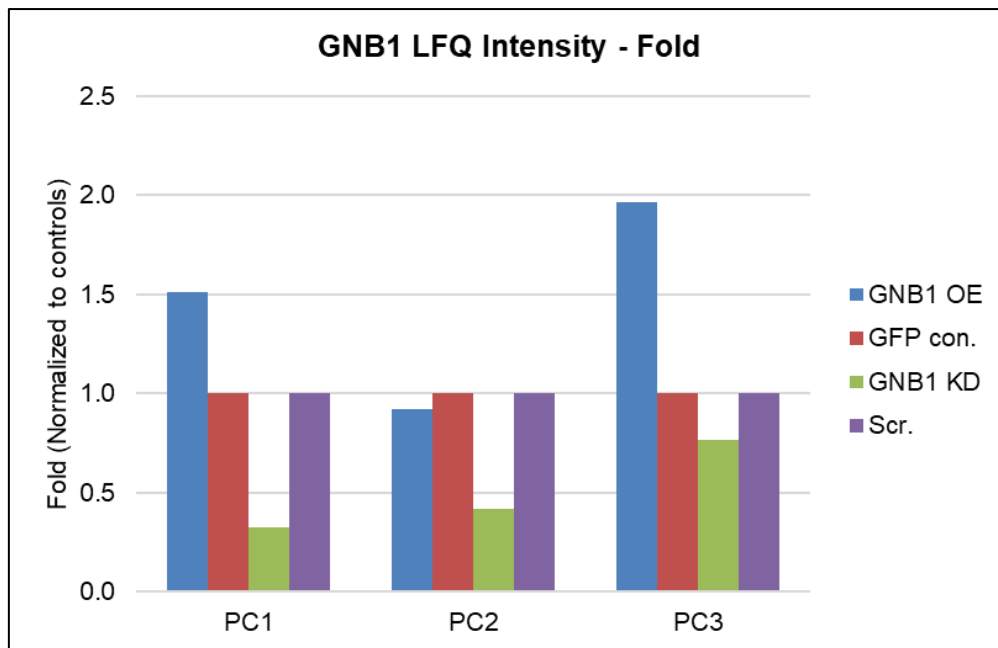


Figure 10: GNB1 overexpression and knockdown on protein level is detected by Mass-spectrometry based whole protein analysis (n=3).

In GNB1 OE group, 1.5-fold and 2-fold increase GNB1 overexpressed were detected compared to GFP con. in PC1 and PC3 GNB1 OE. GNB1 expression decrease in PC2 GNB1 OE. GNB1 was detected knocking down at the efficiency of 70% and 60% in PC1 and PC2 GNB1 KD compared to scramble controls and 20% GNB1 was knocked down in PC3 GNB1 KD. Fold was calculated according to the measured GNB1 Label-Free Quantification (LFQ) intensity. N=3, biological replicates. Y axis: calculated fold change. OE: overexpression; KD: knockdown; con.: control; scr.: scramble; GFP con.: green fluorescent protein control; PC: patient-derived PDAC culture.

G β subunits bind to G α , and G γ subunits and form a complex representing messengers of the GPCRs signalling pathway (McCudden et al. 2005). Therefore, I further filtered out G α subunits and G γ subunits in the retrieved data and compared their LFQ intensity in all three patient-derived PDAC cultures which submitted for mass-spectrometry analysis. In total, eight different G α subunits were detected in all PCs, but among eight G α subunits, G protein subunit alpha 15 (GNA15) expression was low compared to the other seven (Figure 11).

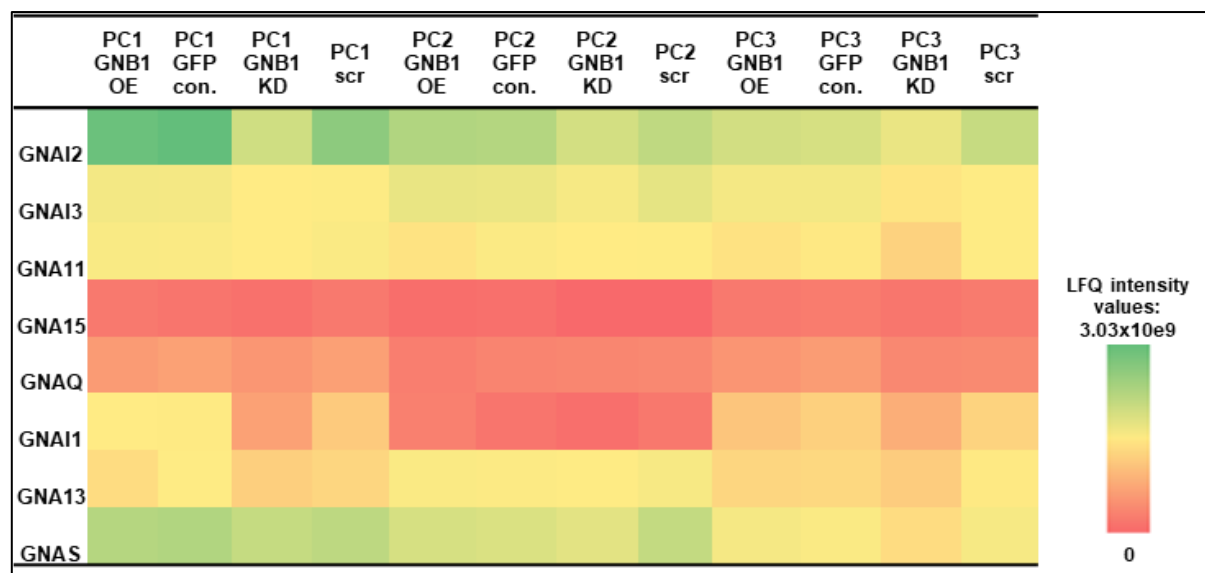


Figure 11: Heat-map of G protein alpha subunits LFQ intensity detected by mass-spectrometry in genetically engineered PCs (n=3).

Eight G protein alpha subunits were detected by mass-spectrometry in genetically engineered PCs. GNAI2 shows the highest expression in all samples, and GNA15 shows the lowest expression. Colour code was set according to the measured Label-Free Quantification (LFQ) intensity, ranged from 0 to 3.03x10e9. N=3, biological replicates, OE: overexpression; KD: knockdown; GFP con.: green fluorescent protein control; scr.: scramble; PC: patient-derived PDAC culture.

Moreover, G γ 12 was the only G protein gamma subunit that was detected in all three PCs, and G γ 5 expressed in PC1 and PC3 (Table 3). In PC2, the detected unique peptides numbers were all below two, which suggested that G γ 5 might not be expressed on the high level (Table 3).

Table 3: Unique peptide numbers of identified G protein gamma subunits detected by mass-spectrometry (n=3).

	PC1 GNB1 OE	PC1 GFP con.	PC1 GNB1 KD	PC1 scr	PC2 GNB1 OE	PC2 GFP con.	PC2 GNB1 KD	PC2 scr	PC3 GNB1 OE	PC3 GFP con.	PC3 GNB1 KD	PC3 scr
GNG5	3	3	3	3	1	1	0	0	3	1	2	1
GNG12	4	4	6	6	5	5	5	5	5	5	4	5

N=3, biological replicates. Abbreviations in the table: OE: overexpression; KD: knockdown; GFP con.: green fluorescent protein control; scr.: scramble; PC: patient-derived PDAC culture.

3.2.1.5 GNB1 overexpression is detectable by immunofluorescence in primary PDAC cultures

Western blot and mass-spectrometry both detected moderate (1.2 - 2-fold increase) GNB1 protein levels in GNB1 OE PCs. It was further suspected, as another possibility, that a high level of GNB1 overexpression was only present in cells with low endogenous GNB1 expression, and this high-level overexpression was diluted in the bulk population. Western blot reflected the mean expression in the bulk population. Therefore, I performed an immunofluorescence experiment using PC1 to investigate the GNB1 protein expression on the single-cell level. LV. GNB1 OE (GNB1 OE) and LV. GFP control vector (GFP con.) transduced cells were triple stained with GNB1-Alexa Fluor 647, GFP-Alexa Fluor 448, and DNA-Hoechst. A GFP single staining was also included to study the percentage of transduced cells directly. I measured and analysed all fluorescence signals under the same settings. I used PC1 GFP control vector transduced cells for parameter settings at first. The long-term laser exposure to adjust the settings caused bleaching of the sample leading to a weaker signal compared to PC1 GNB1 OE. Transduced cells were nearly 100% in the bulk population. GNB1 protein was observed to be located on the cell membrane which was in line with the cellular localization reported in the literature (Campbell and Smrcka 2018). Moreover, GNB1 was overexpressed in PC1 GNB1 OE compared to PC1 GFP control vector transduced cells (Figure 12). This further validated that GNB1 was overexpressed in GNB1 OE vector transduced PCs.

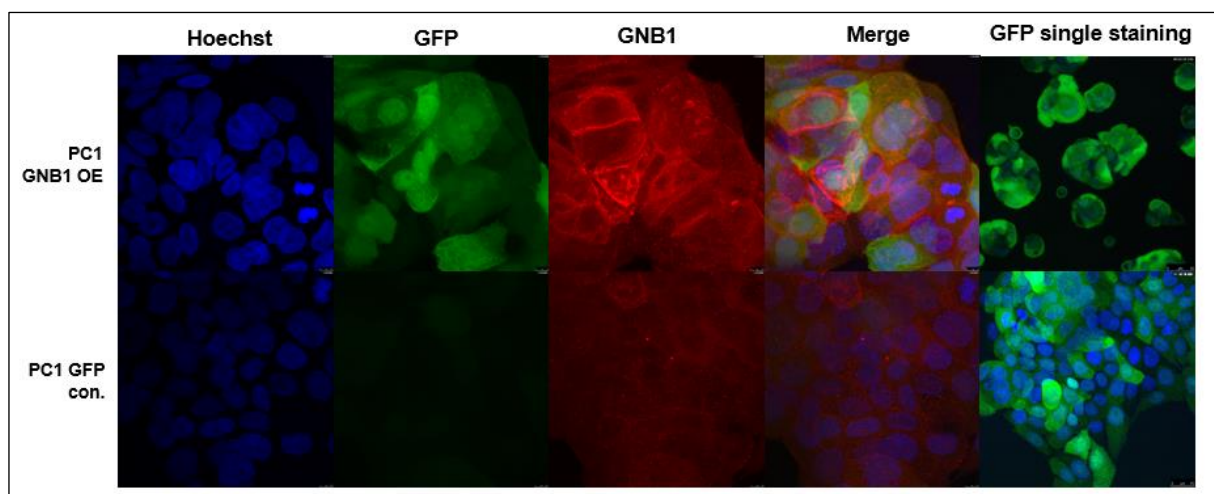


Figure 12: GNB1 overexpression detected by immunofluorescence staining on PC1 (n=1).

PC1 GNB1 OE and PC1 GFP control transduced cells were used in this experiment. GNB1 overexpression could be detected in PC1 GNB1 OE. PC1 GFP con. was used for adjusting the settings of parameters. Nuclear DNA was stained by Hoechst (Blue), then GFP stained by Alexa Fluoro 448 (Green), and Alexa Fluoro 647 as the 2nd antibody was used to visualize GNB1 protein (Red). GFP-Alexa Fluoro 448 was also included reflected the percentage of transduced cells. All fluorescence were measured under the same settings. N=1. OE: overexpression; GFP con.: green fluorescent protein control; PC: patient-derived PDAC culture.

3.2.1.6 Influence of GNB1 expression on cell cycle and cell apoptosis

The contribution in section 3.2.1.6: Dr. med. Jianpeng Gao performed cell cycle analysis by using PC1 GNB1 KD, PC1 Scr., PC2 GNB1 KD and PC2 Scr. cultures. I further expanded the cell cycle analysis dataset by including PC1 GNB1 OE vs PC1 GFP con., PC2 GNB1 OE vs PC2 GFP con., PC3 GNB1 OE vs PC3 GFP con. and PC3 GNB1 KD vs PC3 Scr. Results showed in this section combined the data from Dr. med. Jianpeng Gao and mine.

Previously, Dr. med. Jianpeng Gao demonstrated both *in vivo* and *in vitro* that lentiviral mediated overexpression of GNB1 promoted cell proliferation (Gao 2017). Moreover, the cell cycle analysis was performed using the two individual patient-derived PDACs (PC1 and PC2) which were transduced with two individual GNB1 knockdown vectors to investigate whether the loss of GNB1 alters cell cycle distribution. In this project, to expand the previous cell cycle analysis experimental dataset, I further included PC1 and PC2 GNB1 OE and GFP con. In addition, I analysed cell cycle in PC3 GNB1 KD and PC3 Scr. DNA was stained by PI, and Ki67 antibody staining was used to distinguish cells in G0 and G1 phase. By using this method, the G0 phase as the quiescence phase, first growth phase G1, and DNA replication phase S phase together with G2 and mitosis phase can be detected. I performed the cell cycle analysis three times (n=3, technical replicates) by including PC1, PC2 and PC3 patient-derived cultures (n=3, biological replicates). Then, I performed the t-test to access whether the observed difference between two groups were statistically significant.

In PC1, compared to GNB1 Scr. cells, 17.1% more GNB1 KD cells were enriched in the G0 phase (the change of G0 phase PC1 GNB1 KD vs PC1 Scr. was statistically insignificant, p=0.17, t-test), and the G0 phase cell population were similar in GNB1 OE, GFP con. and GNB1 Scr. (mean value, GNB1 OE:26.77%; GFP con.: 32.95%; GNB1 KD: 46.33%; Scramble: 29.23%; Figure 13). However, in PC2 and PC3, in each cell cycle phases, there was no difference by comparing GNB1 OE or GNB1 KD to each control, respectively (statistically insignificant, all p>0.1, t-test; Figure 13).

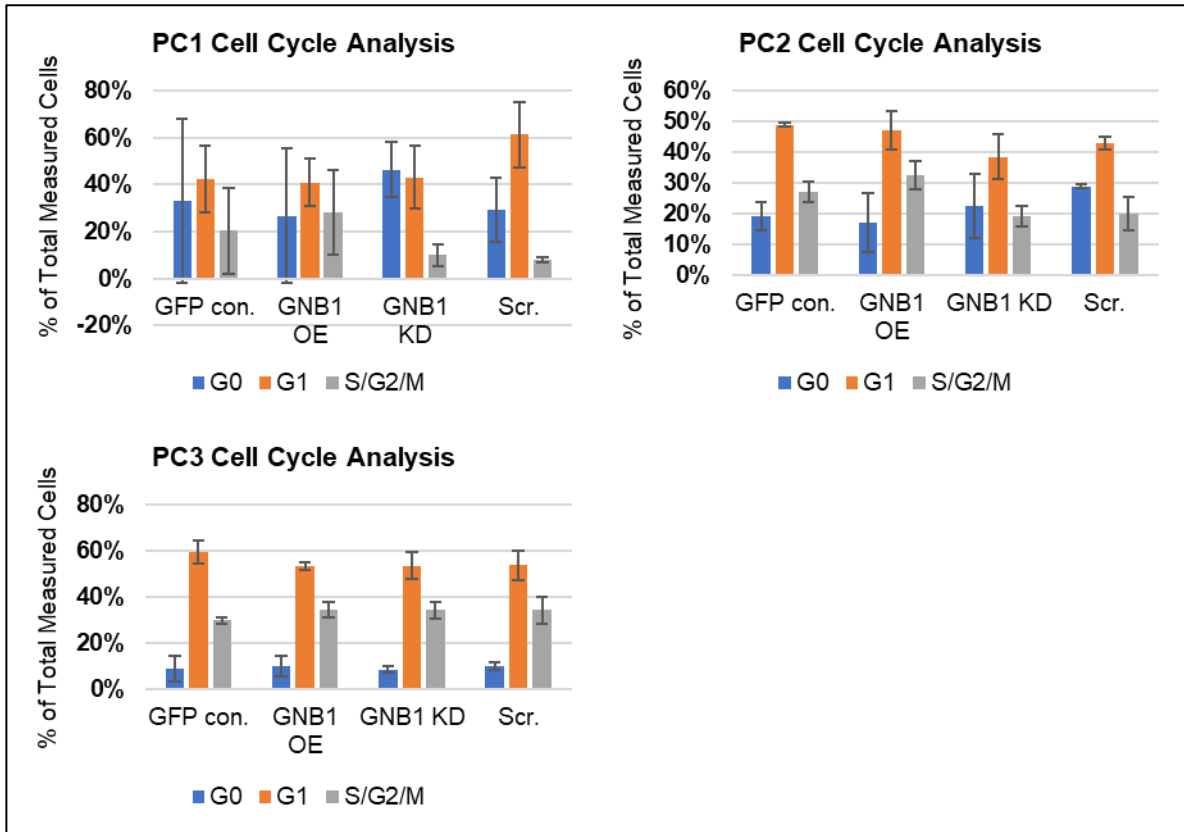


Figure 13: Influence of GNB1 expression on cell cycle in three PCs (n=3).

In PC1 GNB1 KD, 17.1% more cells arresting in G0 phase compared to PC1 scramble control (p=0.17, t-test). And in PC2 and PC3, it showed similar results. However, in all three PCs, GNB1 overexpression did not show the influence on the cell cycle compared to each GFP control (all p > 0.1, t-test). N=3, biological and technical replicates. Triplicates were measured to calculate the mean of each cell cycle phase in each culture. Error bar stands for the standard deviation of the mean. OE: overexpression; KD: knockdown; GFP con.: green fluorescent protein control; Scr.: scramble; G0: cell cycle G0 phase; G1: cell cycle G1 phase; S/G2/M: cell cycle S, G2 and mitosis phases; PC: patient-derived PDAC culture.

And the detailed percentage numbers are summarized in Table 4.

Table 4: Summary of the influence of GNB1 on cell cycle (n=3).

	PC1 (Mean % of total measured cells)			
	GNB1 OE	GFP con.	GNB1 KD	Scramble
G0	26.77%	32.95%	46.33%	29.23%
G1	40.90%	42.50%	43.07%	61.27%
S/G2/M	28.27%	20.45%	9.93%	8.00%

	PC2 (Mean % of total measured cells)			
	GNB1 OE	GFP con.	GNB1 KD	Scramble
G0	19.33%	17.20%	22.55%	28.95%
G1	48.77%	47.17%	38.35%	42.85%
S/G2/M	27.07%	32.60%	19.15%	19.95%

	PC3 (Mean % of total measured cells)			
	GNB1 OE	GFP con.	GNB1 KD	Scramble
G0	9.00%	9.93%	8.43%	10.13%
G1	59.13%	53.40%	53.53%	53.63%
S/G2/M	29.80%	34.50%	34.13%	34.13%

Mean values were calculated from the triplicates of each cell cycle phase in each culture. N=3, biological and technical replicates. OE: overexpression; KD: knockdown; GFP con.: green fluorescent protein control; Scr.: scramble; G0: cell cycle G0 phase; G1: cell cycle G1 phase; S/G2/M: cell cycle S, G2 and mitosis phases; PC: patient-derived PDAC culture.

Of note, cell apoptosis of lentivirally transduced PCs was analysed by Dr. Gao to investigate whether knockdown of GNB1 led to programmed cell death. The proportion of living, early apoptosis, late apoptosis and necrosis cell populations did not have any difference in PC1 (Gao 2017). However, in PC2, 23% of necrotic cells were detected in GNB1 KD culture compared to scramble control transduced cells, with only 10% of necrotic cells (Gao 2017, pg. 80). However, this result was reported as statistically insignificant (Gao 2017, pg. 80).

3.2.2 Validation experiments of SLC35F5 as TIC regulator in PDAC

3.2.2.1 Generation of primary PDAC cultures with stable SLC35F5 knockdown or overexpression

The second candidate of TIC regulators identified was *SLC35F5*. Since little was known of SLC35F5 in PDACs, I first investigated the endogenous *SLC35F5* expression on RNA level by the qRT-PCR method in PC3, PC4, PC5, PC6, PC7 and HeLa cells (n=6, biological replicates, Figure 14). Only in PC3, *SLC35F5* expression on RNA level was about 1.5-fold higher compared to the expression in HeLa cells, whereas in PC4, PC5, PC6 and PC7 the expression was above 4-fold compared to HeLa cells. *SLC35F5* was higher expressed in PDACs compared to in HeLa cells on the RNA level.

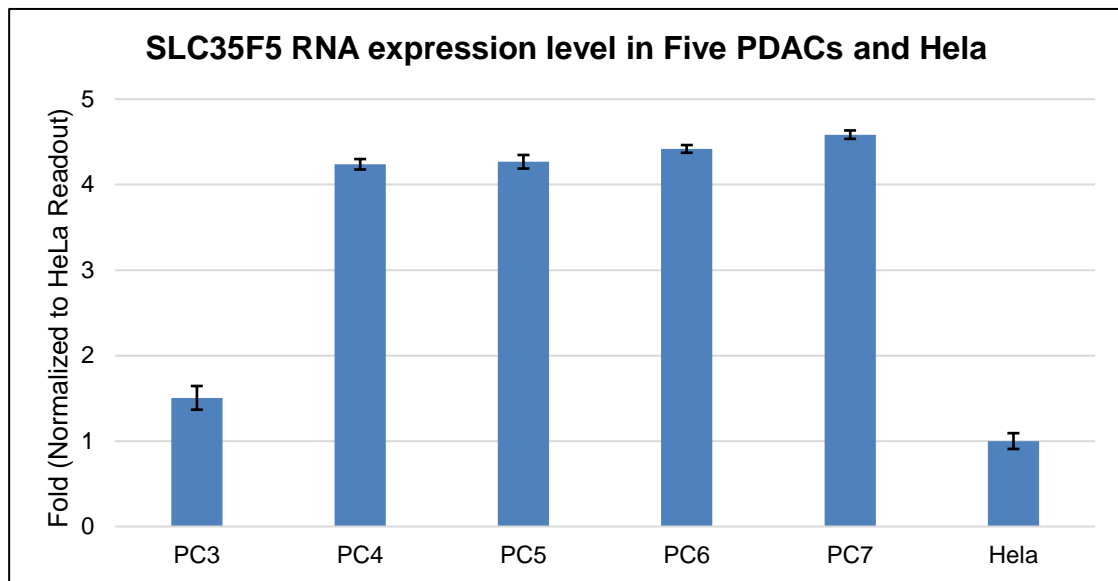


Figure 14: SLC35F5 expression in five primary PDAC cultures compared to HeLa cells on RNA level (n=6).

The designed specific pair of primers was used to detect SLC35F5 mRNAs. β -Actin was used as the house keeping gene. The SLC35F5 mRNA expression level was normalized to the SLC35F5 expression in HeLa cells. 1.5-fold higher expression of SLC35F5 showed in PC3 compared to HeLa, and SLC35F5 expressed over 4-fold in PC4, PC5, PC6 and PC7 compared to HeLa cells on RNA level. N=6, biological replicates. Y axis: calculated fold change. Error bar stands for the standard deviation of the mean. PC: patient-derived PDAC culture.

To establish the stable SLC35F5 knockdown in PDACs, I cloned two individual shRNAs targeting *SLC35F5* into a Doxycycline inducible knockdown vector (pRSIT17-U6Tet-sh-HTS6-CMV-TetRep-2A-TagGFP2-2A-Puro) including GFP as a marker gene. Next, SLC35F5 KD lentivirus vector stocks (SLC35F5 shRNA1 and shRNA5) were produced.

According to the trapping vector screening followed by the genome-wide integration sites analysis, the integration sites of the trapping vector were between Exon 9 and Exon 10 leading to a partially overexpression of the *SLC35F5* gene (Gao 2017, pg. 60). Therefore, I cloned the SLC35F5 full coding sequence (SLC35F5 CDS) and the SLC35F5 truncated (TR, Exon 10 to the end of CDS) sequence into the multiple cloning sites of pCCL_pptPGK_IRES_GFP_PRE vector with GFP expression. Moreover, I generated the lentivirus stocks of both overexpression vectors.

I transduced PC1 cells with LV. SLC35F5 KD (shRNA1 and shRNA5) particles at MOI5, and scramble control at MOI1. LV.SLC35F5 CDS OE, LV. SLC35F5 TR OE and LV. GFP con. particles were transduced into PC1 at MOI 1. I measured the transduction efficiency by flow cytometry on Day 3 post-transduction. The transduction efficiency of PC1 with LV. SLC35F5 KD (shRNA1) was 53.8% of living cells; LV. SLC35F5 KD (shRNA5) was 56.6%, and scramble control was 49.4% (Figure 15).

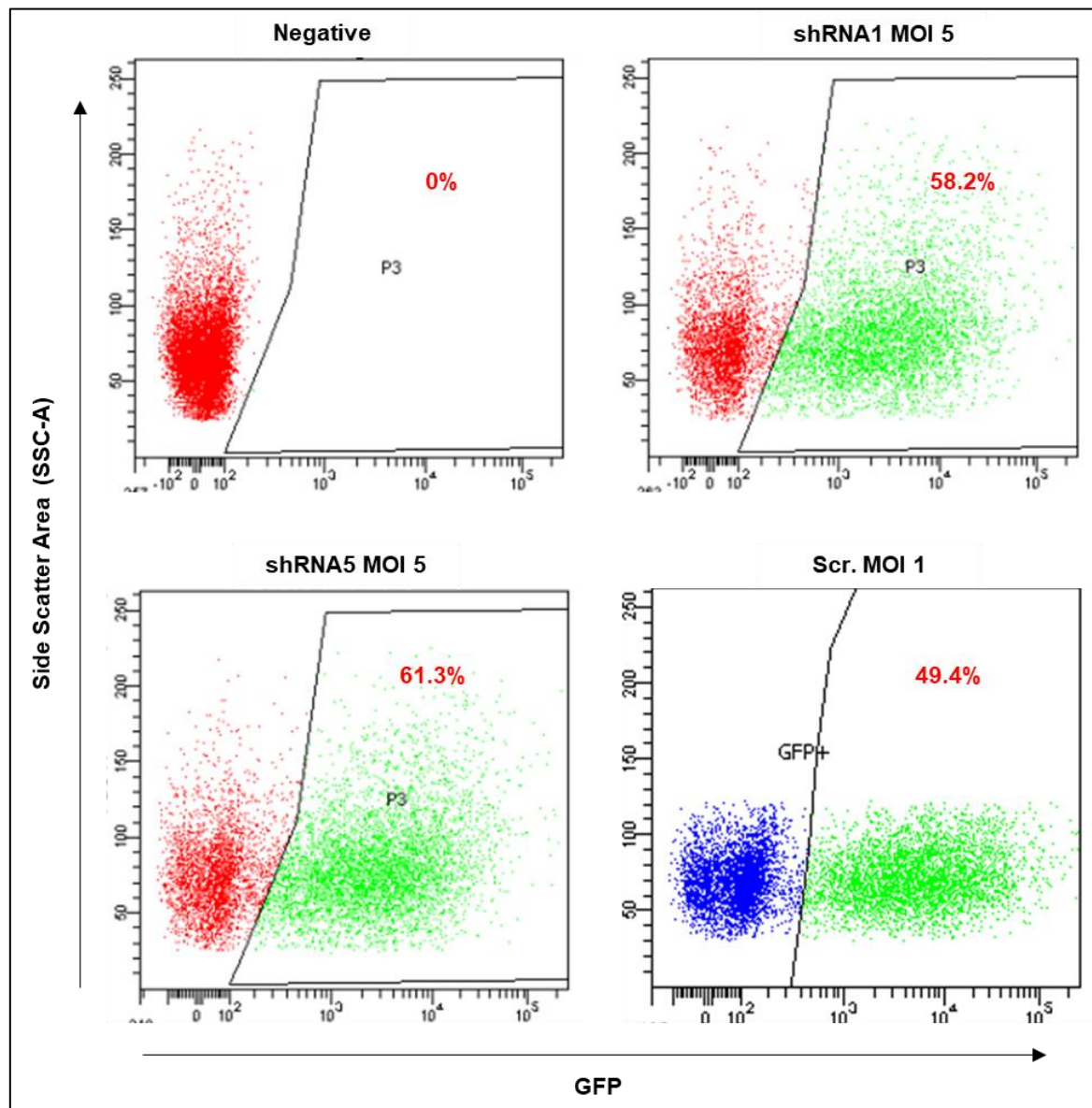


Figure 15: FACS analysis showed efficient marker gene expression in PC1 three days post transduction (n=1).

The established SLC35F5 shRNA1 and shRNA5 were transduced PC1 at MOI 5, and scramble control at MOI 1. The transduction efficiency was measured on Day 3 post-transduction. The transduction efficiency of LV. SLC35F5 KD (shRNA1) and LV. SLC35F5 KD (shRNA5) were 58.2% and 61.3% at MOI5, and 49.4% of LV. sh-scramble at MOI 1. N=1. Scr.: scramble; P3: Gate 3; GFP+: GFP positive; GFP: green fluorescent protein; MOI: multiplicity of infection.

The transduction efficiency of PC1 SLC35F5 CDS overexpression was 32.4% of measured living cells; PC1 SLC35F5 TR overexpression was 21.4%, and GFP control was 17.8% (Figure 16). I further sorted these transduced cells to enrich the GFP positive cells to over 90% and

immediately seeded in the 6-well-plate for the colony formation assays. The later passages of sorted cells were used for PCR and western blot to investigate SLC35F5 expression on RNA and protein levels.

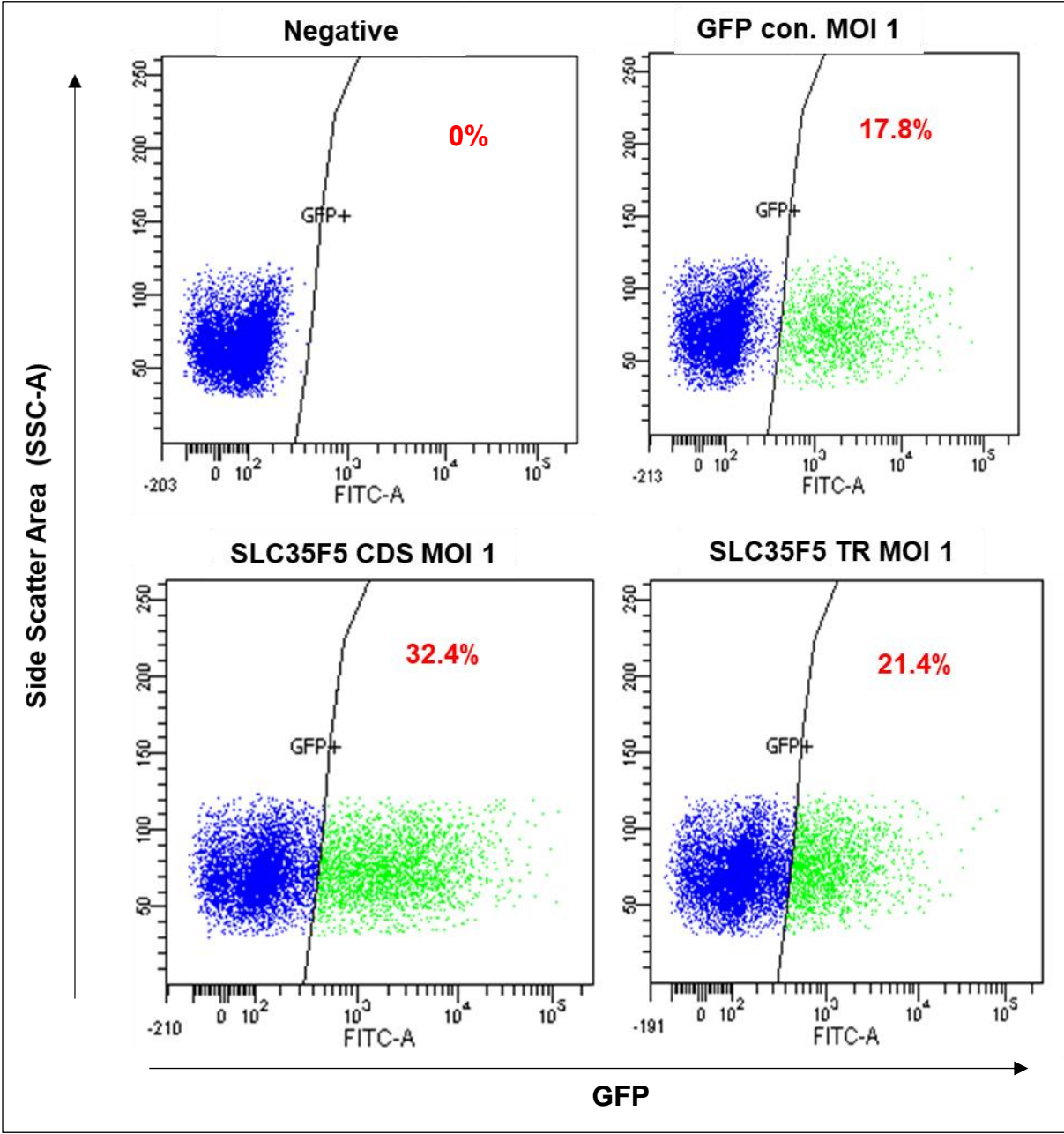


Figure 16: Measurement of lentiviral SLC35F5 overexpression vector transduction efficiency in PC1 (n=1). The established SLC35F5 CDS and TR were transduced PC1 at MOI 1, and GFP control at MOI 1. The transduction efficiency was measured on Day 3 post-transduction. The living GFP+ cells represent the transduced cells. The transduction efficiency of LV. GFP con. was 17.8% with the titer MOI1. 32.4% and 21.4% were the transduction efficiency of LV. SLC35F5 CDS OE and LV. SLC35F5 TR OE. CDS stands for full coding sequence and truncated of TR. N=1.con.: control; CDS: full coding sequence; TR: SLC35F5 truncated; GFP+: GFP positive; FITC: the flow cytometry parameter used to detect GFP signal. GFP: green fluorescent protein.

3.2.2.2 Validation of deregulated SLC35F5 expression on RNA and protein level in primary PDAC

I performed qRT-PCR and western blot to investigate the SLC35F5 expression in SLC35F5 knockdown and overexpression cells. To analyse SLC35F5 knockdown, I harvested LV. SLC35F5 KD shRNA1, 5 or scramble control transduced PC1 cells after 72 hours Doxycycline (1 $\mu\text{g/ml}$) treatment, to induce shRNA expression, for RNA and protein extraction. On the RNA level, SLC35F5 KD shRNA1 showed 53% knockdown efficiency compared to scramble control, and 12% in SLC35F5 KD shRNA5 transduced cells (Figure 17A). On the protein level, 11% less SLC35F5 protein in shRNA1 transduced PC1 was detected compared to PC1 scramble control cells (Figure 17B). Next, I evaluated the overexpression of SLC35F5 after transduction of PC1. LV. SLC35F5 CDS OE and LV. SLC35F5 TR OE transduced cells showed a 7.21-fold and 6.81-fold increase compared to the PC1 GFP con. on RNA level, respectively (Figure 17A). On the protein level, no overexpression of SLC35F5 either the full protein encoded by the CDS or the truncated version (TR) could be observed compared to GFP control (Figure 17B).

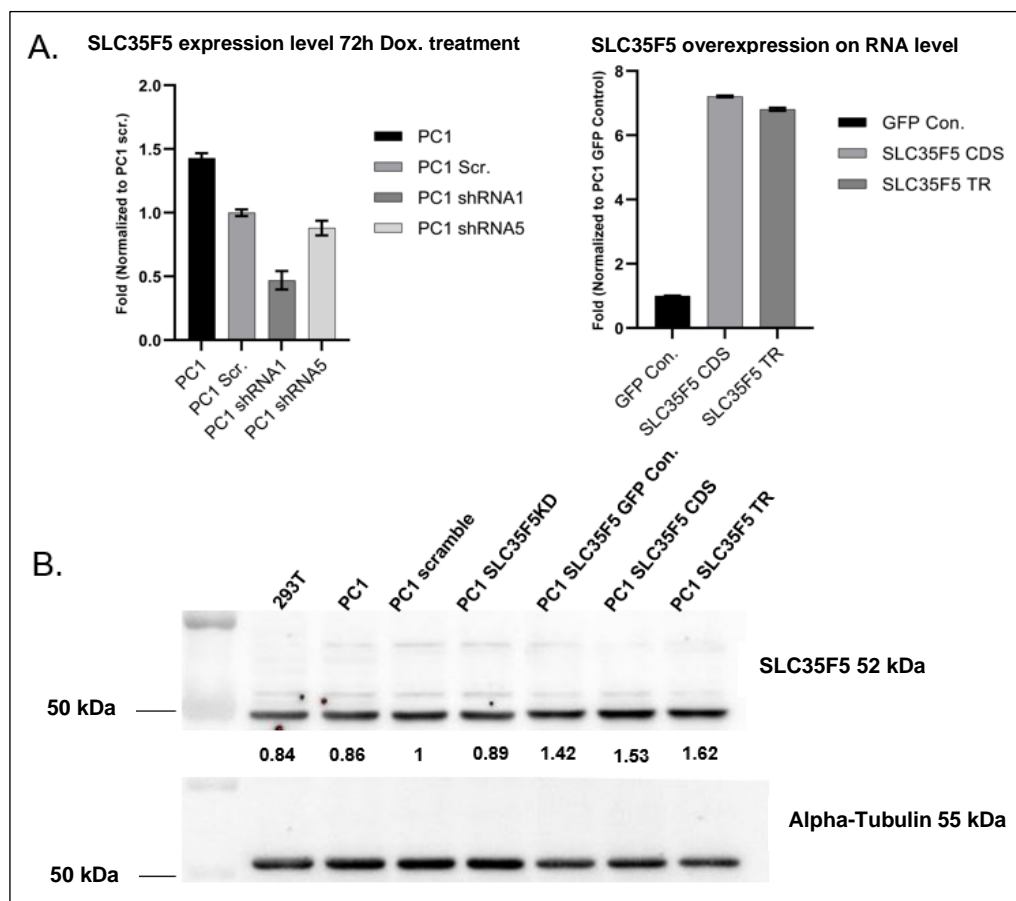


Figure 17: Investigation of SLC35F5 expression on RNA and protein level in PC1 transduced cells (n=1).

A. SLC35F5 expression level on RNA level detected by qRT-PCR. SLC35F5 KD cells were treated with Doxycycline (Dox, 1 $\mu\text{g/ml}$) for 72 hours. 53% knockdown efficiency achieved by using SLC35F5 LV. shRNA1 compared to scramble control, and 12% in SLC35F5 LV. shRNA5 transduced cells. On RNA level, 7.21-fold and 6.81-fold increase of SLC35F5 mRNAs expression were detected in LV. SLC35F5 CDS OE and LV. SLC35F5 TR OE transduced cells compared to GFP con. Error bar stands for the standard deviation of the mean. B. SLC35F5 expression level on protein levels detected by western blot. 293T cells were the positive control of the SLC35F5 antibody. No overexpression and knock down of SLC35F5 detected in both SLC35F5 overexpression and knockdown cells compared to each control. N=1. Alpha-tubulin was used as the loading control. CDS: full coding sequence; TR: SLC35F5 truncated; KD: knockdown; kDa: kilodalton; GFP con.: green fluorescent protein control; PC: patient-derived PDAC culture.

3.2.2.3 Influence of SLC35F5 expression on colony formation

I first performed the colony formation assay *in vitro* to investigate the influence of SLC35F5 deregulation on PDAC cells. Un-transduced PC1 cells were first seeded in 6-well-plate at a density of 50, 100, 200, 400, 800 and 1000 cells/well, to identify the proper seeding number to avoid the colonies merging. I kept this plate in culture for 14 days, and during the culturing time medium was changed every two days to prevent re-seeding of floating cells. On Day 14 after cell seeding, cells were fixed by methanol and stained with 2% crystal violet. Seeding of 400 cells/well revealed that the cells grow well and that colonies did not overlap (Figure 18). Therefore, this concentration was further used in the following colony formation experiments.

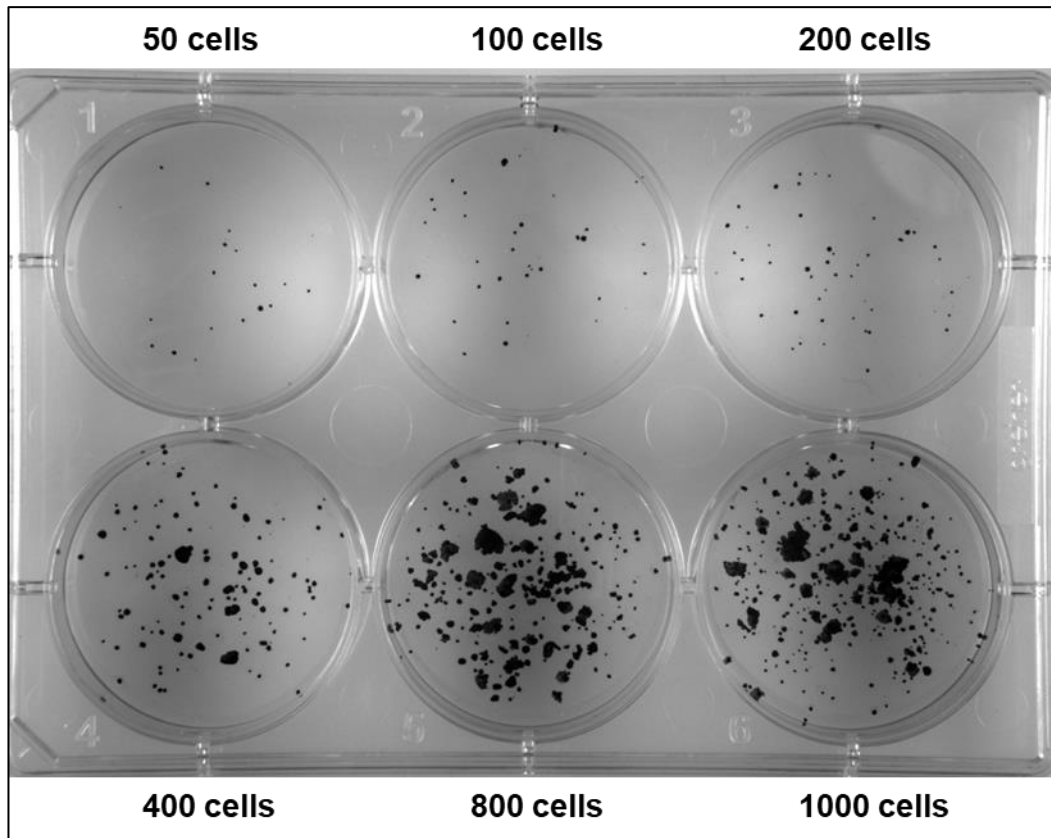


Figure 18: Pre-experiment of PC1 colony formation assay (n=1).

50, 100, 200, 400, 800 and 1000 PC1 cells were seeded into 6-well-plate and cultured for 14 days. After 14 days, cells were fixed with 2% methanol and stained with 2% crystal violet. N=1. PC: patient-derived PDAC culture.

I seeded LV. SLC35F5 KD shRNA1, and scramble control; LV. SLC35F5 CDS OE, LV. SLC35F5 TR OE and GFP control transduced PC1 cells into 6-well-plates (400 cells/well), and triplicates were set for each culture (n=3, technical replicates). Cells were kept in culture for 14 days, fixed and stained and then counted by using ImageJ software.

In the SLC35F5 KD group, colonies formed by PC1 SLC35F5 KD cells showed bigger sizes compared to PC1 un-transduced cells and PC1 scramble controls. The median number of colonies in three wells of PC1 SLC35F5 KD was also more than the other two groups, but compared to scramble control, the difference of colonies numbers between two groups showed statistically insignificant ($p=0.35$, t-test). (Figure 19).

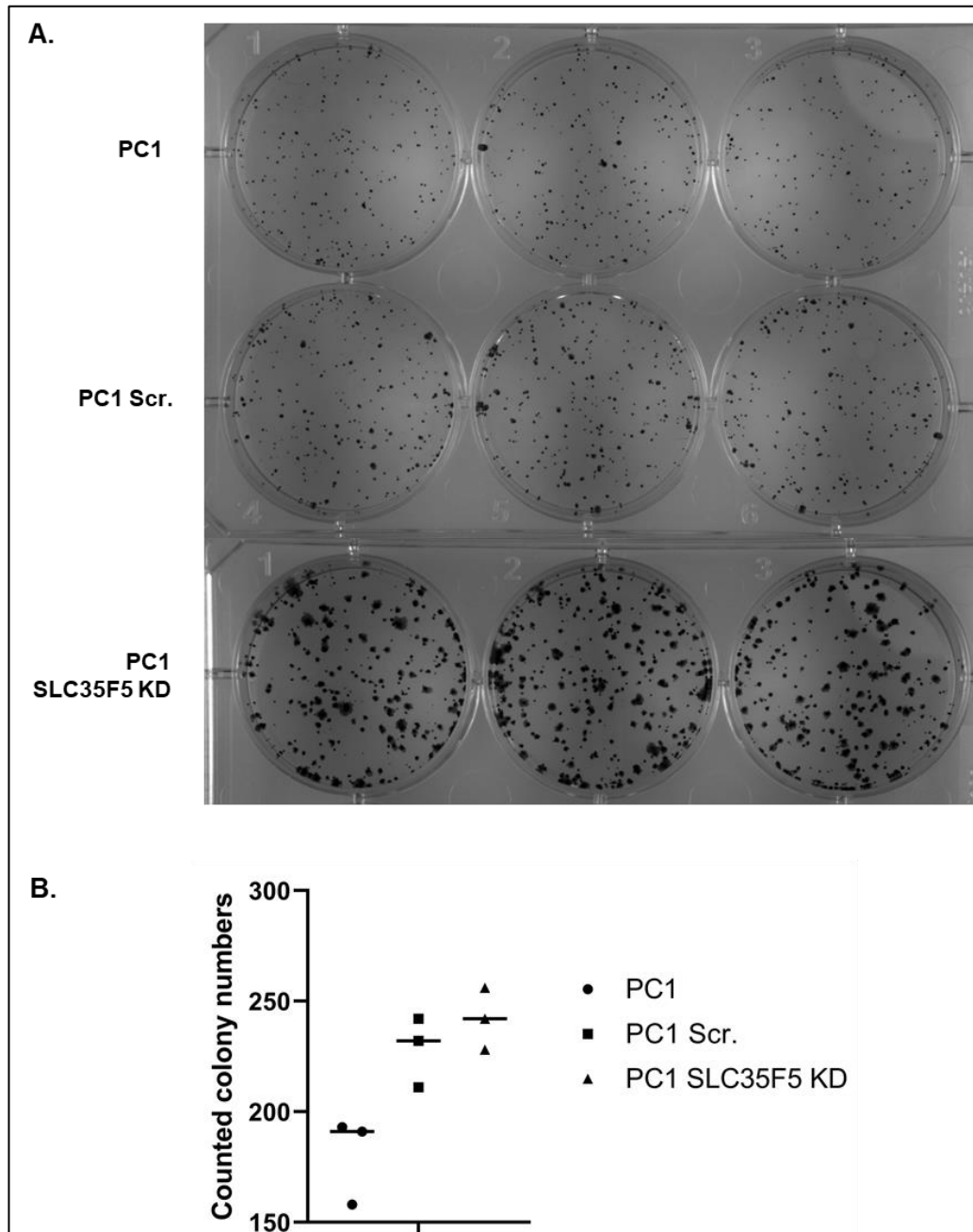


Figure 19: Colony formation of PC1 after lentiviral mediated SLC35F5 knockdown (n=3).

A. Image of colony formation assay. From the image, it was observed that the size of PC1 SLC35F5 KD colonies was bigger as well which suggested SLC35F5 KD may have an influence on cell growth. Established PC1 SLC35F5 KD, scramble and PC1 un-transduced cells were seeded into a 6-well-plate with the 400 cells/well initial seeding. Triplicates were set for each culture, $n=3$, technical replicates. After 14 days of cultures, cells were fixed and stained with 2% crystal violet (containing methanol). B. Colony numbers were counted by using ImageJ software. PC1 SLC35F5 KD formed the most average number of colonies compared to other two groups, but the observed difference was statistically insignificant (SLC35F5 KD versus Scr. group, $p=0.35$, t-test). Each dot, square and triangle represented the number of counted colonies in each well. Horizontal line in each group stands for the median number of each group. KD: knockdown; Scr.: scramble; PC: patient-derived PDAC culture.

On the contrary, in SLC35F5 OE groups, both SLC35F5 CDS and SLC35F5 TR showed a 50% reduced number of colonies compared to PC1 GFP con. group (SLC35F5 CDS vs GFP con. $p=0.005$, t-test, statistically significant and SLC35F5 TR vs GFP con. $p=0.001$, t-test, statistically significant). The size of colonies observed on the images of PC1 GFP con. group was slightly bigger than PC1 SLC35F5 CDS and TR groups (Figure 20).

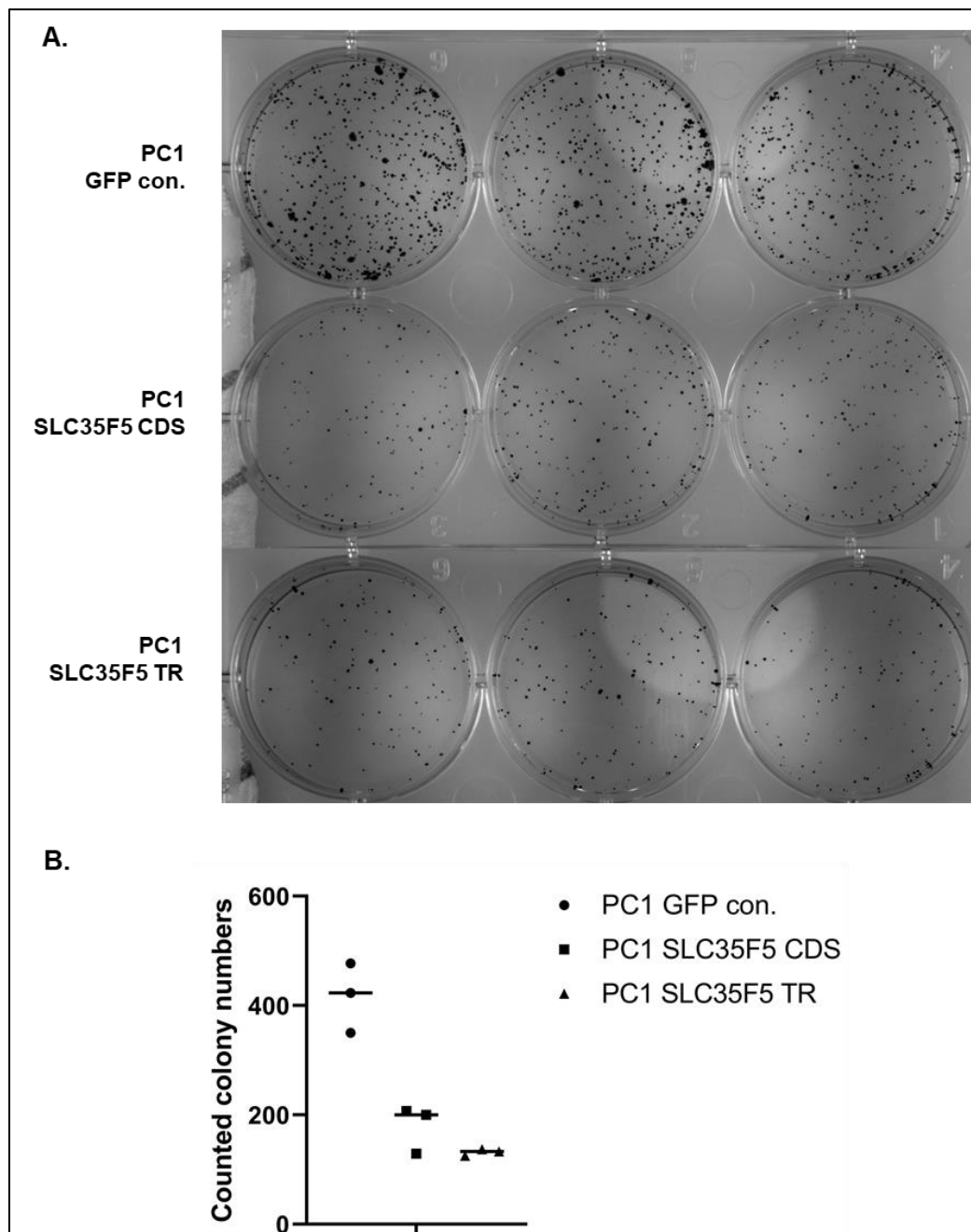


Figure 20: Colony formation of PC1 after lentiviral mediated SLC35F5 overexpression (CDS and TR) (n=3)

A. Image of colony formation assay. Established PC1 SLC35F5 CDS, SLC35F5 TR and GFP con. cells were seeded into 6-well-plate with the 400 cells/well initial seeding. Triplicates were set for each culture, $n=3$, technical replicates. After 14 days of cultures, cells were fixed and stained with 2% crystal violet (containing methanol). B. Colony numbers were counted by using ImageJ software. The observed colony number difference was statistically significant (SLC35F5 CDS vs. GFP con. $p=0.005$ and SLC35F5 TR vs. GFP con. $p=0.001$, t-test). Each dot, square and triangle represented the number of counted colonies in each well. Horizontal line in each group stands for the median number of each group. CDS: full coding sequence; TR: SLC35F5 truncated; con.: control; GFP: green fluorescent protein; PC: patient-derived PDAC culture.

3.2.2.4 Influence of SLC35F5 expression on tumour formation *in vivo*

In the colony formation assay, results showed that knockdown of SLC35F5 led to the increase of cell proliferation *in vitro*; on the contrary, overexpression of SLC35F5 decreased the colony numbers. Therefore, to trace TIC activation, I further serially transplanted PC1 SLC35F5 KD and PC1 scramble control cells into NSG mice. In the first generation, one mouse was transplanted with one million un-transduced PC1 cells as the blank control for detecting the gene marker positive transduced cells. I seeded two million PC1 cells into T25 cell culture flask and transduced with LV. SLC35F5 KD and LV. sh-scrambled particles at the pre-tested MOI 5 and MOI 1 to limit the transduction efficiency for both groups under 50% which suggested the single integration site in each cell, respectively. Within 24 hours, I transplanted one million transduced cells for each mouse into NSG mice. In the first generation, two mice of each group were transplanted with PC1 SLC35F5 KD cells and PC1 scramble controls. In parallel, I kept one million PC1 transduced cells in culture, and on Day 3 post-transduction the percentage of GFP was assessed to determine the transduction efficiency by flow cytometry. The transduction efficiency of two PC1 Scr. mice were 21% and 18.3%, and PC1 SLC35F5 KD were 34.9% and 32.2% respectively (Table 5).

Table 5: Transduction efficiency of transduced and transplanted PDAC patient-derived culture PC1.

	PC1 Scr. (% of living cells)	PC1 SLC35F5 KD (% of living cells)
Mouse 1	21.0%	34.9%
Mouse 2	18.3%	32.2%

N=1. Abbreviation in the table: Scr.: scramble; KD: knockdown; PC: patient-derived PDAC culture.

I harvested tumours when the tumour size reached 1 cm³, purified cells from tumours and determined the percentage of human tumour cells by assessing the percentage of the cell marker EpCAM. I calculated the percentage of living GFP positive cells normalized to the percentage of living EpCAM positive cells. In SLC35F5 KD group, the median of the percentage of GFP positive cells in measured human tumour cells dropped from the initial 33.5% to 6.56% in the 1st generation and increased in the 2nd generation over 10% (Figure 21). In the scramble group, this number decreased from 19.65% to 5% in the 1st generation to further to 1% in the 2nd generation. In both groups, one tumour was collected in the 3rd generation (Figure 21). In SLC35F5 KD group, no transduced cells were detected in the harvested tumour, and in scramble group, 5% transduced cells were detected in the third generation (Figure 21).

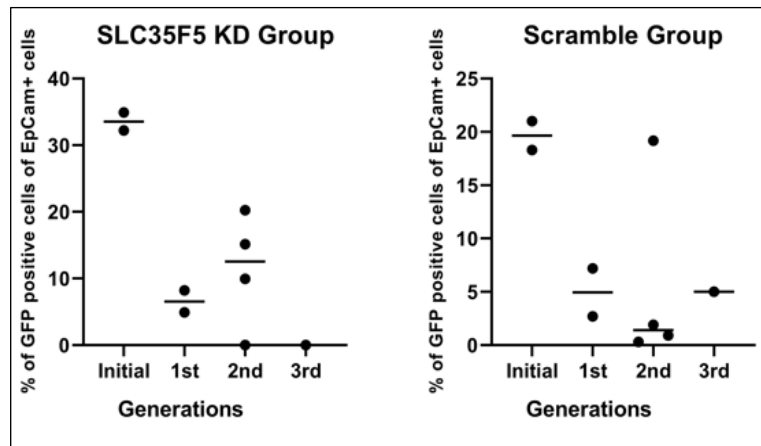


Figure 21: The influence of SLC35F5 knockdown on TIC activation in serial transplantation (n=18)

The initial transduction efficiency was measured *in vitro*. SLC35F5 KD or scramble transduced PC1 cells were serially transplanted into NSG mice. Tumours were harvested when the tumour volume reached to 1.5 cm³ or mouse needed to be sacrificed. The percentage of GFP and EpCAM was traced by flow cytometry. N=18, mice number in total. Each dot represented the data from one mouse, and horizontal line in each group stands for the median number of each group. The single dot located at 20% in the 2nd generation of scramble group was excluded when calculated the median. KD: knockdown; PC: patient-derived PDAC culture; 1st: first; 2nd: second; 3rd: third.

3.2.3 Summary 3.2

GNB1 knockdown and overexpression on RNA and protein level were successfully generated in the patient-derived PDAC cultures. On the RNA level, mRNAs transcribed from the GNB1 codon-optimized sequence were highly expressed. On the protein level, interestingly, only moderate GNB1 overexpression was detected. By performing independent Western blot, mass-spectrometry based whole-cell protein analysis and immunofluorescence experiments, GNB1 overexpression was confirmed in the generated GNB1 overexpression PCs. Eight G α subunits and one G γ subunit were detected in all three PCs. In PC1 GNB1 KD cultures, 20% more cells were found in the G1 phase compared to scramble control transduced cells. GNB1 overexpression showed no impact on cell cycle distribution in three tested PDACs.

SLC35F5 KD in PC1 led to the acceleration of cell growth and overexpression of SLC35F5 in PC1 showed a decrease in cells' colony formation ability. In the *in vivo* serial transplantation experiments, a continuous loss of transduced cells in PC1 scramble group was observed. In the *in vivo* study, SLC35F5 KD group, the percentage of transduced cells in each generation tend to decrease compared to the initial amount of transduced and transplanted cells, but in the 2nd generation, this number increased again. Furthermore, in the scramble group, the impact of transduced cells was also observed in the second and third generations. Due to the small number of xenografts experimental group, it was not possible to draw a statistically sound conclusion.

Overall, together with cell cycle analysis, cell apoptosis data and the cell growth data generated by Dr. Gao, overexpressed GNB1 was demonstrated to accelerate cell proliferation. The *in vitro* colony formation assay data of SLC35F5 KD and SLC35F5 overexpression group showed the opposite trend to the expectation. Therefore, GNB1 was selected as the candidate to further investigate its role in TIC activation.

3.3 Deciphering the transcriptional heterogeneity in pancreatic cancer patient tumours by single-cell RNA sequencing

The contribution in section 3.3: I prepared the PC1 single cell sample for single cell RNA sequencing. And I performed whole procedures of 10x Genomics method including Gel Beads-in-emulsion generation, cDNA amplification and library construction. The generated library was sequenced in Genomics & Proteomics Core Facility in DKFZ, Heidelberg, Germany. Dr. Mario Huerta analysed the sequence data and provided the images.

Previously, Prof. med. Hanno Glimm's lab has shown that PDAC progression is driven by transient activation of TIC activity (Ball et al. 2017). This transient TIC activity suggests that for successful eliminating TIC it may be needed to target a transient functional state. GNB1 was identified as a potential regulator of TIC activity in PDAC (Gao 2017) and further validated in this study (section 3.2.1). Compared to traditional bulk population sequencing, which could provide the average expression of genes in a group of cells, single-cell RNA sequencing allows analysing transcriptomes from every single cell. Therefore, single-cell RNA sequencing (sc-RNA-seq) offers the opportunity to classify cells into subclones and indicate intratumor heterogeneity (Navin 2015). To understand whether the potential TIC regulator GNB1 was expressed heterogeneously or homogeneously within individual PDAC cultures, I performed single-cell mRNA sequencing of one primary patient-derived culture (PC1) using the 10x Genomics platform.

I loaded ten thousand singularized cells of PC1 on the Single Cell A chip and followed with Gel Beads-in-emulsion (GEM) generation, cDNA amplification and library construction critical steps which described in section 2.2.2. I submitted the generated library to the Genomics & Proteomics Core Facility in DKFZ, Heidelberg, Germany. HiSeq 4000 Paired-End 100 base pairs (26+74 bp) sequencing was performed in the core facility. The data of generated library was retrieved and analysed in cooperation with the bioinformatician Dr. Mario Huerta.

The results showed that 7364 living cells were identified after quality control, with an efficiency of 73.64%. The identified PC1 single cells could be grouped into 13 clusters according to their expression profile (Figure 22A). Clusters were further annotated to seven subtypes (epithelial metabolic, epithelial metabolic exocytosis, epithelial metabolic secretion, immunoactivity clearance, migration invasion, migration hypoxia, and proliferation) as described (Peng et al. 2019) (Figure 22B.).

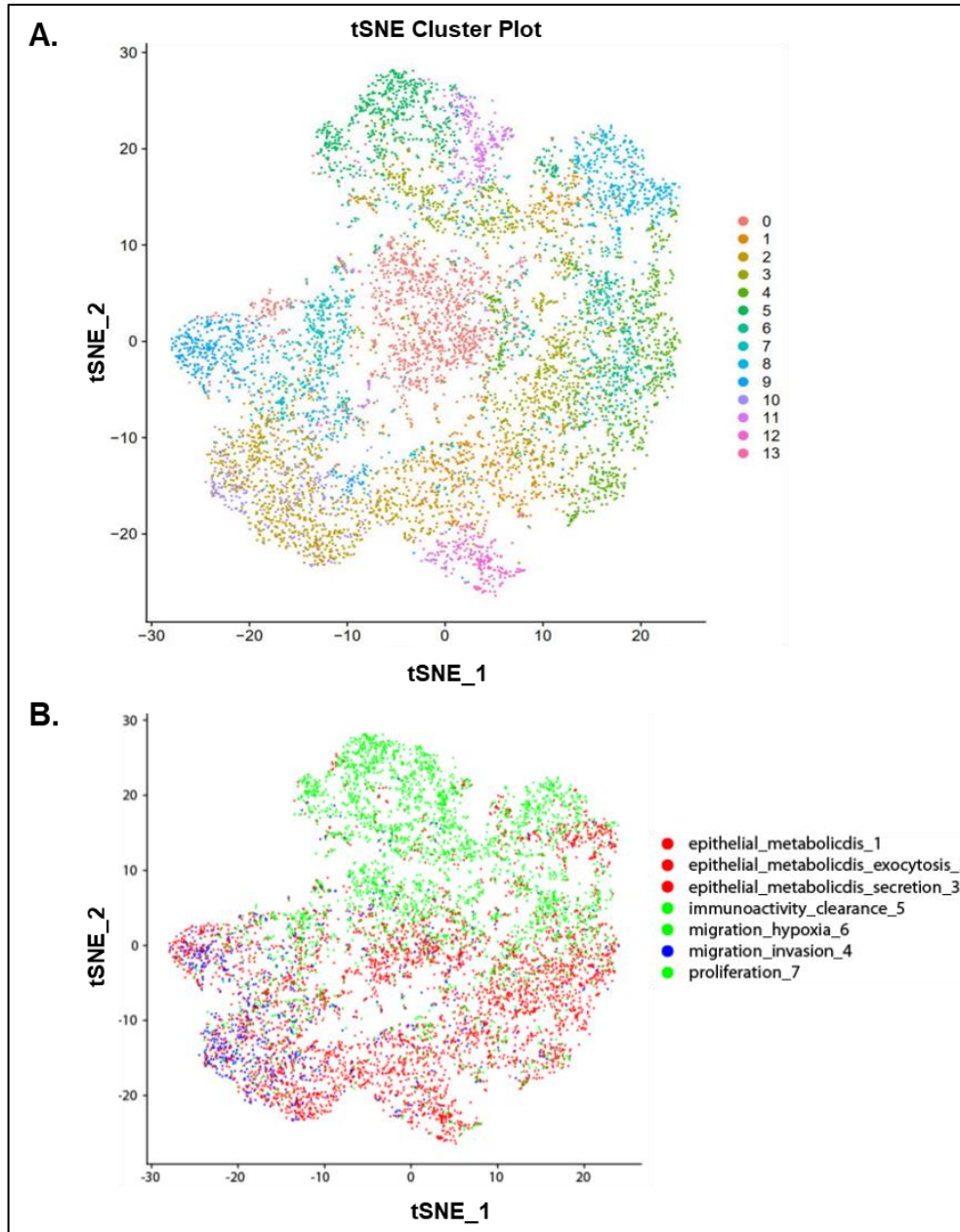


Figure 22: Identification of cell clusters and cell sub-types in PC1 using sc-RNA seq data (n=1).

A. After quality control and data correction, identified cells were clustered into 13 clusters. Each cluster was represented in one colour. B. Cell clusters were annotated into seven subtypes as described in (Peng et al. 2019). Data and images were produced by Dr. Mario Huerta. N=1, PC1. tSNE: t-distributed Stochastic Neighbour Embedding.

Proliferative type contained 2344 cells (31.8% of analysed cells) which were the dominant group of cells. Next, it was interesting that GNB1 expression was detected to be heterogenous. GNB1 positive cells were further divided into quantiles (high-, medium-, and low-GNB1 expression) based on their GNB1 expression level. Classification of the sc-RNA-Seq data revealed that 735 cells (9.98% of analysed cells) were categorized into high GNB1 expression level (quantiles values, >1.11), 1470 cells (19.96% of analysed cells) showed medium GNB1 levels (quantiles, >0.68 and <1.11), 735 cells (9.98% of analysed cells) low level (absolute, <0.68), and in 4424 cells (60.08% of analysed cells) no GNB1 expression was detected (quantiles values, min=0.33|0.68|mediam=0.86|1.11|max=2.43) (Figure 23).

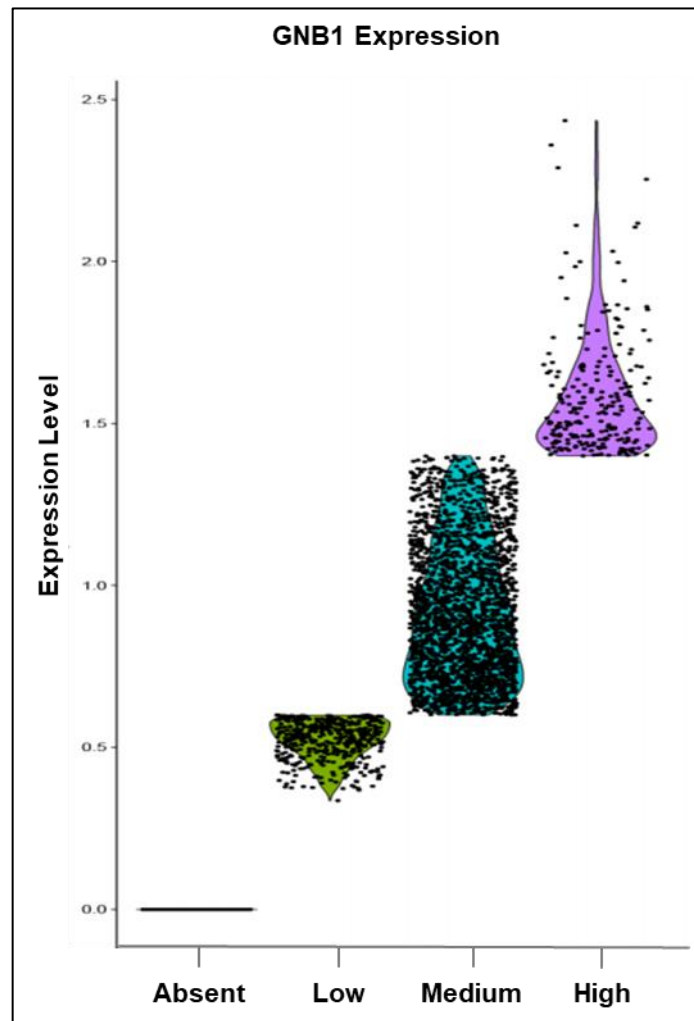


Figure 23: Heterogeneous expression of GNB1 in PC1 on single-cell RNA level.

Violin plot displaying the GNB1 expression and separated into four group, high, medium, low, and absent based on quantile values (min=0.33|0.68|median=0.86|1.11|max=2.43. low<0.68, 0.68< medium<1.11, high>1.11). Each dot represents a single readout value. N=1. Unpublished data, and images were produced by Dr. Mario Huerta.

To identify potential marker genes of GNB1 positive cells, GNB1 expression was correlated with all expressed genes. To further understand the difference of alterations of signalling pathways depending on GNB1 expression level, GNB1 expression was next correlated with signalling pathway signatures. High GNB1 expression was correlated with the signatures of β -arrestin pathway, and Oxidative-Phosphorylation and MYC-targets were correlated with low GNB1 expression (Figure 24).

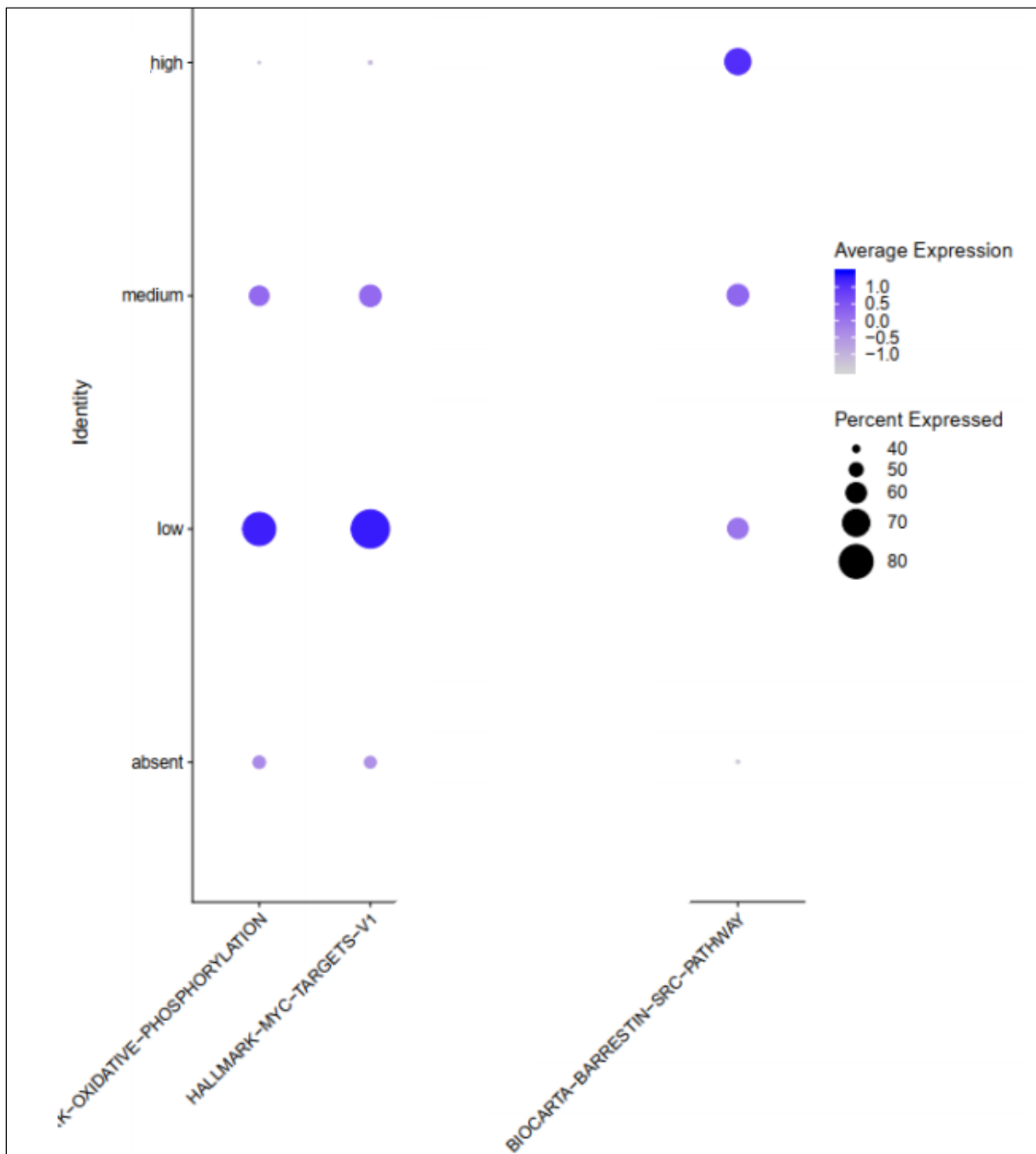


Figure 24: High GNB1 expression correlates with β -arrestin signalling pathway signatures (n=1).

GNB1 expression correlated with common signalling pathway signatures. High GNB1 expression was correlated with the signatures of β -arrestin pathway. In low GNB1 expressing cells, Oxidative-Phosphorylation and MYC-targets signatures were correlated. The average expression and percentage of expressed are indicated by the darkness of purple colour and the size of the circle. Unpublished data and images are produced by Dr. Mario Huerta.

3.4 GNB1 induced pathway alterations in pancreatic cancer cells

3.4.1 Generation of a model system to assess GNB1 induced pathway alterations in pancreatic tumorigenesis

To further investigate the pathway alterations induced by GNB1 overexpression, the immortalized normal pancreas epithelial cell line H6C7 was selected as a model system. As shown in previous studies, oncogenic *KRAS* (mutated *KRAS*) is the main driver of PDAC (di Magliano and Logsdon 2013). In one study, after introducing pancreas-specific mutated *KRAS* into healthy pancreas of mice, focal PanINs formed after 9.7 weeks (Patra et al. 2018). Therefore, in this study, I chose to use H6C7 which introduced mutated *KRAS* to mimic tumorigenesis. This *KRAS* mutated H6C7 cell line was provided by Prof. Dr. med. Claudia Scholl's group, DKFZ, Heidelberg, Germany.

As GNB1 encoded Gβ1 signalling is located upstream of *KRAS* proteins, wildtype *KRAS* and mutated *KRAS* might lead to a different downstream response following additional GNB1 overexpression. Furthermore, the MAPK signalling pathway has extensive cross regulations. Therefore, it was decided to study the pathway alterations in cells with the same genetic background. Moreover, while the majority of PDAC tumours harbour a mutated *KRAS* allele, a small proportion of PDAC tumours is *KRAS* wildtype.

To address this, I received H6C7 cells in whom *KRAS*^{G12V} mutation (EV as the control) was introduced by Prof. Dr. med. Claudia Scholl's group (DKFZ, Heidelberg, Germany). Then, I used GNB1 OE and GFP control lentiviral particles to transduce H6C7 *KRAS* wildtype (H6C7 EV GNB1 OE) cells or H6C7 *KRAS*^{G12V} mutated (H6C7 *KRAS* GNB1 OE) cells separately (Figure 25A.). I measured transduction efficiency on day 3 post-transduction by flow cytometry (Figure 25B).

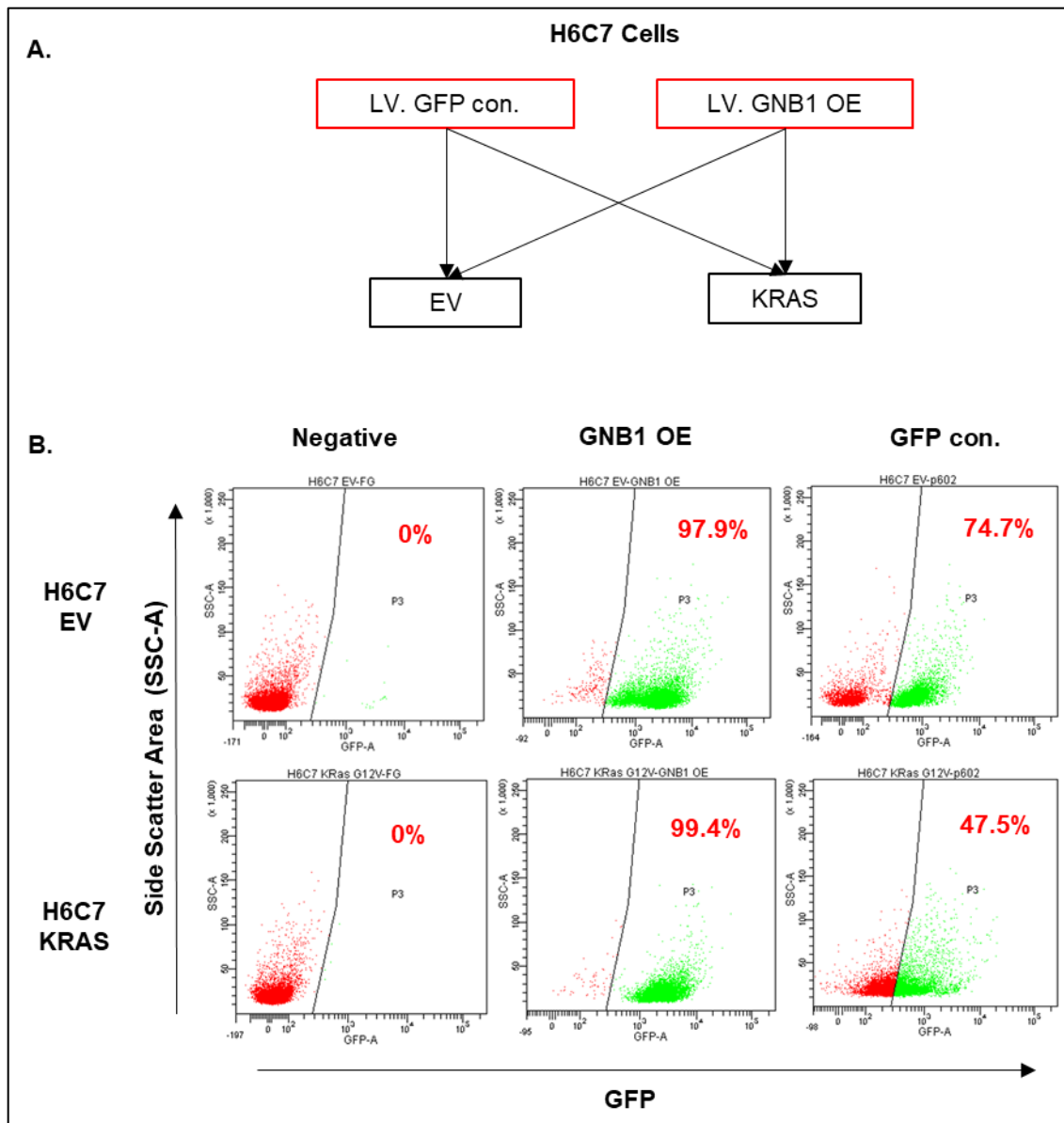


Figure 25: Illustration of established H6C7 cultures with lentiviral mediated GNB1 overexpression and transduction efficiency measurements.

A. Illustration of generated GNB1 OE and GFP control H6C7 cell lines harbouring *KRAS* wildtype and *KRAS*^{G12V} mutation. B. LV. GNB1 OE and LV. GFP con. lentiviral particles transduction efficiency. GFP was traced as the positive cells. Transduction efficiency was measured on Day 3 post-transduction. The transduction efficiency of GNB1 OE in H6C7 EV and H6C7 KRAS were 97.9% and 99.4%, respectively. The transduction efficiency of H6C7 EV GFP control and H6C7 KRAS were 74.7% and 47.5% respectively. N=1, H6C7 culture. Single value. EV: *KRAS* wildtype; KRAS: *KRAS* mutated; OE: overexpression; GFP con.: green fluorescent protein control; LV: lentiviral vector; SSC-A: side scatter area.

The transduction efficiency of LV. GNB1 OE in H6C7 EV and H6C7 KRAS was 97.9% and 99.4%, respectively. The transduction efficiency of H6C7 EV GFP control and H6C7 KRAS were 74.7% and 47.5%, respectively (Table 6).

Table 6: Transduction efficiency of transduced H6C7 cells with lentiviral based GNB1 overexpression and mock vector.

Culture	GNB1 OE (% of living cells)	GFP con. (% of living cells)
H6C7 EV	97.9%	74.7%
H6C7 KRAS	99.4%	47.5%

N=1, H6C7 culture. Single value. Abbreviation in the table: EV: *KRAS* wildtype; KRAS: *KRAS* mutated; OE: overexpression; GFP con.: green fluorescent protein control

Therefore, I sorted these cells to enrich for GFP positive transduced cells on Day 5 after expanding. After sorting, the GFP positive cells were enriched from 74.7% to 100% in H6C7 EV GFP control, and 47.5% to 89.9% in H6C7 KRAS GFP control (Figure 26).

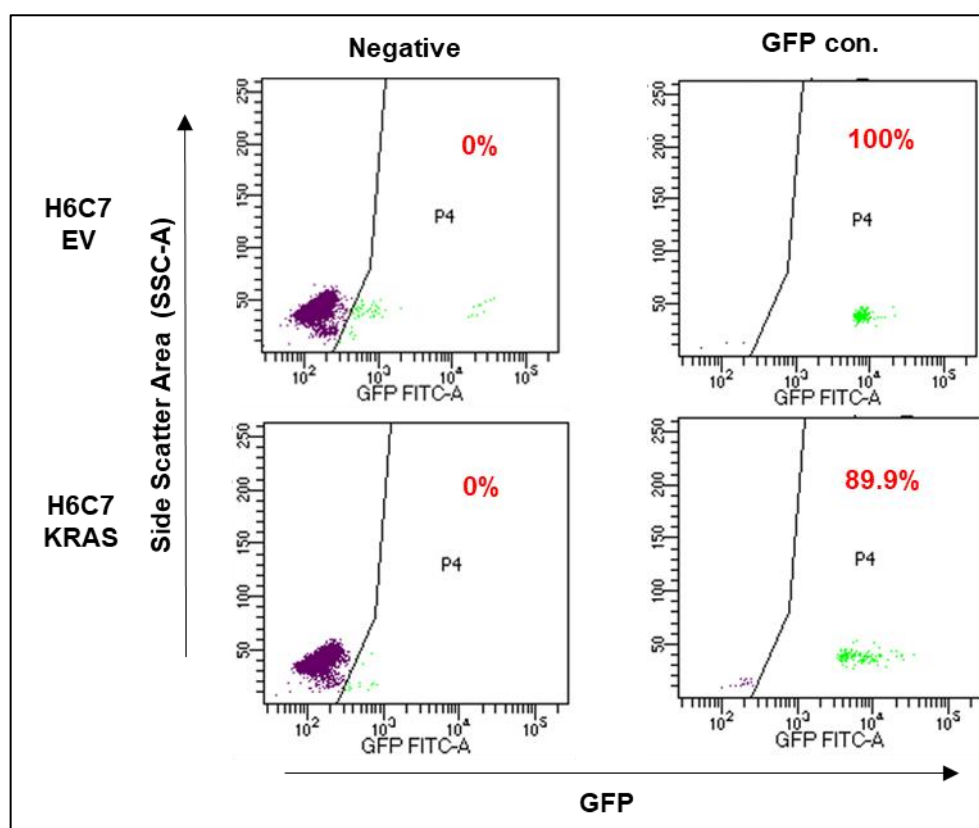


Figure 26: Enrichment of GFP positive cells in H6C7 GFP control by cell sorting.

GFP positive cells represents the transduced cells. FACS analysis showed the GFP positive cells were enriched from 74.7% to 100% in H6C7 EV GFP con., and 47.5% to 89.9% in H6C7 KRAS GFP con. after sorting. The transduction efficiency of LV. GNB1 OE and LV. GFP con. was measured by flow cytometry on Day 5 post transduction. N=1, H6C7 culture. Single value. EV: *KRAS* wildtype; KRAS: *KRAS* mutated; OE: overexpression; GFP con.: green fluorescent protein control; SSC-A: side scatter area; FITC: parameter to show GFP positive cell population. P4: Gate 4.

3.4.2 Ectopic overexpression of GNB1 expression in H6C7 cells on mRNA and protein levels

The GNB1 expression level was validated in the LV. GNB1 OE and LV. GFP con. particles transduced H6C7 *KRAS* wildtype (EV) and *KRAS* mutated (KRAS) cells. Collected cells were separated into two parts, one part was used for western blot and the other part for qRT-PCR. On mRNA level, I performed qRT-PCR to detected codon-optimized (GNB1 Codon.) and endogenous (GNB1 Endo.) GNB1 by specific primers. In H6C7 EV GNB1 OE and KRAS GNB1 OE cells, GNB1 Codon. was 9-fold and 8-fold increase compared to endogenous GNB1 expression, which suggested that GNB1 was overexpressed on RNA level (Figure 27A). As codon-optimized GNB1 coding sequence was not present in GFP control cells, no data was shown (Figure 27A). Next, I performed the western blot, and the western blot analysis showed a 1.13-fold overexpression of GNB1 protein in H6C7 EV GNB1 OE group and 2.29-fold in H6C7 KRAS GNB1 OE (Figure 27B).

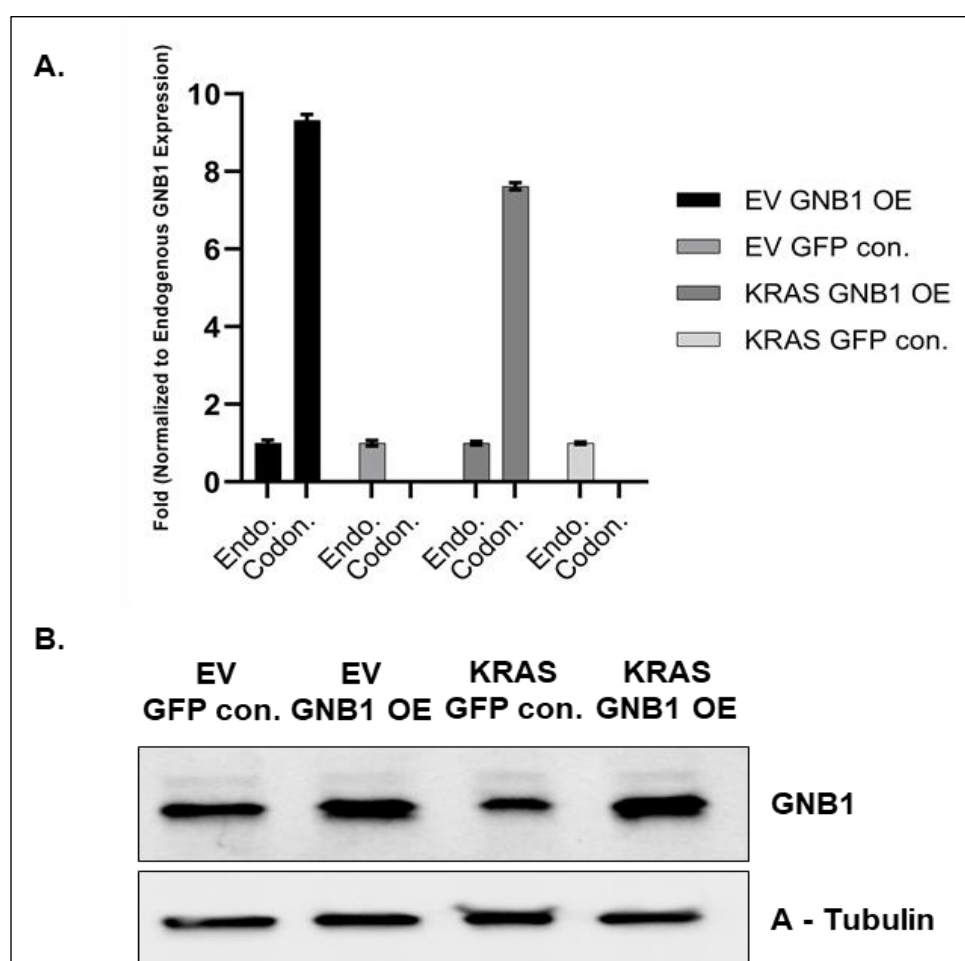


Figure 27: Validation of GNB1 overexpression in pancreatic epithelial cells with and without *KRAS* mutation (n=1).

A. Fold change of GNB1 expression on RNA level. qRT-PCR analysis indicated the 9-fold and 8-fold of codon-optimized GNB1 (Codon.) expression compared to endogenous GNB1 expression (GNB1 Endo.) on mRNA level in H6C7 EV GNB1 OE and H6C7 KRAS GNB1 OE. GNB1 codon-optimized sequence was not present in GFP con., therefore there was no data showed. Error bar: standard deviation of the mean. B. GNB1 expression validated by western blot. GNB1 overexpression was detected 1.13-fold increase in H6C7 EV GNB1 OE transduced group compared to GFP con. and 2.29-fold increase in H6C7 KRAS GNB1 OE. N=1, H6C7 culture. EV: *KRAS* wildtype; KRAS: *KRAS* mutated; OE: overexpression; GFP con.: green fluorescent protein control; A-Tubulin: alpha-tubulin.

3.4.3 Investigation of Akt and ERK1/2 activation in H6C7 transduced cells

GNB1 was reported to be locating upstream of the PI3K and MAPK signalling pathways (Dorsam and Gutkind 2007). Therefore, the activity of key molecules was investigated in both signalling pathways to assess the influence of GNB1 overexpression in H6C7 cells. I first analysed Akt, ERK1/2 and their phosphoprotein type by western blot because it had been shown that Akt could be activated downstream of Gβ1 signalling, and its activity could be regulated via PI3K (Dorsam and Gutkind 2007). Total Akt showed no difference in GNB1 OE versus GFP con. in *KRAS* wild-type, and *KRAS* mutated background. Notably, more p-Akt Ser473 was detected in H6C7 *KRAS* GNB1 OE but not in H6C7 EV GNB1 OE (Figure 28A). Total ERK1/2 protein level was increased in H6C7 *KRAS* mutated cells, as well as p-ERK1/2, but no difference was detected between GNB1 OE and GFP con. (Figure 28B). These results suggested that GNB1 OE might activate the PI3K signalling pathway but not the MAPK signalling in this cell model.

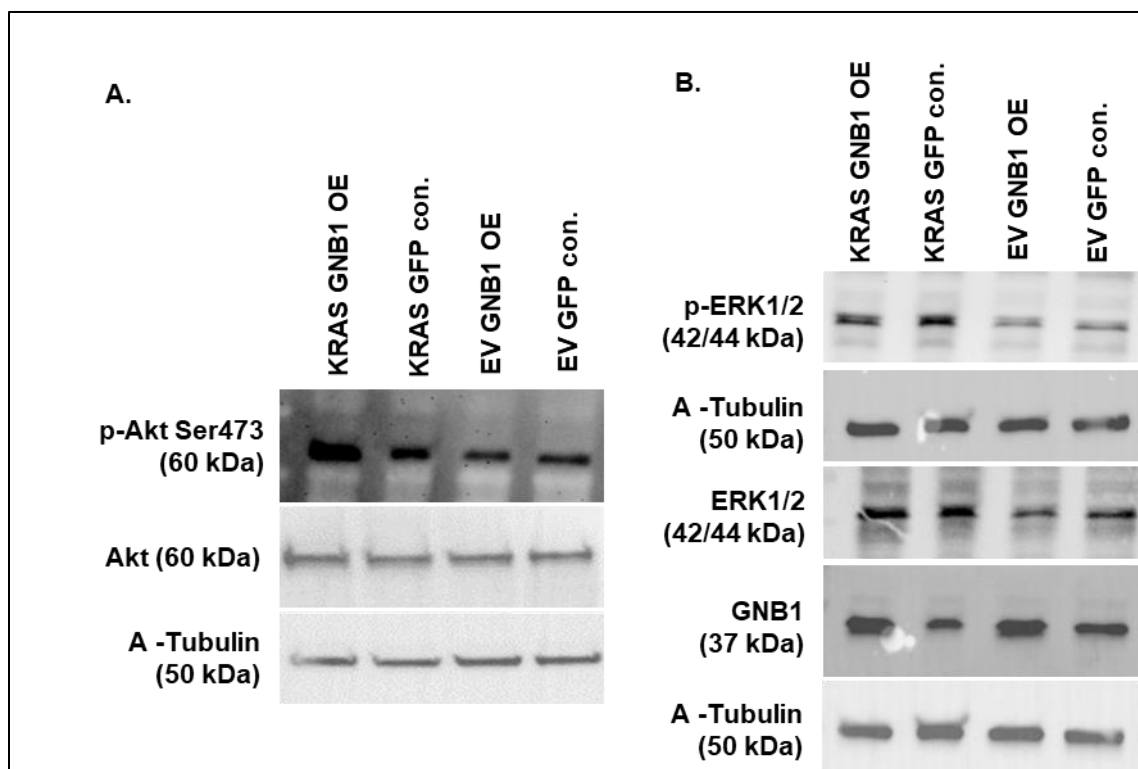


Figure 28: Investigation of PI3K and MAPK signalling after GNB1 overexpression in *KRAS* wildtype or mutated pancreatic epithelial cells (n=1).

A. Western blot using lysates of H6C7 GNB1 OE and GFP con. cells. Total Akt and its phospho-protein type on Ser473 were detected. Phospho-Akt Ser473 (p-Akt Ser473) was found increase in H6C7 *KRAS* GNB1 OE cells, but the total Akt did not change. B. total ERK1/2 and p-ERK1/2 increase in H6C7 *KRAS* mutated cells because of the MAPK pathway continuously activated. However, GNB1 OE did not show any influence on MAPK signalling pathway. N=1, H6C7 culture. EV: *KRAS* wildtype; *KRAS*: *KRAS* mutated; OE: overexpression; GFP con.: green fluorescent protein control; A-Tubulin: alpha-tubulin, kDa: kilodalton.

The following procedures were performed in NMI Technologietransfer GmbH, Reutlingen, Germany. Protein samples were loaded into SDS-PAGE gels to separate the proteins (NMI Technologietransfer GmbH 2020). Then each lane was cut into 96 fractions, and proteins were eluted into 96-well plates (NMI Technologietransfer GmbH 2020). Populations were colour-coded via Luminex[®] Beads, and different protein fractions were pooled (NMI Technologietransfer GmbH 2020). Beads were pooled and then separated into 384 distinct populations and mixed with antibodies (one antibody per well in 384-well-plate) (NMI Technologietransfer GmbH 2020). Luminex[®] instruments were used for the readout, and the proteins were distinguished according to their molecular size (NMI Technologietransfer GmbH 2020). This method provides the chance of analysing a maximum of 800 total and phosphorylated-proteins at one time, which makes the comprehensive pathway analysis easier (NMI Technologietransfer GmbH 2020). Furthermore, the Luminex[®] technology increases the sensitivity of detecting proteins compared to western blot (NMI Technologietransfer GmbH 2020).

The DigiWest analysis was performed in NMI Technologietransfer GmbH, and the panel included 44 antibodies for detecting total proteins (including the different subtypes of one protein), and in total 58 phosphorylated sites of total proteins were detected which were involved in PI3K and MAPK signalling pathways. The chemiluminescence of protein peak signals were measured. Proteins (total proteins or detected different phosphor-sites) with a lower signal than the base line (set by NMI Technologietransfer GmbH, Reutlingen, Germany) were eliminated by NMI Technologietransfer GmbH. Then the data was retrieved.

I further analysed the retrieved data and calculated the mean of the values from two sample sets. Then the chemiluminescence intensity readout of detected proteins in GNB1 OE group was normalized to GFP control groups, respectively. I set the threshold at 1.5-fold by considering the instability of phospho-proteins and the average of the calculated fold difference between GNB1 OE versus GFP con. In H6C7 KRAS GNB1 OE cells, the fold of mean chemiluminescence of TSC complex subunit 2 (TSC2), p-TSC2 S1387, p-SGK1 S78 (SGK1: serum/glucocorticoid regulated kinase 1), p-Raptor S792, Serine/threonine-protein phosphatase 2A (PP2A) C, p-PP2A C Y307, PDPK1 (PDK1 in Figure 30), p-p70 S6 kinase (Ribosomal protein S6 kinase beta-1) T389, mechanistic target of rapamycin kinase (mTOR), p-mTOR-S2448 and p-4E-BP1 S65 (4E-BP1: eukaryotic translation initiation factor 4E-binding protein 1) were above 1.5-fold, which were involved in the PI3K-Akt-mTOR signalling pathway. This might indicate that GNB1 triggers TIC activation via PI3K-Akt-mTOR signalling in PDAC. Among the selected candidates, PDPK1 showed up to 57-fold increase expression in H6C7 KRAS GNB1 OE cells compared to its control (statistically significant, $p=0.000027$, t-test), and a six-fold increase in H6C7 EV GNB1 OE compared to control cells (statistically insignificant, $p=0.11$, t-test) (Figure 30). These candidates which might indirectly or directly regulated by overexpressed GNB1 were selected for further validation by western blot.

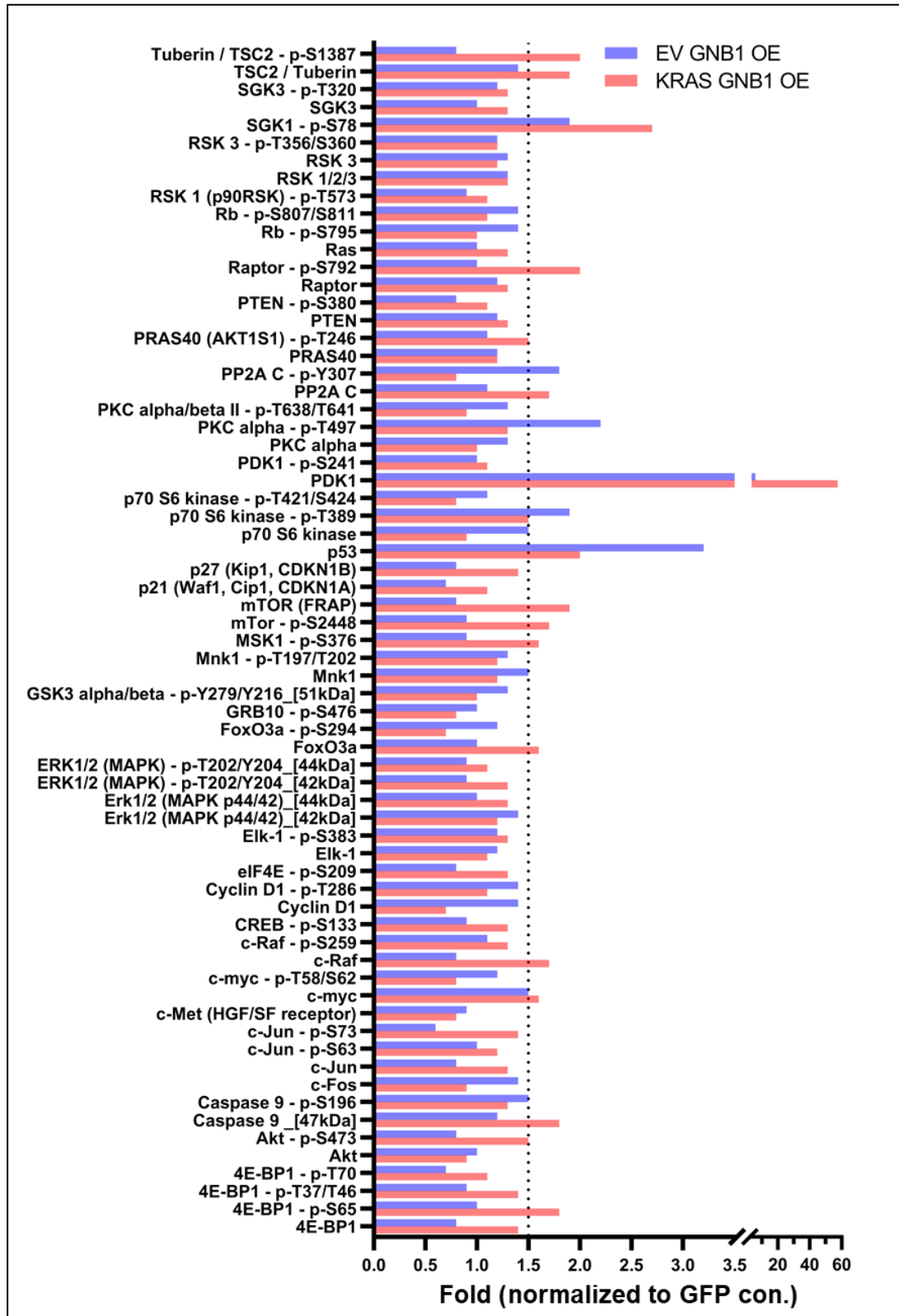


Figure 30: Summary of DigiWest multiplex protein profiling array data analysis (n=2).

This figure indicates the fold change of selected potential indirect or direct downstream effectors of overexpressed GNB1 in H6C7 GNB1 OE cells which normalized to GFP control controls. The threshold was set at 1.5-fold. PDPK1 (PDK1 in the figure) showed highest fold change, 6-fold in H6C7 EV GNB1 and 57-fold in H6C7 KRAS GNB1. Most candidates which fold change above 1.5 involves in PI3K-Akt-mTOR signalling pathway. N=2, technical replicates. EV: *KRAS* wildtype; KRAS: *KRAS* mutated; OE: overexpression.

3.4.5 Validation of PDPK1 expression in GNB1 dysregulated cells

The significant fold increase of PDPK1 detected by DigiWest assay might suggest the strong indirect or direct response to GNB1 overexpression, therefore, I first validated PDPK1 expression in the R2 set. The density of detected protein bands in western blot experiment was normalized to the total loaded proteins (details of normalization to total loaded proteins in section 2.2.7.4). PDPK1 levels were increased in GNB1 OE cells in R2 set, and the fold change was 2.59-fold increase in H6C7 EV GNB1 OE and 1.68-fold increase in H6C7 KRAS mutated cells (Figure 31A and Figure 31B). There was no difference of PDPK1 protein content detectable in an additional set of independently transduced H6C7 cells (replicates 4, R4) (n=2, technical replicates, Figure 31A and Figure 31C).

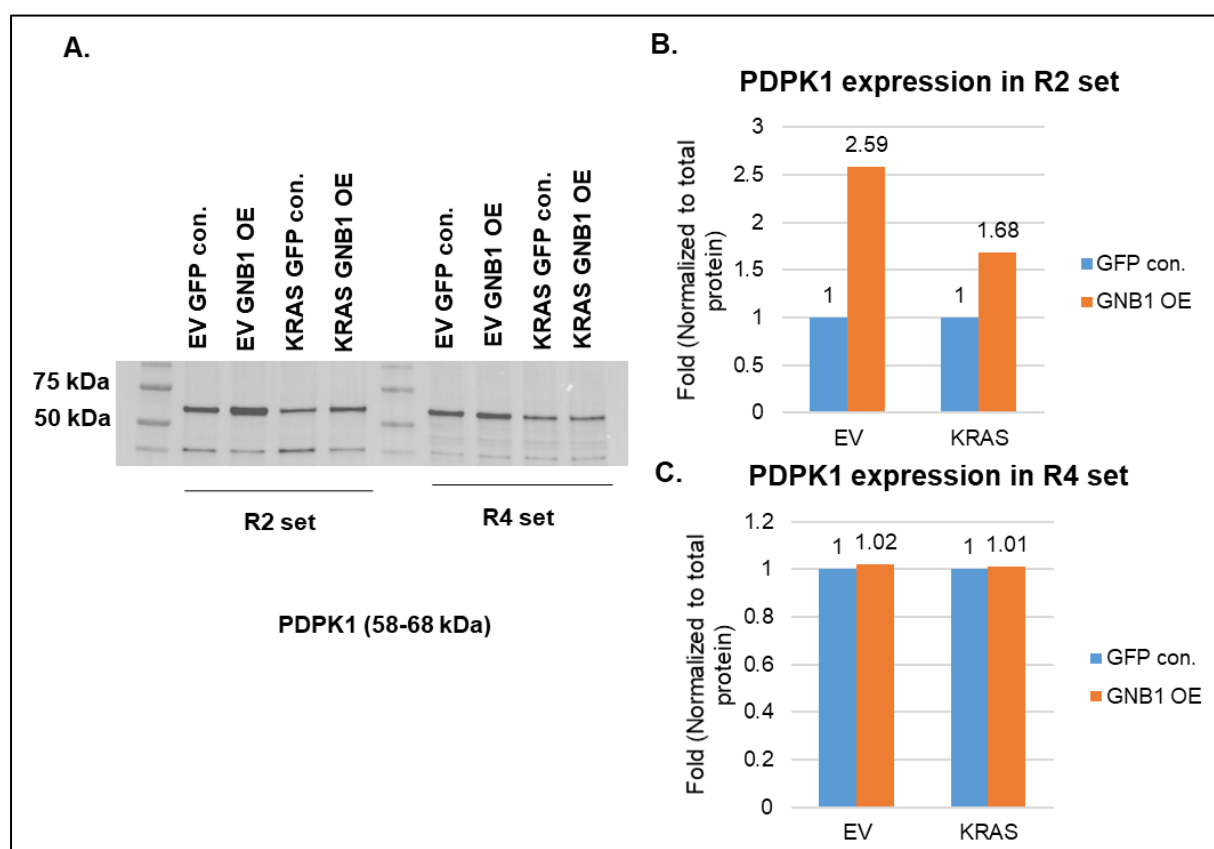


Figure 31: PDPK1 validation by western blot in R2 set and independent transduced (R4) set samples (n=2).

PDPK1 expression was validated by western blot in the replicates 2 (R2) sample set which collected in parallel with the sample sets which sent for antibody array and in an independent transduced set (replicates 4, R4) of H6C7 cells. In R2 set, PDPK1 was found 2.59-fold and 1.68-fold overexpressed in GNB1 OE versus GFP con. in H6C7 EV and H6C7 KRAS cells. In the R4 set, PDPK1 overexpression was not identified. A. PDPK1 protein bands detected in R2 and R4 set. The molecular weight of PDPK1 is between 58 kDa to 68 kDa. B. and C. Quantification figures of PDPK1 expression in R2 and R4 sets. The density of PDPK1 western blot protein bands was first normalized to total loaded proteins in each lane. Then the fold of GNB1 OE versus GFP con. were calculated and showed in bar charts. N=2, technical replicates. EV: KRAS wildtype; KRAS: KRAS mutated; OE: overexpression; GFP con.: green fluorescent protein control; kDa: kilodalton.

I further validated PDPK1 in the original DigiWest analysed protein samples by a different technology, western blot (Figure 32A). In the R1 set, a 2.37-fold increase of PDPK1 protein content in H6C7 EV GNB1 OE was detected and 1.62-fold in H6C7 KRAS G12V GNB1 OE (Figure 32B). And it showed 3.75-fold increase in EV GNB1, and 2.24-fold increase in KRAS GNB1 OE in the R3 set (n=2, technical replicates, Figure 32C).

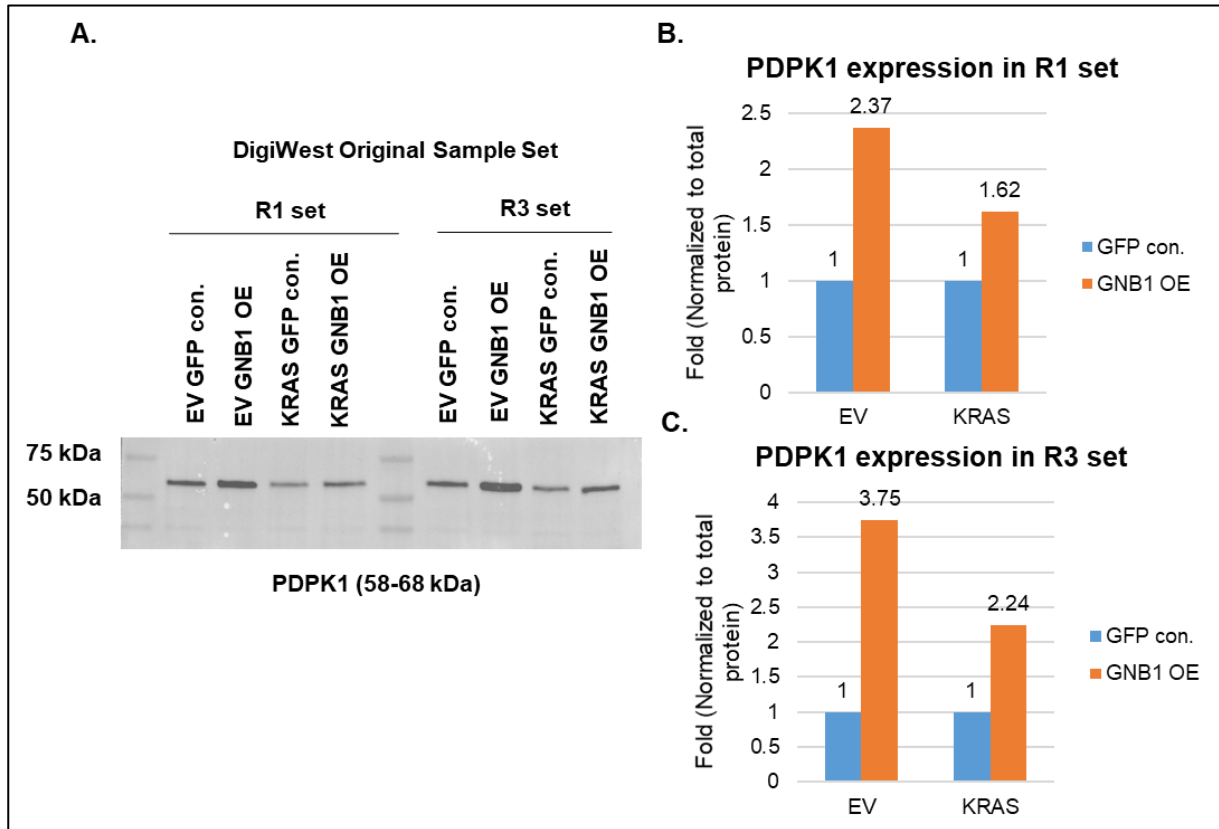


Figure 32: Validation of PDPK1 expression by western blot in the original screening sample set (n=2).

PDPK1 expression was validated in the original antibody array analysed protein sample by western blot. PDPK1 increased in both GNB1 OE cells (EV GNB1 OE vs. GFP con. was 2.37-fold increase in replicates 1(R1), and 3.75-fold increase in replicates 3 (R3); KRAS GNB1 OE vs. GFP con. was detected 1.62-fold increase in R1 set, and 2.24-increase in R3 set), but the fold shifts were not as significant as it detected in DigiWest protein profiling analysis. The PDPK1 antibody that used for DigiWest analysis was also used for western blot. A. PDPK1 protein bands detected in R1 and R3 set. The molecular weight of PDPK1 is between 58 kDa to 68 kDa. B. and C. Quantification figures of PDPK1 expression in R1 and R3 sets. The density of PDPK1 western blot protein bands was first normalized to total loaded proteins in each lane. Then the fold of GNB1 OE versus GFP con. were calculated and showed in bar charts. N=2, technical replicates. EV: *KRAS* wildtype; KRAS: *KRAS* mutated; OE: overexpression; GFP con.: green fluorescent protein control; kDa: kilodalton.

I repeated lentiviral transductions of H6C7 cells using GNB1 OE vectors and GFP control vectors to generate the 2nd independent sample set (replicates 5, R5) which was further used to verify the DigiWest results, and GNB1 KD in both sub-lines, H6C7 EV and H6C7 KRAS, was included (n=1, Figure 33A). I sorted cells according to GFP or RFP signal. The purity of transduced cells after sorting was above 90%, and these sorted cells were used in further experiments. In H6C7 EV GNB1 KD group, PDPK1 protein expression decreased to 53%, but such influence could not be detected in H6C7 KRAS GNB1 KD cells (Figure 33B). Interestingly, within R5 set of cells, the fold change of GNB1 overexpression were 1.5 and 1.3

increase compared to each GFP controls, but 60% of GNB1 proteins were knocked down in both GNB1 KD groups (Figure 33C).

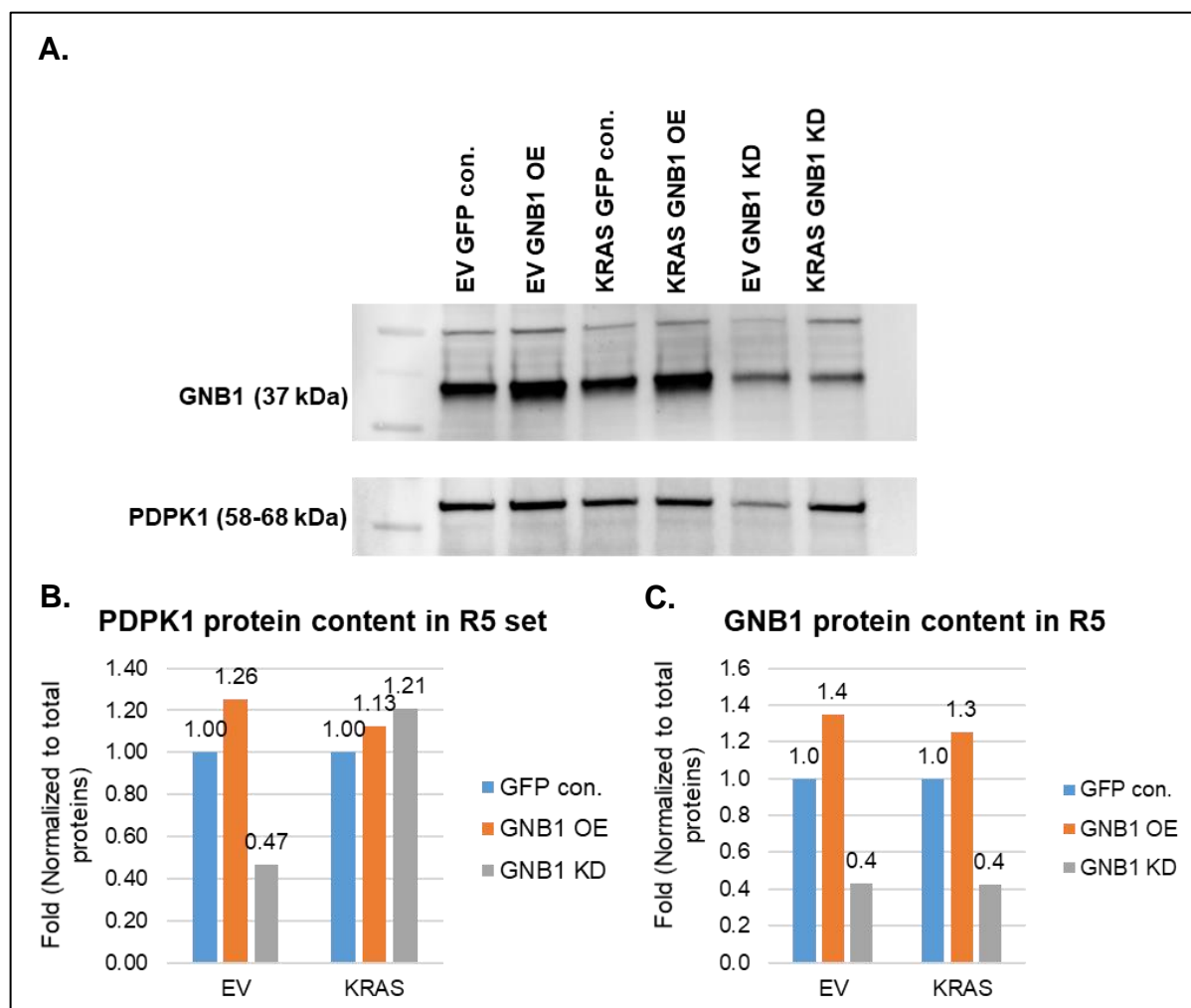


Figure 33: PDPK1 validation by western blot in the newly generated (replicates 5, R5) H6C7 cells (n=1).

A. PDPK1 protein bands detected in R1 and R3 set. The molecular weight of PDPK1 is between 58 kDa to 68 kDa. B. Quantification figure of PDPK1 expression from western blot in R5 set. C. Quantification figure of GNB1 expression from western blot in R5 set. GNB1 overexpression was 1.4- and 1.3-fold increase in H6C7 EV GNB1 OE and H6C7 KRAS GNB1 OE group compared to GFP control controls. 60% of GNB1 proteins were knocked down in both GNB1 knockdown groups. Increase of PDPK1 expression was not detected in this sample set (R5), but interestingly in H6C7 EV GNB1 KD group, around 50% decrease of PDPK1 protein content was detected. The density of PDPK1 western blot protein bands was first normalized to total loaded proteins in each lane. Then the fold of GNB1 OE versus GFP con. were calculated and showed in bar charts (n=1). EV: *KRAS* wildtype; KRAS: *KRAS* mutated; OE: overexpression; KD: knockdown; GFP con.: green fluorescent protein control; kDa: kilodalton.

Furthermore, I also investigated the PDPK1 expression in GNB1-FLAG-Tag transduced primary PC1, PC2 and PC3 cells (n=3, biological replicates). GNB1 expression in these three PCs was validated in previous experiments. Total PDPK1 expression slightly increased in PC1 GNB1-FLAG-Tag cells compared to controls while no difference was detectable in cells from PC2 and PC3 (Figure 34).

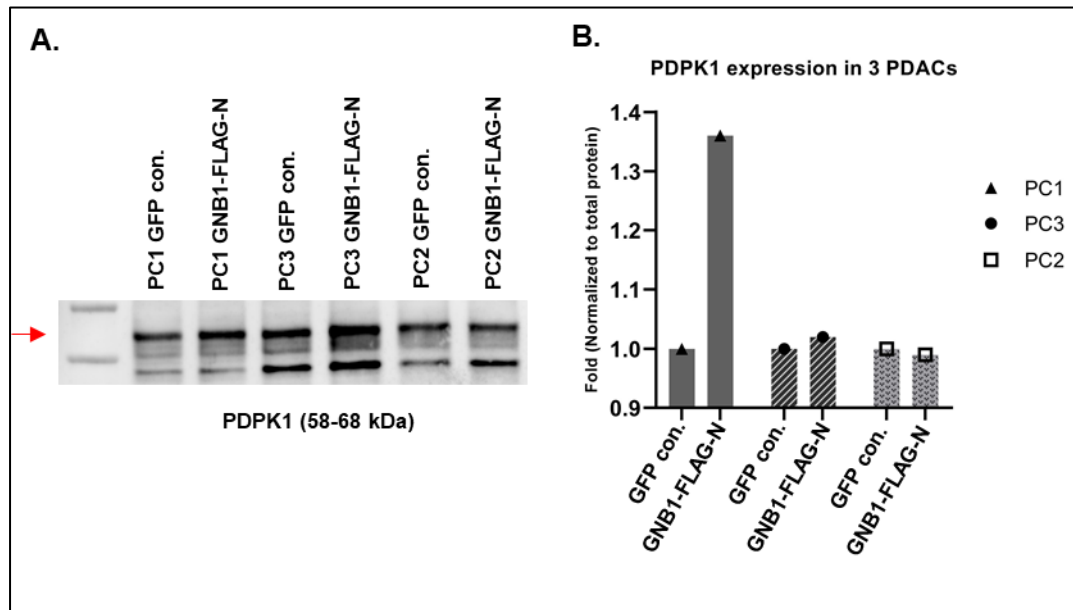


Figure 34: Investigation of PDPK1 expression in three primary PDACs after GNB1 gene dysregulation (n=3).

A. PDPK1 expression detected by western blot in three GNB1 gene overexpression primary PDACs. B. Quantification figure of PDPK1 expression that detected by western blot. In PC1 GNB1-FLAG-Tag transduced cells, PDPK1 expression slightly increased 1.36-fold. In PC2 and PC3, the increase of PDPK1 expression was not detected. The density of PDPK1 western blot protein bands was first normalized to total loaded proteins in each lane. Then the fold of GNB1 OE versus GFP con. were calculated and showed in bar charts (n=3, biological replicates). GNB1-FLAG-N: FLAG-Tag protein coding sequence cloned on the N-terminal of GNB1 coding sequence; GFP con.: green fluorescent protein control; kDa: kilodalton; PC: patient-derived PDAC culture.

In short, data produced in H6C7 cells suggest the strong correlation between GNB1 and PDPK1 which indicated PDPK1 might be one of the key downstream effector of GNB1. However, in primary PDAC cultures, the potential regulatory relevance between GNB1 and PDPK1 might be more dependent on the individual patient derived cultures and genetic backgrounds.

3.4.6 Validation of mTOR expression and mTOR phosphorylation level in GNB1 dysregulated cells

I performed western blot for validating the additional identified targets, mTOR and p-mTOR-S2448 (Figure 35A). Both targets were first validated in the R2 sample set (n=1). mTOR and p-mTOR showed a 20% and 10% decrease in H6C7 EV GNB1 OE compared to controls, respectively (Figure 35B and Figure 35C). In *KRAS* mutated background, mTOR increased 1.35-fold in GNB1 OE compared to its control (Figure 35B).

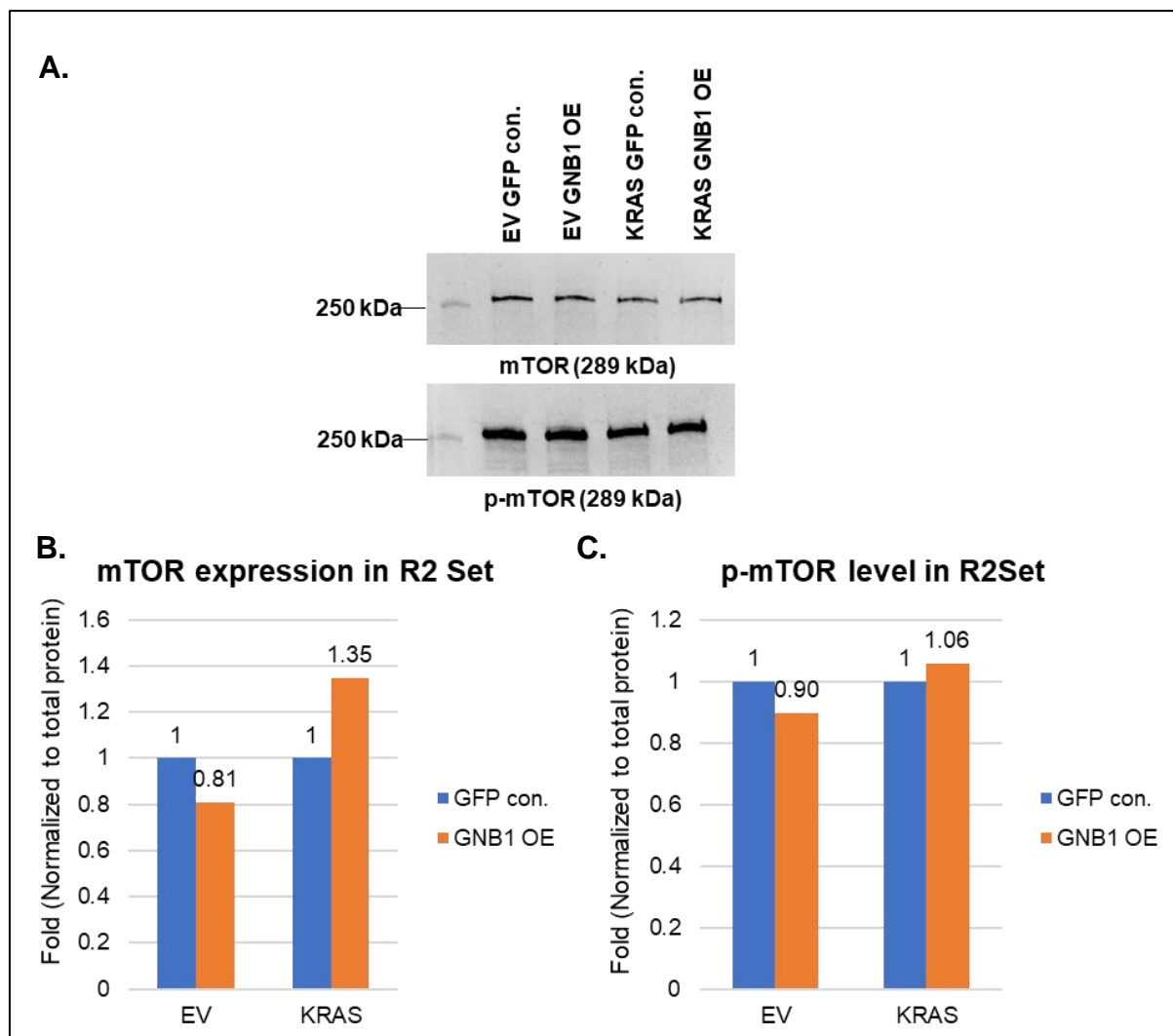


Figure 35: Validation of mTOR and p-mTOR expression in R2 Set (n=1).

A. mTOR and p-mTOR expression in R2 set was validated by western blot. B. and C. Quantification figures of mTOR and p-mTOR from the western blot in R2 set. Total mTOR protein decreased 19% in EV GNB1 OE, and 1.35-fold increase in KRAS GNB1 OE. p-mTOR did not show difference in GNB1 OE compared to controls in *KRAS* wildtype and *KRAS*^{G12V} mutated H6C7. The density of mTOR and p-mTOR western blot protein bands was first normalized to total loaded proteins in each lane. Then the fold of GNB1 OE versus GFP con. were calculated and showed in bar charts (n=1). EV: *KRAS* wildtype; KRAS: *KRAS* mutated; OE: overexpression; GFP con.: green fluorescent protein control; kDa: kilodalton.

Then, I further validated mTOR expression and p-mTOR level by western blot in R1 and R3 Set (n=2, technical replicates, Figure 36A). In R1 set, mTOR increased 1.2-fold in KRAS wildtype and mutated GNB1 OE H6C7, and p-mTOR showed no change in EV GNB1 OE, a 1.16-

fold increase in KRAS GNB1 OE compared to each control (Figure 36B). In R3 Set, a 0.77-fold of mTOR expression was detected in EV GNB1 OE, and 1.36-fold increase in KRAS GNB1 OE. 1.51-fold more p-mTOR was detected by western blot in EV GNB1 OE and 15% decrease in KRAS GNB1 OE compared to each control (Figure 36C).

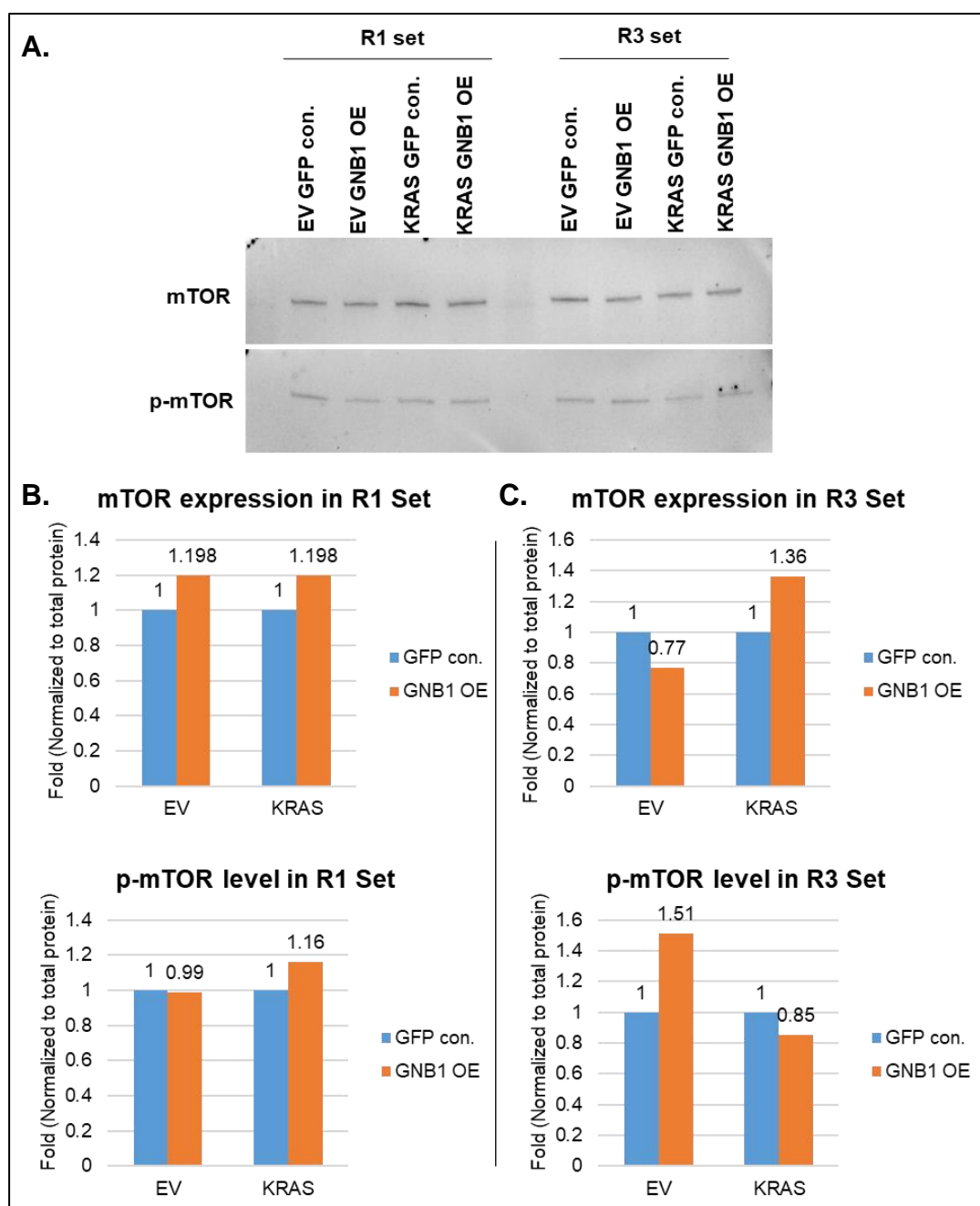


Figure 36: Validation of mTOR and p-mTOR expression in R1 and R3 Sets (n=2).

A. mTOR and p-mTOR detected by western blot in R1 and R3 sets. B. and C. Quantification figures of mTOR and p-mTOR that detected by western blot. Total mTOR protein increased 1.2-fold in both EV GNB1 OE, and KRAS GNB1 OE compared to controls in R1 Set. In R3 set, compared to controls mTOR decreased 30% in EV GNB1 OE, 1.36-fold increase in KRAS GNB1 OE. In R1 Set, p-mTOR did not show difference in EV GNB1 OE, 1.16-fold increase in KRAS GNB1 OE. In R3 Set, a 1.51-fold increase was detected in EV GNB1 OE, 0.85-fold in KRAS GNB1 OE compared to each control. The density of mTOR and p-mTOR western blot protein bands was first normalized to total loaded proteins in each lane. Then the fold of GNB1 OE versus GFP con. were calculated and showed in bar charts (n=2, technical replicates). EV: *KRAS* wildtype; KRAS: *KRAS* mutated; OE: overexpression; GFP con.: green fluorescent protein control; kDa: kilodalton.

3.4.7 Investigation of the PI3K pathway activity in GNB1 overexpressed normal pancreatic epithelial cells

Combining the data from DigiWest protein profiling analysis and western blot validation experiments showed that overexpressed GNB1 might induce PI3K signalling pathway through mediating PDPK1 expression, these data led to the direction of further investigating the correlation between GNB1 and PI3K-Akt-mTOR signalling pathway. In GNB1 OE cells, the PI3K signalling pathway was activated. Therefore, it was asked whether the alteration of this signalling pathway contributes to GNB1 induced TIC activation. To evaluate the hypothesis, I inhibited certain key molecules like PDPK1, Akt, PI3K, phosphatidylinositol-4,5-bisphosphate 3-kinase catalytic subunit alpha (PIK3CA) in the PI3K pathway as well as GNB1. To assess the toxicity of the specific inhibitors, transduced H6C7 cells were seeded in tissue-culture-treated clear F-bottom black 384-well plates for further half maximal inhibitory concentration (IC₅₀) determination. I serially diluted GNB1 inhibitor Gallein, PDPK1 inhibitors GSK2334470 and OSU-03012, PI3K inhibitor Copanlisib, PI3K alpha inhibitor Alpelisib, PIK3CA inhibitor GDC-0032 and Akt inhibitor MK-2206 with a total of 12 dilutions in triplicates (section 2.2.7.9). I used Anisomycin as a positive control (50 μM), and DMSO treated cells as a negative control. The cell viability of DMSO was considered as 100%, then cell viability in each inhibitor treated wells were calculated. Then, IC₅₀ of these inhibitors were first determined, and Y-axis was set as the cell viability (section 2.2.7.9). The IC₅₀ of Gallein, GNB1 inhibitor, of both GNB1 OE H6C7 was nearly doubled to both H6C7 GFP control (EV GFP control: 1.455 μM, EV GNB1 OE: 3.15 μM, KRAS GFP control: 1.677 μM and KRAS GNB1 OE: 2.137 μM) which represented the increase of GNB1 expression in GNB1 OE H6C7 cells. Single PDPK1, Akt, PI3K, PIK3CA inhibitors treated transduced H6C7 cells did not show the impact on the cell viability (Figure 37). GNB1 protein level increase did not alter the sensitivity of cells to PDPK1, PI3K, PIK3CA and Akt inhibition.

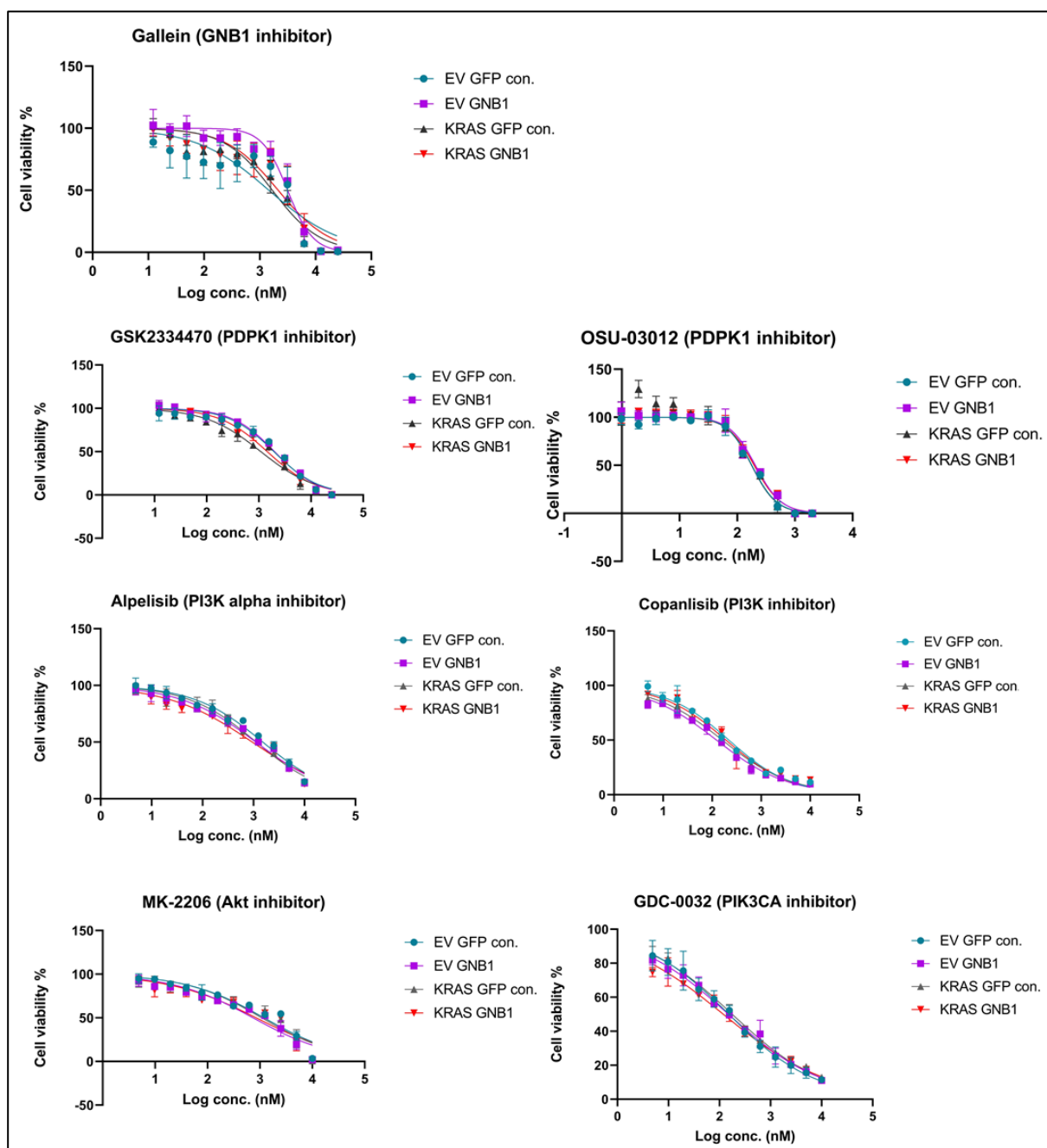


Figure 37: Dose-response curves of inhibitors targeting Akt, PIK3CA, PI3K alpha, PI3K, PDPK1 and GNB1.

Transduced H6C7 cells were treated by inhibitors for 72h. Cell viability was set for the Y-axis and measured by ATP-lite assay. The IC_{50} of Gallein of EV GFP control was 1.455 μ M, 3.15 μ M of EV GNB1 OE, 1.677 μ M of KRAS GFP control and 2.137 μ M of KRAS GNB1 OE. Other inhibitors did not influence the cell viability by 72 hours treatment. Data was normalized to blank control. GSK2334470: PDPK1 inhibitor; OSU-03012: PDPK1 inhibitor; Alpelisib: PI3K alpha inhibitor; Copanlisib: PI3K inhibitor; MK-2206: Akt inhibitor; GDC-0032: PIK3CA inhibitor. In each experiment, triplicates were set for each concentration of inhibitors. Experiments were performed twice under the same conditions, in total six technical replicates ($n=6$) of each concentration of inhibitors. Error bar represented the standard deviation of the mean readout from technical replicates of each concentration. EV: *KRAS* wildtype; KRAS: *KRAS* mutated; GNB1: GNB1 overexpression; GFP con.: green fluorescent protein control.

3.4.8 Summary 3.4

GNB1 was successfully overexpressed on RNA and protein levels in normal pancreas epithelial cells H6C7 with *KRAS* wildtype and mutated background. An increase of activity of Akt was observed in GNB1 overexpressed *KRAS* mutated H6C7 cells. By analysing a digital antibody array DigiWest (NMI Technologietransfer GmbH 2020), the PI3K-Akt-mTOR signalling pathway was found to be activated in GNB1 overexpressed H6C7 cells. Moreover, PDPK1 expression highly increased in H6C7 cells upon GNB1 OE in both, *KRAS* wildtype and *KRAS* mutated cells. However, an increase of GNB1 protein level did not alter the sensitivity of cells to PDPK1, PI3K, PIK3CA and Akt inhibition.

3.5 Identification of GNB1 binding partners in primary PDACs

3.5.1 Cloning of FLAG-tagged GNB1 expression constructs

Formation of fully functional heterotrimeric guanine nucleotide-binding protein (G protein) complexes requires binding of G protein gamma subunits to the G protein subunit beta 1 (GNB1), which then trigger the downstream effectors. There exist different G protein gamma subunits, depending on the cellular context. The identification of the interacting G protein gamma subunits is relevant in PDAC as the assessment of the GNB1 binding partner helps to understand the mechanism of GNB1 induced TIC activation and may help for developing targeted therapies in future. To identify the G protein gamma subunits which bind to GNB1 in primary PDAC cultures, I introduced a 1x FLAG-Tag coding sequence to the N-terminal part of the codon-optimized GNB1 coding sequence of the lentiviral expression vector. I designed specific primers containing a 1x FLAG-Tag protein-coding sequence, and the GNB1 expression vector plasmid was used as the template.

I first performed a gradient PCR to define the best melting temperature (T_m temperature) of PCR product. The temperature was set ranging from 55 degrees to 65 degrees in 12 gradients on the thermal cycler. I loaded the PCR products on an Agarose gel for visualizing the PCR product. The length of GNB1-FLAG-Tag sequence is 1050 bp, according to the size, the brightest band with the least background in the lane (in red frame) was cut out (Figure 38).

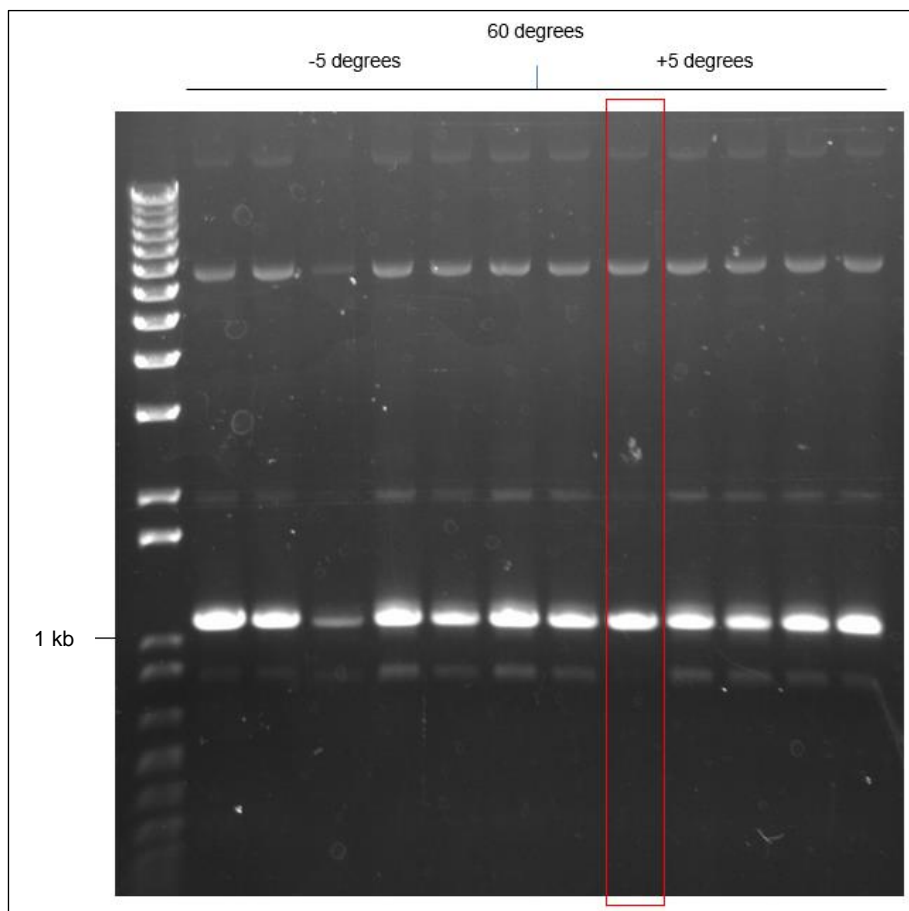


Figure 38: PCR amplification of GNB1-FLAG-Tag sequences.

Gradient PCR was performed to define the best T_m temperature, ranged from 55 degrees to 65 degrees. The length of GNB1-FLAG-Tag sequence is 1050 bp. DNA products were separated by 0.5% agarose gel. The bright band on the desired size (1050 bp) was cut out for further procedures (in red frame). kb: kilobases.

By following the TOPO-TA cloning protocol, I ligated prepared inserts with TOPO-TA vectors and transferred into competent cells for further selection (section 2.2.9.4). I extracted plasmids from selected clones and confirmed the FLAG-Tag coding sequence was successfully cloned to the N-terminal part of GNB1 codon-optimized sequence without mutations. Then, I performed double restriction enzyme digest to cut out the newly generated FLAG-tagged coding sequence and to linearize the expression vector backbone. I used calf alkaline phosphatase (CIP) enzyme in the restriction step to reduce the vector self-ligation. After confirmed the sequence was correct without mutations, I further expanded GNB1-FLAG-Tag inserts in the plasmid's maxi-preparation cultures.

3.5.2 GNB1-FLAG-Tag lentiviral particle production and titration

I transfected GNB1-FLAG-Tag expression vectors into pre-seeded 293T cells. On Day 5 of lentivirus production procedure, I harvested viruses and titrated on HeLa cells. I serially diluted viruses 1:10 (ranged from 10e-3 to 10e-7) in the HeLa cells culture medium and then I incubated cells with prepared viruses containing medium. On Day 3 post-transduction, I measured the proportion of transduced cells in the wells incubated with different amounts of viral supernatant by flow cytometry and then calculated virus titer form this data (Figure 39).

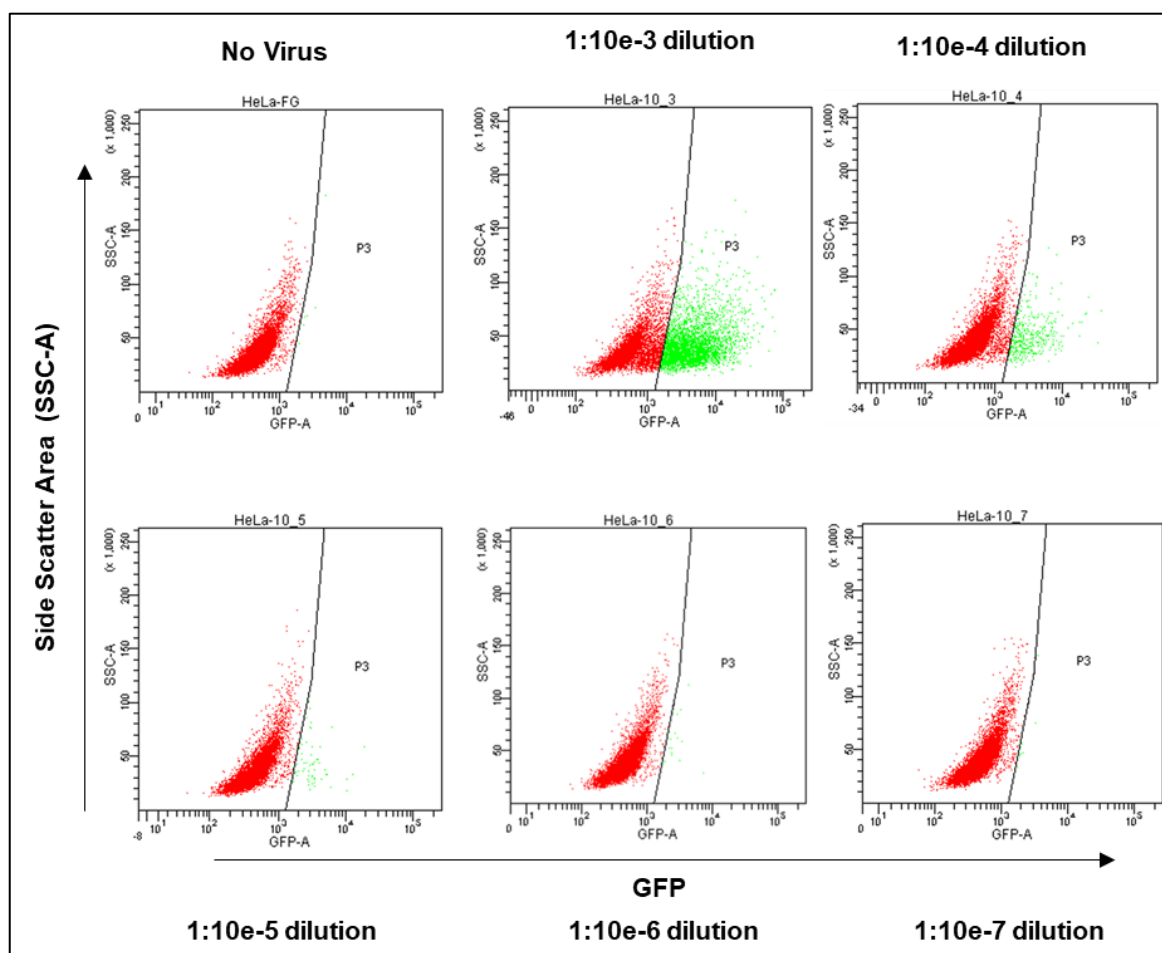


Figure 39: GNBI-FLAG-Tag virus titration using FACS (n=1).

Virus was gradient diluted from 1:10e-3 to 1:10e-7 in culture medium of HeLa cells and incubated with HeLa cells for 4 days. On Day 5, GFP% which represented the transduced cells was measured by flow cytometry. And GFP% between 2%-25% was used for virus titer calculation. The titer was 4.2×10^7 TU/ml. N=1, HeLa culture. SSC-A: side scatter area; GFP: green fluorescent protein control.

The GFP% over 40% is commonly considered as risking multi-integration events per cell which could result underestimation the true virus titer. Therefore, in 1:10e-4 dilution well, GFP% of living cells was 4.2%, and I used this number for titer calculation. According to the formula $[(1 \times 10^5) \times (\% \text{ of GFP-positive living cells})] / (100 \times \text{Dilution})$, the titer of produced GNB1-FLAG-Tag virus was 4.2×10^7 TU/ml (section 2.2.5).

3.5.3 Establishment of constitutive GNB1-FLAG-Tag expression in primary PDACs

I used PC1, PC2 and PC3 to generate GNB1-FLAG-Tag expression cultures. I transduced three PCs with LV. GNB1-FLAG-tagged lentiviral particles at MOI 2 as described in section 2.2.6. I further sorted transduced cells for GFP to enrich the transduced population when the confluency reached 90%. I measured the percentage of GFP positive cells after sorting by flow cytometry (n=3, biological replicates, Figure 40).

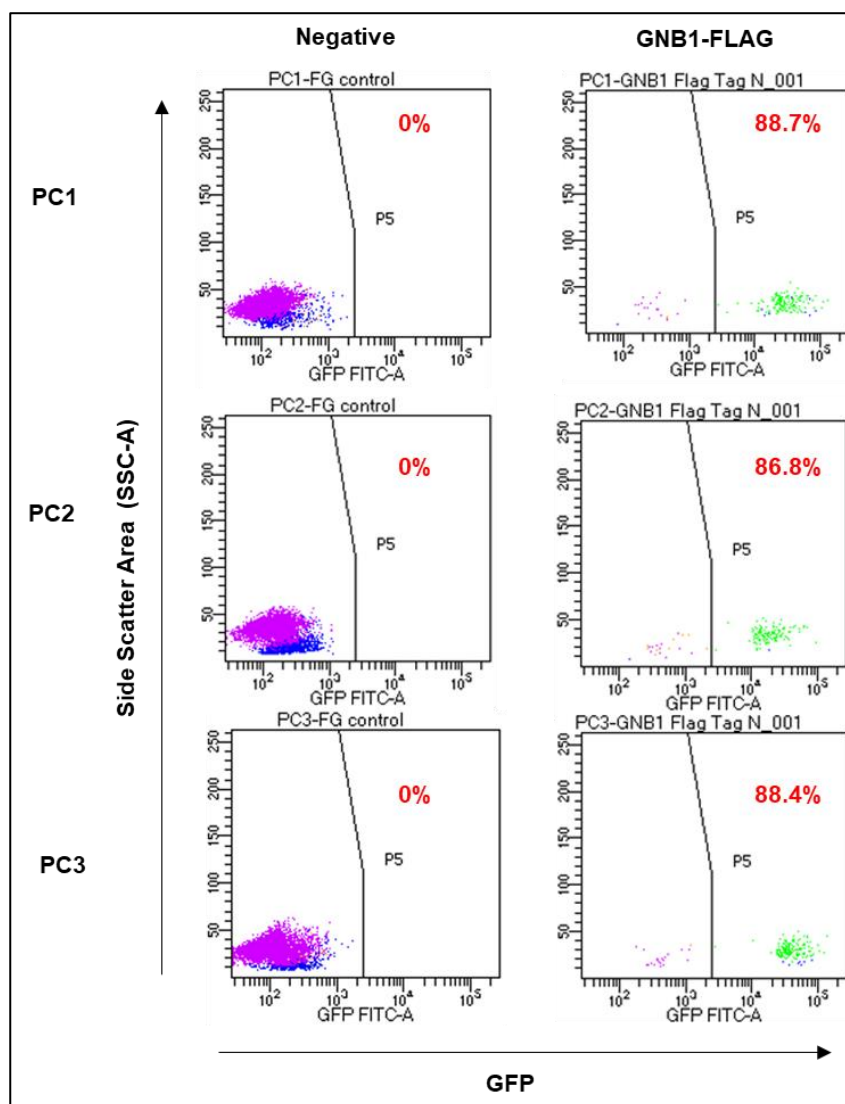


Figure 40: Efficient enrichment of lentivirally transduced cells using a vector for GNB1-FLAG-Tag expression after sorting (n=3).

In all three PCs, GFP positive cells showed as the dominant cells in the total population. GFP% of PC1: 88.7%, PC2: 86.8% and PC3: 88.4%. These data were produced directly after sorting from 200 cells in total. N=3, biological replicates. PC: primary PDAC cultures; SSC-A: side scatter area; FITC: parameter which shows the GFP signals. GFP positive cells represented as the transduced cells; GNB1-FLAG-N: FLAG-Tag protein coding sequence cloned on the N-terminal of GNB1 coding sequence; FG: Fluoro-Gold; GFP: green fluorescent protein; PC: patient-derived PDAC culture.

The proportion of GFP positive cells in PC1 sorted population was 88.7%, 86.8% of PC2 and 88.4% of PC3. These cells were expanded in cell culture flasks. All three PCs were used for further FLAG-Tag protein expression validation. The co-localization of GNB1 proteins and FLAG-Tag proteins were validated in PC1.

3.5.4 Validation of GNB1-FLAG-Tag protein expression by Immunofluorescence staining

I used the generated GNB1-FLAG-Tag expressing PC1 cells (PC1 GNB1-FLAG-N) for the FLAG-Tag protein Co-IP experiments (n=1). I seeded 1×10^7 GNB1-FLAG-Tag transduced PC1 cells, and PC1 GFP control in 15 cm cell culture dishes and cultured overnight. On the second day, I collected cells to generate the cells lysates. Then, I performed pull-down of the FLAG-tagged proteins by using FLAG-Tag antibody-conjugated agarose or magnetic beads. I used 3xFLAG-Tag peptide to elute the GNB1 protein complexes from the beads and sample buffers for the second elution.

I loaded normal cell lysates of PC1 GNB1 OE, GFP control, GNB1 KD, scramble and GNB1-FLAG-N as the loading control, as well as pulled down products into each lane. I first detected GNB1 proteins by using GNB1 antibody.

In the cell lysates, single GNB1-FLAG-Tag protein could be detected only in PC1 GNB1-FLAG-N cells. When GNB1 antibody was used for incubation with the membrane, there were two bands appearing in PC1 GNB1-FLAG-N culture, which indicated the endogenous GNB1 expression and the slightly bigger GNB1-FLAG-Tag protein (Figure 41A). In the FLAG-Tag pull-down sample, a single band was detected on the desired size, and the location of this band was comparable to the size of GNB1 bands in the whole cell lysates suggesting that the FLAG-Tag protein pull-down was successful (Figure 41A).

Furthermore, I investigated the co-localization of GNB1 and FLAG-Tag proteins by immunofluorescence (n=1). I seeded PC1 GNB1-FLAG-Tag and PC1 GFP control cells on coverslips and cultured for 40 hours for attaching. I incubated seeded cells with GNB1 and FLAG-tag antibodies, and further used Alexa Fluoro 647 and Cy3 dye conjugated secondary antibodies to bind to primary antibodies. Then I measured immunofluorescence by Leica TCS SP5 II confocal microscope (Leica company) in the Light Microscopy Facility in DKFZ, Heidelberg, Germany.

The results from immunofluorescence experiment showed that GNB1 proteins were mainly detected on the cell membrane as expected. However, the GNB1 antibody used was not very specific. Unspecific signals could be observed in the cell nucleus. FLAG-Tag antibody worked well, and FLAG-tagged GNB1 proteins were detected on the cell membrane as well. The merged image demonstrated that GNB1 and FLAG-Tag protein were co-localized on the cell membrane (Figure 41B.).

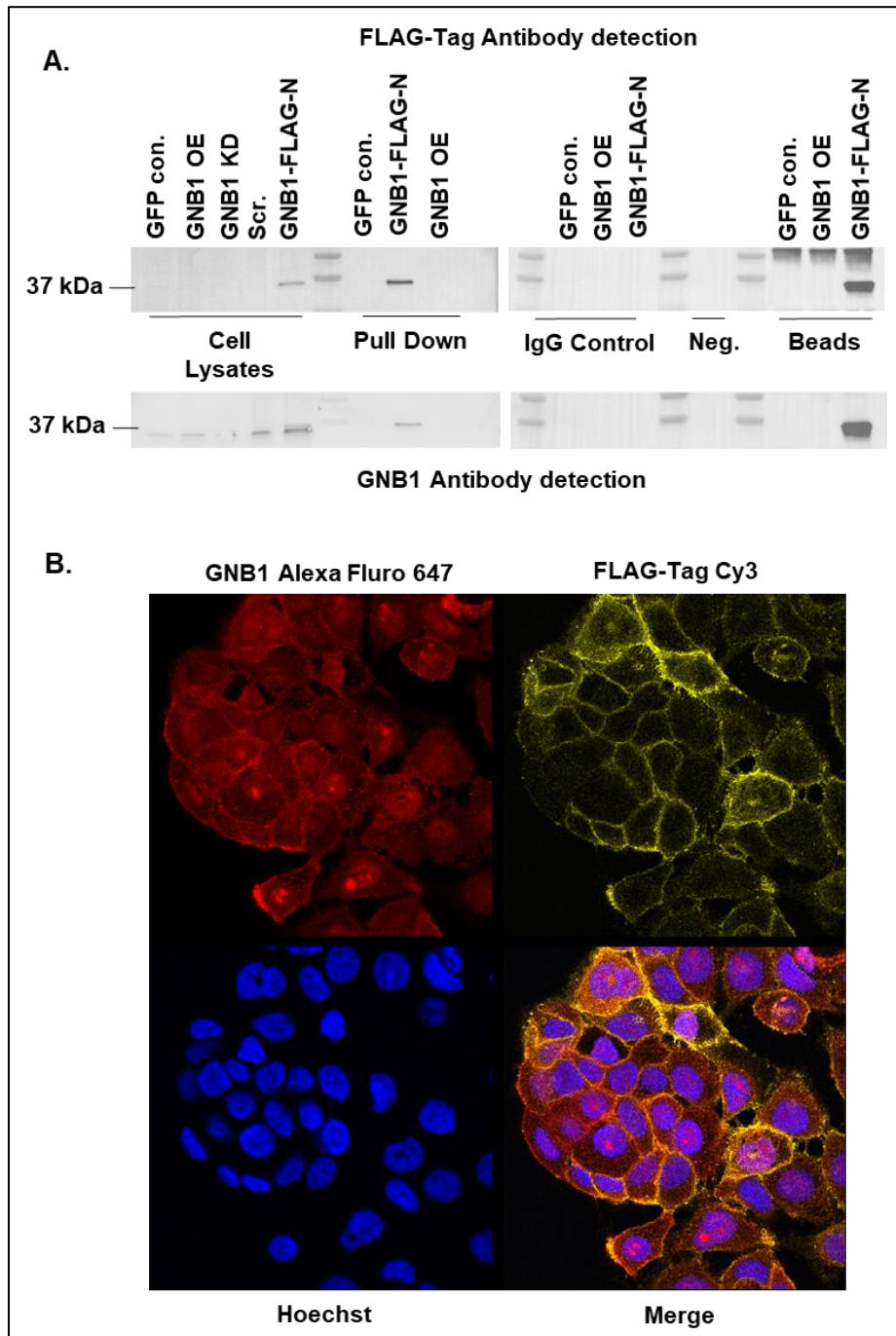


Figure 41: Validation of GNB1 and FLAG-Tag protein expression (n=1).

A. Co-immunoprecipitation of PC1 GNB1-FLAG-N transduced cells. FLAG-Tag protein bands detected in GNB1-FLAG-N cell lysates sample and in FLAG-Tag antibody pulled down GNB1-FLAG-N sample. GNB1 proteins were detected in all cell lysates samples, and in GNB1-FLAG-N cell lysate sample GNB1-FLAG-Tag recombinant protein band was detected on the size of 38 kDa. In FLAG-Tag antibody pull down group, GNB1 protein bands appeared in GNB1-FLAG-N groups. Cell lysates include full set of transduced PC1 (GNB1 OE, GFP control, GNB1 KD, scramble control and GNB1-FLAG-N). FLAG-Tag protein was pulled down by FLAG-Tag antibody conjugated beads, after first elution by using 3x FLAG, beads were boiled in samples buffer and loaded into wells. Membranes were first incubated with FLAG-Tag antibody, and after stripping GNB1 antibody was used for GNB1 proteins detection. B. Immunofluorescence images showed the co-localization of GNB1 and FLAG-Tag protein. Red: GNB1 Alexa Fluro 647, Yellow: FLAG-Tag Cy3, Blue: Hoechst nuclear staining dye. N=1, PC1; Neg.: negative control; OE: overexpression; GFP con.: green fluorescent protein control; KD: knockdown; Scr.: scramble; GNB1-FLAG-N: FLAG-Tag protein coding sequence cloned on the N-terminal of GNB1 coding sequence; kDa: kilodalton.

To investigate the interaction partners like which G gamma subunits binds to GNB1 in primary PDAC cultures comprehensively, mass-spectrometry was performed. Before the samples were sent for mass-spectrometry protein analysis, I performed a final confirmation experiment to validate that FLAG-tagged GNB1 was expressed in PC2 and PC3 (n=2). The molecular weight of FLAG-tag protein is one kDa. Therefore, the molecular weight of FLAG-tagged GNB1 proteins is 38 kDa, and double bands could be observed in the cell lysates part on the membrane in GNB1-FLAG-N groups which suggested that GNB1 were co-expressed with FLAG-Tag proteins in GNB1-FLAG-N groups which suggested that GNB1 were co-expressed with FLAG-Tag proteins (Figure 42). In the next step, to identify the binding partners of GNB1, I pulled down GNB1-FLAG-Tag proteins by FLAG-Tag antibody-conjugated magnetic beads in three PCs (PC1, PC2 and PC3), then these pulled down samples were sent for mass-spectrometry based protein analysis.

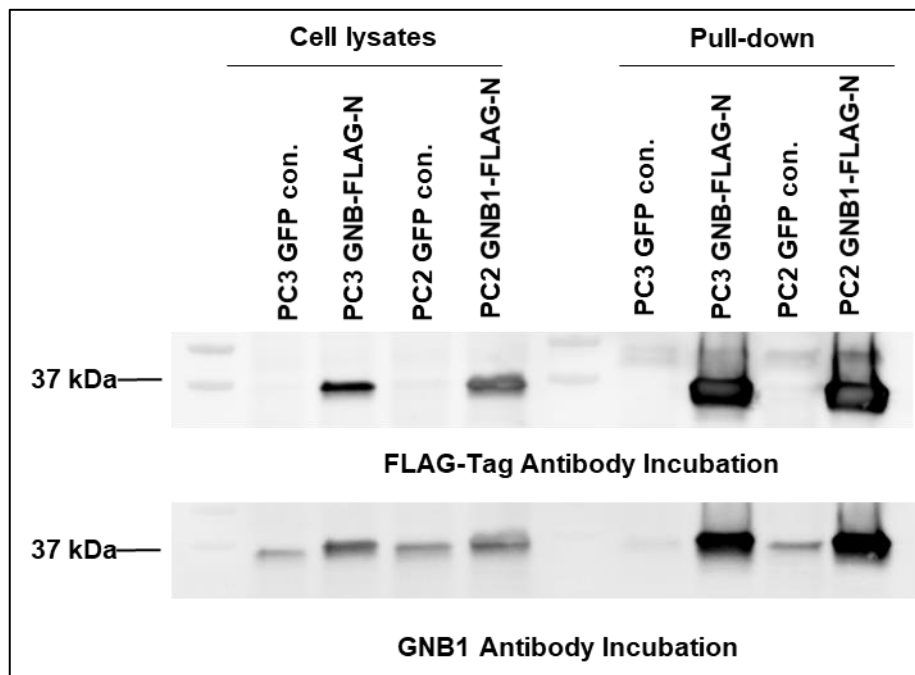


Figure 42: FLAG-Tagged GNB1 expression was detectable in transduced PC2 and PC3 samples (n=2).

FLAG-Tag antibody incubation image shows that GNB1-FLAG-tag recombinant proteins presented in LV. GNB1-FLAG-Tag transduced PC2 and PC3 in cell lysates at the size of 38 kDa. On the GNB1 antibody incubated membrane image, GNB1 bands were detected in all cell lysates, and the GNB1-FLAG-Tag recombinant proteins were detected in pull down samples at the size of 38 kDa. N=2, PC2 and PC3, biological replicates. GFP con.: green fluorescent protein control; GNB1-FLAG-N: FLAG-Tag protein coding sequence cloned on the N-terminal of GNB1 coding sequence; kDa: kilodalton; PC: patient-derived PDAC culture.

3.5.5 Identification and validation of GNB1 binding partners by mass-spectrometry after co-immunoprecipitation

The contribution in section 3.5.5: I prepared all protein samples for mass-spectrometry analysis. The mass-spectrometry analysis was performed in the Core Facility for Mass-spectrometry & Proteomics (CFMP) at Zentrum für Molekulare Biologie der Universität Heidelberg (ZMBH). The raw data was first analysed in the CFMP, then I retrieved these data and further analysed. I performed the co-immunoprecipitation experiments to validate the identified GNB1 binding partners.

I prepared and sent all samples of three PCs including FLAG-Tag protein pull-down, GFP control, transduced PCs, and IgG controls for protein analysis (n=3, biological replicates). Previous mass-spectrometry whole-cell proteome analysis showed expression of G protein subunit gamma 12 (GNG12) as the only G protein subunit in PC1, PC2 and PC3 (Table 3). Therefore, GNG12 could serve as a positive control for evaluating the detected binding partners of GNB1. Mass-spectrometry was performed in the Core Facility for Mass-spectrometry & Proteomics (CFMP) at Zentrum für Molekulare Biologie der Universität Heidelberg (ZMBH), and the raw data was first analysed in there. Then, I further analysed the retrieved data to select the candidates of GNB1 binding partners for further validation. Summarizing from retrieved data, in total, 2201 proteins were identified in three PCs GNB1-FLAG protein pull-down samples, including GNB2 and bait protein GNB1.

I set zero peptides for GFP con. IgG, FLAG-N IgG, and GFP con. FLAG pull down groups and the number of unique peptides number of FLAG-N FLAG pull down group above two as the filtering condition. This condition was applied to all three PCs, then four proteins namely potassium channel tetramerization domain containing 5 (KCTD5), guanine nucleotide-binding protein subunit alpha I1 (GNAI1), GNG12, and phosducin-like protein (PDCL) were identified as the GNB1 binding partners in all three PDAC cultures (Table 7). The detection of GNG12 showed that the results of this method were reliable. GNAI1 were detected in PC2 and PC3. G protein subunit gamma 5 (GNG5) was only identified in PC1.

Table 7: Unique peptide numbers of GNG12 detected by mass-spectrometry based whole cell protein analysis in PC1, PC2 and PC3 (n=3).

	PC3				PC1				PC2			
	GFP con. IgG	FLAG -N IgG	GFP con. FLAG pull down	FLAG -N FLAG pull down	GFP con. IgG	FLAG -N IgG	GFP con. FLAG pull down	FLAG -N FLAG pull down	GFP con. IgG	FLAG -N IgG	GFP con. FLAG pull down	FLAG -N FLAG pull down
GNAI1	0	0	0	8	0	0	0	9	0	0	0	4
PDCL	0	0	0	8	0	0	0	6	0	0	0	1
KCTD5	0	0	0	6	0	0	0	3	0	0	0	4
GNG12	0	0	0	2	0	0	0	2	0	0	0	2

N=3, biological replicates. Abbreviation in the table: PC: patient-derived PDAC culture; FLAG-N: FLAG-Tag protein coding sequence cloned on the N-terminal of GNB1 coding sequence; GFP con.: green fluorescent protein control.

I validated identified KCTD5, GNAI1 and GNG12 by co-immunoprecipitation (co-IP) experiments followed by western blotting (n=3, biological replicates, Figure 43). After co-IP of GNB1 using anti-FLAG-tag beads, KCTD5 and GNAI1 protein were detected at the expected size of 25 kDa and 40 kDa in both FLAG-tag conjugated agarose and magnetic beads pull-down group. No bands were detectable in both GFP control and GNB1-FLAG-Tag IgG samples indicating that KCTD5 and GNAI1 were indeed the binding partners of GNB1. Although the protein amount of GNG12 seemed to be very low in GNB1-FLAG tag samples, no protein band was detected in GFP control and GNB1-FLAG-Tag IgG control lysates (Figure 43).

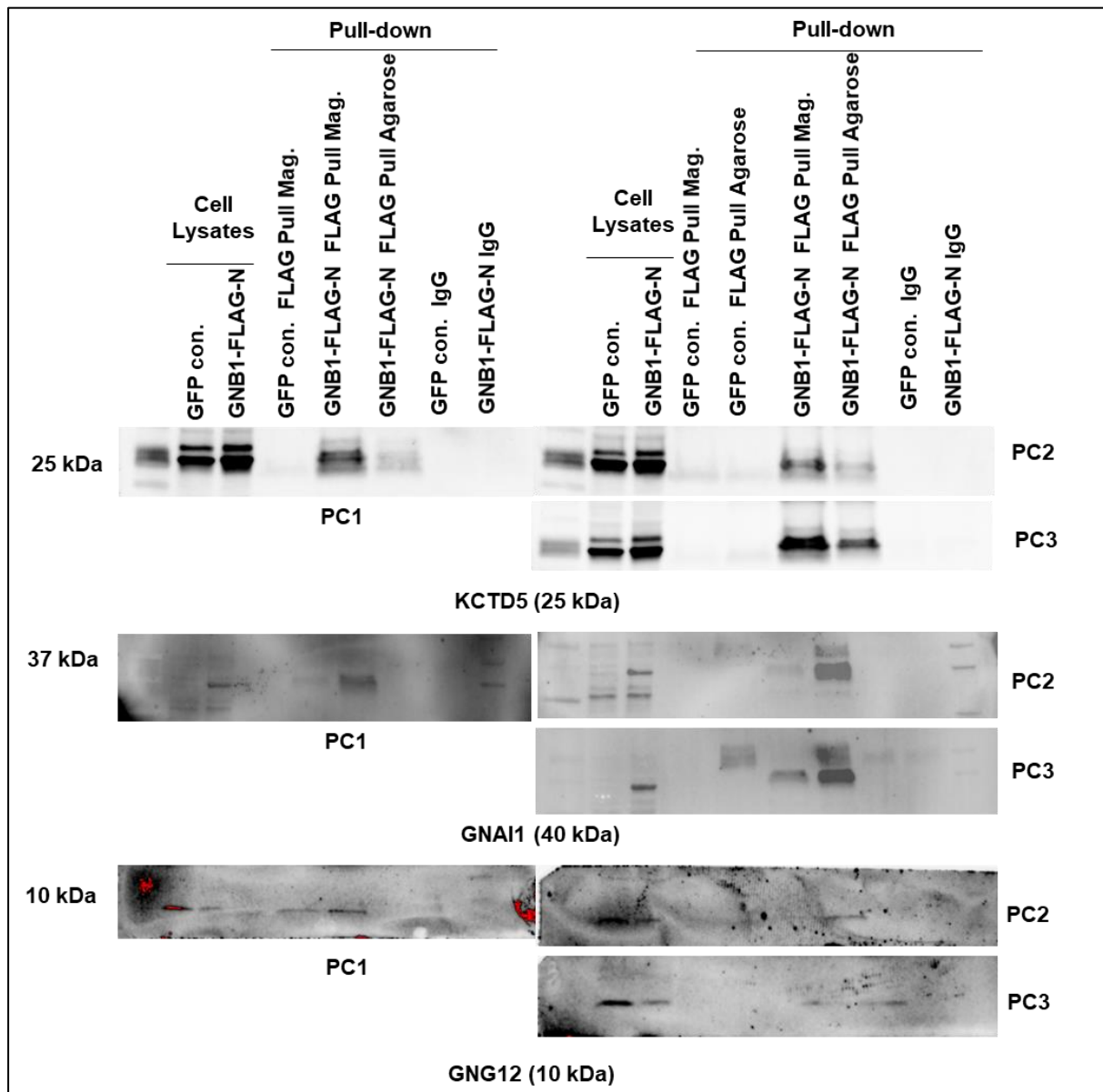


Figure 43: Validation of identified GNB1 binding partners by co-immunoprecipitation (n=3).

Different proteins were detected on the same membrane of each PC, and membranes were strip twice. IgG conjugated agarose beads were used as control, and FLAG-Tag conjugated Agarose and magnetic beads were used for pulling down. KCTD5 (25 kDa), GNAI1 (40 kDa) and GNG12 (10 kDa) were detected on their correct molecular weight which indicated that these three proteins were validated as the binding partners of GNB1. N=3: biological replicates. PC: patient-derived PDAC cultures; GNB1-FLAG-N: FLAG-Tag protein coding sequence cloned on the N-terminal of GNB1 coding sequence; GFP con.: green fluorescent protein control; kDa: kilodalton; PC: patient-derived PDAC culture; Mag.: magnetic.

To further validate GNG12, I re-eluted proteins from FLAG-Tag pull-down beads and subjected to western blot, and old membranes were reactivated to detect GNG12 (Figure 44). In all three PCs (n=3, biological replicates), GNG12 was detected in GNB1-FLAG-Tag transduced PCs, but the absence of detectable protein bands in the control GFP control pull-down samples suggested that GNG12 encoded G γ 12 was the binding partner of GNB1 in primary PDAC cultures.

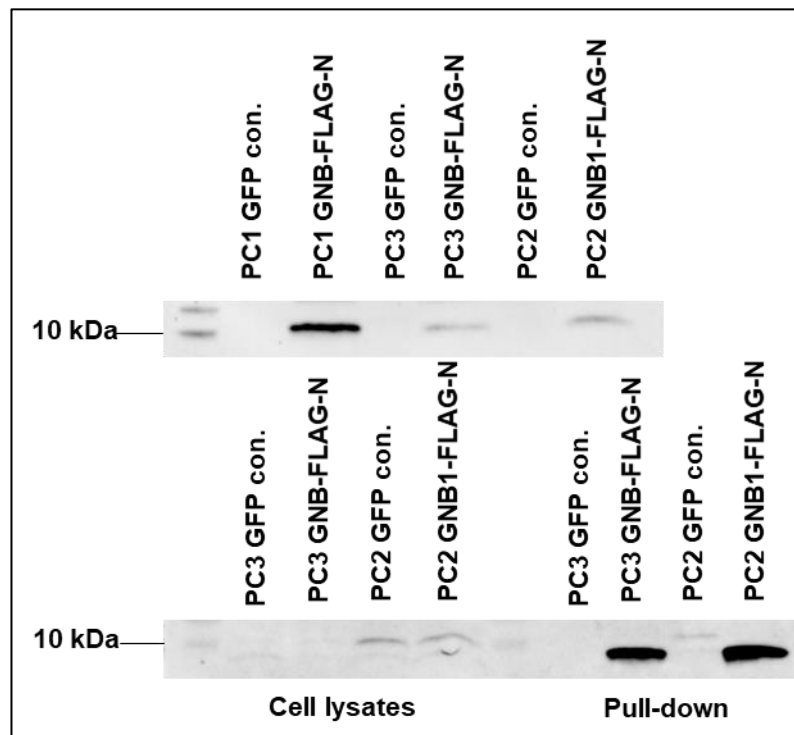


Figure 44: Validation of GNG12 as the binding partner of GNB1 by co-immunoprecipitation (n=3).

Proteins were re-eluted from old FLAG-Tag conjugated pull down beads and performed the western blot. Then old membranes were reactivated to detect GNG12. GNG12 (10 kDa) protein bands were only detected in GNB1-FLAG-Tag PCs. In the cell lysates part of downside image, GNG12 bands were not visible in both PC3 samples might be due to the low protein loading. N=3: technical replicates. GNB1-FLAG-N: FLAG-Tag protein coding sequence cloned on the N-terminal of GNB1 coding sequence; GFP con.: green fluorescent protein control; kDa: kilodalton; PC: patient-derived PDAC culture.

3.5.6 Summary 3.5

Three FLAG-tagged GNB1 expressing PCs were successfully generated, and FLAG-tagged GNB1 protein was observed localized at the cell membrane, suggesting that the FLAG tag did not alter the cellular localization. Co-IP followed by mass spectrometry identified GNAI1, GNG12, and KCTD5 as binding partners of GNB1 which were also validated experimentally.

4 Discussion

4.1 GNB1 possesses PDAC TIC regulator activity

4.1.1 TICs are transiently activated in PDAC

Pancreatic cancer (PDAC) is ranked as the 3rd leading cause of cancer-related death in the US (Ercan et al. 2017). An increasing amount of studies is focusing on PDAC with the aim to improve the outcome by understanding tumour formation and identification of new therapeutic targets. However, recent data revealed that targeting PI3K and ERK in PI3K, and MAPK signalling showed no benefit in respect to the overall survival time of patients (Neoptolemos et al. 2018). Besides intrinsic targets, the microenvironment provides another targetable compartment in PDAC. Unfortunately, antiangiogenic and multi-kinase inhibitors were tested and evaluated as none effective in improving overall survival time (Neoptolemos et al. 2018). Currently, the therapeutic options for PDAC are limited. Therefore, there is an urgent need to deepen the insights of this type of cancer.

According to the famous Hallmarks of Cancer theory from Douglas Hanahan and Robert A. Weinberg, cancer is characterized as a heterogeneous disease (Hanahan and Weinberg 2011). Moreover, tumour initiating cells (TICs) play a critical role in tumour initiation and progression, and TICs show low sensitivity to chemotherapy which suggests its critical role in drug resistance and tumour recurrence (Ercan et al. 2017). Based on the features of TICs, this cell population is considered as an excellent target of cancer therapy. In previous studies from Prof. Dr. med. Hanno Glimm's group, using lentiviral barcoding to follow individual clones in serial transplantation, self-renewing long-term TIC (LT-TIC) were identified which maintain long-term tumour progression in human colon cancer (Dieter et al. 2011). The same genetic clonal marking technology was used to assess clonal dynamics in patient-derived PDAC cultures (Ball et al. 2017; Kreso et al. 2013). Interestingly, in the serial xenografts of PDACs, tumours in different xenograft generations were formed by different cell clones which were active only transiently (Ball et al. 2017), Suggesting that tumour progression in serial transplantation is driven by a succession of transiently active TIC clones (Ball et al. 2017). Therefore, it is crucial for PDACs to understand the underlying mechanisms and to identify regulators of this transient activation.

4.1.2 Overexpression of GNB1 promotes PDAC progression

A trapping vector *in vivo* screening on patient-derived PDAC cultures was performed to identify potential regulators of transient TIC activation in PDAC (Gao 2017). In this screening approach, one PDAC primary culture (PC) derived from a patient's tumour was used and a constant activation of certain clones in serial transplantation (Ehrenberg et al. 2019; Gao 2017) was detected. By mapping the integration sites of the vector using genome-wide high-throughput insertion site analysis, the genes which were upregulated due to a trans-splicing event of the lentiviral vector used were identified. These genes are suggested as candidates of TIC regulation. *GNB1*, *SLC35F5*, and *SOS2* were identified as the TIC regulatory candidates (Gao 2017, pg. 60-64). Previous initial experiments evaluated *GNB1* as potential TIC regulator (Gao 2017, pg. 71-74). Transplantation of PC with ectopic overexpression of *GNB1* showed that *GNB1* overexpression induced continuous contribution of cell clones to tumour formation in all generations (Gao 2017, pg. 71-74).

GNB1 encodes G protein subunit beta 1 which belongs to the G protein superfamily and is activated as the transducer by G protein-coupled receptors (GPCRs) (Choi et al. 2015; Pierce et al. 2002). G protein beta subunits together with G protein gamma subunits separate from G protein alpha subunits and then involve in different cellular response after GPCRs activation (McCudden et al. 2005). In 1998, researchers already found G protein beta gamma subunits regulating cell proliferation via multiple signalling pathways (Dhanasekaran and Prasad 1998). The role of GPCR signalling pathways in cancer has long been studied which revealed that GPCR signalling pathways are involved in different processes to maintain cell survival, proliferation, and migration (Cotton and Claing 2009; Pierce et al. 2002; Schäfer et al. 2004). There is evidence that GPCR signalling plays a central role of GPCRs in stem cell maintenance (Layden et al. 2010; Nakamura et al. 2009). Therefore, GPCR signalling might also be important for stem cell-like cells in cancer. Among GPCRs, leucine-rich repeat-containing G protein-coupled receptor 5 (LGR5) is well characterized as the colon tumour initiating cell marker (Chen and Xue 2019; Morgan et al. 2018). By tracing the cell growth *in vitro* and tumour growth *in vivo*, results from previous study demonstrated that overexpressed GNB1 accelerates cell proliferation, and the knockdown of GNB1 leads to a loss of transduced PC cells. This highly suggests that GNB1 is involved in pathway alterations regulating cell proliferation. Therefore, further GNB1 induced pathway alterations should be studied.

In the previously applied trapping vector screening approach, GNB1 was artificially overexpressed by the integrated trapping vector, thereby possibly enhancing the activation of downstream effectors of G proteins, leading to TIC activation. To understand the molecular consequence of deregulated GNB1 expression in primary PDAC, GNB1 was overexpressed ectopically in patient-derived PDAC cultures. Of note, in this thesis, the three primary PDAC cultures used harboured different *KRAS* mutations (G12V and G12D).

G protein beta gamma subunits negatively or positively regulate adenylyl cyclase (AC) isoforms which generate cAMP from ATP (Sadana and Dessauer 2009). In the following process, protein kinase A (PKA) is activated by cAMP, which further phosphorylates transcription factors and activates other signalling pathways (Hanoune and Defer 2001; New and Wong 2007). G $\beta\gamma$ subunits bind tightly to G α subunits at the inactivated state and are separated from G α subunits when GPCRs are activated (McCudden et al. 2005). The different subgroups of G alpha subunits target on oncogenes to promote tumour growth and generate transformed phenotypes (Radhika and Dhanasekaran 2001; Wong et al. 1995). In PDAC TIC activation, overexpressed GNB1 shows an impact on TIC activation and may also lead to deregulation of G α subunits. However, GPCR-mediated activation of MAPK signalling and transactivation of epidermal growth factor receptor (EGFR); GPCR-mediated PKC-dependent pathways and PI3K-dependent pathways overlap and have cross-regulation (Goldsmith and Dhanasekaran 2007; Wang 2016).

In this thesis, the mechanisms of GNB1 enhanced cell proliferation were further investigated. Cell cycle analysis revealed that knockdown of GNB1 leads to increased G0 cell cycle arrest in one of the three primary cultures, whereas overexpression has no impact. Knockdown (KD) of GNB1 in PC1 and PC2 showed an increase in necrotic cells in PC2 (Gao 2017, pg. 80). The cross-regulation of various signalling pathways may explain this. A series of phosphorylation events control the cell cycle in eukaryote (New and Wong 2007). Cyclins and cyclin-dependent kinases are the relevant master regulators of this process (Poon 2002). During G1 phase, cyclins can react to extracellular signals, so the multi pathways' activation induced by GPCRs can

affect the cell cycle in this phase to either promote cell proliferation or negatively regulating this process or increase the DNA synthesis. (New and Wong 2007).

Furthermore, additional mutations in established cultures may explain the difference influences on the cell cycle of overexpressed GNB1. One study reported that mutated GNB1 induced tumour formation in mouse bone marrow after the loss of *CDKN2A* (Yoda et al. 2014). Mutations in the cell cycle regulator *CDKN2A* are commonly detected in the early stage of PanINs. However, the status of *CDKN2A* in the primary PDACs is unknown and could be analysed in future. Furthermore, it was not clear which treatment these patients received, which could lead to the different signalling response in cells. To address the deregulation of intrinsic signalling pathways, the pathway alterations induced by GNB1 deregulation were further analysed.

4.1.3 GNB1 is heterogeneously expressed in PDAC

Currently, single-cell RNA sequencing is widely used to understand intratumor heterogeneity for biomarker identification. The purpose of performing single-cell RNA sequencing in this study was to investigate the transcriptional heterogeneity of GNB1 expression in PDAC cultures. GNB1 expression was checked in the sequenced cells. Strikingly, 4424 cells (60%) showed no GNB1 expression, 735 cells classified as the high GNB1 expression cells (quantiles values, >1.11). The clonal expansion of a single initiated cell is commonly considered as the source of tumours arisen, and the production of distinct subclones in the following that can cooperate to drive tumour growth or progression (Calbo et al. 2011; Cleary et al. 2014; Greaves and Maley 2012; Nowell 1976; Reeves et al. 2018). The clonal tracking analysis showed that PDAC cells acquire TIC activity only transiently; therefore, different clones primarily drive growth in serial transplantation (Ball et al. 2017). This implies that GNB1 activity may be needed only transiently to trigger TIC activity. Single cell RNA sequencing data done within this thesis further support the hypothesis that GNB1 or targets downstream of GNB1 are responsible for this transient TIC activation. Cells with differential expression levels of GNB1 were identified in the primary PDAC culture supporting this hypothesis further.

Correlation analysis of GNB1 expression and the general pathway signatures, identified β -arrestin signalling pathway, which suggests a high activity of this signalling pathway in high GNB1 expressing cells. Remarkably, it has been shown that the phosphorylated GPCRs activate this pathway, and commonly activated β -arrestins are discovered by GPCR desensitization and internalization (Shenoy and Lefkowitz 2005; Song et al. 2018). β -arrestins can interact with multiple signalling pathways, including MAPK, PI3K, Wnt signalling pathways (Smith and Rajagopal 2016; Song et al. 2018).

It has been demonstrated that β -arrestin1 serves as an adaptor which recruits Src to the obestatin receptor and formed an obestatin receptor/ β -arrestin1/SRC proto-oncogene (Src) complex, which may further promote EGFR transactivation (Alvarez et al. 2009). The transactivation of EGFR promotes the initiation of various signalling pathways, including the PI3K-Akt-mTOR signalling pathway. On the contrary, β -arrestins suppress the activation of the Akt pathway via increasing the activity of PTEN, to inhibit cellular proliferation (Lima-Fernandes et al. 2011). β -arrestins and GNB1 activity are both activated by GPCRs, and by considering the activation of PI3K signalling pathway which was observed in normal pancreas epithelial cells upon GNB1 overexpression, it is suspected that GPCRs/ β -arrestins/PI3K signalling plays a dominant role in PDAC TIC activation. However, so far, there is only one primary PDAC sequenced. To

further identify transcriptional programs which are associated with this TIC regulatory protein, and to gain a better understanding of the role of GNB1 and its downstream effectors involved signalling pathways, more primary PDACs should be sequenced.

These data support the hypothesis that overexpression of GNB1 leads to PDAC TIC activation and encourages to further investigate how GNB1 is involved in PDAC TIC regulation.

4.2 Gβ1 expression seems to be strictly controlled in cancer cells

PDAC cultures could be efficiently transduced with lentiviral vectors encoding for GNB1 leading to successful overexpression in primary PDAC cultures. The mRNAs level of GNB1 which were transcribed from lentiviral expression vectors were overexpressed compared to the endogenous GNB1 mRNAs level. Interestingly, on the protein level the overexpression of GNB1 was below 2-fold in all three transduced PCs, 293T and the normal pancreas epithelial cells H6C7 compared to control transduced cells. This relative low level of overexpression was very similar in three different types of cells. Therefore, it was initially taken into consideration that the endogenous GNB1 expression level was too high, which led to the difficulties to overexpress GNB1 to an even higher degree. According to the PC1 sc-RNA-seq data, in around 60% of cells GNB1 expression was not detectable. Compared to primary PDAC and H6C7 cells, endogenous GNB1 was lower expressed in 293T cells. However, GNB1 proteins cannot be overexpressed significantly in 293T cells either. In line with the data showed in this study, researchers overexpressed wild type GNB1 and two mutated GNB1 isoforms in leukemic cells in a recent study, and the results showed similar GNB1 protein levels by using a different expression vector (Zimmermannova et al. 2017). It seems that an over 2-fold overexpression of GNB1 is hardly achievable in different cancer cells. Altogether, these data suggest that not technical issues but rather an intrinsic regulatory mechanism abrogates high GNB1 protein levels.

Two other possible reasons were then suspected. First, intrinsic post-translational inhibitory mechanisms strictly regulate GNB1 protein expression in cells without affecting mRNAs. The identification of KCTD5 and PDCL, which have been previously reported as a negative regulator of GNB1 (Brockmann et al. 2017; Lukov et al. 2005) in GNB1 pull-down protein mass-spectrometry analysis supports this hypothesis. G proteins are not only regulated by GPCRs, but also can be regulated by various non-GPCR proteins including Ric-8, G protein regulators (GPR), Gα-binding and activating motif-containing protein (GBA proteins), and regulators of G protein signalling proteins (RGS proteins) (Syrovatkina et al. 2016). Among these four types of proteins, Ric-8 can activate Gα subunits but not Gβγ subunits (Tall and Gilman 2005; Thomas et al. 2008). Gα-interacting vesicle-associated proteins (GIV) belonged to GBA proteins and were reported to enhance Gβγ-dependent signalling in cells by displacing Gβγ subunits from Gai-βγ complex (Garcia-Marcos et al. 2009). These identified regulators are mostly regulating Gα subunits, and only a limited number are targeting Gβγ dimers (Syrovatkina et al. 2016). Therefore, further studies investigating GNB1 binding partners will provide additional information to understand the mechanisms of overexpressed GNB1 triggering transient PDAC TIC activation. Second, GNB1 may only be overexpressed in a small population of cells, and average data from the bulk population dilute the deregulation of overexpressed GNB1 proteins. Immunofluorescence staining was performed to address the second hypothesis. Results produced in this study demonstrated that endogenous GNB1 was

heterogeneously expressed. Transduced GNB1 OE PC1 cells showed stable GNB1 overexpression, and only a few cells showed a very high fluorescence level, indicating for a strong and uniform GNB1 expression. As the cells did not grow in monolayer, it was believed that the slight changes in fluorescence intensity were due to the overlapping of signals when 10 layers of images were merged. Therefore, the negative regulation by KCTD5 and PDCL of GNB1 proteins might be the main reason that an over 2-fold GNB1 overexpression in three PCs could not be achieved.

However, it may not be necessary to have very high levels of GNB1 to induce the PDAC TIC activation. In the following, GNB1 overexpression in PC1 and PC2 followed by *in vivo* TIC dynamic validation analysis confirmed this TIC activation. To sum up, these data suggest a strict feedback regulation of GNB1 in cancer cells. Moreover, in the established artificial cell models, slight expression alterations, but the constant activity of GNB1 protein might already be enough to induce TIC activation.

4.3 GNB1 may regulate PDAC TIC activation via PI3K-Akt-mTOR signalling

To further understand the mechanisms of TIC activation triggered by GNB1, a normal pancreatic epithelial cell line model, namely H6C7 cells, was used. As GNB1 seems to signal via PI3K like KRAS for example, the next step was aimed at subtracting the influence of mutated KRAS to the downstream signalling pathways. Therefore, GNB1 was overexpressed in KRAS wild type and KRAS^{G12V} mutated H6C7 cells, respectively. In this established cell line model, Akt activation was found to be upregulated in KRAS GNB1 OE, instead of ERK, which suggests that GNB1 enhanced PI3K signalling.

The network of GPCR signalling pathways and PI3K-Akt-mTOR and MAPK signalling pathways are complex. GNB1 (Gβ1) is located upstream of PI3K-Akt-mTOR and MAPK signalling pathways (Dorsam and Gutkind 2007). When Gβγ dimers separate from Gα subunits, the Src family is activated by Gβγ dimers via recruiting SHC adaptor protein (Shc) and growth factor receptor bound protein (Grb2) adapter proteins to the membrane (Luttrell et al. 1997). Interestingly, Src tyrosine kinase can be directly regulated by Gαs and Gαi as well (Ma et al. 2000). The activated Src further promotes the GTPase activity of Ras (Bunda et al. 2014). Gβγ dimers showed direct activation of the Rac1-specific guanine nucleotide exchange factor (Rac GEF) further triggering the activation of the JNK signalling pathway (Zhang et al. 2009). On the PI3K-Akt-mTOR axis, Gβγ subunits can directly interact with the PI3K p110γ subunit, which influences Akt activation (Leopoldt et al. 1998). Lysophosphatidic acid (LPA) can be activated through GPCRs and alters different cellular responses via G proteins (Lin et al. 2010).

To have the first impression of signalling pathway deregulations in the established GNB1 OE H6C7 cells, a digital western blot based multiplex protein profiling antibody array was used to analyse the key components in both signalling pathways (NMI Technologietransfer GmbH 2020). Through the DigiWest data, the activation of SGK1, TSC2, p70 S6 kinase upon GNB1 overexpression was observed. Especially, a very high increase of PDPK1 protein content was observed in both GNB1 OE transduced H6C7 KRASwt and KRASmut cells. Together with previous observed Akt activation in H6C7 KRAS mutated GNB1 OE cells by western blot, these data showed that, instead of the MAPK signalling pathway, the PI3K-Akt-mTOR signalling pathway was activated in both KRASwt, and KRASmut GNB1 OE H6C7 cells.

PDPK1 is the key molecule leading to Akt phosphorylation on threonine 308 (Thr308) (Jebali and Dumaz 2018). PDPK1 is regulated by phosphatidylinositol 3,4,5 phosphate (PIP3) through

docking on the pleckstrin homology (PH) domain on PDPK1 (Jebali and Dumaz 2018). When PIP3 binds to PDPK1, PDPK1 triggers Akt translocation to the membrane and phosphorylation on Thr308 (Jebali and Dumaz 2018). In this process, PIP3 is controlled by PI3K and activated RAS regulates PI3K (Jebali and Dumaz 2018).

To demonstrate the correlation between GNB1 and PDPK1, western blotting was performed to further validate the DigiWest results by using GNB1 OE H6C7 cells and established GNB1 KD H6C7 cells. The increase of PDPK1 protein was able to verify by western blot. However, the increase was only about 3-fold (*KRAS* wildtype) and 2-fold (*KRAS*^{G12V} mutated) compared to 6-fold (*KRAS* wildtype) and 56-fold (*KRAS*^{G12V} mutated) retrieved in the DigiWest data. This difference might be due to the sensitivity of the different methods. Interestingly, the decrease of PDPK1 expression was observed after knockdown of GNB1 in H6C7 *KRAS* wild type cells, but no change in H6C7 *KRAS* mutated cells. The influence of GNB1 KD was abolished due to continuous activation by mutated *KRAS*. These results indicate that PDPK1 is one of the downstream effectors of GNB1. The PDPK1 protein level shown in both, GNB1 KD H6C7 cells with *KRAS* wild type and *KRAS* mutated background pointed out that mutated *KRAS* interferes with the GNB1-PDPK1 regulating process. *KRAS* mutations occur in over 90% of PDACs and display a gene mutation, which already occurs in PanINs (Vincent et al. 2011). Mutated *KRAS* leads to PDAC cells proliferation and survival (Polireddy and Chen 2016). These findings urged researchers to target mutated *KRAS*. However, following experiments revealed that *KRAS* is an "undruggable" target so far. MAPK and PI3K-Akt-mTOR signalling pathway are the two main pathways in pancreatic cancers. In the meantime, other vital components in PI3K and MAPK signalling pathways, for example, PI3K, Akt, and MEK1/2 were evaluated, which showed potential therapeutic values (Polireddy and Chen 2016).

In summary, the DigiWest array results and the western blot findings after deregulation of GNB1 expression demonstrated that in normal pancreatic epithelial cells, without the influence of mutated *KRAS*, GNB1 modulates the PDPK1 protein content. A study showed the PI3K-PDPK1 signalling was the essential effector of mutated *KRAS* induced pancreatic cancer (Eser et al. 2013). In our study, PDPK1 protein content increased in both *KRAS* wild type and mutated background when GNB1 was overexpressed, and the activation of the downstream kinases can be observed. The PI3K-PDPK1 axis is boldly assumed that it might be essential not only in *KRAS* mutated pancreatic cancer but also seems to be a critical messenger in GNB1 dysregulated pancreatic cancer independent of the *KRAS* genotype.

To target the GNB1 induced PI3K-PDPK1-Akt pathway activation, three different inhibitors were selected targeting PI3K pathway, namely PI3K inhibitor Copanlisib, PIK3CA inhibitor GDC-0032, and PI3K alpha inhibitor Apelisib and used to treat GNB1 expression altered H6C7 cells. Moreover, the Akt inhibitor MK-2206 was included to block the downstream signalling of PDPK1. Firstly, the response of the GNB1 inhibitor Gallein was tested on GNB1 overexpressing cultures. Both, GNB1 OE H6C7 cells with *KRAS* wildtype or mutated showed a two-fold higher IC₅₀ of GNB1 inhibitor compared to each control. However, there was no difference of cell viability between *KRAS* wild type and mutated background when using single PI3K, PIK3CA, PI3K alpha and Akt inhibitor treatment. Due to the intricate cross-regulation that exists in MAPK, and PI3K signalling pathways, single targeting of PI3K, PIK3CA or PI3K alpha may not block the overexpressed GNB1 induced pathway activation. Therefore, in the next step, it is interesting to investigate the activities of the downstream component, for example, the activation status of p70 S6 kinase or S6 kinase. Moreover, since the TIC activation is only initiated in a small population of cells, cell viability which represents the cell survival of the

bulk population cannot reflect the TIC activation. Long-term colony formation *in vitro* with PI3K signalling pathway inhibitors treatment is necessary for observing the influence on the TIC activation in the generated cell models.

4.4 GNG12, GNAI1 and KCTD5 are characterized as the binding partners of GNB1 in primary PDACs.

G $\alpha\beta\gamma$ subunits are binding together and separated to G α and G $\beta\gamma$ subunits when GPCRs are activated (Hilger et al. 2018). The downstream effectors of G α subunits and G $\beta\gamma$ subunits are partially overlapping (McCudden et al. 2005). It is shown that GNB1 can be a TIC activation regulator and it was aimed to understand the underlying mechanisms driving this activity. Therefore, it is necessary to characterize the combination of G $\alpha\beta\gamma$ subunits in different patient-derived PDAC cell models to further understand whether the complex is patient specific in TIC activation. In the past, studies solely reported the expression of G γ subunits in PDACs (Li et al. 2020; Shibata et al. 1998). However, none of them reported the full combinations of G $\alpha\beta\gamma$ subunits. Therefore, characterizing the combination of G $\alpha\beta\gamma$ subunits will provide new insights into G proteins in PDACs. GNAI1, GNG12, KCTD5 and PCDL1 were identified as the binding partners of overexpressed GNB1 by mass-spectrometry based protein pulldown experiments.

GNAI1 encodes for G α_i1 belonging to G α families. G α_i proteins can inhibit specific isoforms of AC and lead to the reduction of intracellular cAMP levels (Syrovatkina et al. 2016). As introduced previously, G protein beta gamma subunits could target AC isoforms as well. And it might be possible that the collaboration between G α_i and G $\beta\gamma$ subunits regulates downstream signalling. Further studies focusing on GNAI1 provide more evidence that signalling through GNAI1 promotes cell proliferation and differentiation (Embry et al. 2004; Ram and Iyengar 2001). In hepatocellular carcinoma, GNAI1 protein was found to be downregulated, causing suppression of tumour cell migration and invasion (Yao et al. 2012). Interestingly, G α_i and G $\beta\gamma$ subunits can co-regulate G $\beta\gamma$ effector G protein-activated K(+) channels (Berlin et al. 2010). However, the role of GNAI1 in pancreatic cancer is still not clear. In this project, it was reported that GNAI1 was identified as the binding partner of the novel TIC regulator GNB1 in pancreatic cancer. The role of GNAI1 in GNB1 induced PDAC TIC activation is interesting to investigate further. Moreover, to understand whether the co-regulation exists during the TIC activation process may help to investigate the pathway alterations triggered by GNB1 in the primary PDACs.

G γ subunits commonly bind tightly to G β subunits and form stable dimers (Sondek et al. 1996). In human, 12 G protein gamma subunits are identified (Syrovatkina et al. 2016). The coding sequence of β -subunits share similarities, but different $\beta\gamma$ complexes could interact with different effectors (Kleuss et al. 1992). Therefore, G protein gamma subunits may determine the function of G $\beta\gamma$ subunits (Kleuss et al. 1992). However, the individual function of G γ subunits is still unknown. Among the three submitted primary PDAC cultures, GNG12 was identified as the only detectable G γ subunit. A previous study showed that GNG12 promoted PDAC cell growth by activating the nuclear factor 'kappa-light-chain-enhancer' of activated B-cells (NF- κ B) pathway in pancreatic cancer cell lines PANC-1 and BxPC-3 (Li et al. 2020). In this study, they did not mention any G β subunits. Therefore, it is unclear whether the findings they reported was initiated from the deregulation of GNG12. At least this study showed that GNG12 is linked to PDAC cell growth. This is in line with the *in vitro* results of previous study showing that GNB1 positively correlates with cell proliferation (Gao 2017, pg. 76-79). This

thesis retrieves that the combination of Gαβγ in the established PDAC primary cultures is the same which helps to further investigate the role of GPCR signalling pathway in PDACs.

Besides GNAI1 and GNG12, KCTD5 and PDCL were also identified as the direct binding partners of GNB1. Co-immunoprecipitation experiments validated KCTD5-GNB1 interaction. KCTD5 is highly expressed in normal tissues of the appendix, colon, esophagus, lymph nodes, small intestine, spleen, stomach, testis, and urinary bladder, but showed the lowest expression in the pancreas (Fagerberg et al. 2014). A study reported that KCTD5 serves as an inhibitor of GPCR signalling pathway by triggering proteolysis of Gβγ dissociated from Gα subunits in HAP1 cells (Brockmann et al. 2017). This study suggested a regulatory role of p-Akt S473 by KCTD5 through Gβγ subunits (Brockmann et al. 2017). These findings may help to identify inhibitors of pathway alterations induced by overexpressed GNB1 in TIC activation.

4.5 Role of SLC35F5 in PDAC TIC activation

In the primary trapping vector screening, *SLC35F5* was identified as a potential TIC regulator. Stable SLC35F5 KD and OE PDAC cultures were established to validate its role in the PDAC TIC activation process. An shRNA based knockdown efficiency of *SLC35F5* of about 50% knockdown on RNA level was achieved, and 11% decrease on the protein level compared to its control. In the SLC35F5 overexpression group, transduction of the full coding sequence (CDS) and a truncated sequence (TR) revealed over 6-fold increase compared to controls on the RNA level, but no difference detected on the protein level. No difference detected of the SLC35F5 protein expression in SLC35F5 KD and OE cells could be due to the non-functioning of the primary antibody. In the colony formation assay, it was remarkable that SLC35F5 KD cells proliferated more during the culturing time compared to its control. It first suspected that this might be due to the shRNA off-target effect, which referred to the unintended transcripts were mediated by siRNA-induced sequence and cause false-positive phenotypes (Jackson and Linsley 2010). However, overexpression of both SLC35F5 CDS and SLC35F5 truncated sequence led to the formation of a smaller number of colonies compared to GFP control transduced cells, which revealed that the data of SLC35F5 KD group was not the off-target effect. Furthermore, SLC35F5 KD cells were serially transplanted into NSG mice. By tracing the GFP marker in transduced cells, it was observed that SLC35F5 KD cells maintained the tumour formation. In the GFP control group, the loss of transduced cells during serial transplantation was observed. Both *in vitro* and *in vivo* data suggested that SLC35 KD triggered cell proliferation and maintains tumour formation. The genome-wide integration site analysis suggested that the trapping vector leads to truncated SLC35F5 overexpression starting from exon 10. Nevertheless, the coding sequence of SLC35F5 covers transcripts from exon one to exon 15 (NM_025181.5) which means that the truncated SLC35F5 only covers a concise part of the coding sequence, from exon 10 to exon 15 which encodes for the last four SLC35F5 protein transmembrane regions. The phosphorylation site of SLC35F5 is not included in the truncated coding protein region. Therefore, it may be that the truncated mRNAs of SLC35F5 were less stable or moreover that the truncated protein was degraded immediately after translation. In addition, SLC35F5 CDS OE cells did not show the increased capacity of colony formation *in vitro*, which suggests that SLC35F5 is no PDAC TIC activator.

4.6 Conclusion

This study evaluates SLC35F5 and GNB1 as potential PDAC TIC regulators to provide a new aspect for the development of PDAC targeted treatment. GNB1 was able to be validated. And

this study sheds light on the molecular mechanisms behind GNB1 in regulating TIC activation. This study aimed at gaining further knowledge of transient TIC activation in PDACs. Moreover, the specific $G\alpha$, $G\gamma$ subunits were identified as well as the regulators which bind to $G\beta 1$ subunits in the distinct patient-derived PDAC cell models.

Previous results of this lab have shown that overexpression of GNB1 induced constant activity of individual cell clones during serial transplantation and promoted cell proliferation (Gao 2017). In this study, GNB1 was found to be heterogeneously expressed in single primary tumour cells supporting the hypothesis that transient GNB1 expression may be relevant for TIC activation. Moreover, it could show that overexpression of GNB1 triggered PI3K signalling pathway in the established cell model. The identification of GNAI1 and GNG12 as interactors of GNB1 revealed all subunits important for the generation of the $G\alpha\beta\gamma$ complex. In addition, KCTD5 was identified as the negative regulator, which was bound to $G\beta 1$ in the PDAC model systems.

4.7 Outlook

Further questions should be addressed to extend the knowledge of GNB1 regulated TIC activation in PDACs.

First, the intra-tumoural heterogenous expression of GNB1 was shown in one primary PDAC culture. To identify and validate transcriptional programs which are associated with PDAC TIC activity in different patients, more primary tumours, metastatic tumours, established PDAC organoids and established semi-adherent cultures should be sequenced by sc-RNA-seq.

Second, KCTD5 was identified as the binding partner and potential off-switch of GNB1. Further experiments are needed to investigate its role in TIC activation. In the established PDAC model system, GNB1 is stably overexpressed. However, within primary tissue, the protein content of GNB1 might only be transiently increased, which leads to transient PDAC activation. During this process, the presence of KCTD5 or other regulators should be clarified. To further investigate the role of KCTD5 which influences GNB1 in the PDAC TIC activation, knocking down of KCTD5 in PDACs followed by pathway alteration analysis and tumour initiating potential should be performed.

Third, it is necessary to validate the findings determined in H6C7 cell lines on primary PDACs. The role of GNB1 and the correlation between GNB1 and PDPK1 in triggering PI3K-Akt-mTOR signalling was reported. It would be interesting to investigate whether multi-inhibitors treatment of PDACs targeting GNB1, PI3K and PDPK1 could block the PI3K-Akt-mTOR signalling pathway completely in KRAS mutated PDAC cells and stop TIC activation. Further *in vivo* validation experiments are required to address this specifically. Results from this study suggest that GNB1, as TIC activator regulator, may serve as a potential druggable target. PI3K inhibitors, combined with gemcitabine used in the chemotherapeutic treatment regimens of PDACs, have already demonstrated no benefit in prolonging patients' overall survival (Neoptolemos et al. 2018). By adding GNB1 or PDPK1 inhibitors to the PI3K inhibitors plus Gemcitabine, the treatment plan may improve the efficiency of the treatment. However, possible side effects have to be evaluated

Fourth, GNB1 is involved in GPCR signalling pathway, and $G\alpha$ departed from $G\beta\gamma$ subunits could activate signalling pathways as well. Moreover, regulation between $G\alpha$ and $G\beta\gamma$ subunits also exist. Nevertheless, in this study, the role of $G\alpha$ subunits was not analysed. Here, GNB1

driven MAPK and PI3K signalling pathway were focused by ignoring other downstream effectors of GPCR signalling pathway, which should be further investigated.

Lastly, from the trapping vector *in vivo* screening, GNB1 has been identified as a promising PDAC TIC regulator. To identify additional TIC regulators, and to increase the statistical power, more PDAC cultures could be screened.

5 Summary

Pancreatic ductal adenocarcinoma is the third of leading cancer-related deaths in the United States of America. It was shown previously that transiently activated tumour initiating cells drove the progression and maintenance of the pancreatic tumours. Due to this observed plasticity, it might be beneficial to target the functional state of tumour initiating cell activation instead of targeting tumour initiating cells themselves. Previous in this lab, studies were performed to investigate the mechanisms and to identify potential regulatory genes of pancreatic ductal adenocarcinoma tumour initiating cells activation. Three candidates for tumour initiating cell activation were identified which named: *guanine nucleotide-binding protein subunit beta 1*, *solute carrier family 35 member F5* and *son of sevenless homolog 2*. Preliminary validation experiments in immune-deficient mice were performed, and *guanine nucleotide-binding protein subunit beta 1* was identified as a potential regulator of pancreatic ductal adenocarcinoma tumour initiating cell activity. Further studies showed that clones overexpressing guanine nucleotide-binding protein subunit beta 1 continuous contribution to tumour formation in xenografts and knocking down this gene led to the loss of transduced cells in xenografts. In addition, the results showed that overexpressed guanine nucleotide-binding protein subunit beta 1 promoted pancreatic ductal adenocarcinoma cell proliferation.

The study aims at further 1) validating identified potential candidate tumour initiating cell regulators, 2) to further investigate the mechanisms of these tumour initiating cell regulators inducing tumour initiating cell activation, and 3) to identify patient-specific guanine nucleotide-binding protein alpha subunits, guanine nucleotide-binding protein gamma subunits and additional regulators which bind to guanine nucleotide-binding protein subunit beta 1 in established pancreatic ductal adenocarcinoma cell cultures.

To further address the role of *guanine nucleotide-binding protein subunit beta 1* in tumour initiating cell activation, one primary pancreatic ductal adenocarcinoma culture was sequenced by single-cell ribonucleic acid sequencing. *Guanine nucleotide-binding protein subunit beta 1* was found to be heterogeneously expressed which strengthened its role as the tumour initiating cell regulator. β -arrestin signalling pathway was identified as the relevant signalling pathway correlating with high guanine nucleotide-binding protein subunit beta 1 expression.

To investigate the mechanisms behind, the pathway alterations triggered by guanine nucleotide-binding protein subunit beta 1 were analysed in normal pancreas epithelial cells H6C7 with *kirsten rat sarcoma viral oncogene homolog* wild type and mutated background. The phosphatidylinositol 3-kinase signalling pathway was identified as the most relevant signalling pathway. 3-phosphoinositide dependent protein kinase 1, one of the critical molecules in the phosphatidylinositol 3-kinase signalling pathway showed a 6-fold increase of protein in H6C7 *kirsten rat sarcoma viral oncogene homolog* wild type guanine nucleotide-binding protein subunit beta 1 overexpressed culture compared to non-overexpressed control, and 56-fold in mutated background. This finding indicated that overexpressed guanine nucleotide-binding protein subunit beta 1 might induce pancreatic ductal adenocarcinoma tumour initiating cell activation via the phosphatidylinositol 3-kinase signalling pathway, and that 3-phosphoinositide dependent protein kinase 1 was one critical downstream effector of guanine nucleotide-binding protein subunit beta 1.

Guanine nucleotide-binding protein subunit beta 1 proteins were pulled down to investigate its binding partners. Guanine nucleotide-binding protein subunit gamma 12, guanine nucleotide-binding protein subunit alpha 11, and potassium channel tetramerization domain containing 5

were identified as the binding partners in primary pancreatic ductal adenocarcinomas by mass-spectrometry based protein analysis and they were validated by co-immunoprecipitation. This combination of guanine nucleotide-binding protein subunits was shown here for pancreatic ductal adenocarcinoma cultures.

Future experiments will mainly focus on investigating the relationship between guanine nucleotide-binding protein subunit beta 1 and 3-phosphoinositide dependent protein kinase 1 to investigate the mechanism of overexpressed guanine nucleotide-binding protein subunit beta 1 initiated phosphatidylinositol 3-kinase signalling pathway activation. Other guanine nucleotide-binding protein-coupled receptor downstream effectors apart from the detected ones should also be addressed. Moreover, the role of guanine nucleotide-binding protein subunit alpha II should be clarified in the guanine nucleotide-binding protein subunit beta 1 enhanced tumour initiating cell activation. More pancreatic ductal adenocarcinoma tumours should be characterized to indicate the shared universal characteristics of pancreatic ductal adenocarcinoma.

To sum up, this study validated guanine nucleotide-binding protein subunit beta 1 as a pancreatic ductal adenocarcinoma tumour initiating cell regulator. Moreover, these results indicate that overexpressed guanine nucleotide-binding protein subunit beta 1 triggers the activation of the phosphatidylinositol 3-kinase signalling pathway, and that 3-phosphoinositide dependent protein kinase 1 plays a role as the downstream responder of guanine nucleotide-binding protein subunit beta 1, which might explain the mechanisms of guanine nucleotide-binding protein subunit beta 1 induced pancreatic ductal adenocarcinoma tumour initiating cell activation. Guanine nucleotide-binding protein subunit beta 1 is heterogeneously expressed in primary pancreatic ductal adenocarcinoma cultures which strengthens the role as the tumour initiating cell regulator, rendering this as an interesting target for future studies. In addition, the combination of guanine nucleotide-binding protein subunits was characterized in pancreatic ductal adenocarcinoma cultures. Lastly, the findings in this study might provide a novel potential therapeutic target of pancreatic ductal adenocarcinoma in tumour initiating cell activation.

6 Zusammenfassung

Das duktales Adenokarzinom des Pankreas ist die dritthäufigste Ursache krebserkrankter Todesfälle in den Vereinigten Staaten von Amerika. In vorausgegangenen Arbeiten wurde gezeigt, dass transient aktive tumor-initiiierende Zellen das Fortschreiten und die Erhaltung von Pankreastumoren vorantreiben. Aufgrund dieser Plastizität mag es förderlich sein, den Zustand der funktionellen Aktivität tumor-initiiierender Zellen therapeutisch anzugreifen und nicht die Zellpopulation tumor-initiiierender Zellen selbst. In vorausgegangenen Arbeiten dieser Gruppe wurden der Mechanismus sowie potentielle Regulatoren der tumor-initiiierenden Aktivität im Pankreaskarzinom untersucht. Hierbei wurden drei Kandidatengene als mögliche Regulatoren tumor-initiiierender Zellaktivität identifiziert: *guanine nucleotide-binding protein subunit beta 1*, *solute carrier family 35 member F5* und *son of sevenless homolog 2*. Diese Ergebnisse wurden in immundefizienten Mäusen validiert, wobei der Beitrag von *guanine nucleotide-binding protein subunit beta 1* als potentieller Regulator tumor-initiiierender Zellaktivität bestätigt werden konnte. Weiterführende Untersuchungen zeigten, dass Zellklone, welche *guanine nucleotide-binding protein subunit beta 1* überexprimierten, kontinuierlich zur Tumorbildung in Xenotransplantaten beitrugen, während Zellen, in denen dieses Gen herunterreguliert wurde, in den Xenotransplantaten verschwanden. Diese Ergebnisse zeigten außerdem, dass die Überexpression von *guanine nucleotide-binding protein subunit beta 1* die Proliferation der Zellen förderte.

In dieser Arbeit werden 1) identifizierte potenzielle Regulatoren tumor-initiiierender Zellen validiert und 2) der Mechanismus der tumor-initiiierenden Zellaktivierung genauer charakterisiert. Des Weiteren werden 3) patienten-spezifische alpha- und gamma-Untereinheiten Guanosin triphosphat-bindender Proteine sowie weitere Regulatoren identifiziert, welche an *guanine nucleotide-binding protein subunit beta 1* in etablierten patientenabgeleiteten Pankreaskarzinomkulturen binden.

Um den Beitrag von *guanine nucleotide-binding protein subunit beta 1* zur tumor-initiiierenden Zellaktivität zu adressieren, wurde eine primäre patientenabgeleitete Pankreaskarzinomkultur mittels Einzelzell-Ribonukleinsäuresequenzierung untersucht. Diese Analyse zeigte eine heterogene Expression des Gens, was dessen Beitrag zur tumor-initiiierenden Zellaktivität unterstreicht. Außerdem konnte hierbei gezeigt werden, dass die Expression des β -Arrestin Signalwegs mit hoher *guanine nucleotide-binding protein subunit beta 1* Expression korreliert.

Der zu Grunde liegende Mechanismus wurde durch *guanine nucleotide-binding protein subunit beta 1* ausgelöste Signalwegsänderungen in der epithelialen Pankreas-Zelllinie H6C7 mit und ohne Mutation im *kirsten rat sarcoma viral oncogene homolog* Gen genauer untersucht. Hierbei wurde der phosphatidylinositol 3-kinase Signalweg als wichtiger Signalweg identifiziert. 3-Phosphoinositide dependent protein kinase 1, ein zentrales Molekül im phosphatidylinositol 3-kinase Signalweg zeigte eine 6-fach höhere Proteinexpression in H6C7 *kirsten rat sarcoma viral oncogene homolog* Wildtyp Zellen mit *guanine nucleotide-binding protein subunit beta 1* Überexpression im Vergleich zu Kontrollzellen. In Zellen mit mutiertem *kirsten rat sarcoma viral oncogene homolog* Gen lag sogar eine 56-fach höhere Expression vor. Diese Beobachtung legte nahe, dass die Überexpression von *guanine nucleotide-binding protein subunit beta 1* die tumor-initiiierende Zellaktivität im duktales Adenokarzinom des Pankreas durch Aktivierung des phosphatidylinositol 3-kinase Signalwegs reguliert und dass 3-phosphoinositide dependent protein kinase 1 ein wichtiger Effektor von *guanine nucleotide-binding protein subunit beta 1* ist.

Um Interaktionspartner von guanine nucleotide-binding protein subunit beta 1 zu identifizieren, wurde ein Pulldown Experiment durchgeführt. Guanine nucleotide-binding protein subunit gamma 12, guanine nucleotide-binding protein subunit alpha 11 und potassium channel tetramerization domain containing 5 wurden mittels Massenspektrometrie als Interaktionspartner in primären duktalem Pankreaskarzinomen identifiziert und durch Ko-Immunopräzipitation validiert. Diese Interaktion mit den genannten Untereinheiten der Guanosintriphosphat-bindenden Proteine konnte hier im duktalem Adenokarzinom des Pankreas gezeigt werden.

Weiterführende Experimente werden darauf abzielen, den Zusammenhang zwischen guanine nucleotide-binding protein subunit beta 1 und 3-phosphoinositide dependent protein kinase 1 zu untersuchen und den Mechanismus der Aktivierung des phosphatidylinositol 3-kinase Signalwegs durch guanine nucleotide-binding protein subunit beta 1 zu verstehen. Zusätzlich sollten weitere Effektoren Guanosintriphosphat-gekoppelter Rezeptoren untersucht werden. Außerdem gilt es zu klären, welche Rolle guanine nucleotide-binding protein subunit alpha 11 in guanine nucleotide-binding protein subunit beta 1 vermittelter tumor-initiiertender Zellaktivität spielt. Hierfür sollten weitere Pankreaskarzinome charakterisiert werden, um gemeinsame universelle Eigenschaften duktalem Adenokarzinomen des Pankreas zu definieren.

Diese Studie konnte den Beitrag von guanine nucleotide-binding protein subunit beta 1 als Regulator tumor-initiiertender Zellaktivität im Pankreaskarzinom validieren und zeigen, dass dessen Überexpression die Aktivierung des phosphatidylinositol 3-kinase Signalwegs bewirkt, in welchem 3-phosphoinositide dependent protein kinase 1 dann als Effektor fungiert. Dieser Zusammenhang könnte den Mechanismus der tumor-initiierten Zellaktivierung durch guanine nucleotide-binding protein subunit beta 1 erklären. Die hier gezeigte heterogene Expression von guanine nucleotide-binding protein subunit beta 1 in einer primären Pankreaskarzinomkultur liefert weitere starke Hinweise auf die Funktion als Regulator tumor-initiiertender Zellen und macht es somit zu einem interessanten Kandidaten für weitere Studien. Zusätzlich wurde außerdem die Kombination verschiedener Untereinheiten Guanosintriphosphat-bindender Proteine in einer Pankreaskarzinomkultur charakterisiert. Diese Erkenntnisse könnten das Angreifen tumor-initiiertender Zellaktivität im duktalem Adenokarzinom des Pankreas als neue therapeutische Strategie ermöglichen.

7 References

- Aguirre, A. J., Bardeesy, N., Sinha, M., Lopez, L., Tuveson, D. A., Horner, J., Redston, M. S. and DePinho, R. A. (2003). **Activated Kras and Ink4a/Arf deficiency cooperate to produce metastatic pancreatic ductal adenocarcinoma.** *Genes Dev* 17 (24), 3112-3126, doi: 10.1101/gad.1158703.
- Al-Hajj, M., Wicha, M. S., Benito-Hernandez, A., Morrison, S. J. and Clarke, M. F. (2003). **Prospective identification of tumorigenic breast cancer cells.** *Proc Natl Acad Sci U S A* 100 (7), 3983-3988, doi: 10.1073/pnas.0530291100.
- Alvarez, C. J., Lodeiro, M., Theodoropoulou, M., Camiña, J. P., Casanueva, F. F. and Pazos, Y. (2009). **Obestatin stimulates Akt signalling in gastric cancer cells through beta-arrestin-mediated epidermal growth factor receptor transactivation.** *Endocr Relat Cancer* 16 (2), 599-611, doi: 10.1677/erc-08-0192.
- American Cancer Society (2020a). **Cancer Facts & Figures 2020.** URL: <https://www.cancer.org/content/dam/cancer-org/research/cancer-facts-and-statistics/annual-cancer-facts-and-figures/2020/cancer-facts-and-figures-2020.pdf> [last accessed 03 April 2020]
- American Cancer Society (2020b). **Survival Rates for Pancreatic Cancer.** URL: <https://www.cancer.org/cancer/pancreatic-cancer/detection-diagnosis-staging/survival-rates.html> [last accessed 03 April 2020].
- Arakaki, A. K. S., Pan, W. A. and Trejo, J. (2018). **GPCRs in Cancer: Protease-Activated Receptors, Endocytic Adaptors and Signaling.** *Int J Mol Sci* 19 (7), doi: 10.3390/ijms19071886.
- Bailey, P., Chang, D. K., Nones, K., Johns, A. L., Patch, A. M., Gingras, M. C., Miller, D. K., Christ, A. N., Bruxner, T. J., Quinn, M. C., Nourse, C., Murtaugh, L. C., Harliwong, I., Idrisoglu, S., Manning, S., Nourbakhsh, E., Wani, S., Fink, L., Holmes, O., Chin, V., Anderson, M. J., Kazakoff, S., Leonard, C., Newell, F., Waddell, N., Wood, S., Xu, Q., Wilson, P. J., Cloonan, N., Kassahn, K. S., Taylor, D., Quek, K., Robertson, A., Pantano, L., Mincarelli, L., Sanchez, L. N., Evers, L., Wu, J., Pinese, M., Cowley, M. J., Jones, M. D., Colvin, E. K., Nagrial, A. M., Humphrey, E. S., Chantrill, L. A., Mawson, A., Humphris, J., Chou, A., Pajic, M., Scarlett, C. J., Pinho, A. V., Giry-Laterriere, M., Rooman, I., Samra, J. S., Kench, J. G., Lovell, J. A., Merrett, N. D., Toon, C. W., Epari, K., Nguyen, N. Q., Barbour, A., Zeps, N., Moran-Jones, K., Jamieson, N. B., Graham, J. S., Duthie, F., Oien, K., Hair, J., Grützmann, R., Maitra, A., Iacobuzio-Donahue, C. A., Wolfgang, C. L., Morgan, R. A., Lawlor, R. T., Corbo, V., Bassi, C., Rusev, B., Capelli, P., Salvia, R., Tortora, G., Mukhopadhyay, D., Petersen, G. M., Munzy, D. M., Fisher, W. E., Karim, S. A., Eshleman, J. R., Hruban, R. H., Pilarsky, C., Morton, J. P., Sansom, O. J., Scarpa, A., Musgrove, E. A., Bailey, U. M., Hofmann, O., Sutherland, R. L., Wheeler, D. A., Gill, A. J., Gibbs, R. A., Pearson, J. V., Waddell, N., Biankin, A. V. and Grimmond, S. M. (2016). **Genomic analyses identify molecular subtypes of pancreatic cancer.** *Nature* 531 (7592), 47-52, doi: 10.1038/nature16965.

- Balkwill, F. R., Capasso, M. and Hagemann, T. (2012). **The tumor microenvironment at a glance.** *J Cell Sci* 125 (Pt 23), 5591-5596, doi: 10.1242/jcs.116392.
- Ball, C. R., Oppel, F., Ehrenberg, K. R., Dubash, T. D., Dieter, S. M., Hoffmann, C. M., Abel, U., Herbst, F., Koch, M., Werner, J., Bergmann, F., Ishaque, N., Schmidt, M., von Kalle, C., Scholl, C., Fröhling, S., Brors, B., Weichert, W., Weitz, J. and Glimm, H. (2017). **Succession of transiently active tumor-initiating cell clones in human pancreatic cancer xenografts.** *EMBO Mol Med* 9 (7), 918-932, doi: 10.15252/emmm.201607354.
- Barati Bagherabad, M., Afzaljavan, F., ShahidSales, S., Hassanian, S. M. and Avan, A. (2019). **Targeted therapies in pancreatic cancer: Promises and failures.** *J Cell Biochem* 120 (3), 2726-2741, doi: 10.1002/jcb.26284.
- Bardeesy, N., Cheng, K. H., Berger, J. H., Chu, G. C., Pahler, J., Olson, P., Hezel, A. F., Horner, J., Lauwers, G. Y., Hanahan, D. and DePinho, R. A. (2006). **Smad4 is dispensable for normal pancreas development yet critical in progression and tumor biology of pancreas cancer.** *Genes Dev* 20 (22), 3130-3146, doi: 10.1101/gad.1478706.
- Berlin, S., Keren-Raifman, T., Castel, R., Rubinstein, M., Dessauer, C. W., Ivanina, T. and Dascal, N. (2010). **G alpha(i) and G betagamma jointly regulate the conformations of a G betagamma effector, the neuronal G protein-activated K⁺ channel (GIRK).** *J Biol Chem* 285 (9), 6179-6185, doi: 10.1074/jbc.M109.085944.
- Blackford, A., Parmigiani, G., Kensler, T. W., Wolfgang, C., Jones, S., Zhang, X., Parsons, D. W., Lin, J. C., Leary, R. J., Eshleman, J. R., Goggins, M., Jaffee, E. M., Iacobuzio-Donahue, C. A., Maitra, A., Klein, A., Cameron, J. L., Olino, K., Schlick, R., Winter, J., Vogelstein, B., Velculescu, V. E., Kinzler, K. W. and Hruban, R. H. (2009). **Genetic mutations associated with cigarette smoking in pancreatic cancer.** *Cancer Res* 69 (8), 3681-3688, doi: 10.1158/0008-5472.Can-09-0015.
- Boire, A., Covic, L., Agarwal, A., Jacques, S., Sherifi, S. and Kuliopulos, A. (2005). **PAR1 Is a Matrix Metalloprotease-1 Receptor that Promotes Invasion and Tumorigenesis of Breast Cancer Cells.** *Cell* 120 (3), 303-313, doi: 10.1016/j.cell.2004.12.018.
- Bradshaw, A., Wickremsekera, A., Tan, S. T., Peng, L., Davis, P. F. and Itinteang, T. (2016). **Cancer Stem Cell Hierarchy in Glioblastoma Multiforme.** *Front Surg* 3, 21, doi: 10.3389/fsurg.2016.00021.
- Brockmann, M., Blomen, V. A., Nieuwenhuis, J., Stickel, E., Raaben, M., Bleijerveld, O. B., Altelaar, A. F. M., Jae, L. T. and Brummelkamp, T. R. (2017). **Genetic wiring maps of single-cell protein states reveal an off-switch for GPCR signalling.** *Nature* 546 (7657), 307-311, doi: 10.1038/nature22376.
- Bunda, S., Heir, P., Srikumar, T., Cook, J. D., Burrell, K., Kano, Y., Lee, J. E., Zadeh, G., Raught, B. and Ohh, M. (2014). **Src promotes GTPase activity of Ras via tyrosine 32 phosphorylation.** *Proc Natl Acad Sci U S A* 111 (36), E3785-3794, doi: 10.1073/pnas.1406559111.

- Buscail, L., Bournet, B. and Cordelier, P. (2020). **Role of oncogenic KRAS in the diagnosis, prognosis and treatment of pancreatic cancer**. *Nat Rev Gastroenterol Hepatol* 17 (3), 153-168, doi: 10.1038/s41575-019-0245-4.
- Calbo, J., van Montfort, E., Proost, N., van Drunen, E., Beverloo, H. B., Meuwissen, R. and Berns, A. (2011). **A functional role for tumor cell heterogeneity in a mouse model of small cell lung cancer**. *Cancer Cell* 19 (2), 244-256, doi: 10.1016/j.ccr.2010.12.021.
- Campbell, A. P. and Smrcka, A. V. (2018). **Targeting G protein-coupled receptor signalling by blocking G proteins**. *Nat Rev Drug Discov* 17 (11), 789-803, doi: 10.1038/nrd.2018.135.
- Carman, C. V., Parent, J. L., Day, P. W., Pronin, A. N., Sternweis, P. M., Wedegaertner, P. B., Gilman, A. G., Benovic, J. L. and Kozasa, T. (1999). **Selective regulation of G α (q/11) by an RGS domain in the G protein-coupled receptor kinase, GRK2**. *J Biol Chem* 274 (48), 34483-34492, doi: 10.1074/jbc.274.48.34483.
- Chen, Z. and Xue, C. (2019). **G-Protein-Coupled Receptor 5 (LGR5) Overexpression Activates β -Catenin Signaling in Breast Cancer Cells via Protein Kinase A**. *Med Sci Monit Basic Res* 25, 15-25, doi: 10.12659/msmbr.912411.
- Chintala, S., Tan, J., Gautam, R., Rusiniak, M. E., Guo, X., Li, W., Gahl, W. A., Huizing, M., Spritz, R. A., Hutton, S., Novak, E. K. and Swank, R. T. (2007). **The Slc35d3 gene, encoding an orphan nucleotide sugar transporter, regulates platelet-dense granules**. *Blood* 109 (4), 1533-1540, doi: 10.1182/blood-2006-08-040196.
- Choi, H. Y., Saha, S. K., Kim, K., Kim, S., Yang, G. M., Kim, B., Kim, J. H. and Cho, S. G. (2015). **G protein-coupled receptors in stem cell maintenance and somatic reprogramming to pluripotent or cancer stem cells**. *BMB Rep* 48 (2), 68-80, doi: 10.5483/bmbrep.2015.48.2.250.
- Cicenas, J., Kvederaviciute, K., Meskinyte, I., Meskinyte-Kausiliene, E., Skeberdyte, A. and Cicenas, J. (2017). **KRAS, TP53, CDKN2A, SMAD4, BRCA1, and BRCA2 Mutations in Pancreatic Cancer**. *Cancers (Basel)* 9 (5), doi: 10.3390/cancers9050042.
- Clapham, D. E. and Neer, E. J. (1997). **G protein beta gamma subunits**. *Annu Rev Pharmacol Toxicol* 37, 167-203, doi: 10.1146/annurev.pharmtox.37.1.167.
- Cleary, A. S., Leonard, T. L., Gestl, S. A. and Gunther, E. J. (2014). **Tumour cell heterogeneity maintained by cooperating subclones in Wnt-driven mammary cancers**. *Nature* 508 (7494), 113-117, doi: 10.1038/nature13187.
- Collisson, E. A., Sadanandam, A., Olson, P., Gibb, W. J., Truitt, M., Gu, S., Cooc, J., Weinkle, J., Kim, G. E., Jakkula, L., Feiler, H. S., Ko, A. H., Olshen, A. B., Danenberg, K. L., Tempero, M. A., Spellman, P. T., Hanahan, D. and Gray, J. W. (2011). **Subtypes of pancreatic ductal adenocarcinoma and their differing responses to therapy**. *Nat Med* 17 (4), 500-503, doi: 10.1038/nm.2344.

- Collisson, E. A., Trejo, C. L., Silva, J. M., Gu, S., Korkola, J. E., Heiser, L. M., Charles, R. P., Rabinovich, B. A., Hann, B., Dankort, D., Spellman, P. T., Phillips, W. A., Gray, J. W. and McMahon, M. (2012). **A central role for RAF→MEK→ERK signaling in the genesis of pancreatic ductal adenocarcinoma.** *Cancer Discov* 2 (8), 685-693, doi: 10.1158/2159-8290.Cd-11-0347.
- Cotton, M. and Claing, A. (2009). **G protein-coupled receptors stimulation and the control of cell migration.** *Cell Signal* 21 (7), 1045-1053, doi: 10.1016/j.cellsig.2009.02.008.
- Couch, F. J., Johnson, M. R., Rabe, K. G., Brune, K., de Andrade, M., Goggins, M., Rothenmund, H., Gallinger, S., Klein, A., Petersen, G. M. and Hruban, R. H. (2007). **The prevalence of BRCA2 mutations in familial pancreatic cancer.** *Cancer Epidemiol Biomarkers Prev* 16 (2), 342-346, doi: 10.1158/1055-9965.Epi-06-0783.
- Crespo, P., Xu, N., Simonds, W. F. and Gutkind, J. S. (1994). **Ras-dependent activation of MAP kinase pathway mediated by G-protein beta gamma subunits.** *Nature* 369 (6479), 418-420, doi: 10.1038/369418a0.
- Dhanasekaran, N. and Prasad, M. V. (1998). **G protein subunits and cell proliferation.** *Biol Signals Recept* 7 (2), 109-117, doi: 10.1159/000014536.
- di Magliano, M. P. and Logsdon, C. D. (2013). **Roles for KRAS in pancreatic tumor development and progression.** *Gastroenterology* 144 (6), 1220-1229, doi: 10.1053/j.gastro.2013.01.071.
- Dieter, S. M., Ball, C. R., Hoffmann, C. M., Nowrouzi, A., Herbst, F., Zavidij, O., Abel, U., Arens, A., Weichert, W., Brand, K., Koch, M., Weitz, J., Schmidt, M., von Kalle, C. and Glimm, H. (2011). **Distinct types of tumor-initiating cells form human colon cancer tumors and metastases.** *Cell Stem Cell* 9 (4), 357-365, doi: 10.1016/j.stem.2011.08.010.
- Dobin, A., Davis, C. A., Schlesinger, F., Drenkow, J., Zaleski, C., Jha, S., Batut, P., Chaisson, M. and Gingeras, T. R. (2013). **STAR: ultrafast universal RNA-seq aligner.** *Bioinformatics* 29 (1), 15-21, doi: 10.1093/bioinformatics/bts635.
- Dorsam, R. T. and Gutkind, J. S. (2007). **G-protein-coupled receptors and cancer.** *Nat Rev Cancer* 7 (2), 79-94, doi: 10.1038/nrc2069.
- Ehrenberg, K. R., Gao, J., Oppel, F., Frank, S., Kang, N., Dieter, S. M., Herbst, F., Möhrmann, L., Dubash, T. D., Schulz, E. R., Strakerjahn, H., Giessler, K. M., Weber, S., Oberlack, A., Rief, E. M., Strobel, O., Bergmann, F., Lasitschka, F., Weitz, J., Glimm, H. and Ball, C. R. (2019). **Systematic Generation of Patient-Derived Tumor Models in Pancreatic Cancer.** *Cells* 8 (2), doi: 10.3390/cells8020142.

- Embry, A. C., Glick, J. L., Linder, M. E. and Casey, P. J. (2004). **Reciprocal signaling between the transcriptional co-factor Eya2 and specific members of the Galphai family**. *Mol Pharmacol* 66 (5), 1325-1331, doi: 10.1124/mol.104.004093.
- Ercan, G., Karlitepe, A. and Ozpolat, B. (2017). **Pancreatic Cancer Stem Cells and Therapeutic Approaches**. *Anticancer Res* 37 (6), 2761-2775, doi: 10.21873/anticancer.11628.
- Eser, S., Reiff, N., Messer, M., Seidler, B., Gottschalk, K., Dobler, M., Hieber, M., Arbeiter, A., Klein, S., Kong, B., Michalski, C. W., Schlitter, A. M., Esposito, I., Kind, A. J., Rad, L., Schnieke, A. E., Baccarini, M., Alessi, D. R., Rad, R., Schmid, R. M., Schneider, G. and Saur, D. (2013). **Selective requirement of PI3K/PDK1 signaling for Kras oncogene-driven pancreatic cell plasticity and cancer**. *Cancer Cell* 23 (3), 406-420, doi: 10.1016/j.ccr.2013.01.023.
- Eser, S., Schnieke, A., Schneider, G. and Saur, D. (2014). **Oncogenic KRAS signalling in pancreatic cancer**. *Br J Cancer* 111 (5), 817-822, doi: 10.1038/bjc.2014.215.
- Fagerberg, L., Hallström, B. M., Oksvold, P., Kampf, C., Djureinovic, D., Odeberg, J., Habuka, M., Tahmasebpoor, S., Danielsson, A., Edlund, K., Asplund, A., Sjöstedt, E., Lundberg, E., Szgyarto, C. A., Skogs, M., Takanen, J. O., Berling, H., Tegel, H., Mulder, J., Nilsson, P., Schwenk, J. M., Lindskog, C., Danielsson, F., Mardinoglu, A., Sivertsson, A., von Feilitzen, K., Forsberg, M., Zwahlen, M., Olsson, I., Navani, S., Huss, M., Nielsen, J., Ponten, F. and Uhlén, M. (2014). **Analysis of the human tissue-specific expression by genome-wide integration of transcriptomics and antibody-based proteomics**. *Mol Cell Proteomics* 13 (2), 397-406, doi: 10.1074/mcp.M113.035600.
- Feldmann, G., Mishra, A., Hong, S. M., Bisht, S., Strock, C. J., Ball, D. W., Goggins, M., Maitra, A. and Nelkin, B. D. (2010). **Inhibiting the cyclin-dependent kinase CDK5 blocks pancreatic cancer formation and progression through the suppression of Ras-Ral signaling**. *Cancer Res* 70 (11), 4460-4469, doi: 10.1158/0008-5472.Can-09-1107.
- Franjic, S. (2019). **A Few Words about Pancreas**. *Journal of Clinical Cancer Research* V1(1), 1-6. URL: <http://jclinicalcancerresearch.org/pdf/JCCR-v1-1005.pdf> [last accessed 20 March 2020]
- Freytag, S., Tian, L., Lönnstedt, I., Ng, M. and Bahlo, M. (2018). **Comparison of clustering tools in R for medium-sized 10x Genomics single-cell RNA-sequencing data**. *F1000Res* 7, 1297, doi: 10.12688/f1000research.15809.2.
- Gao, J. (2017) **Identification and Characterization of Candidate Genes Regulating Tumor-initiating Cell Activity in Human Pancreatic Cancer**. Medical Dissertation, Universität Heidelberg.
- Garcia-Marcos, M., Ghosh, P. and Farquhar, M. G. (2009). **GIV is a nonreceptor GEF for G alpha i with a unique motif that regulates Akt signaling**. *Proc Natl Acad Sci U S A* 106 (9), 3178-3183, doi: 10.1073/pnas.0900294106.

- Giovannetti, E., Funel, N., Peters, G. J., Del Chiaro, M., Erozcenci, L. A., Vasile, E., Leon, L. G., Pollina, L. E., Groen, A., Falcone, A., Danesi, R., Campani, D., Verheul, H. M. and Boggi, U. (2010). **MicroRNA-21 in pancreatic cancer: correlation with clinical outcome and pharmacologic aspects underlying its role in the modulation of gemcitabine activity.** *Cancer Res* 70 (11), 4528-4538, doi: 10.1158/0008-5472.Can-09-4467.
- Goldsmith, Z. G. and Dhanasekaran, D. N. (2007). **G protein regulation of MAPK networks.** *Oncogene* 26 (22), 3122-3142, doi: 10.1038/sj.onc.1210407.
- Gopinathan, A., Morton, J. P., Jodrell, D. I. and Sansom, O. J. (2015). **GEMMs as preclinical models for testing pancreatic cancer therapies.** *Dis Model Mech* 8 (10), 1185-1200, doi: 10.1242/dmm.021055.
- Greaves, M. and Maley, C. C. (2012). **Clonal evolution in cancer.** *Nature* 481 (7381), 306-313, doi: 10.1038/nature10762.
- Hadley, B., Litfin, T., Day, C. J., Haselhorst, T., Zhou, Y. and Tiralongo, J. (2019). **Nucleotide Sugar Transporter SLC35 Family Structure and Function.** *Comput Struct Biotechnol J* 17, 1123-1134, doi: 10.1016/j.csbj.2019.08.002.
- Hahn, S. A., Greenhalf, B., Ellis, I., Sina-Frey, M., Rieder, H., Korte, B., Gerdes, B., Kress, R., Ziegler, A., Raeburn, J. A., Campra, D., Grützmann, R., Rehder, H., Rothmund, M., Schmiegel, W., Neoptolemos, J. P. and Bartsch, D. K. (2003). **BRCA2 germline mutations in familial pancreatic carcinoma.** *J Natl Cancer Inst* 95 (3), 214-221, doi: 10.1093/jnci/95.3.214.
- Hanahan, D. and Weinberg, R. A. (2011). **Hallmarks of cancer: the next generation.** *Cell* 144 (5), 646-674, doi: 10.1016/j.cell.2011.02.013.
- Hanoune, J. and Defer, N. (2001). **Regulation and role of adenylyl cyclase isoforms.** *Annu Rev Pharmacol Toxicol* 41, 145-174, doi: 10.1146/annurev.pharmtox.41.1.145.
- He, J., Jin, Y., Zhou, M., Li, X., Chen, W., Wang, Y., Gu, S., Cao, Y., Chu, C., Liu, X. and Zou, Q. (2018). **Solute carrier family 35 member F2 is indispensable for papillary thyroid carcinoma progression through activation of transforming growth factor- β type I receptor/apoptosis signal-regulating kinase 1/mitogen-activated protein kinase signaling axis.** *Cancer Sci* 109 (3), 642-655, doi: 10.1111/cas.13478.
- He, L., Vasiliou, K. and Nebert, D. W. (2009). **Analysis and update of the human solute carrier (SLC) gene superfamily.** *Hum Genomics* 3 (2), 195-206, doi: 10.1186/1479-7364-3-2-195.
- Heining, C., Horak, P., Uhrig, S., Codo, P. L., Klink, B., Hutter, B., Fröhlich, M., Bonekamp, D., Richter, D., Steiger, K., Penzel, R., Endris, V., Ehrenberg, K. R., Frank, S., Kleinheinz, K., Toprak, U. H., Schlesner, M., Mandal, R., Schulz, L., Lambertz, H.,

- Fetscher, S., Bitzer, M., Malek, N. P., Horger, M., Giese, N. A., Strobel, O., Hackert, T., Springfield, C., Feuerbach, L., Bergmann, F., Schröck, E., von Kalle, C., Weichert, W., Scholl, C., Ball, C. R., Stenzinger, A., Brors, B., Fröhling, S. and Glimm, H. (2018). **NRG1 Fusions in KRAS Wild-Type Pancreatic Cancer**. *Cancer Discov* 8 (9), 1087-1095, doi: 10.1158/2159-8290.Cd-18-0036.
- Hermann, P. C., Huber, S. L., Herrler, T., Aicher, A., Ellwart, J. W., Guba, M., Bruns, C. J. and Heeschen, C. (2007). **Distinct populations of cancer stem cells determine tumor growth and metastatic activity in human pancreatic cancer**. *Cell Stem Cell* 1 (3), 313-323, doi: 10.1016/j.stem.2007.06.002.
- Hilger, D., Masureel, M. and Kobilka, B. K. (2018). **Structure and dynamics of GPCR signaling complexes**. *Nat Struct Mol Biol* 25 (1), 4-12, doi: 10.1038/s41594-017-0011-7.
- Hingorani, S. R., Petricoin, E. F., Maitra, A., Rajapakse, V., King, C., Jacobetz, M. A., Ross, S., Conrads, T. P., Veenstra, T. D., Hitt, B. A., Kawaguchi, Y., Johann, D., Liotta, L. A., Crawford, H. C., Putt, M. E., Jacks, T., Wright, C. V., Hruban, R. H., Lowy, A. M. and Tuveson, D. A. (2003). **Preinvasive and invasive ductal pancreatic cancer and its early detection in the mouse**. *Cancer Cell* 4 (6), 437-450, doi: 10.1016/s1535-6108(03)00309-x.
- Homan, K. T. and Tesmer, J. J. (2015). **Molecular basis for small molecule inhibition of G protein-coupled receptor kinases**. *ACS Chem Biol* 10 (1), 246-256, doi: 10.1021/cb5003976.
- Hruban, R. H., Canto, M. I., Goggins, M., Schulick, R. and Klein, A. P. (2010). **Update on familial pancreatic cancer**. *Adv Surg* 44, 293-311, doi: 10.1016/j.yasu.2010.05.011.
- Jackson, A. L. and Linsley, P. S. (2010). **Recognizing and avoiding siRNA off-target effects for target identification and therapeutic application**. *Nat Rev Drug Discov* 9 (1), 57-67, doi: 10.1038/nrd3010.
- Jebali, A. and Dumaz, N. (2018). **The role of RICTOR downstream of receptor tyrosine kinase in cancers**. *Mol Cancer* 17 (1), 39, doi: 10.1186/s12943-018-0794-0.
- Jones, S., Zhang, X., Parsons, D. W., Lin, J. C., Leary, R. J., Angenendt, P., Mankoo, P., Carter, H., Kamiyama, H., Jimeno, A., Hong, S. M., Fu, B., Lin, M. T., Calhoun, E. S., Kamiyama, M., Walter, K., Nikolskaya, T., Nikolsky, Y., Hartigan, J., Smith, D. R., Hidalgo, M., Leach, S. D., Klein, A. P., Jaffee, E. M., Goggins, M., Maitra, A., Iacobuzio-Donahue, C., Eshleman, J. R., Kern, S. E., Hruban, R. H., Karchin, R., Papadopoulos, N., Parmigiani, G., Vogelstein, B., Velculescu, V. E. and Kinzler, K. W. (2008). **Core signaling pathways in human pancreatic cancers revealed by global genomic analyses**. *Science* 321 (5897), 1801-1806, doi: 10.1126/science.1164368.
- Kamisawa, T., Wood, L. D., Itoi, T. and Takaori, K. (2016). **Pancreatic cancer**. *Lancet* 388 (10039), 73-85, doi: 10.1016/s0140-6736(16)00141-0.
- Karamitopoulou, E. (2019). **Tumour microenvironment of pancreatic cancer: immune**

- landscape is dictated by molecular and histopathological features.** *Br J Cancer* 121 (1), 5-14, doi: 10.1038/s41416-019-0479-5.
- Kent, O. A. (2018). **Increased mutant KRAS gene dosage drives pancreatic cancer progression: evidence for wild-type KRAS as a tumor suppressor?** *Hepatobiliary Surg Nutr* 7 (5), 403-405, doi: 10.21037/hbsn.2018.07.03.
- Kleeff, J., Korc, M., Apte, M., La Vecchia, C., Johnson, C. D., Biankin, A. V., Neale, R. E., Tempero, M., Tuveson, D. A., Hruban, R. H. and Neoptolemos, J. P. (2016). **Pancreatic cancer.** *Nat Rev Dis Primers* 2, 16022, doi: 10.1038/nrdp.2016.22.
- Klein, A. P., Brune, K. A., Petersen, G. M., Goggins, M., Tersmette, A. C., Offerhaus, G. J., Griffin, C., Cameron, J. L., Yeo, C. J., Kern, S. and Hruban, R. H. (2004). **Prospective risk of pancreatic cancer in familial pancreatic cancer kindreds.** *Cancer Res* 64 (7), 2634-2638, doi: 10.1158/0008-5472.can-03-3823.
- Kleuss, C., Scherübl, H., Hescheler, J., Schultz, G. and Wittig, B. (1992). **Different beta-subunits determine G-protein interaction with transmembrane receptors.** *Nature* 358 (6385), 424-426, doi: 10.1038/358424a0.
- Koch, W. J., Hawes, B. E., Allen, L. F. and Lefkowitz, R. J. (1994). **Direct evidence that Gi-coupled receptor stimulation of mitogen-activated protein kinase is mediated by G beta gamma activation of p21ras.** *Proc Natl Acad Sci U S A* 91 (26), 12706-12710, doi: 10.1073/pnas.91.26.12706.
- Kolch, W., Heidecker, G., Kochs, G., Hummel, R., Vahidi, H., Mischak, H., Finkenzeller, G., Marmé, D. and Rapp, U. R. (1993). **Protein kinase C alpha activates RAF-1 by direct phosphorylation.** *Nature* 364 (6434), 249-252, doi: 10.1038/364249a0.
- Komolov, K. E. and Benovic, J. L. (2018). **G protein-coupled receptor kinases: Past, present and future.** *Cell Signal* 41, 17-24, doi: 10.1016/j.cellsig.2017.07.004.
- Krempley, B. D. and Yu, K. H. (2017). **Preclinical models of pancreatic ductal adenocarcinoma.** *Chin Clin Oncol* 6 (3), 25, doi: 10.21037/cco.2017.06.15.
- Kreso, A., O'Brien, C. A., van Galen, P., Gan, O. I., Notta, F., Brown, A. M., Ng, K., Ma, J., Wienholds, E., Dunant, C., Pollett, A., Gallinger, S., McPherson, J., Mullighan, C. G., Shibata, D. and Dick, J. E. (2013). **Variable clonal repopulation dynamics influence chemotherapy response in colorectal cancer.** *Science* 339 (6119), 543-548, doi: 10.1126/science.1227670.
- Lappano, R. and Maggiolini, M. (2011). **G protein-coupled receptors: novel targets for drug discovery in cancer.** *Nature Reviews Drug Discovery* 10 (1), 47-60, doi: 10.1038/nrd3320.
- Layden, B. T., Newman, M., Chen, F., Fisher, A. and Lowe, W. L., Jr. (2010). **G protein coupled receptors in embryonic stem cells: a role for Gs-alpha signaling.** *PLoS One* 5 (2), e9105, doi: 10.1371/journal.pone.0009105.

- Lee, J. W., Komar, C. A., Bengsch, F., Graham, K. and Beatty, G. L. (2016). **Genetically Engineered Mouse Models of Pancreatic Cancer: The KPC Model (LSL-Kras(G12D/+); LSL-Trp53(R172H/+); Pdx-1-Cre), Its Variants, and Their Application in Immuno-oncology Drug Discovery.** *Curr Protoc Pharmacol* 73, 14.39.11-14.39.20, doi: 10.1002/cpph.2.
- Lee, Y. T., Tan, Y. J. and Oon, C. E. (2018). **Molecular targeted therapy: Treating cancer with specificity.** *Eur J Pharmacol* 834, 188-196, doi: 10.1016/j.ejphar.2018.07.034.
- Leopoldt, D., Hanck, T., Exner, T., Maier, U., Wetzker, R. and Nürnberg, B. (1998). **Gbetagamma stimulates phosphoinositide 3-kinase-gamma by direct interaction with two domains of the catalytic p110 subunit.** *J Biol Chem* 273 (12), 7024-7029, doi: 10.1074/jbc.273.12.7024.
- Lev, S., Moreno, H., Martinez, R., Canoll, P., Peles, E., Musacchio, J. M., Plowman, G. D., Rudy, B. and Schlessinger, J. (1995). **Protein tyrosine kinase PYK2 involved in Ca(2+)-induced regulation of ion channel and MAP kinase functions.** *Nature* 376 (6543), 737-745, doi: 10.1038/376737a0.
- Li, C., Heidt, D. G., Dalerba, P., Burant, C. F., Zhang, L., Adsay, V., Wicha, M., Clarke, M. F. and Simeone, D. M. (2007). **Identification of pancreatic cancer stem cells.** *Cancer Res* 67 (3), 1030-1037, doi: 10.1158/0008-5472.Can-06-2030.
- Li, J., Jin, C., Zou, C., Qiao, X., Ma, P., Hu, D., Li, W., Jin, J., Jin, X. and Fan, P. (2020). **GNG12 regulates PD-L1 expression by activating NF-κB signaling in pancreatic ductal adenocarcinoma.** *FEBS Open Bio* 10 (2), 278-287, doi: 10.1002/2211-5463.12784.
- Liao, Y., Smyth, G. K. and Shi, W. (2014). **featureCounts: an efficient general purpose program for assigning sequence reads to genomic features.** *Bioinformatics* 30 (7), 923-930, doi: 10.1093/bioinformatics/btt656.
- Ligorio, M., Sil, S., Malagon-Lopez, J., Nieman, L. T., Misale, S., Di Pilato, M., Ebricht, R. Y., Karabacak, M. N., Kulkarni, A. S., Liu, A., Vincent Jordan, N., Franses, J. W., Philipp, J., Kreuzer, J., Desai, N., Arora, K. S., Rajurkar, M., Horwitz, E., Neyaz, A., Tai, E., Magnus, N. K. C., Vo, K. D., Yashaswini, C. N., Marangoni, F., Boukhali, M., Fatherree, J. P., Damon, L. J., Xega, K., Desai, R., Choz, M., Bersani, F., Langenbucher, A., Thapar, V., Morris, R., Wellner, U. F., Schilling, O., Lawrence, M. S., Liss, A. S., Rivera, M. N., Deshpande, V., Benes, C. H., Maheswaran, S., Haber, D. A., Fernandez-Del-Castillo, C., Ferrone, C. R., Haas, W., Aryee, M. J. and Ting, D. T. (2019). **Stromal Microenvironment Shapes the Intratumoral Architecture of Pancreatic Cancer.** *Cell* 178 (1), 160-175.e127, doi: 10.1016/j.cell.2019.05.012.
- Lim, K. H., Baines, A. T., Fiordalisi, J. J., Shipitsin, M., Feig, L. A., Cox, A. D., Der, C. J. and Counter, C. M. (2005). **Activation of RalA is critical for Ras-induced tumorigenesis of human cells.** *Cancer Cell* 7 (6), 533-545, doi: 10.1016/j.ccr.2005.04.030.
- Lima-Fernandes, E., Enslin, H., Camand, E., Kotelevets, L., Boullaran, C., Achour, L.,

- Benmerah, A., Gibson, L. C., Baillie, G. S., Pitcher, J. A., Chastre, E., Etienne-Manneville, S., Marullo, S. and Scott, M. G. (2011). **Distinct functional outputs of PTEN signalling are controlled by dynamic association with β -arrestins**. *Embo j* 30 (13), 2557-2568, doi: 10.1038/emboj.2011.178.
- Lin, L., Yee, S. W., Kim, R. B. and Giacomini, K. M. (2015). **SLC transporters as therapeutic targets: emerging opportunities**. *Nat Rev Drug Discov* 14 (8), 543-560, doi: 10.1038/nrd4626.
- Lin, M. E., Herr, D. R. and Chun, J. (2010). **Lysophosphatidic acid (LPA) receptors: signaling properties and disease relevance**. *Prostaglandins Other Lipid Mediat* 91 (3-4), 130-138, doi: 10.1016/j.prostaglandins.2009.02.002.
- Liu, T., Han, C., Wang, S., Fang, P., Ma, Z., Xu, L. and Yin, R. (2019). **Cancer-associated fibroblasts: an emerging target of anti-cancer immunotherapy**. *J Hematol Oncol* 12 (1), 86, doi: 10.1186/s13045-019-0770-1.
- Liu, X. (2019). **SLC Family Transporters**. *Adv Exp Med Biol* 1141, 101-202, doi: 10.1007/978-981-13-7647-4_3.
- Logothetis, D. E., Kurachi, Y., Galper, J., Neer, E. J. and Clapham, D. E. (1987). **The beta gamma subunits of GTP-binding proteins activate the muscarinic K⁺ channel in heart**. *Nature* 325 (6102), 321-326, doi: 10.1038/325321a0.
- Longnecker, D. S. (2021). **Anatomy and Histology of the Pancreas**. *Pancreapedia: Exocrine Pancreas Knowledge Base*, DOI: 10.3998/panc.2021.01.
- Lopez-Illasaca, M., Crespo, P., Pellici, P. G., Gutkind, J. S. and Wetzker, R. (1997). **Linkage of G protein-coupled receptors to the MAPK signaling pathway through PI 3-kinase gamma**. *Science* 275 (5298), 394-397, doi: 10.1126/science.275.5298.394.
- Lukov, G. L., Hu, T., McLaughlin, J. N., Hamm, H. E. and Willardson, B. M. (2005). **Phosducin-like protein acts as a molecular chaperone for G protein betagamma dimer assembly**. *Embo j* 24 (11), 1965-1975, doi: 10.1038/sj.emboj.7600673.
- Luttrell, L. M., Della Rocca, G. J., van Biesen, T., Luttrell, D. K. and Lefkowitz, R. J. (1997). **Gbetagamma subunits mediate Src-dependent phosphorylation of the epidermal growth factor receptor. A scaffold for G protein-coupled receptor-mediated Ras activation**. *J Biol Chem* 272 (7), 4637-4644, doi: 10.1074/jbc.272.7.4637.
- Luttrell, L. M., Hawes, B. E., van Biesen, T., Luttrell, D. K., Lansing, T. J. and Lefkowitz, R. J. (1996). **Role of c-Src tyrosine kinase in G protein-coupled receptor- and Gbetagamma subunit-mediated activation of mitogen-activated protein kinases**. *J Biol Chem* 271 (32), 19443-19450, doi: 10.1074/jbc.271.32.19443.
- Ma, Y. C., Huang, J., Ali, S., Lowry, W. and Huang, X. Y. (2000). **Src tyrosine kinase is a novel direct effector of G proteins**. *Cell* 102 (5), 635-646, doi: 10.1016/s0092-8674(00)00086-6.

- Macha, M. A., Seshacharyulu, P., Krishn, S. R., Pai, P., Rachagani, S., Jain, M. and Batra, S. K. (2014). **MicroRNAs (miRNAs) as biomarker(s) for prognosis and diagnosis of gastrointestinal (GI) cancers.** *Curr Pharm Des* 20 (33), 5287-5297, doi: 10.2174/1381612820666140128213117.
- Matsuyama, R., Togo, S., Shimizu, D., Momiyama, N., Ishikawa, T., Ichikawa, Y., Endo, I., Kunisaki, C., Suzuki, H., Hayasizaki, Y. and Shimada, H. (2006). **Predicting 5-fluorouracil chemosensitivity of liver metastases from colorectal cancer using primary tumor specimens: three-gene expression model predicts clinical response.** *Int J Cancer* 119 (2), 406-413, doi: 10.1002/ijc.21843.
- McCudden, C. R., Hains, M. D., Kimple, R. J., Siderovski, D. P. and Willard, F. S. (2005). **G-protein signaling: back to the future.** *Cell Mol Life Sci* 62 (5), 551-577, doi: 10.1007/s00018-004-4462-3.
- McGuigan, A., Kelly, P., Turkington, R. C., Jones, C., Coleman, H. G. and McCain, R. S. (2018). **Pancreatic cancer: A review of clinical diagnosis, epidemiology, treatment and outcomes.** *World J Gastroenterol* 24 (43), 4846-4861, doi: 10.3748/wjg.v24.i43.4846.
- Mendoza, M. C., Er, E. E. and Blenis, J. (2011). **The Ras-ERK and PI3K-mTOR pathways: cross-talk and compensation.** *Trends Biochem Sci* 36 (6), 320-328, doi: 10.1016/j.tibs.2011.03.006.
- Meng, F., Henson, R., Wehbe-Janek, H., Ghoshal, K., Jacob, S. T. and Patel, T. (2007). **MicroRNA-21 regulates expression of the PTEN tumor suppressor gene in human hepatocellular cancer.** *Gastroenterology* 133 (2), 647-658, doi: 10.1053/j.gastro.2007.05.022.
- Moffitt, R. A., Marayati, R., Flate, E. L., Volmar, K. E., Loeza, S. G., Hoadley, K. A., Rashid, N. U., Williams, L. A., Eaton, S. C., Chung, A. H., Smyla, J. K., Anderson, J. M., Kim, H. J., Bentrem, D. J., Talamonti, M. S., Iacobuzio-Donahue, C. A., Hollingsworth, M. A. and Yeh, J. J. (2015). **Virtual microdissection identifies distinct tumor- and stroma-specific subtypes of pancreatic ductal adenocarcinoma.** *Nat Genet* 47 (10), 1168-1178, doi: 10.1038/ng.3398.
- Montini, E., Cesana, D., Schmidt, M., Sanvito, F., Bartholomae, C. C., Ranzani, M., Benedicenti, F., Sergi, L. S., Ambrosi, A., Ponzoni, M., Doglioni, C., Di Serio, C., von Kalle, C. and Naldini, L. (2009). **The genotoxic potential of retroviral vectors is strongly modulated by vector design and integration site selection in a mouse model of HSC gene therapy.** *J Clin Invest* 119 (4), 964-975, doi: 10.1172/jci37630.
- Morgan, R. G., Mortenson, E. and Williams, A. C. (2018). **Targeting LGR5 in Colorectal Cancer: therapeutic gold or too plastic?** *Br J Cancer* 118 (11), 1410-1418, doi: 10.1038/s41416-018-0118-6.

- Mueller, S., Engleitner, T., Maresch, R., Zukowska, M., Lange, S., Kaltenbacher, T., Konukiewicz, B., Öllinger, R., Zwiebel, M., Strong, A., Yen, H. Y., Banerjee, R., Louzada, S., Fu, B., Seidler, B., Götzfried, J., Schuck, K., Hassan, Z., Arbeiter, A., Schönhuber, N., Klein, S., Veltkamp, C., Friedrich, M., Rad, L., Barenboim, M., Ziegenhain, C., Hess, J., Dovey, O. M., Eser, S., Parekh, S., Constantino-Casas, F., de la Rosa, J., Sierra, M. I., Fraga, M., Mayerle, J., Klöppel, G., Cadiñanos, J., Liu, P., Vassiliou, G., Weichert, W., Steiger, K., Enard, W., Schmid, R. M., Yang, F., Unger, K., Schneider, G., Varela, I., Bradley, A., Saur, D. and Rad, R. (2018). **Evolutionary routes and KRAS dosage define pancreatic cancer phenotypes.** *Nature* 554 (7690), 62-68, doi: 10.1038/nature25459.
- Multiplexion (2020). **Cell lysate Preparation Protocol.** URL: https://www.multiplexion.de/images/Multiplexion/Cell_Lysate_Preparation_Protocol.pdf [last accessed 26 June 2020].
- Murakami, T., Hiroshima, Y., Matsuyama, R., Homma, Y., Hoffman, R. M. and Endo, I. (2019). **Role of the tumor microenvironment in pancreatic cancer.** *Ann Gastroenterol Surg* 3 (2), 130-137, doi: 10.1002/ags3.12225.
- Murga, C., Arcones, A. C., Cruces-Sande, M., Briones, A. M., Salaces, M. and Mayor, F., Jr. (2019). **G Protein-Coupled Receptor Kinase 2 (GRK2) as a Potential Therapeutic Target in Cardiovascular and Metabolic Diseases.** *Front Pharmacol* 10, 112, doi: 10.3389/fphar.2019.00112.
- Murphy, K. M., Brune, K. A., Griffin, C., Sollenberger, J. E., Petersen, G. M., Bansal, R., Hruban, R. H. and Kern, S. E. (2002). **Evaluation of candidate genes MAP2K4, MADH4, ACVR1B, and BRCA2 in familial pancreatic cancer: deleterious BRCA2 mutations in 17%.** *Cancer Res* 62 (13), 3789-3793.
- Nakamura, K., Salomonis, N., Tomoda, K., Yamanaka, S. and Conklin, B. R. (2009). **G(i)-coupled GPCR signaling controls the formation and organization of human pluripotent colonies.** *PLoS One* 4 (11), e7780, doi: 10.1371/journal.pone.0007780.
- Navin, N. E. (2015). **The first five years of single-cell cancer genomics and beyond.** *Genome Res* 25 (10), 1499-1507, doi: 10.1101/gr.191098.115.
- Neer, E. J., Schmidt, C. J., Nambudripad, R. and Smith, T. F. (1994). **The ancient regulatory-protein family of WD-repeat proteins.** *Nature* 371 (6495), 297-300, doi: 10.1038/371297a0.
- Neoptolemos, J. P., Kleeff, J., Michl, P., Costello, E., Greenhalf, W. and Palmer, D. H. (2018). **Therapeutic developments in pancreatic cancer: current and future perspectives.** *Nat Rev Gastroenterol Hepatol* 15 (6), 333-348, doi: 10.1038/s41575-018-0005-x.
- New, D. C. and Wong, Y. H. (2007). **Molecular mechanisms mediating the G protein-coupled receptor regulation of cell cycle progression.** *J Mol Signal* 2, 2, doi:

10.1186/1750-2187-2-2.

NMI Technologietransfer GmbH, N. T. P. (2020). **DigiWest® Protein Profiling Services**. URL: <https://www.nmi-tt.de/pharmaservices/digiwest/> [last accessed 21 June 2020].

Nogués, L., Reglero, C., Rivas, V., Neves, M., Penela, P. and Mayor, F., Jr. (2017). **G-Protein-Coupled Receptor Kinase 2 as a Potential Modulator of the Hallmarks of Cancer**. *Mol Pharmacol* *91* (3), 220-228, doi: 10.1124/mol.116.107185.

Nowell, P. C. (1976). **The clonal evolution of tumor cell populations**. *Science* *194* (4260), 23-28, doi: 10.1126/science.959840.

O'Brien, C. A., Pollett, A., Gallinger, S. and Dick, J. E. (2007). **A human colon cancer cell capable of initiating tumour growth in immunodeficient mice**. *Nature* *445* (7123), 106-110, doi: 10.1038/nature05372.

O'Brien, L. E., Soliman, S. S., Li, X. and Bilder, D. (2011). **Altered modes of stem cell division drive adaptive intestinal growth**. *Cell* *147* (3), 603-614, doi: 10.1016/j.cell.2011.08.048.

O'Flaherty, J. D., Barr, M., Fennell, D., Richard, D., Reynolds, J., O'Leary, J. and O'Byrne, K. (2012). **The cancer stem-cell hypothesis: its emerging role in lung cancer biology and its relevance for future therapy**. *J Thorac Oncol* *7* (12), 1880-1890, doi: 10.1097/JTO.0b013e31826bfbc6.

Paradis, J. S., Ly, S., Blondel-Tepaz, É., Galan, J. A., Beautrait, A., Scott, M. G., Enslin, H., Marullo, S., Roux, P. P. and Bouvier, M. (2015). **Receptor sequestration in response to β -arrestin-2 phosphorylation by ERK1/2 governs steady-state levels of GPCR cell-surface expression**. *Proc Natl Acad Sci U S A* *112* (37), E5160-5168, doi: 10.1073/pnas.1508836112.

Parker, S. J., Amendola, C. R., Hollinshead, K. E. R., Yu, Q., Yamamoto, K., Encarnación-Rosado, J., Rose, R. E., LaRue, M. M., Sohn, A. S. W., Biancur, D. E., Paulo, J. A., Gygi, S. P., Jones, D. R., Wang, H., Philips, M. R., Bar-Sagi, D., Mancias, J. D. and Kimmelman, A. C. (2020). **Selective Alanine Transporter Utilization Creates a Targetable Metabolic Niche in Pancreatic Cancer**. *Cancer Discov* *10* (7), 1018-1037, doi: 10.1158/2159-8290.Cd-19-0959.

Patra, K. C., Kato, Y., Mizukami, Y., Widholz, S., Boukhali, M., Revenco, I., Grossman, E. A., Ji, F., Sadreyev, R. I., Liss, A. S., Sreaton, R. A., Sakamoto, K., Ryan, D. P., Mino-Kenudson, M., Castillo, C. F., Nomura, D. K., Haas, W. and Bardeesy, N. (2018). **Mutant GNAS drives pancreatic tumorigenesis by inducing PKA-mediated SIK suppression and reprogramming lipid metabolism**. *Nat Cell Biol* *20* (7), 811-822, doi: 10.1038/s41556-018-0122-3.

Peng, J., Sun, B. F., Chen, C. Y., Zhou, J. Y., Chen, Y. S., Chen, H., Liu, L., Huang, D., Jiang, J., Cui, G. S., Yang, Y., Wang, W., Guo, D., Dai, M., Guo, J., Zhang, T., Liao, Q., Liu, Y., Zhao, Y. L., Han, D. L., Zhao, Y., Yang, Y. G. and Wu, W. (2019). **Single-cell**

- RNA-seq highlights intra-tumoral heterogeneity and malignant progression in pancreatic ductal adenocarcinoma.** *Cell Res* 29 (9), 725-738, doi: 10.1038/s41422-019-0195-y.
- Pliner, H. A., Shendure, J. and Trapnell, C. (2019). **Supervised classification enables rapid annotation of cell atlases.** *Nat Methods* 16 (10), 983-986, doi: 10.1038/s41592-019-0535-3.
- Pierce, K. L., Premont, R. T. and Lefkowitz, R. J. (2002). **Seven-transmembrane receptors.** *Nat Rev Mol Cell Biol* 3 (9), 639-650, doi: 10.1038/nrm908.
- Polireddy, K. and Chen, Q. (2016). **Cancer of the Pancreas: Molecular Pathways and Current Advancement in Treatment.** *J Cancer* 7 (11), 1497-1514, doi: 10.7150/jca.14922.
- Poon, R. Y. C. (2002). **Cell Cycle Control.** In: *Encyclopedia of Cancer* (Second Edition), ed. Bertino, J. R., 2nd Edition, Academic Press, New York, pg. 393-403.
- R Core Team (2021). **R: A Language and Environment for Statistical Computing** (R Foundation for Statistical Computing). URL: <https://www.R-project.org> [last accessed 25 March 2021]
- Radhika, V. and Dhanasekaran, N. (2001). **Transforming G proteins.** *Oncogene* 20 (13), 1607-1614, doi: 10.1038/sj.onc.1204274.
- Rahman, M., Deleyrolle, L., Vedam-Mai, V., Azari, H., Abd-El-Barr, M. and Reynolds, B. A. (2011). **The cancer stem cell hypothesis: failures and pitfalls.** *Neurosurgery* 68 (2), 531-545; discussion 545, doi: 10.1227/NEU.0b013e3181ff9eb5.
- Ram, P. T. and Iyengar, R. (2001). **G protein coupled receptor signaling through the Src and Stat3 pathway: role in proliferation and transformation.** *Oncogene* 20 (13), 1601-1606, doi: 10.1038/sj.onc.1204186.
- Ranzani, M., Cesana, D., Bartholomae, C. C., Sanvito, F., Pala, M., Benedicenti, F., Gallina, P., Sergi, L. S., Merella, S., Bulfone, A., Doglioni, C., von Kalle, C., Kim, Y. J., Schmidt, M., Tonon, G., Naldini, L. and Montini, E. (2013). **Lentiviral vector-based insertional mutagenesis identifies genes associated with liver cancer.** *Nat Methods* 10 (2), 155-161, doi: 10.1038/nmeth.2331.
- Rawat, M., Kadian, K., Gupta, Y., Kumar, A., Chain, P. S. G., Kovbasnjuk, O., Kumar, S. and Parasher, G. (2019). **MicroRNA in Pancreatic Cancer: From Biology to Therapeutic Potential.** *Genes (Basel)* 10 (10), doi: 10.3390/genes10100752.
- Rawla, P., Sunkara, T. and Gaduputi, V. (2019). **Epidemiology of Pancreatic Cancer: Global Trends, Etiology and Risk Factors.** *World J Oncol* 10 (1), 10-27, doi: 10.14740/wjon1166.

- Reeves, M. Q., Kandyba, E., Harris, S., Del Rosario, R. and Balmain, A. (2018). **Multicolour lineage tracing reveals clonal dynamics of squamous carcinoma evolution from initiation to metastasis**. *Nat Cell Biol* 20 (6), 699-709, doi: 10.1038/s41556-018-0109-0.
- Ribas, C., Penela, P., Murga, C., Salcedo, A., García-Hoz, C., Jurado-Pueyo, M., Aymerich, I. and Mayor, F., Jr. (2007). **The G protein-coupled receptor kinase (GRK) interactome: role of GRKs in GPCR regulation and signaling**. *Biochim Biophys Acta* 1768 (4), 913-922, doi: 10.1016/j.bbamem.2006.09.019.
- Sadana, R. and Dessauer, C. W. (2009). **Physiological roles for G protein-regulated adenylyl cyclase isoforms: insights from knockout and overexpression studies**. *Neurosignals* 17 (1), 5-22, doi: 10.1159/000166277.
- Sahai, E., Astsaturov, I., Cukierman, E., DeNardo, D. G., Egeblad, M., Evans, R. M., Fearon, D., Greten, F. R., Hingorani, S. R., Hunter, T., Hynes, R. O., Jain, R. K., Janowitz, T., Jorgensen, C., Kimmelman, A. C., Kolonin, M. G., Maki, R. G., Powers, R. S., Puré, E., Ramirez, D. C., Scherz-Shouval, R., Sherman, M. H., Stewart, S., Tlsty, T. D., Tuveson, D. A., Watt, F. M., Weaver, V., Weeraratna, A. T. and Werb, Z. (2020). **A framework for advancing our understanding of cancer-associated fibroblasts**. *Nat Rev Cancer* 20 (3), 174-186, doi: 10.1038/s41568-019-0238-1.
- Salcedo, A., Mayor, F., Jr. and Penela, P. (2006). **Mdm2 is involved in the ubiquitination and degradation of G-protein-coupled receptor kinase 2**. *Embo j* 25 (20), 4752-4762, doi: 10.1038/sj.emboj.7601351.
- Schäfer, B., Marg, B., Gschwind, A. and Ullrich, A. (2004). **Distinct ADAM metalloproteinases regulate G protein-coupled receptor-induced cell proliferation and survival**. *J Biol Chem* 279 (46), 47929-47938, doi: 10.1074/jbc.M400129200.
- Shenoy, S. K. and Lefkowitz, R. J. (2005). **Seven-transmembrane receptor signaling through beta-arrestin**. *Sci STKE* 2005 (308), cm10, doi: 10.1126/stke.2005/308/cm10.
- Shibata, K., Mori, M., Tanaka, S., Kitano, S. and Akiyoshi, T. (1998). **Identification and cloning of human G-protein gamma 7, down-regulated in pancreatic cancer**. *Biochem Biophys Res Commun* 246 (1), 205-209, doi: 10.1006/bbrc.1998.8581.
- Singh, S. K., Hawkins, C., Clarke, I. D., Squire, J. A., Bayani, J., Hide, T., Henkelman, R. M., Cusimano, M. D. and Dirks, P. B. (2004). **Identification of human brain tumour initiating cells**. *Nature* 432 (7015), 396-401, doi: 10.1038/nature03128.
- Smith, J. S. and Rajagopal, S. (2016). **The β -Arrestins: Multifunctional Regulators of G Protein-coupled Receptors**. *J Biol Chem* 291 (17), 8969-8977, doi: 10.1074/jbc.R115.713313.

- Smith, T., Heger, A. and Sudbery, I. (2017). **UMI-tools: modeling sequencing errors in Unique Molecular Identifiers to improve quantification accuracy**. *Genome Res* 27 (3), 491-499, doi: 10.1101/gr.209601.116.
- Sondek, J., Bohm, A., Lambright, D. G., Hamm, H. E. and Sigler, P. B. (1996). **Crystal structure of a G-protein beta gamma dimer at 2.1A resolution**. *Nature* 379 (6563), 369-374, doi: 10.1038/379369a0.
- Song, Q., Ji, Q. and Li, Q. (2018). **The role and mechanism of β -arrestins in cancer invasion and metastasis (Review)**. *Int J Mol Med* 41 (2), 631-639, doi: 10.3892/ijmm.2017.3288.
- Stuart, T., Butler, A., Hoffman, P., Hafemeister, C., Papalexi, E., Mauck, W. M., 3rd, Hao, Y., Stoeckius, M., Smibert, P. and Satija, R. (2019). **Comprehensive Integration of Single-Cell Data**. *Cell* 177 (7), 1888-1902.e1821, doi: 10.1016/j.cell.2019.05.031.
- Syrovatkina, V., Alegre, K. O., Dey, R. and Huang, X. Y. (2016). **Regulation, Signaling, and Physiological Functions of G-Proteins**. *J Mol Biol* 428 (19), 3850-3868, doi: 10.1016/j.jmb.2016.08.002.
- Tall, G. G. and Gilman, A. G. (2005). **Resistance to inhibitors of cholinesterase 8A catalyzes release of G α 1-GTP and nuclear mitotic apparatus protein (NuMA) from NuMA/LGN/G α 1-GDP complexes**. *Proc Natl Acad Sci U S A* 102 (46), 16584-16589, doi: 10.1073/pnas.0508306102.
- Tan, B. T., Park, C. Y., Ailles, L. E. and Weissman, I. L. (2006). **The cancer stem cell hypothesis: a work in progress**. *Lab Invest* 86 (12), 1203-1207, doi: 10.1038/labinvest.3700488.
- Tang, D. G. (2012). **Understanding cancer stem cell heterogeneity and plasticity**. *Cell Res* 22 (3), 457-472, doi: 10.1038/cr.2012.13.
- Thomas, C. J., Tall, G. G., Adhikari, A. and Sprang, S. R. (2008). **Ric-8A catalyzes guanine nucleotide exchange on G α 1 bound to the GPR/GoLoco exchange inhibitor AGS3**. *J Biol Chem* 283 (34), 23150-23160, doi: 10.1074/jbc.M802422200.
- Tuteja, N. (2009). **Signaling through G protein coupled receptors**. *Plant Signal Behav* 4 (10), 942-947, doi: 10.4161/psb.4.10.9530.
- van Geel, R., van Brummelen, E. M. J., Eskens, F., Huijberts, S., de Vos, F., Lolkema, M., Devriese, L. A., Opdam, F. L., Marchetti, S., Steeghs, N., Monkhorst, K., Thijssen, B., Rosing, H., Huitema, A. D. R., Beijnen, J. H., Bernardis, R. and Schellens, J. H. M. (2020). **Phase 1 study of the pan-HER inhibitor dacomitinib plus the MEK1/2 inhibitor PD-0325901 in patients with KRAS-mutation-positive colorectal, non-small-cell lung and pancreatic cancer**. *Br J Cancer* 122 (8), 1166-1174, doi: 10.1038/s41416-020-0776-z.

- Vincent, A., Herman, J., Schulick, R., Hruban, R. H. and Goggins, M. (2011). **Pancreatic cancer**. *Lancet* 378 (9791), 607-620, doi: 10.1016/s0140-6736(10)62307-0.
- Vinogradov, S. and Wei, X. (2012). **Cancer stem cells and drug resistance: the potential of nanomedicine**. *Nanomedicine (Lond)* 7 (4), 597-615, doi: 10.2217/nnm.12.22.
- De Waard, M., Liu, H., Walker, D., Scott, V. E., Gurnett, C. A. and Campbell, K. P. (1997). **Direct binding of G-protein betagamma complex to voltage-dependent calcium channels**. *Nature* 385 (6615), 446-450, doi: 10.1038/385446a0.
- Wang, Z. (2016). **Transactivation of Epidermal Growth Factor Receptor by G Protein-Coupled Receptors: Recent Progress, Challenges and Future Research**. *Int J Mol Sci* 17 (1), doi: 10.3390/ijms17010095.
- Waters, A. M. and Der, C. J. (2018). **KRAS: The Critical Driver and Therapeutic Target for Pancreatic Cancer**. *Cold Spring Harb Perspect Med* 8 (9), doi: 10.1101/cshperspect.a031435.
- Weissmueller, S., Manchado, E., Saborowski, M., Morris, J. P. t., Wagenblast, E., Davis, C. A., Moon, S. H., Pfister, N. T., Tschaharganeh, D. F., Kitzing, T., Aust, D., Markert, E. K., Wu, J., Grimmond, S. M., Pilarsky, C., Prives, C., Biankin, A. V. and Lowe, S. W. (2014). **Mutant p53 drives pancreatic cancer metastasis through cell-autonomous PDGF receptor β signaling**. *Cell* 157 (2), 382-394, doi: 10.1016/j.cell.2014.01.066.
- Winter, G. E., Radic, B., Mayor-Ruiz, C., Blomen, V. A., Trefzer, C., Kandasamy, R. K., Huber, K. V. M., Gridling, M., Chen, D., Klampfl, T., Kralovics, R., Kubicek, S., Fernandez-Capetillo, O., Brummelkamp, T. R. and Superti-Furga, G. (2014). **The solute carrier SLC35F2 enables YM155-mediated DNA damage toxicity**. *Nat Chem Biol* 10 (9), 768-773, doi: 10.1038/nchembio.1590.
- Wong, Y. H., Chan, J. S., Yung, L. Y. and Bourne, H. R. (1995). **Mutant alpha subunit of Gz transforms Swiss 3T3 cells**. *Oncogene* 10 (10), 1927-1933.
- Wootten, D., Christopoulos, A., Marti-Solano, M., Babu, M. M. and Sexton, P. M. (2018). **Mechanisms of signalling and biased agonism in G protein-coupled receptors**. *Nat Rev Mol Cell Biol* 19 (10), 638-653, doi: 10.1038/s41580-018-0049-3.
- Yang, Z. F., Ho, D. W., Ng, M. N., Lau, C. K., Yu, W. C., Ngai, P., Chu, P. W., Lam, C. T., Poon, R. T. and Fan, S. T. (2008). **Significance of CD90+ cancer stem cells in human liver cancer**. *Cancer Cell* 13 (2), 153-166, doi: 10.1016/j.ccr.2008.01.013.
- Yao, J., Liang, L. H., Zhang, Y., Ding, J., Tian, Q., Li, J. J. and He, X. H. (2012). **GNAI1 Suppresses Tumor Cell Migration and Invasion and is Post-Transcriptionally Regulated by Mir-320a/c/d in Hepatocellular Carcinoma**. *Cancer Biol Med* 9 (4), 234-241, doi: 10.7497/j.issn.2095-3941.2012.04.003.

- Yoda, A., Adelmant, G., Tamburini, J., Chapuy, B., Shindoh, N., Yoda, Y., Weigert, O., Kopp, N., Wu, S.-C., Kim, S. S., Liu, H., Tivey, T., Christie, A. L., Elpek, K. G., Card, J., Gritsman, K., Gotlib, J., Deininger, M. W., Makishima, H., Turley, S., Javidi-Sharifi, N., Maciejewski, J. P., Rodig, S. J., Tyner, J. W., Marto, J. A., Weinstock, D. M. and Lane, A. A. (2014). **GNB1 Activating Mutations Promote Myeloid and Lymphoid Neoplasms Targetable By Combined PI3K/mTOR Inhibition**. *Blood* 124 (21), 3567-3567, doi: 10.1182/blood.V124.21.3567.3567.
- Yoda, A., Adelmant, G., Tamburini, J., Chapuy, B., Shindoh, N., Yoda, Y., Weigert, O., Kopp, N., Wu, S. C., Kim, S. S., Liu, H., Tivey, T., Christie, A. L., Elpek, K. G., Card, J., Gritsman, K., Gotlib, J., Deininger, M. W., Makishima, H., Turley, S. J., Javidi-Sharifi, N., Maciejewski, J. P., Jaiswal, S., Ebert, B. L., Rodig, S. J., Tyner, J. W., Marto, J. A., Weinstock, D. M. and Lane, A. A. (2015). **Mutations in G protein β subunits promote transformation and kinase inhibitor resistance**. *Nat Med* 21 (1), 71-75, doi: 10.1038/nm.3751.
- Yonemori, K., Kurahara, H., Maemura, K. and Natsugoe, S. (2017). **MicroRNA in pancreatic cancer**. *J Hum Genet* 62 (1), 33-40, doi: 10.1038/jhg.2016.59.
- Zhang, Q. G., Wang, R., Han, D., Dong, Y. and Brann, D. W. (2009). **Role of Rac1 GTPase in JNK signaling and delayed neuronal cell death following global cerebral ischemia**. *Brain Res* 1265, 138-147, doi: 10.1016/j.brainres.2009.01.033.
- Zhao, W. G., Yu, S. N., Lu, Z. H., Ma, Y. H., Gu, Y. M. and Chen, J. (2010). **The miR-217 microRNA functions as a potential tumor suppressor in pancreatic ductal adenocarcinoma by targeting KRAS**. *Carcinogenesis* 31 (10), 1726-1733, doi: 10.1093/carcin/bgq160.
- Zheng, G. X., Terry, J. M., Belgrader, P., Ryvkin, P., Bent, Z. W., Wilson, R., Ziraldo, S. B., Wheeler, T. D., McDermott, G. P., Zhu, J., Gregory, M. T., Shuga, J., Montesclaros, L., Underwood, J. G., Masquelier, D. A., Nishimura, S. Y., Schnall-Levin, M., Wyatt, P. W., Hindson, C. M., Bharadwaj, R., Wong, A., Ness, K. D., Beppu, L. W., Deeg, H. J., McFarland, C., Loeb, K. R., Valente, W. J., Ericson, N. G., Stevens, E. A., Radich, J. P., Mikkelsen, T. S., Hindson, B. J. and Bielas, J. H. (2017). **Massively parallel digital transcriptional profiling of single cells**. *Nat Commun* 8, 14049, doi: 10.1038/ncomms14049.
- Zhou, Q. and Melton, D. A. (2018). **Pancreas regeneration**. *Nature* 557 (7705), 351-358, doi: 10.1038/s41586-018-0088-0.
- Zimmermannova, O., Doktorova, E., Stuchly, J., Kanderova, V., Kuzilkova, D., Strnad, H., Starkova, J., Alberich-Jorda, M., Falkenburg, J. H. F., Trka, J., Petrak, J., Zuna, J. and Zaliova, M. (2017). **An activating mutation of GNB1 is associated with resistance to tyrosine kinase inhibitors in ETV6-ABL1-positive leukemia**. *Oncogene* 36 (43), 5985-5994, doi: 10.1038/onc.2017.210.
- 10x Genomics (2019). **Chromium Single Cell 3' Reagent Kits v2 User Guide**. URL: <https://assets.ctfassets.net/an68im79xiti/RT8DYozzhDJRBMrJCmVxl/6a0ed8015d89>

[bf9602128a4c9f8962c8/CG00052_SingleCell3_ReagentKitv2UserGuide_RevF.pdf](#)
[last accessed 06 April 2020].

8 Personal Contribution to Data Acquisition, Assessment and Publications

This project was based on results gained within a previous PhD thesis project in Prof. Dr. med. Hanno Glimm's group performed by Dr. med. Jianpeng Gao (Gao 2017). Dr. Gao had identified GNB1 as a potential TIC regulator in a screening approach and performed initial validation experiments in patient derived cultures. Within my thesis, I completed the dataset for experimental validation of the identified candidate. After successful validation, I further investigated the underlying mechanisms and aimed to identify relevant binding partners of GNB1 in human pancreatic cancer.

In brief, Dr. med. Jianpeng Gao generated the GNB1 codon-optimized overexpression (GNB1 OE), and shRNA-based GNB1 knockdown (GNB1 KD) constructs, which were used in this study. Dr. Gao produced the concentrated GNB1 OE, GNB1 KD, GFP control (vector control for GNB1 OE) lentiviral vector stocks which were further used for the transduction of patient-derived PCs and H6C7 cultures. Dr. Gao performed cell cycle analysis and cell apoptosis analysis of PC1 and PC2 GNB1 KD (including scramble control) as shown and declared in section 3.2, Figure 13 and Table 4. Moreover, PC1 and PC2 GNB1 KD and scramble control cultures used in this thesis were generated by Dr. Gao. I produced the scramble control concentrated lentiviral vector stocks and generated the GNB1 OE and GFP control (control of overexpression vector) PC cultures, PC3 GNB1 KD, and PC3 scramble control cultures. Based on Dr. Gao's experimental setup, I performed PC1, PC2, PC3 GNB1 OE (with GFP control vector control) and PC3 GNB1 KD (including scramble control) cell cycle analysis to complete the analysis.

I prepared protein sample for mass-spectrometry based whole protein analysis, DigiWest antibody array, and GNB1 binding partners mass-spectrometry. Then samples for mass-spectrometry based whole protein analysis were submitted to the Genomics & Proteomics Core Facility of DKFZ, Heidelberg, Germany for analysis. Raw data was first analysed in the Genomics & Proteomics Core Facility of DKFZ, Heidelberg, Germany, then data was retrieved. I further summarized and analysed retrieved data which showed in Figure 8, Figure 9, Figure 10, Figure 11, and Table 3.

Sample preparation and the library establishments of single cell RNA sequencing were performed by me in scOpenLab, Heidelberg, Germany. And library sequencing was done in the Genomics & Proteomics Core Facility of DKFZ, Heidelberg, Germany. Sequencing data was retrieved and analysed together with bioinformatician Dr. Mario Huerta which was shown in section 3.3. Results images shown in Figure 22, Figure 23 and Figure 24 were produced by Dr. Mario Huerta.

Protein samples for DigiWest antibody array were submitted to NMI TT Technologietransfer GmbH, Reutlingen, Germany. Quality control and raw data pre-analyse were performed by NMI TT Technologietransfer GmbH, Reutlingen, Germany. Then I further analysed retrieved data to generated Figure 30.

Protein samples for GNB1 binding partners mass-spectrometry analysis was submitted to the Core Facility for Mass-spectrometry & Proteomics (CFMP) at Zentrum für Molekulare Biologie der Universität Heidelberg (ZMBH). The peptides readout data of proteins were retrieved from the core facility and further analysed by me.

Immunofluorescence images were taken at the Light Microscopy Facility, DKFZ, Heidelberg, Germany by using the Leica TCS SP5 confocal microscope as indicated in section 2.2.7.7.

Curriculum Vitae

Personal data

Name: Na Kang
Date of Birth: 31.08.1987
Place of Birth: Harbin, China
Nationality: Chinese
Study Subject: Oncology

School Career

2003-2006 Harbin No.6 High School, China

University Career

2006-2011 B.Sc. Clinical Medicine, Harbin Medical University, China.

2013-2014 M.Res. Cancer Research, Newcastle University, UK
Received a Faculty of Medical Sciences MRes Scholarship

2015-2016 Ph.D. Heidelberg University, Germany
Prof. Dr. med. Margot Zöller at Tumourzellbiologie, Chirurgische
Universitätsklinik

2016-Present Ph.D. Heidelberg University, Germany
Doctoral thesis: Characterization of G Protein Subunit Beta 1 as
Regulator of Tumour Initiating Cell Activity in Human
Pancreatic Cancer
Prof. Dr. med. Hanno Glimm at National Center for Tumour
Disease (NCT), Heidelberg & Dresden, Germany
Received a Chinese Government Scholarship from the Chinese
Scholarship Council.

I declare that all the above information given by me is valid.

Acknowledgement

PhD study is a tough, challenging, exhausting life. Till now, four years have passed since I joined AG Glimm, and I have experienced them all, as expected. However, those are not all, and I also experienced the fun part of doing science, enjoy the exciting feelings that working with professionals, and involved in the warm and lively atmosphere in the lab office.

First, I would like to thank my Doctor Father Mr. Prof. Dr. med. Hanno Glimm, who "adopted" me as a PhD student in his lab. In the research life, I am impressed by how knowledgeable he is whenever we are in the lab meetings or the project discussions. Mr. Prof. Dr. med. Hanno Glimm also influenced me in the way of thinking when facing problems and the attitude of life that I interpreted as humble, grace, rigorous, kind, and cool always.

Second, I want to express my gratitude to all my PIs, Ms. Dr. rer. nat. Claudia Ball, Ms. Dr. rer. nat. Friederike Herbst, and Mr. Dr. med. Roland Ehrenberg. They supervised and guided me to keep me on the right track in doing my PhD project. Their guidance trained me to be as a researcher.

PhD candidates Ms. Karin Laaber and Ms. Martina Zowada whose names always showed together as "Katina", joined AG Glimm around the same time with me. They bring the "warm, lively, noisy" atmosphere, which I mentioned above to the lab office. They generously provided their help when I asked. Ms. Karin Laaber kindly helped me to translate the Summary into German version. And there are so many funny moments to remember which will be my precious memories in the rest of my life. Next, I would like to thank Ms. Dr. sc. nat. Paula Codo. She is very professional in working with proteins and doing analysis. She is a kind person as well. With time pass, we found we shared the same interests, which made us good teammates both in lab work and leisure time. Then I want to thank our know-everything-in-lab technicians Mr. Tim Kindinger, Ms. Sylvia Martin, and former TA Ms. Nina Hofmann. They showed great patience for helping me when I faced the technical problems in doing sorting, cloning, even looking for experiments' materials etc. Mr. Tim Kindinger is very experienced in animal experiments which helped me a lot when my mouse experiments ongoing. And Ms. Nina Hofmann also provided a lot of help in checking the mice. Ms. Sylvia Martin, who knows a lot about *in vitro* assays and offered her time in helping me to improve my protocols. Ms. Dr. rer. nat. Anna Lena Ostermann-Parucha is a very lovely supervisor and shared her ideas for helping me overcome the problems that I met in my project. In AG Glimm, Ms. Stephanie Frank, an MD student, also worked with PDACs, taught me a great number of assays. In the last year, AG Glimm expanded a lot, and more lab members joined in Dresden. I would specially thank Ms. Dr. rer. nat. Zunamys Carrero, who indeed sacrifice her precious time in helping me to do mass-spectrometry data analysis. And in here, I want to thank Ms. Sara Hrabovska and all the other lab members in Dresden who provided me with their ideas in the lab meeting. Back to Heidelberg, Mr. Dr. Mario Huerta helped me doing single-cell RNA sequencing analysis. Mr. Haidar Kasem, Ms. Dr. med. Stella Arelaki are my good friends and thank you for kindly providing me with all kinds of help when I requested. Finally, for our lab members and former colleagues, Ms. Hannah Walzer, Mr. Leon Wambach, Mr. Dr. rer. nat. Elias Eckert, Mr. Dr. rer. nat. Peer Wünsche, Ms. Dr. sc. hum. Mariam Haffa, Mr. Dr. med. Jianpeng Gao, and Ms. Dr. rer. nat. Christine Siegl also helped me a lot in the lab.

I also want to thank my TAC members, Mr. Prof. Dr. rer. nat. Holger Sülthmann and Mr. Prof. rer. nat. Dr. Kai Breuhahn. During the TAC meeting, they gave me beneficial suggestions, not only about my project but also cares about my PhD life and my future career.

I would not forget my dearest families. They are supporting me to chase my dreams and left me no worries behind.

EIDESSTATTLICHE VERSICHERUNG

1. Bei der eingereichten Dissertation zu dem Thema

Characterization of G Protein Subunit Beta 1 as Regulator of Tumour Initiating Cell Activity in Human Pancreatic Cancer

handelt es sich um meine eigenständig erbrachte Leistung.

2. Ich habe nur die angegebenen Quellen und Hilfsmittel benutzt und mich keiner unzulässigen Hilfe Dritter bedient. Insbesondere habe ich wörtlich oder sinngemäß aus anderen Werken übernommene Inhalte als solche kenntlich gemacht.
3. Die Arbeit oder Teile davon habe ich bislang nicht an einer Hochschule des In- oder Auslands als Bestandteil einer Prüfungs- oder Qualifikationsleistung vorgelegt.*
4. Die Richtigkeit der vorstehenden Erklärungen bestätige ich.
5. Die Bedeutung der eidesstattlichen Versicherung und die strafrechtlichen Folgen einer unrichtigen oder unvollständigen eidesstattlichen Versicherung sind mir bekannt. Ich versichere an Eides statt, dass ich nach bestem Wissen die reine Wahrheit erklärt und nichts verschwiegen habe.

Ort und Datum

Harbin, China
26 March 2021

Unterschrift

Na Kang